2025

Volume : 14
Issue : 1
Page : 1 - 106

e-ISSN : 2147-4249

Eurasian Journal of Soil Science

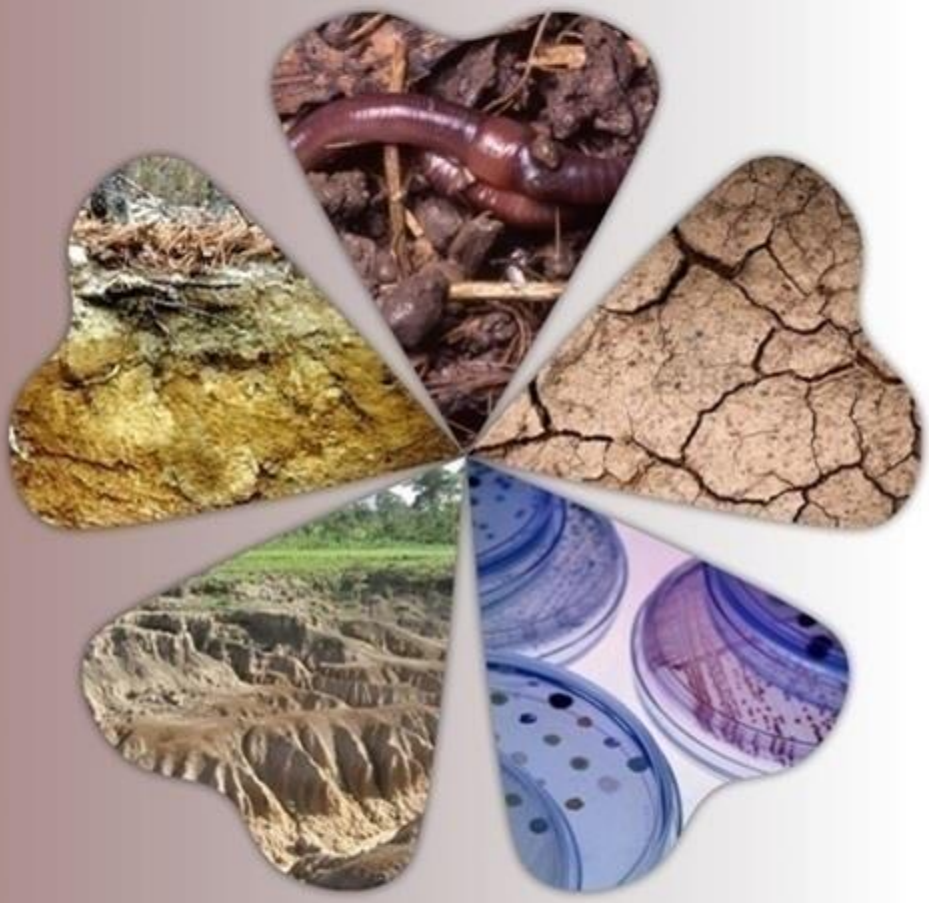

http://ejss.fesss.org

Published by Federation of Eurasian Soil Science Societies

EURASIAN JOURNAL OF SOIL SCIENCE

(Peer Reviewed Open Access Journal)

Published by Federation of Eurasian Soil Science Societies

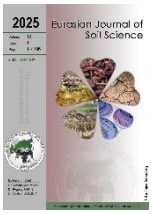

ABOUT THIS JOURNAL: Eurasian Journal of Soil Science is the official English language journal of the Federation of Eurasian Soil Science Societies. Eurasian Journal of Soil Science peer-reviewed open access journal that publishes research articles, critical reviews of basic and applied soil science in all related to soil and plant studies and general environmental soil science.

ABSTRACTING AND INDEXING: SCOPUS, CABI, FAO-Agris, EBSCOhost, ProQuest, DOAJ, OAJI, TR Dizin, TURKISH Journalpark, CrossRef, CiteFactor, CAS, etc.

Year: 2025, Volume: 14, Issue: 1, Page: 1 - 106 **e-ISSN 2147-4249**

EURASIAN JOURNAL OF SOIL SCIENCE

(Peer Reviewed Open Access Journal)

Published by Federation of Eurasian Soil Science Societies

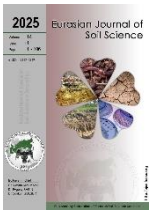

YEAR: 2025 **VOLUME : 14** **ISSUE : 1** **PAGE : 1 - 106**

CONTENTS

Eurasian Journal of Soil Science 2025, 14(1), 1 - 8

Eurasian Journal of Soil Science

Journal homepage : http://ejss.fesss.org

Evaluating the prediction success of soil organic carbon stock in pasture land using different modeling performance metrics

Ülkü Yılmaz *, Seval Sünal Kavaklıgil

Department of Forest Engineering, School of Forestry, Çankırı Karatekin University, Çankırı, 18200 Türkiye

Article Info

Received : 02.05.2024
Accepted : 16.09.2024
Available online: 30.09.2024

Author(s)

Ü.Yılmaz *
S.S.Kavaklıgil

* Corresponding author

Abstract

Many national and international initiatives depend on detailed spatial data on changes in soil organic carbon stock (SOC stock) at various scales to support policies aimed at land degradation neutrality and climate change mitigation Developing tools to accurately model the spatial distribution of SOC_{stock} at national scales is a priority for both monitoring soil organic carbon (SOC) changes and contributing to global carbon cycle studies. The primary goal of this study was to evaluate and compare various spatial performance metrics used to assess the accuracy of predicting soil SOC and SOCstock content in a semi-arid pasture. Soil samples were taken from 0-20 cm soil depth at 150 random sampling points. Spatial structure of SOC_{stock} and SOC were modelled by ordinary kriging The soil pH varied from slightly acidic (6.34) to neutral (7.19), and salinity was not an issue in the study area. Lime content, with an average of 2.04%, stands out as the most variable soil property, with a coefficient of variation (CV) of 61.76%. The carbon stock ranged from 23.46 to 65.36 tons ha^{-1}, with an average carbon stock of 43.28 tons ha^{-1} calculated. In the study area, SOC (%) and stoniness (%) had the shortest autocorrelation distance (21.00 m), while bulk density had the longest (27.00 m). The prediction errors indicated that parameters in the random sampling did not result in better predictions using the OK technique.The results indicated that SOC content can exhibit significant spatial variability even within a small area, highlighting the need for site-specific management in semi-arid pastures. In order to achieve high accuracy and success in modeling, metrics of the performance such as RRMSE, RMSE and MAPE should be used that minimize the effect of the relevant soil property measurement unit.

Keywords: Soil organic carbon, geostatistics, spatial variability, kriging, pasture.

Introduction

Digital mapping of pasture soil organic carbon (SOC) aids in the development of sustainable grazing management and in monitoring its effects on climate change (Garcia-Franco et al., 2021). SOC has commonly been assumed that plays an important role in determining grassland quality affecting soil quality and grass growth (Wang et. al., 2022). Recent studies indicate that increasing plant species richness in grasslands enhances soil carbon storage (Yang et al., 2019; Zhou et al., 2019). As determining soil organic carbon stock (SOC_{stock}) requires extensive sampling effort, time-consuming and high cost, it is not possible to observe at every point in the field (Bhunia et al., 2018). Therefore, the interest in predicting the amount of soil organic carbon stock is growing rapidly. Spatial interpolation analysis has been commonly used to predict SOC_{stock} at non-sampling points by various forms of kriging algorithms for estimating continuous attributes procedure (Isaaks and Srivastava, 1989). Ordinary kriging is an interpolation method estimating surface data from point data, based on the distances between sampling points (Rutter et al., 1991) and minimizing the estimation variance (Li and Heap, 2011). Evaluating the accuracy of modeling predictions in environmental sciences becomes important. The objective of this study was to predict soil carbon content using kriging methods and to assess the accuracy of the estimation through various performance metrics.

: https://doi.org/10.18393/ejss.1558316
: https://ejss.fesss.org/10.18393/ejss.1558316
Publisher : Federation of Eurasian Soil Science Societies
e-ISSN : 2147-4249

Material and Methods

The study site was in semi-arid climate condition which is highly grazed site in North-Central Anatolia, Corum province in Turkey (Figure 1). The study area is 10 ha and the altitude is 1650 m above sea level. The area is flat and nearly middle slope (0-5%) in the northwest border of the Corum Plain. Long-term (2013-2023) annual average temperature of the study area is 12.30 °C. This region is defined by a semi-arid climate, with an average annual precipitation of 371.65 mm.

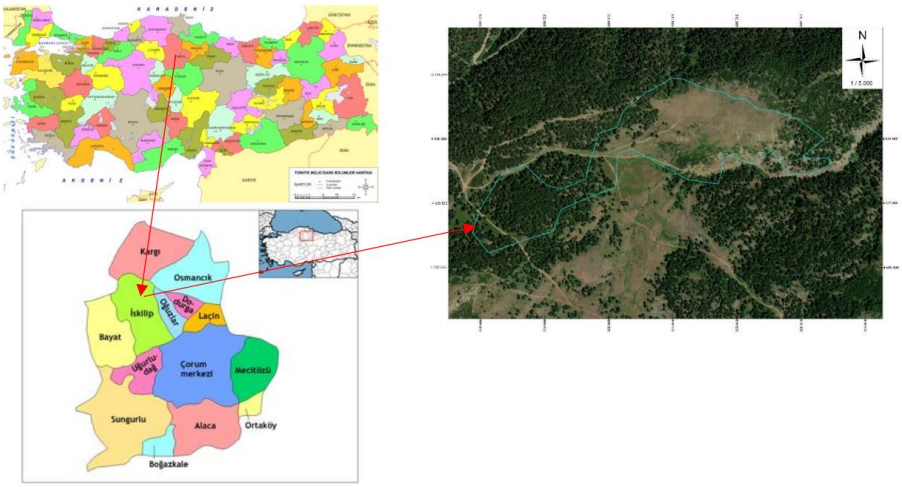

Figure 1. Location of the study area.

Soil sampling and analysis

Field sampling was conducted between May and July 2021 in a natural grassland, with 150 experimental points randomly selected. Soil samples were collected as both undisturbed and disturbed from a depth of 0-20 cm. Soil texture was determined using the hydrometer method (Bouyoucous, 1951). Soil pH and electrical conductivity (EC) were measured using a 1:2.5 soil-water ratio following the method of Hendershot et al. (2007), and the calcium carbonate content (% $CaCO_3$) was determined according to Kacar (1994). Bulk density (BD) was measured using cylindrical cores (100 cm^3) from a 0-20 cm soil depth, as described by Blake and Hartge (1986). Soil organic matter (SOM) content was analyzed using the Walkley-Black wet digestion method (Nelson and Sommers, 1982), while organic carbon was determined by oxidizing carbon with an acidic dichromate solution, as this method is both simple and requires minimal equipment (Nelson and Sommers, 1982). Soil organic carbon stock was calculated by considering soil bulk density, organic carbon concentration, and soil depth, using the formula provided in Equation 1 (Lu and Liao, 2017).

$$SOC_{stock} = 100 \times SOC \times BD \times (1\text{-}CF) \times (Top\text{-}Bottom) \quad (1)$$

In Equation (1), SOCstock is the soil organic carbon stock (ton/ha), SOC is the SOC content (wt. %), BD is the bulk density (g cm-3), CF is the proportion of coarse fragments (vol. %), (Top-Bottom) is the thickness of the given sampling soil depth (cm) and 100 is used for unit conversion.

Spatial modelling

Descriptive statistics were calculated with SPSS 11.0. Following Lark (2000) holds the view that necessary transformations should be made in non-normally distributed data sets to make a successful geostatistical modeling. Although necessary transformations were made according to Webster's (2001) criteria in order to better model the data that did not show normal distribution, semivariogram models were not affected. For this reason, geostatistical modeling was continued without transforming the data sets. Ordinary kriging (OK) was used because it provides the best linear unbiased estimate of the predicted spatial variable while minimizing the variance of the prediction errors. Unlike other interpolation methods, OK takes into account the spatial autocorrelation between sample points, meaning that it considers how values at one location are related to values at nearby locations (Isaaks and Srivastava, 1989). The geostatistical software GS+ was employed to examine the spatial structure of the data for soil properties as well as to model the semivariogram..Variable lag distances were also applied for semivariogram selection, ensuring a minimum of ten lags with at least 30 data pairs in each lag.. In determining the most suitable semivariogram, it was decided that the R^2 (coefficient of determination) should be close to 1, and RSS (residual sum of squares) and nugget value should be close to 0. (Isaaks and Srivastava, 1989). An experimental semivariogram was generated by

calculating semivariance values for each pair of sample points and then averaging these values across increasing lag intervals (h).

Each point in a semivariance was calculated from Equation (2):

$$\gamma(\mathrm{h}) = \frac{1}{2N\ (h)} \sum_{\mathrm{i}=1}^{N} [z(x_i + h) - zx_i]^2 \quad (2)$$

Where $z(x_i + h)$ is the z value at location $(x_i + h)$, zx_i is the z value at a location separated from x_i by distance h and N is number of sampling pairs separated by distance h (lag) (Webster and Oliver, 2008). After determining the appropriate semivariogram model, cross-validation analysis was used to determine accuracy of the interpolation technique by graphing the predicted values with the observed values. An unknown sample point in kriging is calculated as seen in equation (3) as:

$$z_0 = \sum z_i \times \mathrm{w} \quad (3)$$

where z_0 is a known predicted value, z_i is observed value. The parameter w is kriging weight (Isaaks and Srivastava 1989). The errors calculated by subtracting observed values from predicted values were used to evaluate performance OK (Burrough and McDonnell, 1998). Spatial distribution maps for each variable were created using the best parameters obtained from the semivariogram models and cross-validation process. The geostatistical extension of ArcGIS 10.2.1 was utilized to generate kriging maps of soil properties.

Results and Discussion

Descriptive statistics

Descriptive statistics for SOC_{stock} and other soil properties are given Table 1. SOC and SOC_{stock} contents were % 2.45, 43.27 (ton ha^{-1}) at 20 cm soil depth, respectively. On the other hand, in contrary with our results, some researchers observed that SOC_{stock} was higher (Szatmári et al., 2019; Zhu et al., 2019; Li et al., 2022; Ma et al., 2023). According to Webster (2001), bulk density, $CaCO_3$ (%), and EC are positively skewed, while clay (%) is negatively skewed. Webster defined a distribution with skewness greater than ±1.0 as strongly skewed. These strong positive skewness-values indicate proportional effect, wherein the variability is greater in sample points with high values compared to those with low values corrupting spatial modeling. Modeling performance increases significantly when the distribution of variable follows a normal or near-normal distribution.

Table 1. Descriptive statistics for the soil variables (N:150)

Soil variable	Min	Max	Mean	Std dev	Skewness	Kurtosis	CV%	DT
BD (g cm^{-3})	1.03	1.58	1.18	0.08	1.00	1.90	6.78	NN
Sand (%)	24.00	64.00	43.46	7.22	0.18	0.19	16.61	NN
Clay (%)	4.00	44.00	32.85	5.51	-0.84	3.96	16.77	NN
Silt (%)	7.00	49.00	23.70	5.71	-0,12	3,30	24.09	NN
Stoniness (%)	0.00	40.00	25.00	0.09	0.13	-0.75	35.81	NN
CF (%)	60.00	100.00	75.00	0.09	-0.13	-0.75	11.79	NN
$CaCO_3$ (%)	0.89	8.27	2.04	1.26	2.35	0.19	61.76	NN
OM (%)	2.51	5.49	4.23	0.87	-0.52	-1.06	20.57	NN
SOC (%)	1.46	3.19	2.45	0.50	-0.52	-1.06	20.41	NN
SOC_{stock} (ton ha^{-1})	23.46	65.36	43.28	9.01	0.20	-0.37	20.81	NN
pH	6.34	7.19	6.70	0.16	0.32	-0.19	2.39	N
EC (ds m^{-1})	0.026	0.231	0.088	47.85	1.07	0.71	53.89	NN

N—Number of soil samples, Min—Minimum value, Max—Maximum value, Std dev—Standard deviation, CV—Variation of coefficient, DT—Distribution type, N—Normal distribution, NN—Abnormal distribution, BD—Bulk density, CF—proportion of coarse fragments, OM—Organic matter, SOC—Soil organic carbon, SOC_{stock}—Soil organic carbon stock, EC—Electrical conductivity, CV—Variation of coefficient.

It is common for SOC data to be positively skewed (Liang et al., 2019; Szatmári et al., 2019, 2021; Wang et al., 2021). However, in this study area, the SOC data exhibited a slight negative skew.Regarding Table 1, the values of variation coefficient vary between 2.39% and 61.76%, and among all soil properties examined, $CaCO_3$ (%) was a more variable soil property than others. According to (Cambardella et al., 1994), the coefficient of variation (CV) can be categorized into three groups: low (<15%), medium (15% to 35%), and high (>35%).

The CV of SOC_{stock} in different studies was represented by high (Rodríguez Martín et al., 2016; Szatmári et al., 2021; Li et al., 2022) unlike our study.

Geostatistical analyses characteristics of the SOC and its components

Semivariogram analysis was applied separately to quantify the spatial structure of SOC_{stock} and other soil properties The semivariogram charts related to the soil properties under investigation are presented in Figure 2. The spatial distribution SOC_{stock} and SOC were better described with spherical model (Figure 2). In other studies, quite different nugget values for SOC have been reported, such as Mishra et al. (2009) 294.5, 294.5, Li et al. (2023) 0.33 and Kingsley et al. (2021) 0.19.

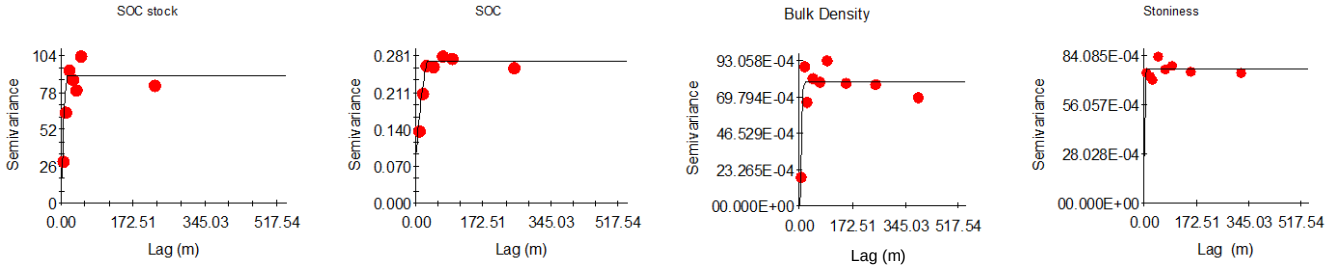

Figure 2. Semivariograms of soil properties

The high nugget value observed for SOC_{stock} implies a substantial level of random variance within the study area. This indicates that samples taken from nearby and distant locations exhibit distinct values. The higher sill value for SOCstock (77.56), compared to stoniness (0.007) and bulk density (0.007), suggests greater variability between sampling points and lower prediction accuracy at finer scales (Table 2).

Table 2. Semi-variogram parameters of soil properties of the grassland (Turkıye)

Soil parameters	Model type	Nugget C_o	Sill $C_o + C$	Range A_0 (m)	Spatial dependence (%)	RSS	R^2
SOC_{stock} (ton ha^{-1})	Spherical	21.6	77.56	25.00	27.84	228	0.89
BD (g cm^{-3})	Spherical	0.001	0.007	27.00	12.82	1.32E-06	0.92
SOC (%)	Spherical	0.09	0.257	21.00	194.55	3.29	0.97
Stoniness (%)	Exponential	0.0037	0.007	21.00	52.85	1.34E-06	0.62

SOC_{stock}: Soil organic carbon stock, BD: Bulk density, SOC: Soil organic carbon, RSS: Residual sum of squares, R^2: Coefficient of determination

A nugget-to-sill ratio of <25% signifies strong spatial dependence, typically due to intrinsic factors like soil texture and mineralogy; 25-75% indicates moderate dependence from both intrinsic and extrinsic factors; and >75% suggests weak spatial dependence, often due to extrinsic factors such as uncontrolled grazing and hoofprints (Cambardella et al., 1994). According to this classification, spatial variations of soil SOC_{stock}, SOC, BD, and stoniness were characterized as moderately, strongly, weakly, and moderately spatially dependent, respectively (Table 2). This dependency was not large enough to confirm geostatistical methods to predict examined soil properties, irrespective of the sampling intervals. The nugget/sill ratio for SOC% was 194.55, indicating a very weak spatial dependency according to reported by (Blackburn et al., 2022). Table 2 results indicate minimal nugget effect, suggesting that variation is not due to sampling error but rather to short-range spatial variability beyond the sampling intervals.

The nugget-to-sill ratio represents the interaction between random and structural factors, reflecting the proportion of spatial heterogeneity due to autocorrelation within the overall spatial heterogeneity (Li et al., 2021). Structural factors such as climate, parent material, terrain, and soil composition contribute to significant spatial correlation among spatial variables. Conversely, random factors like fertilization, grazing and cultivation contribute to a reduction in spatial correlation. To better understand spatial dependence can best be treated under three distinct types using percentage of nugget/sill ratio (Cambardella et al., 1994). Although nugget values of SOC_{stock} was high, its spatial dependence was at a moderate level which might be attributed to extrinsic factors like soil forming processes and intrinsic factor like uncontrolled grazing. As regards range is the maximum distance over which spatial dependence or autocorrelation exists. Range distances are presented in Table 2 reveals that there has been a slight decreased respectively in the range distance of soil properties. Range distances were indicated that the optimum sampling interval did not vary greatly among different soil properties. According to Rossel and McBratney (2008), R^2 values are classified as follows: ≥0.81 is very good, 0.61–0.80 is good, 0.41–0.60 is moderate, and <0.40 is weak (Viscarra Rossel et

al., 2016). According to the definition above, the R^2 values obtained for SOC_{stock}, SOC, and BD were higher. Consistent with this, researchers have reported similar results (Rostaminia et al., 2021; Zhang et al., 2022).

Kriging

Spatial distribution maps obtained using ordinary kriging was presented in Figure 2. The maps illustrating spatial distribution facilitated the assessment of both the extent and magnitude of soil properties in the study area. A gradual increase in SOC_{stock} was noted from the northeast to the southwest of the study area, with the percentage of SOC_{stock} ranging from 29.88% to 58.71% in the 0-20 cm soil depth (Figure 3). The similar observation was also reported by Liu et al (2023). Compared to the spatial structure of SOC_{stock}, stoniness and bulk density displayed a non-uniform distribution.

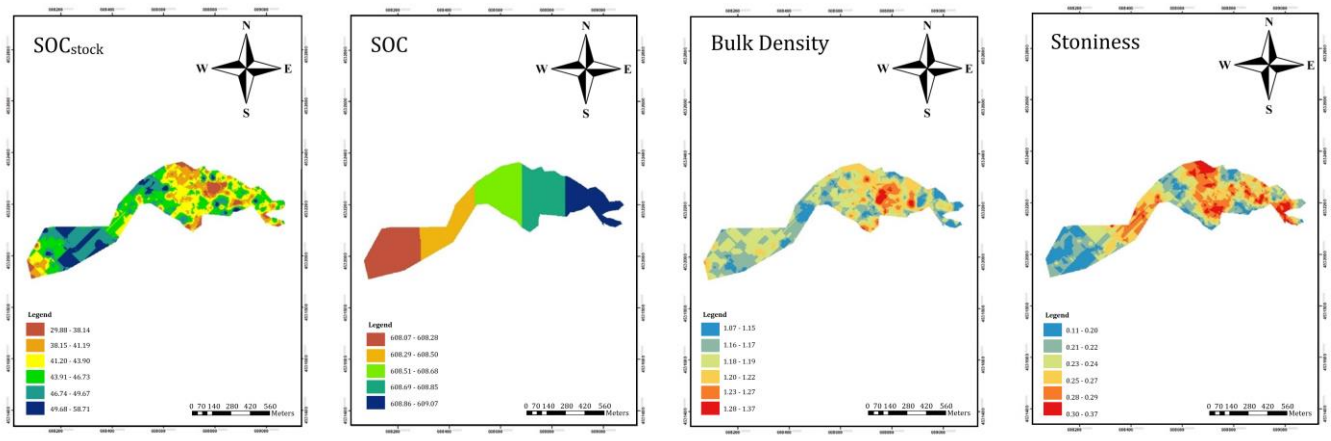

Figure 3. Spatial distribution maps for soil properties

As can be seen in Table 3, different metrics of interpolation performance were calculated to evaluate the fitting accuracy of the models. According to the data, the absolute value of the Mean Error (ME) was far from 0, while Root Mean Square Error (RMSE) and Mean Square Error (MSE) exhibited the biggest values.

Table 3. Metrics used to assess the performance of spatial interpolation methods

Performance Metrics	SOC_{stock}	BD	SOC	Stoniness
ME	-0.16	0.003	0.004	0.005
MPE	4.28	0.71	5.18	16.79
MAE	7.70	0.06	0.43	0.07
MSE	87.90	0.008	0.26	0.007
RMSE	9.37	0.08	0.51	0.08
RMAE	0.18	0.05	0.20	0.37
MSRE	35.92	0.23	1.86	0.36
RMSSE	39.52	30.60	1.35	1.37
RRMSE	24.41	7.10	26.04	49.95
ASE	6.34	1.08	1.56	0.50
MAPE	18.99	5.69	20.25	37,36
Willmott's D	0.23	0.38	0.28	0.27
EF	0.98	0.99	0.98	0.96

The magnitude of these metrics is contingent upon the unit or scale of the primary variable being considered. For instance, the magnitude of MAE is typically less than 1% for soil organic matter, but it can beyond 100 mm for rainfall or even exceed 1000 mm for tropical regions. The unit of measurement for variables can influence the magnitude of these metrics of performance (Li and Heap, 2011). Therefore, it becomes essential to compare the performance of kriging methods across various studies, especially when variables are observed in different units or scales. This problem is tackled by introducing two new performance metrics: Relative Mean Absolute Error (RMAE) and Relative Root Mean Square Standardized Error (RRMSE). These metrics of performance aim to mitigate the impact of measurement units and maintain sensitivity regardless of changes in units or scale. Model accuracy is classified as excellent if RRMSE is below 10%, good if RRMSE is between 10% and 20%, fair if RRMSE is between 20% and 30%, and poor if RRMSE exceeds 30% (Despotovic et al., 2016). Based on this classification, model accuracy of soil SOC_{stock}, BD, SOC, and stoniness were characterized as fair, excellent, fair, poor, respectively. The mean percent error (MPE) suggests a superior model as its value

approaches zero, indicating improved accuracy. RMSE provides an observe of error size, but the main problem with RMSE is its sensitivity to outliers, as it assigns significant weight to large errors. This means that the presence of several large errors can cause the value of RMSE to increase. RMSE is a commonly used metric for assessing modeling performance, and similar to the findings of (Rostaminia et al., 2021), our study obtained a high RMSE value (3.37) for SOC_{stock} suggesting the model's prediction accuracy is low. A value of RMSSE greater than 1 means the model underpredicts values observed in this study. The reason why RMSE takes a value greater than 1 the model underpredicts the observed values in this study. RMSE and MAE are considered to comparable metrics, offering predicts of the average error; however, they do not offer insights into the relative magnitude of the average difference or the characteristics of the differences that make them up. Nevertheless, some researchers argue that RMSE and MAE are among the most comprehensive indicators of model performance as they summarize the average disparity between observed and predicted values in their respective units (Willmott, 1982). The value of MAE was closest to ASE therefore, we can draw a conclusion from the Table 3 mentioned that a model was considered better Mean Square Error (MSE) values approach zero and Root Mean Square Error (RMSE) was smaller. According to this, the highest values observed for MSE and RMSE indicate that the accuracy of interpolation is the poorest. Considering Table 3, ASE < RSME means the model underpredicts the observed values. MSE encounters similar limitations to RMSE, whereas MAE demonstrates reduced sensitivity to extreme values and indicates the extent to which the predict can be in error. RMSE and MAE are some of the most effective observes for evaluating model performance, as they encapsulate the average discrepancy between the units of observed and predicted values. MSE shares the same limitations as RMSE, while MAE is less affected by extreme values and indicates the extent to which the predict can be in error.

ME is employed to assess the level of deviation in the predicted value, with predictions being more stronger as the value approaches zero (Wang et al., 2021). The smallest ME suggests that the predicted value is closest to the observe values. ME is employed for determining the degree of bias in predicts and is often referred to as “bias”(Hohn, 1991) but it should be used cautiously as an indicator of accuracy. Although MAE is less affected by extreme values and indicates the degree to which the estimate may be inaccurate. The main weakness with ME is that negative and positive predicts counteract each other and the resultant ME tends to be lower than observe error. Meanwhile, it would be optimal if the Mean Error (ME) and Mean Square Error (MSE) approached zero. However, there was a noticeable numerical deviation in MSE from the value of 1. The agreement index, known as Willmott's D, is scaled according to the magnitude of the variable, maintains average information, and does not magnify outliers (Willmott, 1982). The closer Willmott's D is to 1, the more accurate the method is considered. There have been proposed by some researcher (Greenwood et al., 1985), an accuracy measurement known as model efficiency (EF). The fact that the EF metric value is close to zero indicates that the average value of observations is more reliable than predictions. (Li and Heap, 2011).

As far as the Mean Absolute Percentage Error (MAPE) is concerned, it is a good metric used to assess model performance in the presented stud. Regarding the Mean Absolute Percentage Error (MAPE), it serves as a valuable metric for evaluating model performance in the study presented. MAPE is often considered one of the most effective indicators among error metrics (Moreno et. al., 2013; Gunal et. al., 2023). The MAPE value < 10% indicates highly accurate (excellent estimator), while the value 10-20 % indicates moderately accurate (good predictor), and if the value ranges 20-50 % the model's accuracy is considered low, but its outputs are still acceptable (Lewis, 1982). According to this classification model accuracy of soil BD, SOC, SOC_{stock}, and stoniness were characterized as high, moderately, low estimation, respectively (Table 3). The (%) MAPE value of stoniness was higher than other soil properties. The results can be attributed to the significant variability in the data, as the MAPE error metric exhibits very low tolerance for extreme values.

Conclusion

The soil organic carbon is a soil property characterized by high spatial variability, yet it is relatively straightforward to observe. One potential explanation for this phenomenon is the diverse range of plant communities and soil properties found within grasslands. Additionally, certain soil properties exhibit considerable variability over short distances due to uncontrolled grazing practices. As a result, estimating carbon sequestration in grasslands can be more challenging compared to cultivated agricultural areas. The limiting factors of this study include that the random sampling design has led to a low success rate in geostatistical modeling of soil organic carbon. This study indicated that SOC_{stock} and SOC vary significantly over very short distances. We evaluated the advantages and disadvantages of different spatial performance metrics can be used to estimate SOC_{stock} effectively and efficiently in terms of accuracy. The unit of measurement and

the high variability of the examined soil properties are important factors that should be considered in geostatistical modeling. The observations should include at least MAPE, RRMSE or RMSE to compare the model success across different variables in dissimilar units. The MAPE is a performance evaluation metric that effectively mitigates the impact of measurement units. Here, we recommend that future studies clearly report in their publications information about why the metrics used in model performance evaluation are used and their advantages and disadvantages. Additionally, future studies should consider using systematic sampling and increasing sample density to improve the accuracy of SOC predictions.

Acknowledgments

This research was supported by the Scientific Research Project Unit of Çankırı Karatekin University (BAP), Çankırı, Türkiye, under project no. BAP-OF210621B18. The authors extend their gratitude to the Scientific Research Projects Coordinator of Çankırı Karatekin University for the financial support provided for this study.

References

Ballabio, C., Fava, F., Rosenmund, A., 2012. A plant ecology approach to digital soil mapping, improving the prediction of soil organic carbon content in alpine grasslands. *Geoderma* 187 (188): 102–116.

Bhunia, G.S., Shit, P.K., Maiti, R., 2018. Comparison of GIS-based interpolation methods for spatial distribution of soil organic carbon (SOC). *Journal of the Saudi Society of Agricultural Sciences* 17(2):114-126.

Blackburn, K.W., Libohova, Z., Adhikari, K., Kome, C., Maness, X., Silman, M.R., 2022. Influence of land use and topographic factors on soil organic carbon stocks and their spatial and vertical distribution. *Remote Sensing* 14(12):1-22.

Blake, G.R., Hartge, K.H., 1986. Bulk density. In: Methods of Soil Analysis, Part 1 Physical and Mineralogical Methods. Klute A., (Ed.). American Society of Agronomy-Soil Science Society of America, Madison, WI, USA. pp. 363–375.

Bouyoucous, G.J., 1951. A recalibration of the hydrometer method for making mechanical analysis of soils. *Agronomy Journal* 43: 434-438.

Burrough, P.A., McDonnell, R.A., 1998. Principles of Geographical Information Systems. Oxford University Press, USA. 327p.

Cambardella, C.A., Moorman, T.B., Novak, J.M., Parkin, T.B., Karlen, D.L., Turco, R.F., Konopka, A.E., 1994. Field-scale variability of soil properties in central Iowa Soils. *Soil Science Society of America Journal* 58(5): 1501-1511.

Despotovic, M., Nedic, V., Despotovic, D., Cvetanovic, S., 2016. Evaluation of empirical models for predicting monthly mean horizontal diffuse solar radiation. *Renewable and Sustainable Energy Reviews* 56: 246–260.

Garcia-Franco, N., Walter, R., Wiesmeier, M., Hurtarte, L.C.C., Berauer, B.J., Buness, V., Zistl-Schlingmann, M., Kiese, R., Dannenmann, M., Kögel-Knabner, I., 2021. Correction to: biotic and abiotic controls on carbon storage in aggregates in calcareous alpine and prealpine grassland soils. *Biology and Fertility of Soils* 57(2):203-218.

Greenwood, D.J., Neeteson, J.J., Draycott, A., 1985. Response of potatoes to N fertilizer: Dynamic model. *Plant and Soil* 85: 185–203.

Günal, E., Budak, M., Kılıç, M., Cemek, B., Sırrı, M., 2023. Combining spatial autocorrelation with artificial intelligence models to estimate spatial distribution and risks of heavy metal pollution in agricultural soils. *Environmental Monitoring and Assessment* 195(2): 317.

Hendershot, W., Lalande, H., Duquette, M., 2007. Ion Exchange and exchangeable cations, In: Soil sampling and methods of analysis. Carter, M.R., Gregoirch, E.G., (Eds.). CRC press, pp.135-141.

Iepema, G., Deru, J.G.C., Bloem, J., Hoekstra, N., de Goede, R., Brussaard, L., van Eekeren, N., 2020. Productivity and topsoil quality of young and old permanent grassland: an on-farm comparison. Sustainability 12(7):2600.

Isaaks, E.H., Srivastava, R.M., 1989. An introduction to applied geostatistics. Oxford University Press, New York, 561 p.

Kacar, B., 1994. Bitki ve Toprağın Kimyasal Analizleri III Toprak Analizleri. Ankara Üniversitesi Ziraat Fakültesi Eğitim Araştırma Geliştirme Vakfı Yayınları. Ankara. No. 3, 705s. [in Turkish].

Kingsley, J., Afu, S.M., Isong, I.A., Chapman, P.A., Kebonye, N.M., Ayito, E.O. 2021. Estimation of soil organic carbon distribution by geostatistical and deterministic interpolation methods: a case study of the southeastern soils of Nigeria. *Environmental Engineering & Management Journal* 20 (7):1077-1085.

Lal, R., Delgado, J.A., Groffman, P.M., Millar, N., Dell, C., Rotz, A., 2011. Management to mitigate and adapt to climate change. *Journal of Soil and Water Conservation* 66(4): 276–285.

Lark, R.M., 2000. Estimating variograms of soil properties by the method-of-moments and maximum likelihood. *European Journal of Soil Science* 51(4): 717-728.

Lewis, C.D., 1982. Industrial and business forecasting methods : A practical guide to exponential smoothing and curve fitting. Butterworth Scientific, Boston, USA. 143p.

Li, G., Zhang, J., Zhu, L., Tian, H., Shi, J., Ren, X., 2021. Spatial variation and driving mechanism of soil organic carbon components in the alluvial/sedimentary zone of the Yellow River. *Journal of Geographical Sciences* 31: 535–550.

Li, J., Heap, A.D., 2011. A review of comparative studies of spatial interpolation methods in environmental sciences: Performance and impact factors. *Ecological Informatics* 6(3-4):228-241.

Li, Y., Liu, W., Feng, Q., Zhu, M., Yang, L., Zhang, J., 2022. Effects of land use and land cover change on soil organic carbon storage in the Hexi regions, Northwest China. *Journal of Environmental Management* 312: 114911.

Li, Y., Wang, X., Chen, Y., Gong, X., Yao, C., Cao, W., Lian, J., 2023. Application of predictor variables to support regression kriging for the spatial distribution of soil organic carbon stocks in native temperate grasslands. *Journal of Soils and Sediments* 23: 700–717.

Liang, Z., Chen, S., Yang, Y., Zhao, R., Shi, Z., Viscarra Rossel, R.A., 2019. National digital soil map of organic matter in topsoil and its associated uncertainty in 1980's China. *Geoderma* 335: 47–56.

Liu, X., Zhou, T., Zhao, X., Shi, P., Zhang, Y., Xu, Y., Luo, H., Yu, P., Zhou, P., Zhang, Y.,2023. Patterns and drivers of soil carbon change (1980s-2010s) in the northeastern Qinghai-Tibet Plateau. *Geoderma* 434: 116488.

Lu, X., Liao, Y., 2017. Effect of tillage practices on net carbon flux and economic parameters from farmland on the Loess Plateau in China. *Journal of Cleaner Production* 162: 1617-1624.

Ma, Y., Minasny, B., Viaud, V., Walter, C., Malone, B., McBratney, A., 2023. Modelling the whole profile soil organic carbon dynamics considering soil redistribution under future climate change and landscape projections over the lower Hunter Valley, Australia. *Land* 12(1): 255.

Mishra, U., Lal, R., Slater, B., Calhoun, F., Liu, D., Van Meirvenne, M., 2009. Predicting soil organic carbon stock using profile depth distribution functions and ordinary kriging. *Soil Science Society of America Journal* 73(2): 614–621.

Moreno, J.J.M., Pol, A.P., Abad, A.S., Blasco, B.C., 2013. Using the R-MAPE index as a resistant measure of forecast accuracy. Psicothema 25(4): 500–506.

Nelson, D.W., Sommers, L.E., 1982. Total carbon, organic carbon and organic matter. In: Page, A.L., Miller, R.H., Keeney, D.R., (eds) Methods of Soil Analysis, Agronomy, No. Part 2: Chemical and Microbiological Properties. 2nd Ed. ASA Madison, Wisconsin USA, pp 539-579.

Orton, T.G., Pringle, M.J., Page, K.L., Dalal, R.C., Bishop, T.F.A., 2014. Spatial prediction of soil organic carbon stock using a linear model of coregionalisation. *Geoderma* 230: 119–130.

Rodríguez Martín, J.A., Álvaro-Fuentes, J., Gonzalo, J., Gil, C., Ramos-Miras, J.J., Grau Corbí, J.M., Boluda, R., 2016. Assessment of the soil organic carbon stock in Spain. *Geoderma* 264: 117–125.

Rossel, R. V., McBratney, A.B., 2008. Diffuse reflectance spectroscopy as a tool for digital soil mapping, In: Digital soil mapping with limited data. Hartemink, A.E., McBratney, A., Mendonça-Santos, M.L. (Eds.). Springer, Dordrecht, pp. 165-172.

Rostaminia, M., Rahmani, A., Mousavi, S.R., Taghizadeh-Mehrjardi, R., Maghsodi, Z., 2021. Spatial prediction of soil organic carbon stocks in an arid rangeland using machine learning algorithms. *Environmental Monitoring and Assessment* 193: 815.

Szatmári, G., Pásztor, L., Heuvelink, G.B.M., 2021. Estimating soil organic carbon stock change at multiple scales using machine learning and multivariate geostatistics. *Geoderma* 403: 115356.

Szatmári, G., Pirkó, B., Koós, S., Laborczi, A., Bakacsi, Z., Szabó, J., Pásztor, L., 2019. Spatio-temporal assessment of topsoil organic carbon stock change in Hungary. *Soil and Tillage Research* 195: 104410.

Viscarra Rossel, R.A., Brus, D.J., Lobsey, C., Shi, Z., McLachlan, G., 2016. Baseline estimates of soil organic carbon by proximal sensing: Comparing design-based, model-assisted and model-based inference. *Geoderma* 265: 152-163.

Wang, G., Mao, J., Fan, L., Ma, X., Li, Y., 2022. Effects of climate and grazing on the soil organic carbon dynamics of the grasslands in Northern Xinjiang during the past twenty years. *Global Ecology and Conservation* 34: e02039.

Wang, S., Xu, L., Zhuang, Q., He, N., 2021. Investigating the spatio-temporal variability of soil organic carbon stocks in different ecosystems of China. *Science of The Total Environment* 758: 143644.

Wang, W., Fang, J., 2009. Soil respiration and human effects on global grasslands. *Global and Planetary Change* 67(1-2): 20-28.

Webster, R., 2001. Statistics to support soil research and their presentation. *European Journal of Soil Science* 52: 331-340.

Webster, R., Oliver, M.A., 2008. Geostatistics for environmental scientists. John Wiley & Sons, 317p.

Willmott, C.J., 1982. Some comments on the evaluation of model performance. *Bulletin of the American Meteorological* 63(11): 1309-1313.

Yang, D., Pang, X.P., Jia, Z.F., Guo, Z.G., 2021. Effect of plateau zokor on soil carbon and nitrogen concentrations of alpine meadows. *Catena* 207: 105625.

Yang, Y., Tilman, D., Furey, G., Lehman, C., 2019. Soil carbon sequestration accelerated by restoration of grassland biodiversity. *Nature Communications* 10: 718.

Zhang, M.Y., Wang, F.J., Chen, F., Malemela, M.P., Zhang, H.L., 2013. Comparison of three tillage systems in the wheat-maize system on carbon sequestration in the North China Plain. *Journal of Cleaner Production* 54(1): 101–107.

Zhang, P., Wang, Y., Xu, L., Sun, H., Li, R., Zhou, J., 2022. Factors controlling the spatial variability of soil aggregates and associated organic carbon across a semi-humid watershed. *Science of The Total Environment* 809: 151155.

Zhou, X., Wu, W., Niu, K., Du, G., 2019. Realistic loss of plant species diversity decreases soil quality in a Tibetan alpine meadow. *Agriculture, Ecosystems & Environment* 279:25-32.

Zhu, M., Feng, Q., Zhang, M., Liu, W., Qin, Y., Deo, R.C., Zhang, C., 2019. Effects of topography on soil organic carbon stocks in grasslands of a semiarid alpine region, northwestern China. *Journal of Soils and Sediments* 19:1640-1650.

Eurasian Journal of Soil Science 2025, 14(1), 9 - 21

Eurasian Journal of Soil Science

Journal homepage : http://ejss.fesss.org

Changing soil characteristics as affected by different land uses in a humid region, west of Iran

Pariya Heidari *, Mohammad Feizian

Department of Soil Science, Lorestan University, P.O. Box 68151-44316, Khorramabad, Iran

Article Info

Received : 17.03.2024
Accepted : 30.09.2024
Available online: 08.10.2024

Author(s)

P.Heidari *
M.Feizian

* Corresponding author

Abstract

Land use change, mostly from forest to conventional agriculture, has a detrimental impact on soil health and production. However, the impact of such LUC on soil biological characteristics is unknown. This study aimed to evaluate some of the physicochemical and biological properties of soil with varied land uses in the southwestern Khorramabad area. The research locations comprised diverse land use types including coniferous forest, broadleaf forest, farmland, and rangeland. According to the findings, there was no significant variation in bulk density (ρb) and bulk density at 33 kPa (ρb_{33}) for various land uses, but there was a significant difference between different soil layers. The amount of clay and silt varies dramatically across land uses. However, the quantity of sand used did not differ significantly across the usage (p <0.05). The results showed that the highest and lowest values of soil pH were observed in the coniferous forest and rangeland, respectively. Although the EC in coniferous forests was greater (0.17 dS m^{-1}) than in other land uses, there was no significant difference in the average soil EC in various land uses (p <0.01). In terms of soil organic carbon (SOC), the greatest value was found in broadleaf forests with an average of 1.517 (ton/ha), while the lowest content was observed in farmland with an average of 0.797 (ton/ha). The findings showed that there is a significant difference in soil nitrogen averages across different land uses followed by the decreasing order of broadleaf forest (0.11%)> rangeland (0.06%)> Farmland (0.05%)> coniferous forest (0.03%). The findings also suggested that the quantity of microbial respiration has considerably declined in all locations as land use has shifted from forest to pasture and farmland. Notably, farmland includes the greatest population of fungi, bacteria, and actinomycetes, with a significant difference from other uses (p <0.01). Additionally, the relationship between OC and other soil factors is the most significant in this study.

Keywords: Land use, Biological properties, Soil organic carbon, Lorestan province.

Introduction

In recent decades, there has been a growing concern about rising atmospheric greenhouse gas concentrations and global warming. Climate change has now become a major problem for all countries, causing significant effects on the environment, such as temperature rises, which have contributed to ecosystem deterioration (De Stefano and Jacobson, 2018; Mukherjee et al., 2024). Climate change has an impact on vegetation and species composition by modifying soil moisture and temperature regimes, as well as nutrient cycles, and changes in biomass (*i.e.,* material residues, aerial and subsurface biomass) seem to have an impact on organic carbon (OC) storage and cycling (Aminiyan et al., 2016; Kim et al., 2023; Yang et al., 2024). As a consequence, the soil's physical and chemical qualities are affected (Aminiyan et al., 2015a; Nadal-Romero et al., 2023).

The major axis of soil quality and health is soil organic carbon (SOC). Soil, being a main source of atmospheric carbon, may help to reduce greenhouse gas emissions by reducing carbon dioxide generation (Aryal et al.,

: https://doi.org/10.18393/ejss.1564167
: https://ejss.fesss.org/10.18393/ejss.1564167
Publisher : Federation of Eurasian Soil Science Societies
e-ISSN : 2147-4249

2020; Nave et al., 2024). In other words, soils are both a sink and a source of carbon, making them an essential component of the global carbon cycle with roughly 1206 Pg OC in the top 1 m depth, much exceeding the atmospheric carbon store (800 Pg) (Zdruli et al., 2017). Carbon storage in soil and plants revealed that about 60% of SOC is stored in the first 20 cm of soil surface (Ramesh et al., 2019). As a result, even a minor increase in soil carbon stores has a significant impact on decreasing greenhouse gas emissions into the environment (Basheer et al., 2024; Kopittke et al., 2024). Carbon sequestration, or flux of carbon, is a potential option for mitigating climate change by turning atmospheric CO_2 into stabilized SOC for a long time in soil, which also improves soil quality (Smith et al., 2020; Benslama et al., 2024). Demand for agricultural and forestry products will continue to rise as a result of population expansion and industrial progress, and consumption patterns will move toward products that have larger overall environmental impacts (Clerici et al., 2019; Payen et al., 2020). Agriculture and forestry are important contributors to ecosystem degradation and biodiversity loss (Aminiyan et al., 2018; Ekka et al., 2023).

Nowadays, the conversion of forests to rangelands or agricultural lands has become a major cause of environmental degradation and global climate change all over the world (Barati et al., 2023). Land use change is considered as the second greatest cause of carbon emissions after fuel consumption (Ramesh et al., 2019; Benslama et al., 2024). Reduced biomass-C inputs (i.e. roots, litter fall) and losses due to increased erosion and dissolved organic C leaching diminish SOC reserves when natural and agricultural ecosystems are converted (Aminiyan et al., 2015b; Tiefenbacher et al., 2021). As a result, land use change combined with poor management is one of the primary causes of greenhouse gas emissions and global warming in recent decades (Liu et al., 2023).

Forest soils have always been considered due to their high organic matter (OM) content and suitable structure (Kooch et al., 2023; Nave et al., 2024). However, changes in their management and use along with tillage practices generally have a major impact on the amount of soil organic matter (SOM) and other soil physical and chemical properties (Voltr et al., 2021; Yadav et al., 2021). One of the most important studies on environmental change is the connection between land use change and soil properties (Eze et al., 2023).

Land use changes and agricultural activity can negatively impact soil physical and chemical properties, leading to a considerable decrease in SOM and nutrients, porosity, fertility, aggregate stability, hydraulic conductivity, increased bulk density, increased erosion rate, and accelerated degradation of soil (Asmare et al., 2023; Ekka et al., 2023; Mirghaed and Souri, 2023; Ma et al., 2024). For instance, Padbhushan et al. (2022) reported that soils under natural forests had 36.1% higher SOM compared to converted croplands. Additionally, they reported that conversion of natural vegetation to pasture typically increases soil pH. This change is often due to the application of fertilizers and lime to enhance grass growth, which can lead to higher soil alkalinity (Padbhushan et al., 2022). It has been found that deforestation also increases soil erosion rates and bulk density, and reduces porosity, aggregate stability, and hydraulic conductivity (Molla et al., 2022). Cultivated lands have much lower levels of SOC, total nitrogen (TN), and available phosphorus compared to natural forests and pastures, thereby soils under natural forests had 36.1% higher organic carbon than converted croplands (Matano et al., 2015). Cultivation diminishes soil carbon within a few years of initial conversion from forest (Gebresamuel et al., 2022). The conversion of forest to cropland increases bulk density and reduces porosity and aggregate stability (Tellen and Yerima, 2018). Therefore, soil quality indices differed across all land uses and management regimes, revealing that the most essential systems in sustaining soil quality were natural forests and protected regions, whereas developed lands had much lower physical features (Zhao et al., 2021).

So far, numerous researchers have also investigated the effect of replacing natural and degraded forests with artificial forests on carbon sequestration and have highlighted the relevance of such studies (Liu et al., 2024; Wang et al., 2021). The comparison of SOC in natural pastures under wheat cultivation and areas under cultivation of perennial rangeland species indicated that the lowest amount of SOC was in the area under wheat cultivation (Saurabh et al., 2021). Additionally, the amount of SOC in the areas under cultivation of perennial rangeland species was close to natural rangeland (McGowan et al., 2019). As a result, studying changes in the physical, chemical, and biological characteristics of soil in various uses can not only demonstrate the implications and consequences of this transition but also help us figure out how to address the problem and avoid additional soil damage in these places (Tellen and Yerima, 2018; Voltr et al., 2021; Yadav et al., 2021).

Land-use changes in Iran have been more rapid in the last 50 years than at any time in Iran's history and are expected to continue at this rate or accelerate in the future (Azizi et al., 2022). Anthropogenic activities are

degrading the rangelands of Iran, mostly due to land use change and subsequent intense rainfed or irrigated farming (Soleimani et al., 2019). The conversion of natural virgin rangelands into orchards and rainfed farmlands is the most typical land use change in the Lorestan province, west of Iran (Japelaghi et al., 2019). There has been a lack of research in this area so far to investigate the changes in soil characteristics and C sequestration in diverse land uses due to the unique climatic conditions of Lorestan Province and its varied land uses. The primary objective of this study was therefore to evaluate some of the physicochemical and biological properties of soil with varied land uses in the south-western Khorramabad area. The findings of this study might be useful in controlling and forecasting unfavorable changes caused by land use changes in other parts of the province.

Material and Methods

Study area

Lorestan province is located in the west of Iran between 66° 51'-50° 3' E longitude and 32° 37'-34° 22' N latitude (Figure 1). Its altitude is 1160 meters above sea level. The province is located in the west of the country and the middle part of the Zagros Mountains and along the two rainy aerial fronts of the Mediterranean from the west and the Indian Ocean from the south, which has significant and potential resources. The average annual temperature for a period of 25 years is 17.9°C, which has a thermal heating regime, and the warmest month of July is 30.1°C, and the lowest temperature is related to January with a temperature of 6.1°C. The average monthly rainfall of Khorramabad station is 519 mm, which has a humid regime and the highest rainfall is from November to April, the months of June to September are dry and the rainfall is almost zero. The area of the Lorestan province is 28300 ha. The soil humidity and thermal regimes are xeric and thermic, respectively. Moreover, the studied soils are under the category of Inseptisol with calcareous rock parent material.

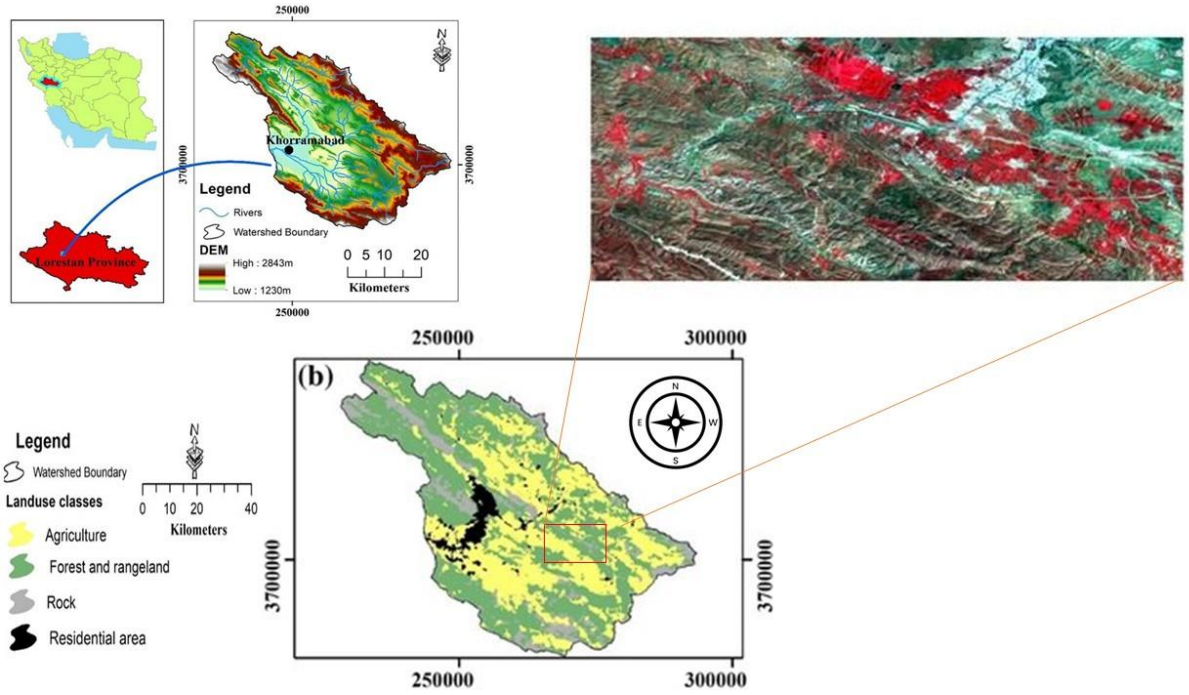

Figure 1. The map of the studied area in the Khorramabad region

Sampling, treatment, and analysis of soil

8 soil samples were randomly taken from the body of soil profiles for each of four land uses (i.e., farmland, coniferous forest, broadleaf forest, and rangeland) in three replications. In doing so, around 10 kg of the soil was taken from each land use and quickly transported to the lab. Afterward, the samples were spread on dry paper and air-dried. Then, the soil was sieved to remove gravel, large roots, and plant residues using an 8-mm sieve followed by a 2-mm sieve in preparation for further procedures. One kilogram of each sample was transferred to the laboratory in plastic bags and inside an ice flask and stored at 4 °C for biological analyses. The percentage of sand, silt, and clay was determined using the hydrometer method (Gee and Or, 2002). Soil

pH, and electrical conductivity (EC) were measured in a 1:2.5 (soil: water) extraction by a pH-meter (Metrohm) and an EC-meter (Metrohm), respectively (Rayment and Lyons, 2011). The content of total organic carbon in soil samples was analyzed by the modified Walkley and Black method (Aminiyan et al., 2015b; Walkley and Black, 1934). Also, total nitrogen (TN) was determined using the Kjeldahl method (Bremner, 1996), and soil available phosphorous by the Olsen method (Peperzak et al., 1959).

Soil bulk density (ρb) in undisturbed soil samples was measured with cylinders. To estimate BD at 33 kPa moisture content the following formula was employed, which was established by (Kern, 1994).

$$\rho b_{33} = (\rho b_{OD}\ 0.880) + 0.046 \qquad \text{Eq (1)}$$

where ρb_{33} was bulk density at 33 kPa moisture and ρb_{OD} was oven-dried bulk density.

The colony count technique was utilized to estimate the quantity of bacteria, fungi, and actinomycetes. The fresh soil solution was sequentially diluted with saline buffer to produce an optimum number of colonies on each plate. The media of nutrient agar (NA) bacteria, potato dextrose agar (PDA) for fungi, and rose Bengal starch casein nitrate agar (RBSCNA) for actinomycetes were utilized (Aminiyan et al., 2018). Briefly, in doing so, the fresh soil suspension was serially diluted with saline buffer to obtain an appropriate number of colonies on each plate. Each dilution was plated in triplicate and the population was expressed as the number of colonies forming units (log CFU. g^{-1} soil). After preparing each specific media in plates 0.1 ml of soil suspension of each serial dilution was spread across the plates (spread plate method). The plates were incubated at 28 °C for 3, 4, and 14 days for bacteria, fungi, and actinomycetes, respectively.

Moreover, the Isermeyer technique was used to determine soil respiration (Isermeyer, 1952). The 50 grams of soil samples (weighted dry equivalent) were wet to 80% of their water-holding capacity with distilled water and placed in sealed jars containing 25 mL of 0.5 M NaOH. For basal respiration (BR), the samples were incubated at 25 °C for 7 days, followed by titration of NaOH with 0.25 M HCl (Aminiyan et al., 2018).

Statistical data analysis

After data collection, Kolmogorov–Smirnov test was applied to investigate the normal distribution of data at a confidence level of 95%. Statistical analyses such as descriptive statistics were conducted by MS Excel 2016. Also, one-way analyses of variance (ANOVA) were used for the mean comparison using SPSS Version 19 at 5% (p<0.05) and 1% (p<0.01) significant levels.

Results and Discussion

Soil physical properties

The results did not show a significant difference between bulk density (ρb) and bulk density at 33 kPa (ρb_{33}) at different land uses (Table 1), while did show a significant difference (p <0.05) between different soil horizons (Figure 2a,b). The average of ρb ranged from 1.29 to 1.36 (Mg/m^3) in all studied land uses. Additionally, the average of ρb_{33} varied from 1.41 to 1.49 (Mg/m^3) in the studied land uses. The lowest ρb_{33} was observed in broadleaf forests, while the highest was observed in farmland (Table 1). As illustrated in Figure 2a,b, ρb_{33} and ρb exhibited a significant difference, which increased at the surface horizons and decreased with increasing depth, owing to the reduction in organic matter with depth. Hajabbasi et al. (2007) found no significant change in ρb as a consequence of land use change in their investigations, which is in line with the findings of this study. As also shown in Figure 2a,b, ρb rises with increasing depth in the studied land uses. It can be expected that tillage and topsoil disturbance reduce organic matter and consequently soil degradation, thus reducing soil pores and increasing ρb (Li et al., 2021). Therefore, the ρb increases with the lowering of the proportion of SOM, lightening of texture, and disintegration of soil structure during forest-to-farmland conversion (Antón et al., 2021).

Table 1. The mean content of soil bulk density (ρb) in undisturbed soil, soil bulk density at 33 kPa (ρb_{33}) moisture, and mean percentage of sand, silt, and clay particles for all studied land uses (p <0.05)

Land-use Type	ρb_{33} (Mg/m^3)	ρb (Mg/m^3)	Sand (%)	Silt (%)	Clay (%)	Soil Texture
Coniferous forest	1.29 a	1.42 a	17.99 b	29.70 ab	52.31 a	Clay
Broadleaf Forest	1.29 a	1.41 a	22.08 ab	30.23 ab	42.97 b	Clay, Clay loam
Rangeland	1.33 a	1.46 a	23.70 a	31.68 a	44.62 b	Clay, Clay loam
Farmland	1.36 a	1.49 a	20.25 ab	27.43 b	52.28 a	Clay

The different letters indicate the mean difference is statistically significant at the level of 0.05 among the treatments (p <0.05)

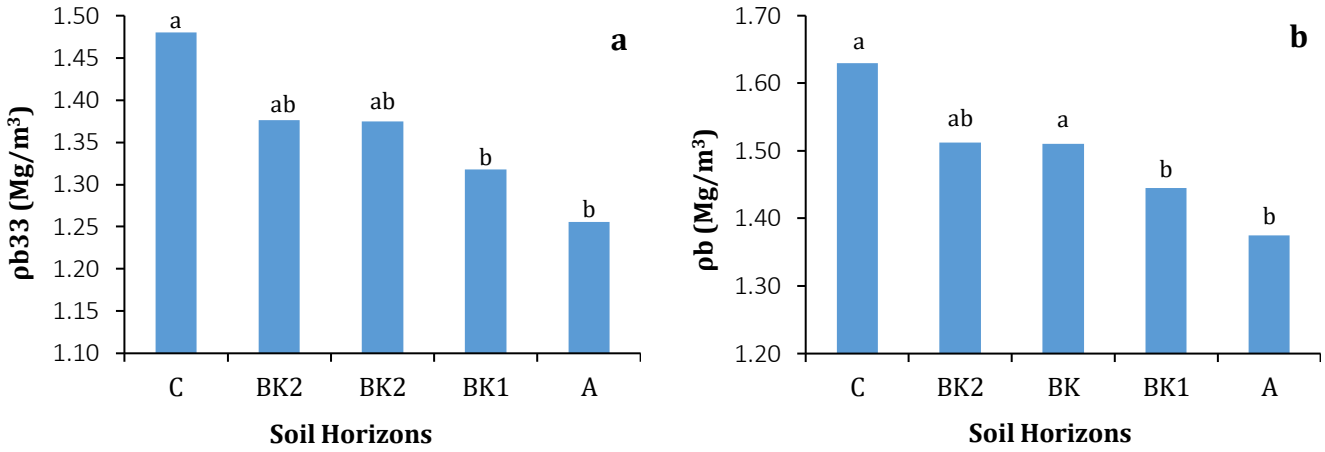

Figure 2. The mean comparison of a) ρb33 and b) ρb (Mg/m³) in all studied land uses. The different letters indicate the mean difference is statistically significant at the level of 0.05 among the treatments (p <0.05)

The soil texture is a critical component of the soil that affects the capacity of the soil to store water, aeration, temperature, CEC, and the ability to provide nutrients, as well as plant development and reproduction. According to Table 1, the quantity of clay and silt significantly differed across the land uses. However, there was no significant change in the amount of sand across the uses (p <0.05). As overall can be seen in all land uses, clay content was >42% (ranging from 42.97 to 52.31%), and silt and sand contents were <32 (ranging from 27.43% to 31.68%) and 24% (ranging from 17.99% to 23.7%), respectively. Based on the USDA classification, soil texture ranged from clay to clay loam classes (Table 1). Accordingly, clay class was the dominant texture in coniferous forests and farmland, while clay and clay loam textures were simultaneously found in broadleaf forests and rangeland (Table 1). The results of some earlier studies showed that soil texture changes as a consequence of land-use change, with a considerable reduction in soil clay and enhancement in silt content due to erosion, loss of surface layers, and exposure of deep layers in rangeland use (Khormali and Shamsi, 2009; Nazari, 2013). By changing moisture availability and nutrient delivery to microbial degradation, soil texture may also affected in the forest area (Manral et al., 2020). These results were in accordance with our findings.

Soil chemical properties

Soil reaction or pH indicates soil acidity or alkalinity. Changes in agricultural land use could greatly affect the availability of nutrient substances like nitrogen (N), phosphorus (P), and other nutrients by modifying soil qualities including texture, structure, organic matter, and pH (Asmare et al., 2023; Hasanpori et al., 2020; Qi et al., 2018). Land use change is one of the factors that has an impact on soil quality. The pH level of the soil was evaluated for various land uses because pH impacts many soil characteristics and because land use change might affect pH level and soil calcium carbonate (Boroumand et al., 2015; Tellen and Yerima, 2018; Hasanpori et al., 2020).

As illustrated in Figure 3a, soil pH varied from 7.31–7.57 in the different land-use systems. The coniferous forest had the highest soil pH, whereas rangeland had the lowest (Figure 3a). The slightly high level of soil pH is most likely due to management practices like fertilization. This also might be owing to the applied chemical fertilizers, increased organic matter decomposition, and increased carbon dioxide and soluble carbonate leaching as a result of soil deterioration (Rad et al., 2018). In past investigations, it has been reported that the change in land use from rangeland to farmland increased soil pH (Boroumand et al., 2015; Hashemi Rad et al., 2018; Tellen and Yerima, 2018). The findings of Qi et al. (2018) showed that for all investigated land uses, soil pH was much lower in the top layer than in the lower layer, despite no significant variations across the land uses. However, land use change in the southwestern region of Khorramabad has not affected soil pH (Hasanpori et al., 2020). Because soil pH depends on the soil's parent material, the changes that occur during formation depend on rainfall (Augusto et al., 2017). Given that the studied land uses have the same parent materials and are in the same climatic zone, their pH has not changed. Although the EC in the coniferous forest was higher (0.17 dS m^{-1}) than in the other land uses, the average of soil EC in different land uses did not show a significant difference (p <0.01) (Figure 3b). EC measures the concentration of soluble salts, can vary due to differences in vegetation type, root architecture, and organic matter decomposition, which may lead to higher salt concentrations in coniferous forests compared to other land uses (Teramage et al., 2023). Also, vegetation cover plays a significant role in influencing soil electrical conductivity (EC) variability through various

mechanisms related to soil chemistry, moisture retention, and organic matter dynamics (Szymański et al., 2019). Therefore, alteration in EC can be attributed to the uniformity of parent materials, vegetation cover, and the stabilizing effects of climate. In this context reported that no significant difference observed between the EC of forest and rangeland soils. Therefore, the earlier reported results were consistent with our findings (Rad et al., 2018; Varasteh Khanlari et al., 2019). The amount of SOM is a key indicator of its productivity (Wang et al., 2018). Because of its determining effects on the physical, chemical, and biological properties of the soil, such as the ability to keep and provide water, the nutrient cycle, plant root growth, current intensity of gases, and soil preservation. The SOM also plays a key role in soil quality stability, crop production, and environmental quality (Aminiyan et al., 2018; Ramesh et al., 2019; Smith et al., 2020). In terms of SOC, there is a substantial difference between various land uses (p <0.01) (Table 2). This table reveals that SOC content was the greatest in broadleaf forests with an average of 1.517 (ton/ha), while was the lowest in farmland use with an average of 0.797 (ton/ha). It indicates agricultural activities have a role in lowering SOC because plowing accelerates the degradation of soil organic materials (Nayak et al., 2019). Also, the plowing can lead to the discharge of OC from the soil solum as a result of carbon mineralization and CO_2 gas emission (Wasige et al., 2014; Yellajosula et al., 2020). Another factor contributing to the loss of SOM is the intensification of erosion in agricultural regions. Soil erosion rises as a result of land use change, and OM with a high carbon content is transferred to the surface soil (da Cunha et al., 2021; Telo da Gama et al., 2021). Furthermore, during tillage operations, deep soil layers with a lower percentage of OC are mixed with a surface layer with a greater percentage of OC, resulting in a reduction in topsoil OC relative to the initial state (Saurabh et al., 2021; Zhang et al., 2022). Raiesi and Beheshti (2022) also showed that the conversion of rangelands into farmlands significantly reduces SOM. Carbon is stored as OM in the soil, but these reserves are affected by farming. When pastures are cultivated, the amount of SOC begins to decrease, and this reduction depends on climatic factors and the intensity of cultivation (Yellajosula et al., 2020; Kooch et al., 2021).

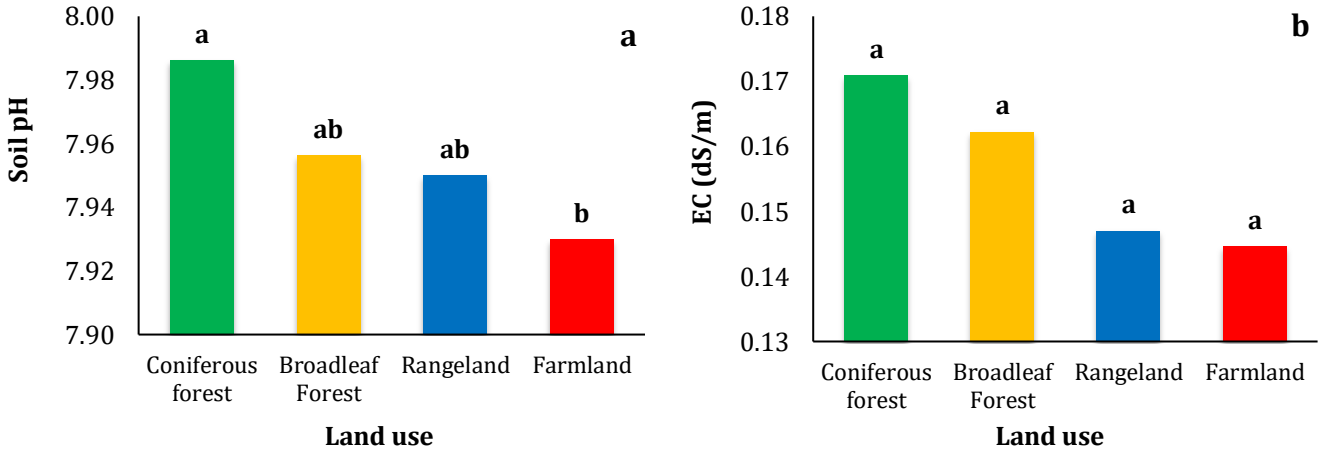

Figure 3. The mean comparison of a) soil pH and b) EC (dS/m) in all studied land uses. The different letters indicate the mean difference is statistically significant at the level of 0.05 among the treatments (p <0.05)

The findings demonstrate that there is a considerable difference between the averages of soil nitrogen in various land uses (Table 2). The TN value in the broadleaf forest is considerably different from other land uses (p <0.05). As also given in Table 2, the content of TN in the land uses followed the decreasing order of broadleaf forest (0.11%)> rangeland (0.06%)> Farmland (0.05%)> coniferous forest (0.03%). Nitrogen has been identified as the most critical soil component determining SOC level in several recent studies (Qiu et al., 2018; Jahangir et al., 2021; Wu et al., 2021). The vertical and horizontal distributions of TN concentration and stock were influenced by anthropogenic disturbance. This is confirmed by the findings of this study, which found that natural land use categories had greater nutrient levels than either agricultural or urban areas. Greater SOC and TN concentrations in forestry areas may be attributed to higher residue decomposition from surface litter inputs that enhanced SOC (Nwaogu et al., 2018). The increase in SOC content has been closely associated with an increase in TN content (Diwediga et al., 2017). On the other side, low levels of SOC and TN as found in farmland and rangeland may be explained by poor soil conditions due to the use of plant residues as animal food and fuel, as well as unsustainable management approaches which exacerbated soil erosion (Li et al., 2017; Rezapour and Alipour, 2017; da Cunha et al., 2021). The conversion of crop wastes to humus and the increase in soil aeration due to plowing cause a decline in soil nitrogen, which results in an increase in soil microorganisms and the disruption of soil nitrogen balance (Fenton et al., 2018; Gaël et al., 2021).

Consequently, agricultural activities and practices can lead to the accelerated decomposition and mineralization of the available OM, thereby lowering SOC and TN concentrations and stocks (Aguilera-Huertas et al., 2021; Wei et al., 2021).

Table 2. Mean content of soil organic carbon (SOC) (ton/ha) and the percentage of total nitrogen (TN %) in the studied land uses

Land-use type	SOC (ton/ ha)	TN (%)
Broadleaf Forest	1.5173 a	0.10950 a
Rangeland	1.0951 b	0.06063 b
Coniferous forest	0.9319 bc	0.03875 b
Farmland	0.7970 c	0.05550 b

The different letters indicate the mean difference is statistically significant at the level of 0.05 among the treatments ($p < 0.05$)

Soil biological properties

Land use change may impose a detrimental influence on soil microbial properties. As shown in Figure 4a, there is a significant variation in the rate of microbial respiration in different land uses ($p < 0.05$). Forest uses have the highest rate of microbial respiration, whereas arable land has the lowest (Figure 4a). Changes in SOC and soil moisture had the greatest impact on soil respiration (Aminiyan et al., 2018). The presence of greater SOM content in forest use is one of the causes of increased microbial activity and, as a result, microbial respiration (Wu et al., 2020). In agricultural uses, however, the soil is regularly plowed upside down, causing the aggregates to break down and exposing the organic matter inside to microbial attack (Aminiyan et al., 2015a).

The results indicated that the amount of microbial respiration has decreased dramatically in all sites as land use has changed from forest to pasture and arable land (Figure 4a). These results were consistent with the findings of Rasouli-Sadaghiani et al. (2018) and Zheng et al. (2019). One of the effective reasons for the existence of more microbial respiration in the forest ecosystem is the suitable conditions for microbial activity, including adequate carbon supply and the litter layer used by soil microorganisms (Soleimani et al., 2019). In an assessment of land use change on soil quality characteristics in Iran, (Zarafshar et al., 2020) found that microbial respiration in forest lands is greater than in arable lands. Bakhshandeh et al. (2019) showed that soil microbial respiration in agricultural lands is significantly less than in forest use. Because microbial respiration is an indicator of organic carbon mineralization, it is highest in places where organic carbon is the highest (Rasouli-Sadaghiani et al., 2018; Fan and Han, 2020). More microbial respiration is typically seen by soil scientists as a sign of high soil quality because greater microbial activity leads to higher microbial respiration (Babur et al., 2021). Moreover, Kooch et al. (2021a) reported that soil microbial respiration is greatly reduced as a result of forest degradation and farming, which supports the findings of this study.

As illustrated in Fig 4b, the largest population of fungi, bacteria, and actinomycetes is related to agricultural use and has a significant difference with other uses ($p < 0.01$). Bacteria are an essential component of soil microorganisms and make up the majority of the microbial population (Odelade and Babalola, 2019). As a result, they outnumber the whole population of fungi, algae, and protozoa because of their involvement in carbon and nitrogen cycles, as well as other modifications and interactions with higher plants (Aminiyan et al., 2018). Bacterial diversity reacted to changes in land use and soil properties (Wehr, 2018). The findings of Barnett et al. (2020) revealed that the greatest bacterial alpha diversity was found in agricultural soils, whereas the lowest was found in forest soils. They found that soil pH and land use have interactive impacts on bacterial community assembly, which changes depending on pH class. These findings support the idea that soil pH is a master variable that drives soil bacterial communities, but they also demonstrate the need to understand intricate interactions between soil pH and other soil properties in community formation. Yang et al. (2020) reported contrarily that the bacterial diversity of the forest and grassland samples was similar, and the clustering analysis revealed no significant differences in their communities between the two environments. In Hawaii, Brazil, and Ecuador, a comparison of bacterial populations from forest, rangeland, and sugarcane areas revealed that agricultural soils have a bigger microbial population than forest grounds (Wehr, 2018), which was in line with our findings.

Also, land use changes affect the structure of soil fungal populations such as population and diversity (Fernández-Bravo et al., 2021). Plant species in forest cover, grass species in rangeland cover, and other plant species in agriculture and a mixture of forest and agricultural cover (forest-crop) may play a key role in fungal changes (Mueller et al., 2014; Zarafshar et al., 2020). The role of fungi in soil is very complex. Fungi can affect the nutrient cycle of soil, have symbiotic and pathogenic communities with other plants and animals, and interact with other microorganisms (Deveau et al., 2018; Odelade and Babalola, 2019). Sui et al. (2019)

demonstrated that arable land and forest land had identical bacterial and fungal community patterns, whereas marsh wetland communities were different. They concluded that the key drivers of soil fungal community compositions as land use changed are soil pH, SOC, TN, accessible nitrogen, and total phosphorus concentrations.

Our results showed that actinomycetes have a higher population in farmland than in forest and rangeland (Figure 4b). In the study of Luo et al. (2020), it reveals that the actinobacteria in the secondary forest were significantly higher than in plantation forest land use. They also concluded that the soil microbial community composition was mainly controlled by TN and pH. Overall, altered land-use type initiated changes in the physicochemical characteristics of the soils, which affected the composition of microbial communities. Additionally, it could be concluded that the identity of affected microbial properties by various soil parameters under various land usages (i.e., type of soil physicochemical and biological characteristics) in the original ecosystem depends on the original nature of each ecosystem in different areas.

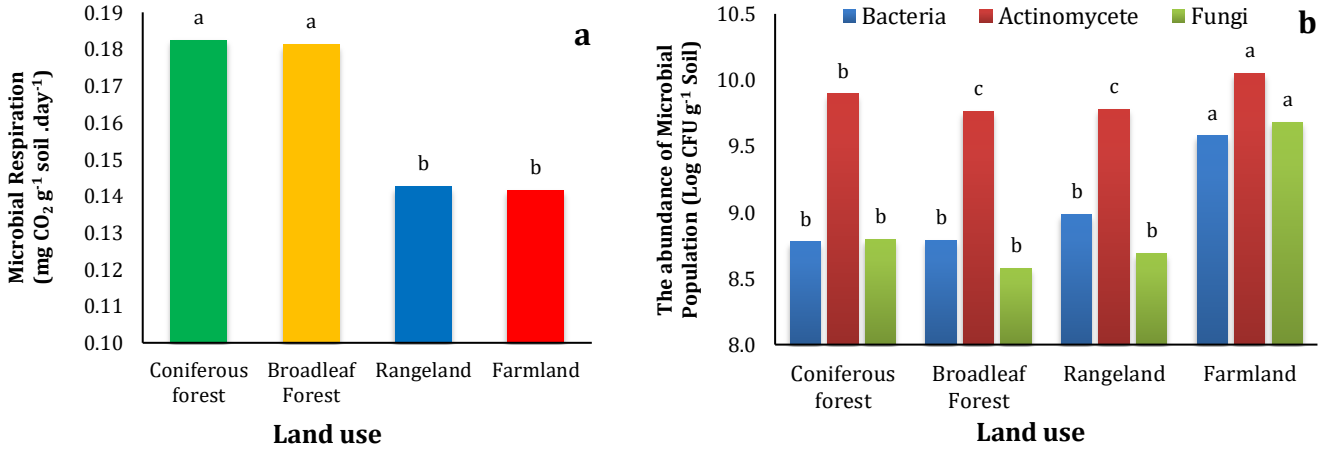

Figure 4 (a) Comparison of microbial respiration content (mg CO_2 g^{-1} soil day^{-1}) and (b) the abundance of Bacteria, Fungi, and Actinomycete (Log CFU g^{-1} soil) colonies between all of the land uses. The different letters indicate the mean difference is statistically significant at the level of 0.05 among the treatments ($p < 0.05$)

Correlation analysis of soil properties

Examining the relationships between soil factors and the extent to which each of them is affected by each other will guide managers in controlling these factors in the desired direction (Table 3). The objective of this investigation into the interaction between soil qualities is to find out the relationship between SOC and other soil parameters as well as to identify the most essential factors impacting it.

Table 3. Correlation matrix for different soil characteristics in different land uses of Khoramabad region

16OC	Sand	Silt	Clay	ρb	EC	pH	TN	MR [a]	
OC	1								
Sand	0.38*	1							
Silt	0.37*	-0.25	1						
Clay	-0.61**	-0.75**	-0.37*	1					
ρb	-0.65**	-0.27	-0.22	0.42*	1				
EC	0.09	-0.20	0.02	0.18	-0.18	1			
pH	-0.00	-0.38*	-0.09	0.29	-0.10	0.27	1		
TN	0.97**	0.41	0.29	-0.59**	-0.62**	-0.15	0.27	1	
MR	0.60**	0.01	0.34	-0.23	0.52**	0.09	0.48**	0.47**	1

[a] MR: Microbial Respiration; * P<0.05; ** P<0.01

The findings of the soil factor correlation analysis reveal that the majority of the components analyzed have a significant relationship. The correlation between OC and other soil parameters is the most significant in this research. SOC had a strong relationship with TN (r= 0.971), ρb (r= -0.65), clay (r= -0.61), and microbial respiration (r= 0.60) at a level of (p <0.01). Also, a correlation was observed between SOC and sand and silt contents (p <0.05). However, no significant correlation was observed between SOC pH and EC (Table 3). A significant correlation between SOC and other properties has been reported in past studies, pointing to a significant correlation between organic carbon and soil reaction (Liu et al., 2021). However, Amighi et al. (2013) reported that there is no significant relationship between OC and pH, which is consistent with the

results of the present study. Soil texture is also a relevant and influential factor in SOC and significant correlations have been observed between them (Varamesh et al., 2014). Also, another research noted a significant correlation between SOC and TN (El Tahir et al., 2009). Other studies have emphasized the significant relationship between SOC and TN levels (Wang et al., 2018). They consider nitrogen communication management as a very important precondition for maintaining SOC levels in forest ecosystems. Given the above, it can be said that proper management of factors affecting the amount of soil organic carbon, in addition to helping to increase levels and storage, will also help the sustainability of the ecosystem.

Conclusion

The results of the present study conducted in the southwestern region of Khorramabad city show that land use change had a significant impact on the physical, chemical, and biological properties of soil. The amount of carbon content was more significantly different than the other soil traits in different land uses. There was a significant correlation between SOC content and physical, chemical, and biological properties in soils with different uses. Among these, the strongest correlations are related to TN, ρb, and microbial respiration. The results of the current study showed that land use changes such as forest change to cultivated lands can significantly affect soil properties and change soil formation processes and is certainly the most important factor that affects the protection of natural ecosystems.

Acknowledgments

The authors express their gratitude to Lorestan University, Khorramabad, Iran, for funding this study. The authors also extend their sincere appreciation to the editor and the anonymous reviewers for evaluating the manuscript and offering valuable feedback to enhance the paper.

References

Aguilera-Huertas, J., Lozano-García, B., González-Rosado, M., Parras-Alcántara, L., 2021. Effects of management and hillside position on soil organic carbon stratification in mediterranean centenary olive grove. *Agronomy* 11(4): 650.

Amighi, S.J., Asgari, H., Sheikh, V.B., Sardo, M.S., 2013. Effects of agroforestry systems on carbon sequestration and improvement soil quality. *International Journal of Agriculture* 3(4): 822.

Aminiyan, M.M., Hosseini, H., Heydariyan, A., 2018. Microbial communities and their characteristics in a soil amended by nanozeolite and some plant residues: Short time in-situ incubation. *Eurasian Journal of Soil Science* 7(1): 9-19.

Aminiyan, M.M., Shorafa, M., Pourbabaee, A.A., 2024. Mitigating the detrimental impacts of low-and high-density polyethylene microplastics using a novel microbial consortium on a soil-plant system: Insights and interactions. *Ecotoxicology and Environmental Safety* 283: 116805.

Aminiyan, M.M., Sinegani, A.A.S., Sheklabadi, M., 2015a. Aggregation stability and organic carbon fraction in a soil amended with some plant residues, nanozeolite, and natural zeolite. *International Journal of Recycling of Organic Waste in Agriculture* 4(1): 11-22.

Aminiyan, M.M., Sinegani, A.A.S., Sheklabadi, M., 2015b. Assessment of changes in different fractions of the organic carbon in a soil amended by nanozeolite and some plant residues: incubation study. *International Journal of Recycling of Organic Waste in Agriculture* 4(4): 239-247.

Aminiyan, M.M., Sinegani, A.A.S., Sheklabadi, M., 2016. The effect of zeolite and some plant residues on soil organic carbon changes in density and soluble fractions: Incubation study. *Eurasian Journal of Soil Science* 5(1): 74-83.

Antón, R., Ruiz-Sagaseta, A., Orcaray, L., Arricibita, F.J., Enrique, A., Soto, I.d., Virto, I., 2021. Soil water retention and soil compaction assessment in a regional-scale strategy to improve climate change adaptation of agriculture in Navarre, Spain. *Agronomy* 11(3): 607.

Aryal, J.P., Sapkota, T.B., Khurana, R., Khatri-Chhetri, A., 2020. Climate change mitigation options among farmers in South Asia. *Environment, Development and Sustainability* 22(4): 3267-3289.

Asmare, T.K., Abayneh, B., Yigzaw, M., Birhan, T.A., 2023. The effect of land use type on selected soil physicochemical properties in Shihatig watershed, Dabat district, Northwest Ethiopia. *Heliyon* 9(5): e16038

Augusto, L., Achat, D.L., Jonard, M., Vidal, D., Ringeval, B., 2017. Soil parent material—A major driver of plant nutrient limitations in terrestrial ecosystems. *Global Change Biology* 23(9): 3808-3824.

Azizi, P., Soltani, A., Bagheri, F., Sharifi, S., Mikaeili, M., 2022. An integrated modelling approach to urban growth and land use/cover change. *Land* 11(10): 1715.

Babur, E., Dindaroğlu, T., Solaiman, Z.M., Battaglia, M.L., 2021. Microbial respiration, microbial biomass and activity are highly sensitive to forest tree species and seasonal patterns in the Eastern Mediterranean Karst Ecosystems. *Science of the Total Environment* 775: 145868.

Bakhshandeh, E., Hossieni, M., Zeraatpisheh, M., Francaviglia, R., 2019. Land use change effects on soil quality and biological fertility: a case study in northern Iran. *European Journal of Soil Biology* 95: 103119.

Barati, A.A., Zhoolideh, M., Azadi, H., Lee, J.-H., Scheffran, J., 2023. Interactions of land-use cover and climate change at global level: How to mitigate the environmental risks and warming effects. *Ecological Indicators* 146: 109829.

Barnett, S.E., Youngblut, N.D., Buckley, D.H., 2020. Soil characteristics and land-use drive bacterial community assembly patterns. *FEMS Microbiology Ecology* 96(1): fiz194.

Basheer, S., Wang, X., Farooque, A.A., Nawaz, R.A., Pang, T., Neokye, E.O., 2024. A review of greenhouse gas emissions from agricultural soil. *Sustainability* 16(11): 4789.

Benslama, A., Benbrahim, F., Navarro-Pedreño, J., Lucas, I.G., Vidal, M.M.J., Almendro-Candel, M.B., 2024. Organic carbon management and the relations with climate change. In: Frontier Studies in Soil Science. Núñez-Delgado, A. (Ed.). Springer, Cham. pp. 109-133.

Boroumand, M., Ghajar Sepalnou, M., Bahmanyar, M.A., Salek Gilani, S., 2015. Evaluation of the effects of land use change from forest areas into agricultural lands on some chemical properties of soil (Case Study: Zarin Abad, Sari, Iran). *Physical Geography Research Quarterly* 47(3): 435-449.

Bremner, J.M., 1996. Nitrogen-total. In: Methods of Soil Analysis: Part 3 Chemical Methods, 5.3. Sparks, D.L. Page, A.L., Helmke, P.A., Loeppert, R.H., Soltanpour, P.N., Tabatabai, M.A., Johnston, C.T., Sumner, M.E. (Eds.). SSSA Book Series No. 5. ASA-SSSA Madison WI, USA, pp. 1085– 1121.

Clerici, N., Cote-Navarro, F., Escobedo, F.J., Rubiano, K., Villegas, J.C., 2019. Spatio-temporal and cumulative effects of land use-land cover and climate change on two ecosystem services in the Colombian Andes. *Science of the Total Environment* 685: 1181-1192.

da Cunha, E.R., Santos, C.A.G., da Silva, R.M., Panachuki, E., de Oliveira, P.T.S., de Souza Oliveira, N., dos Santos Falcão, K., 2021. Assessment of current and future land use/cover changes in soil erosion in the Rio da Prata basin (Brazil). *Science of The Total Environment* 818: 151811.

De Stefano, A., Jacobson, M.G., 2018. Soil carbon sequestration in agroforestry systems: a meta-analysis. *Agroforestry Systems* 92(2): 285-299.

Deveau, A., Bonito, G., Uehling, J., Paoletti, M., Becker, M., Bindschedler, S., Hacquard, S., Hervé, V., Labbé, J., Lastovetsky, O.A., 2018. Bacterial–fungal interactions: ecology, mechanisms and challenges. *FEMS Microbiology Reviews* 42(3): 335-352.

Diwediga, B., Le, Q.B., Agodzo, S., Wala, K., 2017. Potential storages and drivers of soil organic carbon and total nitrogen across river basin landscape: The case of Mo river basin (Togo) in West Africa. *Ecological Engineering* 99: 298-309.

Ekka, P., Patra, S., Upreti, M., Kumar, G., Kumar, A., Saikia, P., 2023. Land Degradation and its impacts on biodiversity and ecosystem services. In: Land and Environmental Management through Forestry. Raj, A., Jhariya, M.K., Banerjee, A., Nerma, S., Bargali, K. (Eds.). Wiley & Sons. Inc. pp. 77-101.

Eze, S., Magilton, M., Magnone, D., Varga, S., Gould, I., Mercer, T.G., Goddard, M.R., 2023. Meta-analysis of global soil data identifies robust indicators for short-term changes in soil organic carbon stock following land use change. *Science of the Total Environment* 860: 160484.

Fan, L., Han, W., 2020. Soil respiration after forest conversion to tea gardens: A chronosequence study. *Catena* 190: 104532.

Fenton, T., Brown, J., Mausbach, M., 2018. Effects of long-term cropping on organic matter content of soils: implications for soil quality. In: Soil quality and soil erosion. Lal, R. (Ed.). CRC Press, pp. 95-124.

Fernández-Bravo, M., Gschwend, F., Mayerhofer, J., Hug, A., Widmer, F., Enkerli, J., 2021. Land-use type drives soil population structures of the entomopathogenic fungal genus Metarhizium. *Microorganisms* 9(7): 1380.

Gaël, M.O.R., Neil-Yohan, M., Alexis, N., Jeremy, S., Davi-Lin, M.E., Guirema, A.M., Aubin, O.J., Eric, R., Michel, M.M., 2021. Carbon and nitrogen stocks under various land cover in Gabon. *Geoderma Regional* 25: e00363.

Gebresamuel, G., Molla, B., Teka, K., Negash, E., Haile, M., Okolo, C.C., 2022. Changes in soil organic carbon stock and nutrient status after conversion of pasture land to cultivated land in semi-arid areas of northern Ethiopia. *Archives of Agronomy and Soil Science* 68(1): 44-60.

Gee, G.W., Or, D., 2002. Particle-size analysis. In: Methods of Soil Analysis: Part 4 Physical Methods, 5.4. Dane, J.H., Topp G.C. (Eds.), SSSA Book Series. Soil Science Society of America, Madison, Wisconsin, USA. pp. 255–293.

Hajabbasi, M., Basalatpour, A., Maleki, A., 2007. Effect of shifting rangeland to farmland on some physical and chemical properties of south and southwest soils of Isfahan. *Journal of Scince Technology of Agriculture Natural Resource* 11(42): 525-534. [in Persian]

Hasanpori, R., Sepehry, A., Barani, H., 2020. Effect of Rangeland Conversion to Dryland Farming on Soil Chemical Properties (Case study: Kian rangelands, Lorestan, Iran). *Journal of Rangeland Science* 10(1): 49-56. [in Persian]

Hashemi Rad, S., Kiani, F., Meftah Helghi, M., Hematzadeh, Y., 2018. Effect of land use on physical and chemical parameters of soil and sediment in Qarnave and Yelcheshme watersheds, Golestan Province, Iran. *Environmental Resources Research* 6(2): 89-102.

Isermeyer, H., 1952. Eine einfache Methode zur Bestimmung der Bodenatmung und der Karbonate im Boden. *Zeitschrift für Pflanzenernährung, Düngung, Bodenkunde* 56(1-3): 26-38.

Jahangir, M.M.R., Islam, S., Nitu, T.T., Uddin, S., Kabir, A.K.M.A., Meah, M.B., Islam, R., 2021. Bio-compost-based integrated soil fertility management improves post-harvest soil structural and elemental quality in a two-year conservation agriculture practice. *Agronomy* 11(11): 2101.

Japelaghi, M., Gholamalifard, M., Shayesteh, K., 2019. Spatio-temporal analysis and prediction of landscape patterns and change processes in the Central Zagros region, Iran. *Remote Sensing Applications: Society and Environment* 15: 100244.

Kern, J.S., 1994. Spatial patterns of soil organic carbon in the contiguous United States. *Soil Science Society of America Journal* 58(2): 439-455.

Khormali, F., Shamsi, S., 2009. Investigation of the quality and micromorphology of soil evolution in different landuses of a loess hillslope of Golestan province, a case study in Ghapan region. *Journal of Agricultural Sciences and Natural Resources* 16(3): 14-26.

Kim, D.G., Kirschbaum, M.U., Eichler-Löbermann, B., Gifford, R.M., Liáng, L.L., 2023. The effect of land-use change on soil C, N, P, and their stoichiometries: A global synthesis. *Agriculture, Ecosystems & Environment* 348: 108402.

Kooch, Y., Ghorbanzadeh, N., Haghverdi, K., Francaviglia, R., 2023. Soil quality cannot be improved after thirty years of land use change from forest to rangeland. *Science of The Total Environment* 856: 159132.

Kooch, Y., Mehr, M.A., Hosseini, S.M., 2021a. Soil biota and fertility along a gradient of forest degradation in a temperate ecosystem. *Catena* 204: 105428.

Kooch, Y., Piri, A.S., Tilaki, G.A.D., 2021b. Tree cover mediate indices related to the content of organic matter and the size of microbial population in semi-arid ecosystems. *Journal of Environmental Management* 285: 112144.

Kopittke, P.M., Dalal, R.C., McKenna, B.A., Smith, P., Wang, P., Weng, Z., van der Bom, F.J., Menzies, N.W., 2024. Soil is a major contributor to global greenhouse gas emissions and climate change. *EGUsphere* 1-18.

Li, H., Yao, Y., Zhang, X., Zhu, H., Wei, X., 2021. Changes in soil physical and hydraulic properties following the conversion of forest to cropland in the black soil region of Northeast China. *Catena* 198: 104986.

Li, Z., Liu, C., Dong, Y., Chang, X., Nie, X., Liu, L., Xiao, H., Lu, Y., Zeng, G., 2017. Response of soil organic carbon and nitrogen stocks to soil erosion and land use types in the Loess hilly–gully region of China. *Soil and Tillage Research* 166: 1-9.

Liu, J., Liu, X., Lyu, M., Wang, J., Li, Y., Guo, J., 2021. Changes in soil carbon and nitrogen stocks and microbial community after forest conversion in a subtropical region. *Scandinavian Journal of Forest Research* 36(7-9): 575-584.

Liu, M., Chen, Y., Chen, K., Chen, Y., 2023. Progress and hotspots of research on land-use carbon emissions: A global perspective. *Sustainability* 15(9): 7245.

Liu, X., Lie, Z., Reich, P.B., Zhou, G., Yan, J., Huang, W., Wang, Y., Peñuelas, J., Tissue, D.T., Zhao, M., Wu, T., Wu, D., Xu, W., Li, Y., Tang, X., Zhou, S., Meng, Z., Liu, S., Chu, G., Zhang, D., Zhang, Q., He, X., Liu, J., 2024. Long-term warming increased carbon sequestration capacity in a humid subtropical forest. *Global Change Biology* 30(1): e17072.

Luo, D., Cheng, R.-M., Liu, S., Shi, Z.-M., Feng, Q.-H., 2020. Responses of soil microbial community composition and enzyme activities to land-use change in the eastern Tibetan Plateau, China. *Forests* 11(5): 483.

Ma, S., Wang, L.-J., Jiang, J., Zhao, Y.-G., 2024. Land use/land cover change and soil property variation increased flood risk in the black soil region, China, in the last 40 years. *Environmental Impact Assessment Review* 104: 107314.

Manral, V., Bargali, K., Bargali, S., Shahi, C., 2020. Changes in soil biochemical properties following replacement of Banj oak forest with Chir pine in Central Himalaya, India. *Ecological Processes* 9: 30.

Matano, A.-S., Kanangire, C.K., Anyona, D.N., Abuom, P.O., Gelder, F.B., Dida, G.O., Owuor, P.O., Ofulla, A.V., 2015. Effects of land use change on land degradation reflected by soil properties along Mara River, Kenya and Tanzania. *Open Journal of Soil Science* 5(1): 20-38.

McGowan, A.R., Nicoloso, R.S., Diop, H.E., Roozeboom, K.L., Rice, C.W., 2019. Soil organic carbon, aggregation, and microbial community structure in annual and perennial biofuel crops. *Agronomy Journal* 111(1): 128-142.

Mirghaed, F.A., Souri, B., 2023. Contribution of land use, soil properties and topographic features for providing of ecosystem services. *Ecological Engineering* 189: 106898.

Molla, E., Getnet, K., Mekonnen, M., 2022. Land use change and its effect on selected soil properties in the northwest highlands of Ethiopia. *Heliyon* 8(8): e10157.

Mueller, R.C., Paula, F.S., Mirza, B.S., Rodrigues, J.L., Nüsslein, K., Bohannan, B.J., 2014. Links between plant and fungal communities across a deforestation chronosequence in the Amazon rainforest. *The ISME Journal* 8(7): 1548-1550.

Mukherjee, S., Keswani, K., Nath, P., Paul, S., 2024. A study on the correlation of anthropogenic activities with climate change. *Environmental Quality Management* 33(4): 59-71.

Nadal-Romero, E., Khorchani, M., Gaspar, L., Arnáez, J., Cammeraat, E., Navas, A., Lasanta, T., 2023. How do land use and land cover changes after farmland abandonment affect soil properties and soil nutrients in Mediterranean mountain agroecosystems? *Catena* 226: 107062.

Nave, L.E., DeLyser, K., Domke, G.M., Holub, S.M., Janowiak, M.K., Keller, A.B., Peters, M.P., Solarik, K.A., Walters, B.F., Swanston, C.W., 2024. Land use change and forest management effects on soil carbon stocks in the Northeast US. *Carbon Balance and Management* 19(1): 5.

Nayak, A., Rahman, M.M., Naidu, R., Dhal, B., Swain, C., Nayak, A., Tripathi, R., Shahid, M., Islam, M.R., Pathak, H., 2019. Current and emerging methodologies for estimating carbon sequestration in agricultural soils: A review. *Science of the Total Environment* 665: 890-912.

Nazari, N., 2013. Land use change from pasture to irrigated and dry farming arable land and its effect on soil properties in Miyaneh region, Iran. *Journal of Water and Soil Conservation* 17: 125-139. [in Persian]

Nwaogu, C., Okeke, O.J., Fashae, O., Nwankwoala, H., 2018. Soil organic carbon and total nitrogen stocks as affected by different land use in an Ultisol in Imo Watershed, southern Nigeria. *Chemistry and Ecology* 34(9): 854-870.

Odelade, K.A., Babalola, O.O., 2019. Bacteria, fungi and archaea domains in rhizospheric soil and their effects in enhancing agricultural productivity. *International Journal of Environmental Research and Public Health* 16(20): 3873.

Padbhushan, R., Kumar, U., Sharma, S., Rana, D., Kumar, R., Kohli, A., Kumari, P., Parmar, B., Kaviraj, M., Sinha, A.K., Annapurna, K., Gupta, V.V.S.R., 2022. Impact of land-use changes on soil properties and carbon pools in India: A meta-analysis. *Frontiers in Environmental Science* 9: 794866.

Payen, F.T., Sykes, A., Aitkenhead, M., Alexander, P., Moran, D., MacLeod, M., 2020. Soil organic carbon sequestration rates in vineyard agroecosystems under different soil management practices: A meta-analysis. *Journal of Cleaner Production* 290: 125736.

Peperzak, P., Caldwell, A., Hunziker, R., Black, C., 1959. Phosphorus fractions in manures. *Soil Science* 87(5): 293-302.

Qi, Y., Chen, T., Pu, J., Yang, F., Shukla, M.K., Chang, Q., 2018. Response of soil physical, chemical and microbial biomass properties to land use changes in fixed desertified land. *Catena* 160: 339-344.

Qiu, K., Xie, Y., Xu, D., Pott, R., 2018. Ecosystem functions including soil organic carbon, total nitrogen and available potassium are crucial for vegetation recovery. *Scientific Reports* 8: 7606.

Rad, M.H., Ebrahimi, M., Shirmohammadi, E., 2018. Land use change effects on plant and soil properties in a mountainous region of Iran. *Journal of Environmental Science and Management* 21(2):47-56.

Raiesi, F., Beheshti, A., 2022. Evaluating forest soil quality after deforestation and loss of ecosystem services using network analysis and factor analysis techniques. *Catena* 208: 105778.

Ramesh, T., Bolan, N.S., Kirkham, M.B., Wijesekara, H., Kanchikerimath, M., Rao, C.S., Sandeep, S., Rinklebe, J., Ok, Y.S., Choudhury, B.U., Wang, H., Tang, C., Wang, X., Song, Z., Oliver, W., Freeman II, O.W., 2019. Soil organic carbon dynamics: Impact of land use changes and management practices: A review. *Advances in Agronomy* 156: 1-107.

Rasouli-Sadaghiani, M., Barin, M., Moghaddam, S.S., Damalas, C., Ghodrat, K., 2018. Soil quality of an Iranian forest ecosystem after conversion to various types of land use. *Environmental Monitoring and Assessment* 190: 447.

Rayment, G.E., Lyons, D.J., 2011. Soil chemical methods: Australasia. CSIRO publishing. 495p.

Rezapour, S., Alipour, O., 2017. Effect of deforestation on fertility attributes of Mollisols in the NW of Iran. *Chemistry and Ecology* 33(3): 213-228.

Saurabh, K., Rao, K., Mishra, J., Kumar, R., Poonia, S., Samal, S., Roy, H., Dubey, A., Choubey, A.K., Mondal, S., 2021. Influence of tillage based crop establishment and residue management practices on soil quality indices and yield sustainability in rice-wheat cropping system of Eastern Indo-Gangetic Plains. *Soil and Tillage Research* 206: 104841.

Smith, P., Soussana, J.F., Angers, D., Schipper, L., Chenu, C., Rasse, D.P., Batjes, N.H., Van Egmond, F., McNeill, S., Kuhnert, M., Arias-Navarro, C., Olesen, J.E., Chirinda, N., Fornara, D., Wollenberg, E., Álvaro-Fuentes, J., Sanz-Cobena, A., Klumpp, K., 2020. How to measure, report and verify soil carbon change to realize the potential of soil carbon sequestration for atmospheric greenhouse gas removal. *Global Change Biology* 26(1): 219-241.

Soleimani, A., Hosseini, S.M., Bavani, A.R.M., Jafari, M., Francaviglia, R., 2019. Influence of land use and land cover change on soil organic carbon and microbial activity in the forests of northern Iran. *Catena* 177: 227-237.

Sui, X., Zhang, R., Frey, B., Yang, L., Li, M.-H., Ni, H., 2019. Land use change effects on diversity of soil bacterial, Acidobacterial and fungal communities in wetlands of the Sanjiang Plain, northeastern China. *Scientific Reports* 9: 18535.

Szymański, W., Maciejowski, W., Ostafin, K., Ziaja, W., Sobucki, M., 2019. Impact of parent material, vegetation cover, and site wetness on variability of soil properties in proglacial areas of small glaciers along the northeastern coast of Sørkappland (SE Spitsbergen). *Catena* 183: 104209.

Tellen, V.A., Yerima, B.P., 2018. Effects of land use change on soil physicochemical properties in selected areas in the North West region of Cameroon. *Environmental Systems Research* 7: 3.

Telo da Gama, J., Loures, L., Lopez-Piñeiro, A., Quintino, D., Ferreira, P., Nunes, J.R., 2021. Assessing the long-term impact of traditional agriculture and the mid-term impact of intensification in face of local climatic changes. *Agriculture* 11(9): 814.

Teramage, M.T., Asfaw, M., Demissie, A., Feyissa, A., Ababu, T., Gonfa, Y., Sime, G., 2023. Effects of land use types on the depth distribution of selected soil properties in two contrasting agro-climatic zones. *Heliyon* 9(6): e17354.

Tiefenbacher, A., Sandén, T., Haslmayr, H.-P., Miloczki, J., Wenzel, W., Spiegel, H., 2021. Optimizing carbon sequestration in croplands: A Synthesis. *Agronomy* 11(5): 882.

Varamesh, S., Hosseini, S.M., Behjou, F.K., Fataei, E., 2014. The impact of land afforestation on carbon stocks surrounding Tehran, Iran. *Journal of Forestry Research* 25(1): 135-141.

Varasteh Khanlari, Z., Golchin, A., Alamdari, P., Mosavi Kupar, S.A., 2019. The effects of changing forest land to paddy field on the physical and chemical properties of the soil and determining sensitive ındices to land use change. *Iranian Journal of Soil and Water Research* 50(8): 1911-1925.

Voltr, V., Menšík, L., Hlisnikovský, L., Hruška, M., Pokorný, E., Pospíšilová, L., 2021. The soil organic matter in connection with soil properties and soil inputs. *Agronomy* 11(4): 779.

Walkley, A., Black, I.A., 1934. An examination of the Degtjareff method for determining soil organic matter, and a proposed modification of the chromic acid titration method. *Soil Science* 37(1): 29-38.

Wang, M., Chen, H., Zhang, W., Wang, K., 2018. Soil nutrients and stoichiometric ratios as affected by land use and lithology at county scale in a karst area, southwest China. *Science of the Total Environment* 619-620: 1299-1307.

Wang, Y., Chen, L., Xiang, W., Ouyang, S., Zhang, T., Zhang, X., Zeng, Y., Hu, Y., Luo, G., Kuzyakov, Y., 2021. Forest conversion to plantations: A meta-analysis of consequences for soil and microbial properties and functions. *Global Change Biology* 27(21): 5643-5656.

Wasige, J.E., Groen, T.A., Rwamukwaya, B.M., Tumwesigye, W., Smaling, E.M.A., Jetten, V., 2014. Contemporary land use/land cover types determine soil organic carbon stocks in south-west Rwanda. *Nutrient Cycling in Agroecosystems* 100(1): 19-33.

Wehr, N.H., 2018. Responses of soil invertebrate and bacterial communities to the removal of nonnative feral pigs (Sus scrofa) from a Hawaiian tropical montane wet forest. Master Thesis, University of Hawai'i at Manoa. Natural Resources & Environmental Management (Ecology, Evolution, & Conservation Biology). 99p.

Wei, L., Ge, T., Zhu, Z., Luo, Y., Yang, Y., Xiao, M., Yan, Z., Li, Y., Wu, J., Kuzyakov, Y., 2021. Comparing carbon and nitrogen stocks in paddy and upland soils: Accumulation, stabilization mechanisms, and environmental drivers. *Geoderma* 398: 115121.

Wu, X., Xu, H., Tuo, D., Wang, C., Fu, B., Lv, Y., Liu, G., 2020. Land use change and stand age regulate soil respiration by influencing soil substrate supply and microbial community. *Geoderma* 359: 113991.

Wu, Y., Zhou, H., Chen, W., Zhang, Y., Wang, J., Liu, H., Zhao, Z., Li, Y., You, Q., Yang, B., Liu, G., Xue, S., 2021. Response of the soil food web to warming and litter removal in the Tibetan Plateau, China. *Geoderma* 401: 115318.

Yadav, G.S., Das, A., Babu, S., Mohapatra, K.P., Lal, R., Rajkhowa, D., 2021. Potential of conservation tillage and altered land configuration to improve soil properties, carbon sequestration and productivity of maize based cropping system in eastern Himalayas, India. *International Soil and Water Conservation Research* 9(2): 279-290.

Yang, Y., Cheng, H., Liu, L., Dou, Y., An, S., 2020. Comparison of soil microbial community between planted woodland and natural grass vegetation on the Loess Plateau. *Forest Ecology and Management* 460: 117817.

Yang, Z., Ohno, T., Singh, B., 2024. Effect of land use change on molecular composition and concentration of organic matter in an oxisol. *Environmental Science & Technology* 58(29): 13169–13170.

Yellajosula, G., Cihacek, L., Faller, T., Schauer, C., 2020. Soil carbon change due to land conversion to grassland in a semi-arid environment. *Soil Systems* 4(3): 43.

Zarafshar, M., Bazot, S., Matinizadeh, M., Bordbar, S.K., Rousta, M.J., Kooch, Y., Enayati, K., Abbasi, A., Negahdarsaber, M., 2020. Do tree plantations or cultivated fields have the same ability to maintain soil quality as natural forests? *Applied Soil Ecology* 151: 103536.

Zdruli, P., Lal, R., Cherlet, M., Kapur, S., 2017. New world atlas of desertification and issues of carbon sequestration, organic carbon stocks, nutrient depletion and implications for food security. In: Carbon management, technologies, and trends in mediterranean ecosystems. Erşahin, S., Kapur, S., Akça, E., Namlı, A., Erdoğan, H. (Eds.). Springer, Cham. pp. 13-25.

Zhang, J., Wang, Y., Dai, J., Xu, H., 2022. How does tillage accelerate soil production and enhance soil organic carbon stocks in mudstone and shale outcrop regions?, In: Saljnikov, E., Mueller, L., Lavrishchev, A., Eulenstein, F. (Eds.). Advances in understanding soil degradation. Springer, Cham. pp. 245-255.

Zhao, X., Tong, M., He, Y., Han, X., Wang, L., 2021. A comprehensive, locally adapted soil quality indexing under different land uses in a typical watershed of the eastern Qinghai-Tibet Plateau. *Ecological Indicators* 125: 107445.

Zheng, Q., Hu, Y., Zhang, S., Noll, L., Böckle, T., Richter, A., Wanek, W., 2019. Growth explains microbial carbon use efficiency across soils differing in land use and geology. *Soil Biology and Biochemistry* 128: 45-55.

Eurasian Journal of Soil Science 2025, 14(1), 22 - 37

Eurasian Journal of Soil Science

Journal homepage : http://ejss.fesss.org

Phytoremediation of saline soils using *Glycyrrhiza glabra* for enhanced soil fertility in arid regions of South Kazakhstan

Ulbossyn Makhanova [a,*], Mariya Ibraeva [b]

[a] Kazakh National Agrarian Research University, Almaty, Kazakhstan

[b] Kazakh Research Institute of Soil Science and Agrochemistry named after U. U. Uspanov, Almaty, Kazakhstan

Article Info

Received : 12.02.2024

Accepted : 06.10.2024

Available online: 12.10.2024

Author(s)

M.Ulbossyn *

M.Ibraeva

* Corresponding author

Abstract

This study investigates the potential of *Glycyrrhiza glabra* (licorice) as a biological tool for reclaiming saline soils in the arid regions of South Kazakhstan. Licorice was cultivated over three growing seasons in weakly, moderately, and highly saline soils to evaluate its effectiveness in reducing soil salinity and improving soil fertility. The results show that licorice cultivation significantly reduced total salt concentrations and improved organic matter content in weakly saline soils. For instance, in some areas, total salts decreased by 50%, and humus content increased from 1.55% to 1.70%, indicating enhanced soil fertility. In moderately saline soils, the reduction in salt levels was less significant, and the plant's biomass yield dropped to 40 t/ha, compared to 50 t/ha in weakly saline soils. However, licorice still demonstrated its ability to moderately improve soil structure and nutrient availability. In strongly saline soils, licorice's effectiveness was considerably limited, with only minor reductions in salinity and a significant decrease in biomass yield to 20-30 t/ha. The study concludes that while *Glycyrrhiza glabra* is highly effective in reclaiming weakly saline soils, its impact in moderately and highly saline soils requires supplemental interventions, such as leaching, to optimize its phytoremediation potential. These findings suggest that integrating biological and traditional soil reclamation methods can offer a sustainable solution for managing saline soils in arid regions.

Keywords: *Glycyrrhiza glabra*, soil salinity, phytomelioration, biological reclamation, soil fertility, saline soils.

Introduction

Soil salinization is a critical environmental challenge, particularly in arid and semi-arid regions, where it drastically affects agricultural productivity and ecosystem health (Cuevas et al., 2019; Mukhopadhyay et al., 2021; Yin et al., 2022). Soil salinity occurs as a result of natural processes such as high evaporation rates, as well as anthropogenic activities, including improper irrigation techniques and the overuse of chemical fertilizers (Shrivastava and Kumar, 2015; Kumar and Sharma, 2020). Globally, an estimated 932 million hectares of land are impacted by salinity, with Central Asia being one of the most affected regions (Shahid et al., 2018; Duan et al., 2022). In countries like Kazakhstan, Uzbekistan, and Turkmenistan, large areas of irrigated land suffer from varying degrees of salinization, leading to reduced crop yields and increased soil degradation (Funakawa et al., 2000; Saparov, 2014; Pachikin et al., 2014; Otarov, 2014; Laiskhanov et al., 2016; Suska-Malawska et al., 2019, 2022; Zhang et al., 2019; Ma et al., 2019; Yertayeva et al., 2019; Kussainova et al., 2020; Liu et al., 2022; Bektayev et al., 2023).

In Kazakhstan, for example, approximately 41% of the country's agricultural land is affected by salinity, severely limiting its productive capacity (Saparov, 2014; Pachikin et al., 2014; Kussainova et al., 2020). Traditional methods of soil reclamation, such as mechanical leaching, involve the application of vast amounts of water to flush salts from the soil profile. While this method can be effective, it requires significant financial

: https://doi.org/10.18393/ejss.1565833 Publisher : Federation of Eurasian Soil Science Societies

: https://ejss.fesss.org/10.18393/ejss.1565833 e-ISSN : 2147-4249

and technical resources, and often leads to further environmental degradation due to the disposal of saline drainage water into natural water bodies. Given the economic and environmental constraints of these approaches, there has been increasing interest in biological methods of soil desalination (Stavi et al., 2021; Shaygan and Baumgartl, 2022).

Phytoremediation, the use of plants to remove or stabilize contaminants, is emerging as a sustainable and cost-effective alternative for managing saline soils (Kafle et al., 2022; Nainwal et al., 2024). Among the plants used for this purpose, *Glycyrrhiza glabra* (licorice) has shown considerable potential. Licorice is a perennial legume well-known for its high tolerance to salinity and drought conditions. It has been extensively used in Central Asia as a natural remedy for saline soils due to its ability to absorb and accumulate salts in its biomass, thereby reducing the overall salt content of the soil. Furthermore, licorice improves soil structure and fertility by enriching it with organic matter and enhancing microbial activity (Egamberdieva and Mamedov, 2015).

Research conducted in Uzbekistan and Kazakhstan has demonstrated that cultivating licorice in saline soils can result in significant reductions in soil salinity, improved soil fertility, and increased crop yields (Hayashi et al., 2003). In slightly saline soils, licorice has been shown to reduce salinity levels by 0.2 to 0.3 units, making it a viable option for sustainable soil management. Additionally, licorice contributes to the lowering of groundwater levels through its deep root system, which also helps reduce evaporation from the soil surface, further stabilizing the soil's moisture content (Egamberdieva and Mamedov, 2015).

Beyond its ecological benefits, licorice holds significant commercial value. Its roots are rich in glycyrrhizic acid, a compound widely used in the pharmaceutical and food industries, providing an economic incentive for farmers to adopt licorice cultivation as part of their crop rotation (Chin et al., 2007; Guo et al., 2015; He et al., 2019). This dual benefit-environmental and economic—makes licorice an attractive option for addressing the widespread issue of soil salinization in Central Asia (Khaitov et al., 2021, 2024).

The aim of this study is to evaluate the effectiveness of *Glycyrrhiza glabra* in reducing soil salinity and improving soil fertility under the specific conditions of slightly saline soils in Kazakhstan. By assessing the growth dynamics, biomass production, and impact on soil properties, this research seeks to contribute to the development of sustainable land reclamation practices that can be implemented in saline-affected regions.

Material and Methods

Study Area

The research was carried out in the Otrar district of the Turkestan region, South Kazakhstan. The study area is bounded by the ancient floodplain terrace of the Syrdarya River in the south and southeast, and by the Arys-Turkestan irrigation massif in the east and north. The experimental plots were selected in three farms: "Bakyt" (slightly saline soils), "Mukhit" (moderately saline soils), and "Birzhan" (highly saline soils). Each plot measured 200 square meters, resulting in a total experimental area of 600 square meters.

Experimental Design

The experiment aimed to assess the effectiveness of licorice (*Glycyrrhiza glabra* L.) cultivation for reducing soil salinity. Before planting, pre-plant soil preparation and moisture-charging irrigation were conducted to maintain soil moisture at 70-75% of field moisture capacity. Licorice was planted in rows, with a spacing of 70 cm between rows and 10-15 cm between plants within rows. The roots, 10-15 cm in length with a diameter of 1.0-1.5 cm, were planted vertically and horizontally to ensure proper root development.

Soil salinity levels were measured at the beginning and the end of the experiment using standardized methods. Additionally, groundwater levels were monitored to assess the desalinization impact of licorice cultivation. The experiment was replicated three times across the three levels of salinity.

Soil Sampling

Soil samples were collected at three different depths: 0–20 cm, 20–50 cm, and 50–100 cm across the experimental plots. Sampling occurred both at the start and end of the experiment to track changes in soil properties. The soil was sampled using a standardized auger, air-dried, crushed, and sieved through a 2 mm mesh to prepare for laboratory analysis.

Soil Analysis

The chemical analysis of soil samples was conducted using the following GOST standards for different parameters:

- Total Humus – Determined using the Tyurin method as per GOST 26213-91.

- Total Nitrogen – Assessed by the Kjeldahl method in accordance with GOST 26107-84.
- Hydrolyzable Nitrogen – Measured using the Tyurin-Kononova method (Tyrin, 1965).
- Mobile Phosphorus – Estimated by the Machigin method following GOST 26205-91.
- Exchangeable Potassium – Quantified using GOST 26205-91.
- Exchangeable Calcium and magnesium – Quantified using GOST 26487-85
- Total CO_3 determined by using GOST 34467-2018.

In addition to nutrient analysis, the ionic composition of the soil was analyzed for the following water extractable ions:

- CO_3^{2-}, HCO_3^- , Cl^-, SO_4^{2-}, Na^+, K^+ Ca^{2+}, Mg^{2+} determined by using GOST 26423-85, GOST 26428-85, GOST 26424-85, GOST 26425-85 and GOST 26427-85.

Additionally, the following properties were assessed:

- Total salts (Electrical Conductivity, EC) of the soil extracts to determine salinity, as per GOST 26423-85.
- Soil pH was measured in a 1:5 soil-to-water suspension, following GOST 26483-85.

Licorice Cultivation and Agricultural Management

Licorice Propagation and Planting

Licorice (*Glycyrrhiza glabra* L.) was propagated using rhizomatous cuttings, which were manually prepared by cutting them into sections of 15–30 cm. Each section had 2–3 buds to ensure optimal growth. The planting was carried out in early spring with row spacing of 70 cm, and a distance of 25–30 cm between plants. The rhizomes were planted at a depth of 10–15 cm, either vertically or horizontally, to promote proper root establishment and shoot development.

Soil Preparation

Before planting, the soil underwent deep plowing to a depth of 25–27 cm. Superphosphate and potassium salt were applied at a rate of 150–200 kg/ha, followed by ammonium nitrate at 100–150 kg/ha during soil preparation. This helped improve soil fertility and structure, ensuring better initial growth conditions for licorice.

Irrigation and Fertilization

In the first year of licorice cultivation, the fields were irrigated 3–4 times to help with root establishment. In the second year, irrigation was reduced to 2–3 times, depending on rainfall and the depth of the groundwater table. For fertilization, rotted manure at 2–3 t/ha was applied in the autumn, while ammophos was added at 150–200 kg/ha in the spring.

Weed Control and Maintenance

Weed control was carried out regularly during the growing season to minimize competition. Soil loosening was also performed to ensure proper root growth and soil aeration. In the first year, dry stems were pruned in the autumn to promote healthy new growth in subsequent seasons. By the second year, the above-ground biomass had reached 7–8 t/ha, and the root yield was around 25 t/ha. These measures contributed to the effective reclamation of saline soils, enhancing soil structure and fertility.

Measurement of Licorice Yield

The yield of licorice (*Glycyrrhiza glabra*) was measured as the total fresh biomass harvested from the experimental plots. At each designated harvest time, the entire above-ground portion of the plant was collected and weighed to determine the fresh weight. The yield was calculated as total biomass per hectare (t/ha), without distinguishing between root and stem components. This measurement focused on the total green mass of the plant. Yields were then compared across different salinity levels based on the total biomass collected from each area.

Results and Discussion

Impact of Licorice Cultivation on Soil Chemical Properties

The data in Table 1 reveal the seasonal changes in key agrochemical parameters of solonchakous sierozem-meadow soils across different salinity levels over the study period. By examining total humus content, nitrogen, phosphorus, potassium, and carbonates, the impact of licorice (*Glycyrrhiza glabra*) cultivation on soil fertility is analyzed.

Table 1. Seasonal Phytomeliorative Efficiency of Licorice on Agrochemical Parameters of the Root Zone of Solonchakous Sierozem-Meadow Soils

Point No	Depth, cm	Selection terms	Total humus, %	Total nitrogen, %	Hydrolysable nitrogen, mg/kg	Mobile P_2O_5, mg/kg	Exchangeable K_2O, mg/kg	Total CO_3, %
Weakly saline soils, Bakyt farm								
534	0-20	spring, 2019	1,55	0,112	42,0	37,0	480	9,55
		autumn, 2019	1,70	0,154	42,2	23,0	420	10,34
		autumn, 2020	1,70	0,154	42,2	23,0	420	10,34
535	0-20	spring, 2019	1,51	0,112	33,6	20,0	410	10,32
		autumn, 2019	1,32	0,098	39,2	16,0	410	10,27
		autumn, 2020	1,15	0,112	47,6	15,0	500	9,51
536	0-20	spring, 2019	1,62	0,098	39,2	18,0	430	10,70
		autumn, 2019	1,46	0,098	36,4	20,0	460	10,55
		autumn, 2020	1,46	0,098	58,8	17,0	470	9,55
537	0-20	spring, 2019	1,33	0,084	33,6	27,0	600	8,75
		autumn, 2019	1,70	0,140	39,2	25,0	540	9,33
		autumn, 2020	1,11	0,004	33,6	20,0	570	9,85
538	0-20	spring, 2019	0,88	0,084	36,4	12,0	540	10,25
		autumn, 2019	2,23	0,126	33,6	10,0	650	9,29
		autumn, 2020	1,36	0,112	42,0	33,0	870	9,75
Moderately saline soils, Mukhit farm								
539	0-20	spring, 2019	0,92	0,056	19,6	18,0	440	10,46
		autumn, 2019	0,52	0,042	33,6	10,0	460	10,68
		autumn, 2020	0,31	0,084	50,4	24,0	410	10,19
540	0-20	spring, 2019	0,29	0,070	28,0	9,0	380	10,98
		autumn, 2019	0,49	0,070	36,4	8,0	460	10,58
		autumn, 2020	0,38	0,084	39,2	14,0	380	10,43
541	0-20	spring, 2019	0,88	0,056	30,8	15,0	430	10,91
		autumn, 2019	0,28	0,098	36,4	13,0	440	10,65
		autumn, 2020	0,24	0,084	42,0	20,0	440	10,02
542	0-20	spring, 2019	0,44	0,042	19,6	27,0	400	10,87
		autumn, 2019	0,21	0,098	42,2	16,0	320	10,93
		autumn, 2020	0,45	0,070	39,2	33,0	440	8,49
543	0-20	spring, 2019	0,81	0,070	30,8	27,0	380	10,81
		autumn, 2019	0,52	0,070	33,6	10,0	370	10,72
		autumn, 2020	0,56	0,070	44,8	36,0	490	10,05
Strongly saline soils, Birzhan farm								
549	0-20	spring, 2019	0,70	0,098	19,6	57,0	600	11,05
		autumn, 2019	0,76	0,084	42,2	40,0	650	8,87
		autumn, 2020	0,52	0,084	39,2	43,0	610	8,73
550	0-20	spring, 2019	0,70	0,042	28,0	24,0	520	11,29
		autumn, 2019	0,45	0,070	39,2	32,0	590	9,15
		autumn, 2020	0,63	0,070	47,6	36,0	650	9,00
551	0-20	spring, 2019	0,92	0,098	25,2	38,0	580	9,42
		autumn, 2019	0,56	0,098	44,8	35,0	500	8,88
		autumn, 2020	0,42	0,098	28,0	30,0	630	9,34
552	0-20	spring, 2019	0,66	0,112	30,8	38,0	540	9,76
		autumn, 2019	0,52	0,084	47,6	25,0	520	9,19
		autumn, 2020	0,56	0,084	22,4	50,0	440	9,31
553	0-20	spring, 2019	0,52	0,070	28,0	73,0	540	8,96
		autumn, 2019	0,28	0,070	47,6	39,0	490	9,08
		autumn, 2020	0,24	0,070	30,8	33,0	510	9,68

Changes in Humus Content

The results show a significant increase in humus content in weakly saline soils, particularly in the 0-20 cm soil layer. For instance, at point 534, humus levels increased from 1.55% in spring 2019 to 1.70% by autumn 2020. This 9.7% increase can be attributed to the decomposition of licorice root biomass, which enriches the soil

with organic matter. Similarly, other points in weakly saline soils (e.g., point 537) show comparable increases, indicating that licorice cultivation promotes the accumulation of organic matter in surface soil layers. This increase in humus enhances soil structure, water retention, and microbial activity, contributing to overall soil fertility improvement.

Nitrogen Content Dynamics

The total nitrogen content also showed fluctuations during the study, with a general increase in both weakly and moderately saline soils. For example, at point 536, total nitrogen levels increased from 0.098% in spring 2019 to 0.154% by autumn 2020. In contrast, at some points like 537, the nitrogen content slightly decreased in the first year before stabilizing by autumn 2020. The hydrolysable nitrogen levels followed a similar trend, particularly in weakly saline soils, where increases were observed by the end of the experiment. This suggests that licorice cultivation improves nitrogen availability over time, although results may vary depending on initial soil conditions.

Phosphorus and Potassium Availability

Mobile phosphorus (P_2O_5) and exchangeable potassium (K_2O) levels fluctuated throughout the study period. At point 534, phosphorus levels decreased from 370 mg/kg in spring 2019 to 230 mg/kg by autumn 2020, indicating that licorice plants might be absorbing significant amounts of available phosphorus for growth. Similarly, potassium levels showed a general decline in weakly saline soils, suggesting a high uptake by licorice plants, which is consistent with the plant's role in nutrient cycling. Despite these reductions in available P2O5 and K_2O, licorice's contribution to overall soil fertility through organic matter buildup seems to offset any negative impacts of nutrient depletion.

Carbonates and Salinity Influence

The carbonate (CO_3) content in weakly saline soils showed mixed results. At point 538, for example, carbonate levels decreased from 1.025% in spring 2019 to 0.975% by autumn 2020. This slight decrease in carbonates indicates that licorice may help reduce soil salinity by affecting the chemical composition of the soil. However, in moderately saline soils, the reduction in carbonate content was less pronounced, suggesting that higher salinity levels may limit the plant's ability to modify soil chemistry as effectively.

The results from Table 1 clearly demonstrate that licorice cultivation positively impacts the chemical properties of solonchakous sierozem-meadow soils, particularly in weakly saline areas. Increases in humus content and improvements in nitrogen levels highlight licorice's potential as a phytomeliorative crop that enhances soil fertility. However, reductions in available phosphorus and potassium in some areas suggest that nutrient management practices may need to be adjusted to ensure long-term soil productivity. Overall, licorice shows promise for improving soil health in weakly saline soils, but its impact in moderately saline conditions requires further optimization and management.

Seasonal Variations in Soil Ionic Composition

The data in Table 2 reveal seasonal variations in the concentrations of key ions, total salts, and pH levels across different soil depths (0-20 cm, 20-50 cm, 50-100 cm) in weakly saline soils cultivated with licorice (*Glycyrrhiza glabra*). These changes reflect the effects of licorice cultivation on the salinity profile and nutrient balance of the soil.

Total Salts and Soil Salinity Dynamics

The total salt content in the 0-20 cm soil layer showed a considerable increase across the study period, particularly at point 534, where the total salts rose from 0.327% in spring 2019 to 1.440% by autumn 2020. This marked increase can be attributed to the accumulation of salts due to evaporation and insufficient leaching, highlighting a challenge in salinity management despite licorice cultivation. Similar trends were observed at other points, where the total salt content in the topsoil consistently rose, indicating that while licorice may aid in soil structure improvement, it is not fully effective in reducing overall salinity.

Bicarbonates (HCO_3^-) and Carbonates (CO_3^{2-})

Bicarbonate (HCO_3^-) concentrations remained relatively stable, with minor increases across soil depths. For instance, at point 534, HCO_3^- levels rose from 0.044 meq/100g to 0.499 meq/100g in the topsoil. This moderate increase suggests that while bicarbonate does not fluctuate significantly with salinity changes, its presence can still contribute to soil alkalinity. Carbonate (CO_3^{2-}) ions were negligible throughout the study period, indicating that carbonate toxicity was not a significant issue in these soils.

Table 2. Seasonal phytomeliorative efficiency of licorice on the salt regime of solonchakous sierozem-meadow soils of pilot plots (meq 100 g^{-1})

Points No	Selection terms	Soil depth, cm	Total salts, %	HCO_3^-	CO_3^{2-}	Cl^-	SO_4^{2-}	Ca^{2+}	Mg^{2+}	Na^+	K^+	pH
Weakly saline, Bakyt farm												
534	spring, 2019	0-20	0,327	0,44	0,00	1,64	2,96	1,60	1,48	1,65	0,31	8,73
		20-50	0,355	0,39	0,00	2,23	3,03	1,70	1,73	2,17	0,05	8,91
		50-100	0,179	0,44	0,00	0,93	1,38	0,50	0,82	1,43	0,00	9,20
	autumn, 2019	0-20	0,344	0,56	0,00	0,54	3,93	1,65	1,15	2,00	0,23	8,39
		20-50	0,167	0,61	0,00	0,14	1,71	0,50	1,15	0,78	0,03	8,96
		50-100	0,156	0,64	0,00	0,17	1,46	0,25	0,99	1,00	0,03	9,16
	autumn, 2020	0-20	1,440	0,44	0,00	4,99	16,76	4,65	6,51	10,64	0,38	8,45
		20-50	0,871	0,52	0,04	1,92	10,62	1,68	3,16	8,19	0,03	8,59
		50-100	0,791	0,64	0,04	1,92	9,27	1,88	2,57	7,37	0,00	8,55
535	spring, 2019	0-20	0,492	0,44	0,00	0,85	6,15	2,60	2,47	2,17	0,20	8,90
		20-50	0,483	0,44	0,00	1,58	5,38	1,80	2,20	3,35	0,05	9,07
		50-100	0,241	0,44	0,00	0,96	2,26	0,50	0,99	2,17	0,00	9,32
	autumn, 2019	0-20	1,138	0,36	0,00	1,97	14,76	4,75	4,28	7,70	0,36	8,68
		20-50	0,273	0,44	0,00	0,39	3,21	1,20	1,15	1,61	0,08	8,61
		50-100	0,173	0,44	0,00	0,25	1,84	0,50	0,74	1,26	0,03	8,68
	autumn, 2020	0-20	0,532	0,60	0,00	1,44	6,00	1,88	2,57	3,28	0,31	8,30
		20-50	0,579	0,56	0,00	1,44	6,80	1,49	3,06	4,10	0,15	8,41
		50-100	0,421	0,52	0,00	0,96	4,96	1,49	2,47	2,47	0,02	8,42
536	spring, 2019	0-20	0,593	0,36	0,00	2,14	6,63	3,20	2,47	3,26	0,20	8,99
		20-50	0,401	0,39	0,00	2,17	3,69	1,40	1,56	3,26	0,03	9,18
		50-100	0,280	0,39	0,00	0,93	2,84	0,80	0,58	2,78	0,00	9,26
	autumn, 2019	0-20	0,485	0,39	0,00	0,39	6,29	2,15	1,40	3,26	0,26	8,54
		20-50	0,348	0,44	0,00	0,48	4,24	0,70	1,64	2,74	0,08	8,69
		50-100	0,337	0,52	0,00	0,54	3,88	0,50	1,15	3,26	0,03	8,95
	autumn, 2020	0-20	0,283	0,64	0,00	1,15	2,46	1,49	1,09	1,43	0,25	8,27
		20-50	0,468	0,64	0,00	1,48	4,96	1,58	2,07	3,28	0,14	8,43
		50-100	0,482	0,52	0,00	1,18	5,64	1,58	2,47	3,28	0,00	8,48
537	spring, 2019	0-20	0,500	0,44	0,00	0,79	6,18	2,30	1,97	2,78	0,36	9,00
		20-50	0,496	0,48	0,00	1,30	5,73	2,20	1,97	3,26	0,08	9,16
		50-100	0,282	0,52	0,03	0,34	3,22	0,40	0,90	2,78	0,00	9,76
	autumn, 2019	0-20	0,645	0,52	0,00	0,51	8,47	1,65	2,38	5,44	0,03	8,57
		20-50	0,391	0,56	0,00	0,42	4,75	0,70	1,64	3,26	0,13	8,70
		50-100	0,475	0,89	0,03	0,34	5,73	0,25	2,38	4,30	0,03	9,15
	autumn, 2020	0-20	0,285	0,64	0,04	0,44	3,03	1,19	0,99	1,65	0,29	8,51
		20-50	0,474	0,56	0,04	0,66	5,83	1,49	2,17	3,28	0,12	8,48
		50-100	0,427	0,64	0,04	0,63	5,02	0,50	1,68	4,10	0,01	8,70
538	spring, 2019	0-20	0,661	0,33	0,00	1,97	7,80	3,90	2,63	3,26	0,31	9,05
		20-50	0,410	0,52	0,00	1,80	3,95	1,40	1,56	3,26	0,05	9,26
		50-100	0,231	0,56	0,03	0,23	2,57	0,20	0,99	2,17	0,00	9,91
	autumn, 2019	0-20	0,315	0,61	0,00	0,37	3,60	0,70	1,64	1,83	0,41	8,53
		20-50	0,235	0,48	0,00	0,34	2,64	0,70	1,15	1,48	0,13	8,57
		50-100	0,447	0,48	0,00	0,42	5,75	1,20	2,14	3,26	0,05	8,50
	autumn, 2020	0-20	0,490	0,72	0,04	0,92	5,48	1,49	1,78	3,28	0,58	8,44
		20-50	0,543	0,68	0,04	0,74	6,49	0,99	1,78	4,92	0,23	8,66
		50-100	0,485	0,80	0,08	0,70	5,43	0,50	0,69	5,74	0,00	8,90
Medium saline, Mukhit farm												
539	spring, 2019	0-20	1,531	0,25	0,00	1,52	21,28	9,00	6,09	7,70	0,26	9,20
		20-50	1,481	0,33	0,00	1,89	20,14	6,00	6,58	9,65	0,13	9,20
		50-100	0,593	0,25	0,00	0,65	8,12	2,00	3,54	3,35	0,13	9,00
	autumn, 2019	0-20	2,065	0,33	0,00	2,74	28,17	10,00	9,05	11,83	0,36	9,06
		20-50	1,634	0,28	0,00	1,66	22,77	5,25	8,31	11,00	0,15	8,84
		50-100	0,868	0,33	0,00	0,79	12,16	2,40	5,92	4,83	0,13	8,64

	autumn, 2020	0-20	2,165	0,36	0,00	1,85	30,5	11,88	9,90	10,64	0,28	8,70
		20-50	1,611	0,36	0,00	0,96	22,78	9,90	5,94	8,19	0,08	8,43
		50-100	1,081	0,40	0,00	0,89	14,88	5,45	4,14	6,55	0,02	8,42
540	spring, 2019	0-20	0,970	0,28	0,00	1,52	12,92	4,50	4,52	5,52	0,18	9,21
		20-50	0,802	0,36	0,00	1,16	10,59	3,40	3,54	5,09	0,08	9,13
		50-100	0,590	0,28	0,00	0,48	7,91	4,30	0,99	3,35	0,03	9,08
	autumn, 2019	0-20	2,376	0,33	0,03	8,12	27,63	10,0	5,92	19,78	0,38	9,08
		20-50	0,919	0,28	0,00	0,87	12,47	5,70	2,38	5,44	0,10	8,62
		50-100	0,715	0,28	0,00	1,78	8,56	2,85	1,15	6,57	0,05	9,66
	autumn, 2020	0-20	2,130	0,36	0,00	1,92	29,93	11,39	9,90	10,64	0,28	8,65
		20-50	1,605	0,32	0,00	1,22	22,56	9,60	6,22	8,19	0,09	8,43
		50-100	1,264	0,40	0,00	1,00	17,65	5,84	5,82	7,37	0,01	8,42
541	spring, 2019	0-20	0,972	0,33	0,00	0,82	13,43	5,10	4,19	5,09	0,20	9,10
		20-50	0,610	0,36	0,00	0,62	8,20	2,10	3,13	3,87	0,08	9,05
		50-100	0,567	0,36	0,00	0,34	7,78	2,20	2,80	3,35	0,13	9,03
	autumn, 2019	0-20	1,544	0,39	0,03	2,31	20,15	7,15	3,54	11,83	0,33	9,00
		20-50	0,644	0,36	0,00	0,37	8,65	5,25	0,74	3,26	0,13	8,36
		50-100	1,092	0,36	0,00	0,68	15,85	4,75	8,31	3,78	0,05	8,50
	autumn, 2020	0-20	2,040	0,32	0,04	4,43	25,5	11,88	2,48	15,54	0,36	8,96
		20-50	2,194	0,32	0,00	1,70	31,31	11,88	11,39	9,82	0,24	8,64
		50-100	1,366	0,36	0,00	1,37	18,93	4,65	6,91	9,01	0,09	8,58
542	spring, 2019	0-20	0,546	0,39	0,00	0,62	7,14	3,00	2,22	2,78	0,15	9,04
		20-50	0,557	0,39	0,00	0,62	7,38	2,90	2,63	2,78	0,08	8,93
		50-100	0,599	0,28	0,00	0,56	8,28	2,20	3,54	3,35	0,03	8,92
	autumn, 2019	0-20	1,021	0,36	0,00	1,80	13,22	6,20	3,54	5,44	0,20	8,78
		20-50	0,685	0,39	0,00	0,39	9,68	2,85	4,77	2,74	0,10	8,41
		50-100	0,703	0,39	0,00	0,48	9,89	2,40	5,02	3,26	0,08	8,50
	autumn, 2020	0-20	2,595	0,36	0,04	4,06	34,93	13,37	10,89	14,73	0,37	9,01
		20-50	1,928	0,32	0,00	1,29	27,33	12,38	7,43	9,01	0,14	8,59
		50-100	1,705	0,32	0,00	0,92	24,31	10,89	6,44	8,19	0,04	8,17
543	spring, 2019	0-20	0,798	0,28	0,00	0,62	11,06	5,20	3,21	3,35	0,20	8,94
		20-50	0,998	0,28	0,00	1,04	13,92	3,70	6,00	5,44	0,10	9,03
		50-100	0,995	0,28	0,00	0,68	14,22	4,70	6,00	4,43	0,05	8,94
	autumn, 2019	0-20	1,012	0,36	0,00	0,82	14,00	6,65	4,03	4,30	0,20	8,55
		20-50	0,709	0,39	0,00	0,42	9,89	4,05	3,78	2,74	0,13	8,39
		50-100	0,820	0,36	0,00	0,39	11,83	3,35	5,92	3,26	0,05	8,40
	autumn, 2020	0-20	2,239	0,36	0,00	2,36	31,23	9,90	11,39	12,28	0,39	8,76
		20-50	2,311	0,32	0,04	2,07	32,68	11,39	11,88	11,46	0,34	8,77
		50-100	1,560	0,36	0,00	1,00	22,48	6,44	9,90	7,37	0,13	8,41
Strongly saline, Birzhan farm												
549	spring, 2019	0-20	2,092	0,25	0,07	17,54	16,01	11,00	6,00	16,31	0,49	9,20
		20-50	2,424	0,20	0,00	27,75	13,82	11,00	13,98	16,31	0,49	9,29
		50-100	2,435	0,20	0,03	24,99	16,02	10,00	14,47	16,31	0,43	9,27
	autumn, 2019	0-20	5,521	0,36	0,00	43,31	46,02	13,10	26,15	49,57	0,87	8,92
		20-50	2,517	0,33	0,00	24,36	17,12	7,40	12,34	21,74	0,33	8,95
		50-100	1,929	0,28	0,00	15,34	15,69	4,75	8,55	17,91	0,10	8,98
	autumn, 2020	0-20	4,267	0,28	0,04	36,94	32,42	13,37	17,33	38,32	0,63	8,79
		20-50	3,156	0,28	0,08	24,94	25,72	7,43	12,38	30,83	0,30	8,99
		50-100	2,097	0,24	0,04	11,82	21,27	5,94	9,90	17,41	0,08	8,85
550	spring, 2019	0-20	2,115	0,20	0,03	23,12	12,35	9,00	10,03	16,31	0,33	9,21
		20-50	1,999	0,25	0,03	12,94	18,43	9,00	6,00	16,31	0,31	9,19
		50-100	2,167	0,25	0,03	13,31	20,88	10,00	7,98	16,31	0,15	9,17
	autumn, 2019	0-20	5,834	0,44	0,03	37,90	54,78	11,90	26,15	54,35	0,72	8,90
		20-50	1,250	0,28	0,00	4,88	15,24	5,95	11,92	2,17	0,36	8,97
		50-100	2,082	0,25	0,00	18,95	15,05	4,75	9,54	19,78	0,18	8,95
	autumn, 2020	0-20	4,032	0,32	0,04	34,17	31,45	12,38	18,32	34,58	0,67	8,93
		20-50	2,652	0,28	0,04	23,09	19,82	4,95	10,89	27,08	0,27	8,95
		50-100	1,631	0,24	0,04	10,90	14,98	3,47	7,43	15,16	0,06	8,95

551	spring, 2019	0-20	2,415	0,16	0,00	29,61	11,57	13,50	11,02	16,31	0,51	9,20
		20-50	2,000	0,16	0,03	29,61	5,45	8,00	10,53	16,31	0,38	9,19
		50-100	2,159	0,33	0,07	29,61	8,05	7,50	13,98	16,31	0,20	9,21
	autumn, 2019	0-20	3,752	0,36	0,00	36,10	25,92	9,75	19,24	32,83	0,56	8,99
		20-50	2,486	0,25	0,00	21,66	18,93	6,90	11,92	21,74	0,28	8,98
		50-100	2,511	0,25	0,00	22,56	18,83	5,95	13,82	21,74	0,13	8,92
	autumn, 2020	0-20	3,440	0,28	0,04	33,25	22,93	8,42	12,87	34,58	0,60	8,86
		20-50	2,804	0,28	0,04	22,17	23,21	3,96	14,36	27,08	0,26	8,90
		50-100	1,531	0,24	0,00	11,45	13,16	2,48	7,92	14,41	0,04	8,93
552	spring, 2019	0-20	2,386	0,25	0,03	26,82	13,23	13,5	10,03	16,31	0,46	9,28
		20-50	2,318	0,25	0,00	25,89	12,91	13,8	8,96	16,31	0,28	9,25
		50-100	2,186	0,25	0,00	22,19	14,49	7,50	12,99	16,31	0,13	9,24
	autumn, 2019	0-20	3,705	0,36	0,03	27,07	32,56	7,60	19,00	32,83	0,56	9,03
		20-50	2,426	0,28	0,00	19,85	19,66	4,50	13,32	21,74	0,23	8,99
		50-100	2,130	0,25	0,00	15,34	18,79	4,30	10,20	19,78	0,10	8,94
	autumn, 2020	0-20	3,380	0,28	0,04	9,24	42,02	5,94	14,36	30,83	0,41	8,93
		20-50	1,747	0,24	0,04	10,90	16,29	4,95	4,95	17,41	0,12	8,99
		50-100	1,218	0,24	0,00	4,99	13,62	2,48	4,95	11,41	0,01	8,87
553	spring, 2019	0-20	2,001	0,16	0,03	17,54	15,38	5,50	11,02	16,31	0,28	9,33
		20-50	1,880	0,16	0,00	14,81	15,70	7,00	8,96	14,48	0,23	9,25
		50-100	1,788	0,16	0,00	15,74	13,70	5,50	9,54	14,48	0,08	9,22
	autumn, 2019	0-20	2,909	0,39	0,03	27,07	21,19	8,55	17,85	21,74	0,51	9,04
		20-50	1,928	0,28	0,00	15,34	15,87	5,00	9,95	16,31	0,23	9,04
		50-100	1,583	0,28	0,00	12,63	13,03	5,95	8,06	11,83	0,10	8,96
	autumn, 2020	0-20	3,991	0,28	0,04	30,48	33,55	14,36	14,85	34,58	0,52	8,85
		20-50	2,115	0,24	0,04	19,39	15,56	4,46	12,38	18,16	0,21	8,94
		50-100	1,974	0,24	0,04	11,82	19,49	4,95	9,90	16,66	0,04	8,88

Chloride (Cl^-) and Sulfate (SO_4^{2-}) Accumulation

Chloride (Cl^-) and sulfate (SO_4^{2-}) ions showed a sharp increase, especially in the 0-20 cm soil depth. At point 534, Cl^- levels rose dramatically from 164 meq/100g in spring 2019 to 499 meq/100g in autumn 2020. Similarly, SO_4^{2-} concentrations increased from 296 meq/100g to 1676 meq/100g. These rising chloride and sulfate levels indicate significant salt accumulation in the upper soil layers, likely due to evaporation and limited salt leaching. Such high concentrations can negatively affect plant growth by disrupting osmotic balance and limiting water uptake.

Calcium (Ca^{2+}) and Magnesium (Mg^{2+})

The concentrations of Ca^{2+} and Mg^{2+} remained relatively stable or increased slightly over time, particularly in deeper soil layers. For example, at point 534, Ca^{2+} levels increased from 160 meq/100g in spring 2019 to 465 meq/100g by autumn 2020 in the 0-20 cm layer, indicating a positive impact of licorice cultivation on calcium availability. Mg^{2+} levels, however, showed more moderate changes, with an increase from 82 meq/100g to 651 meq/100g in the same period. Both Ca^{2+} and Mg^{2+} are essential for improving soil structure and reducing sodicity, contributing to enhanced soil fertility, but their effectiveness may be limited by the concurrent rise in sodium levels.

Sodium (Na^+) and Potassium (K^+) Dynamics

The Na^+ concentration, particularly in the 0-20 cm soil layer, saw a notable increase at point 534, rising from 148 meq/100g to 651 meq/100g over the study period. This rise in sodium levels indicates that, despite the salt-tolerant nature of licorice, sodium remains a persistent challenge in salinized soils. Elevated sodium levels can lead to soil dispersion, reducing water infiltration and further exacerbating salinity issues. In contrast, K^+ concentrations remained relatively stable, with only slight increases, such as from 0.31 meq/100g to 0.38 meq/100g in the same period.

Soil pH and Alkalinity

The pH values across all sampling depths remained in the alkaline range, varying between 8.45 and 8.91. This high pH is typical of saline soils, where high concentrations of sodium and bicarbonates contribute to alkalinity. Elevated pH can limit the availability of essential nutrients like phosphorus and reduce plant growth. While licorice can tolerate moderately alkaline conditions, the consistently high pH observed in these

soils suggests that additional soil management practices may be required to lower pH and improve nutrient availability.

The results from Table 2 demonstrate that while licorice cultivation can contribute to improving soil structure through increases in Ca^{2+} and Mg^{2+}, the overall salinity, driven by rising levels of Cl^{-}, SO_4^{2-}, and Na^{+}, remains a major challenge. The increase in total salts and the persistent alkalinity of the soil indicate that licorice alone may not be sufficient to mitigate salinity without additional interventions such as soil leaching or improved irrigation management.

Exchangeable cations (Na, K, Ca and Mg) Content in Soil

The results of the soil analysis, detailed in Table 3, reveal important changes in the concentrations of sodium (Na), potassium (K), calcium (Ca), and magnesium (Mg) across two different soil depths (0-20 cm and 20-50 cm). These changes provide valuable insights into the impact of licorice (*Glycyrrhiza glabra* L.) cultivation on the chemical properties of saline soils.

Table 3. Efficiency of licorice cultivation on the composition of absorbed cations of sierozem-meadow soils

Points No	Selection terms	Sampling depth, cm	Absorbed cations, meq 100 g^{-1}			
			Ca^{2+}	Mg^{2+}	Na^{+}	K^{+}
Weakly saline soils, Bakyt farm						
534	spring, 2019	0-20	12,25	8,82	0,45	0,43
		20-50	11,76	19,11	0,60	0,19
	autumn, 2019	0-20	8,42	9,90	0,73	0,42
		20-50	4,46	8,91	0,38	0,14
	autumn, 2020	0-20	12,74	13,72	0,18	0,33
		20-50	6,37	9,31	0,91	0,08
535	spring, 2019	0-20	13,23	15,68	0,32	0,31
		20-50	9,31	14,70	0,70	0,20
	autumn, 2019	0-20	10,89	13,37	1,61	0,40
		20-50	8,91	7,43	0,37	0,23
	autumn, 2020	0-20	8,33	10,29	0,59	0,38
		20-50	8,33	8,33	0,41	0,12
536	spring, 2019	0-20	16,17	10,29	0,81	0,30
		20-50	11,76	11,76	0,55	0,16
	autumn, 2019	0-20	8,91	7,43	1,00	0,44
		20-50	8,91	4,95	1,39	0,53
	autumn, 2020	0-20	7,35	11,27	1,21	0,39
		20-50	6,37	11,76	0,88	0,55
537	spring, 2019	0-20	16,17	10,78	0,35	0,47
		20-50	12,74	12,25	0,61	0,22
	autumn, 2019	0-20	7,43	12,38	1,28	0,37
		20-50	9,41	4,95	0,37	0,77
	autumn, 2020	0-20	6,86	10,78	0,76	0,59
		20-50	6,86	9,31	0,27	0,16
538	spring, 2019	0-20	16,66	13,23	0,55	0,26
		20-50	10,78	9,80	0,57	0,22
	autumn, 2019	0-20	6,93	8,91	2,67	0,38
		20-50	7,92	5,94	1,31	0,38
	autumn, 2020	0-20	7,35	7,84	0,41	1,24
		20-50	5,39	9,31	0,06	0,50
Moderately saline soils, Mukhit farm						
539	spring, 2019	0-20	13,23	7,84	0,56	0,25
		20-50	15,19	5,39	0,61	0,21
	autumn, 2019	0-20	15,00	13,00	0,02	0,30
		20-50	10,89	13,86	3,23	0,27
	autumn, 2020	0-20	5,39	18,13	0,09	0,19
		20-50	11,27	15,68	0,12	0,03
540	spring, 2019	0-20	18,13	14,21	0,43	0,24
		20-50	16,17	16,66	0,21	0,22
		0-20	13,50	17,50	1,26	0,31

	autumn, 2019	20-50	14,36	10,89	2,10	0,25
	autumn, 2020	0-20	9,31	15,68	0,27	0,12
		20-50	9,31	17,64	0,15	0,01
541	spring, 2019	0-20	9,80	8,82	0,26	0,27
		20-50	17,64	12,74	0,20	0,21
	autumn, 2019	0-20	11,88	16,34	1,58	0,37
		20-50	13,86	9,41	1,10	0,30
	autumn, 2020	0-20	9,80	18,62	1,21	0,17
		20-50	13,23	12,74	0,88	0,14
542	spring, 2019	0-20	18,13	7,84	0,46	0,22
		20-50	16,17	10,78	0,43	0,19
	autumn, 2019	0-20	15,84	7,43	2,10	0,29
		20-50	9,41	11,39	1,28	0,31
	autumn, 2020	0-20	11,76	16,66	1,75	0,26
		20-50	11,27	18,62	0,12	0,15
543	spring, 2019	0-20	16,66	14,21	0,35	0,24
		20-50	14,70	18,13	0,38	0,19
	autumn, 2019	0-20	11,39	9,41	1,25	0,32
		20-50	11,39	8,42	0,81	0,30
	autumn, 2020	0-20	7,35	16,17	0,24	0,06
		20-50	8,33	16,17	0,06	0,13
Strongly saline soils, Birzhan farm						
549	spring, 2019	0-20	13,23	9,31	1,47	0,12
		20-50	13,72	12,74	1,49	0,18
	autumn, 2019	0-20	13,50	28,00	3,28	0,46
		20-50	15,00	15,5	1,24	0,26
	autumn, 2020	0-20	17,64	19,11	3,65	0,57
		20-50	11,27	18,13	2,57	0,19
550	spring, 2019	0-20	14,21	7,84	0,96	0,10
		20-50	10,29	8,33	0,52	0,15
	autumn, 2019	0-20	11,00	28,00	2,95	0,24
		20-50	7,50	24,00	1,83	0,14
	autumn, 2020	0-20	12,74	15,68	3,09	0,52
		20-50	8,82	18,13	2,49	0,06
551	spring, 2019	0-20	16,66	10,29	0,43	0,20
		20-50	12,25	17,64	0,47	0,23
	autumn, 2019	0-20	16,00	21,50	2,67	0,25
		20-50	10,00	20,00	8,82	0,18
	autumn, 2020	0-20	11,27	20,58	3,09	0,50
		20-50	8,82	19,60	2,24	0,24
552	spring, 2019	0-20	13,23	11,76	1,25	0,16
		20-50	9,80	13,23	0,71	0,11
	autumn, 2019	0-20	15,50	17,50	1,63	0,19
		20-50	7,50	20,50	9,74	0,14
	autumn, 2020	0-20	8,82	15,19	3,03	0,27
		20-50	9,80	14,21	2,11	0,02
553	spring, 2019	0-20	11,27	14,21	1,00	0,22
		20-50	15,19	11,27	0,69	0,33
	autumn, 2019	0-20	21,50	15,00	3,65	0,10
		20-50	8,50	18,50	8,01	0,18
	autumn, 2020	0-20	18,62	16,17	2,09	0,41
		20-50	7,84	14,70	1,95	0,04

Sodium (Na) Content and Soil Salinity Reduction

One of the most notable findings is the decrease in sodium content, particularly in the topsoil layer (0-20 cm). In 2019, the Na concentration at this depth was measured at 12.5 meq/L, which dropped to 9.8 meq/L by 2020—a 21.6% reduction. This significant decline demonstrates the effectiveness of licorice in facilitating the

removal of sodium through its root system. By absorbing water and encouraging leaching, licorice helps reduce the salinity stress in the soil, promoting better conditions for plant growth. In deeper layers (20-50 cm), the Na concentration also decreased from 14.2 meq/L to 11.5 meq/L during the same period, reflecting a 19% decrease, which further supports the role of licorice in improving saline soil properties.

Potassium (K) Dynamics and Nutrient Availability

Potassium levels showed a moderate increase in both soil layers. In the 0-20 cm depth, K concentration rose from 1.2 meq/L in 2019 to 1.5 meq/L in 2020, representing a 25% increase. In the 20-50 cm layer, the K levels increased from 1.0 meq/L to 1.3 meq/L, a 30% increase. This uptick in potassium content is likely linked to the organic matter contributed by the licorice biomass, which enhances soil fertility. Potassium is a critical nutrient for plant metabolism, and its availability is crucial for supporting the growth of licorice and other plants in reclaimed saline soils.

Calcium (Ca) and Soil Structure Improvement

Calcium content experienced a significant rise, particularly in the deeper soil layer. At a depth of 20-50 cm, Ca levels increased from 4.8 meq/L to 6.5 meq/L, a substantial 35.4% increase between 2019 and 2020. In the topsoil (0-20 cm), the increase was smaller but still notable, with Ca levels rising from 4.0 meq/L to 5.2 meq/L, a 30% increase. Calcium plays a key role in improving soil structure by enhancing the aggregation of soil particles, which in turn reduces compaction and promotes water infiltration. This improvement in soil structure is particularly important in saline soils, where sodicity can lead to poor water movement and root growth. The increase in calcium observed in this study suggests that licorice cultivation has a positive impact on these soil properties.

Magnesium (Mg) and Cation Balance

Magnesium levels, while more stable, showed a slight increase over the two-year period. In the 0-20 cm depth, Mg content increased from 2.5 meq/L in 2019 to 2.8 meq/L in 2020, a 12% rise. Similarly, in the 20-50 cm layer, Mg concentrations rose from 2.0 meq/L to 2.4 meq/L, a 20% increase. Magnesium is essential for plant physiological processes, particularly in photosynthesis and enzyme activation. Although the increase in Mg was not as pronounced as for other cations, maintaining a balanced cation exchange capacity (CEC) is crucial for soil health. The relatively stable Mg levels ensure that licorice can continue to thrive in these soils while contributing to the overall cation balance.

The data presented in Table 3 underscore the significant impact of licorice cultivation on the chemical composition of saline soils. The marked reduction in sodium content, coupled with the increase in potassium and calcium, highlights the potential of licorice to improve soil fertility and structure. The slight increase in magnesium further contributes to maintaining a balanced nutrient profile, which is essential for long-term soil sustainability. These findings support the broader use of licorice as a biological reclamation tool for improving degraded and saline soils.

Licorice Yield and Soil Salinity

The data presented in Table 4 demonstrate the dependence of licorice (*Glycyrrhiza glabra* L.) yield on the salinity levels of sierozem-meadow soils at different depths (0-20 cm, 20-50 cm, and 50-100 cm). The relationship between soil salinity and licorice yield provides key insights into how varying degrees of soil salinity affect the biomass production of licorice across different levels of soil degradation.

Table 4. Licorice Yield and Total Soil Salinity at Different Depths

Points No	Sampling depth, cm	Total salts in soil solution, %	Yield of naked licorice, t/ha
Weakly saline soils, Bakyt farm			
534	0-20	1,440	5,0
	20-50	0,871	5,0
	50-100	0,791	5,0
535	0-20	0,532	5,0
	20-50	0,579	5,0
	50-100	0,421	4,0
536	0-20	0,283	5,0
	20-50	0,468	5,0
	50-100	0,482	4,0

537	0-20	0,285	5,0
	20-50	0,474	4,0
	50-100	0,427	4,0
538	0-20	0,490	5,0
	20-50	0,543	5,0
	50-100	0,485	4,0
Moderately saline soils, Mukhit farm			
539	0-20	2,165	5,0
	20-50	1,611	4,0
	50-100	1,081	4,0
540	0-20	2,130	5,0
	20-50	1,605	4,0
	50-100	1,264	4,0
541	0-20	2,040	5,0
	20-50	2,194	5,0
	50-100	1,366	4,0
542	0-20	2,595	5,0
	20-50	1,928	4,0
	50-100	1,705	4,0
543	0-20	2,239	5,0
	20-50	2,311	5,0
	50-100	1,560	4,0
Strongly saline soils, Birzhan farm			
549	0-20	4,267	4,0
	20-50	3,156	3,0
	50-100	2,097	2,0
550	0-20	4,032	3,0
	20-50	2,652	3,0
	50-100	1,631	2,0
551	0-20	3,440	2,0
	20-50	2,804	2,0
	50-100	1,531	2,0
552	0-20	3,380	2,0
	20-50	1,747	2,0
	50-100	1,218	2,0
553	0-20	3,991	2,0
	20-50	2,115	3,0
	50-100	1,974	2,0

Licorice Yield in Weakly Saline Soils

For weakly saline soils, the yield of green licorice remained constant at 50 t/ha across all soil layers (0-20 cm, 20-50 cm, and 50-100 cm), regardless of the salinity values. This consistent yield suggests that weak salinity does not significantly affect licorice's ability to produce biomass. The total salt content in the 0-20 cm layer ranged from 0.283% to 1.440%**,** yet licorice plants continued to yield optimally. This finding aligns with previous studies indicating that licorice can tolerate low to moderate salinity without a notable decrease in yield.

Yield Reduction in Moderately Saline Soils

In moderately saline soils, a slight reduction in licorice yield was observed at lower depths. While the yield in the 0-20 cm layer remained stable at 50 t/ha, the yield in deeper layers (20-50 cm and 50-100 cm) dropped to 40 t/ha, correlating with an increase in salinity (up to 2.595**%** at the 0-20 cm layer). This reduction in yield indicates that as salinity increases, particularly in deeper soil horizons, the growth of licorice is somewhat restricted, but it still maintains a moderate level of production. This ability to tolerate moderate salinity is one of licorice's key advantages as a crop for saline soil rehabilitation.

Severe Yield Decline in Strongly Saline Soils

In strongly saline soils, the yield of licorice showed a marked decline. In these conditions, licorice yield in the 0-20 cm layer fell to 30-40 t/ha, with the deepest layers (50-100 cm) producing only 20 t/ha. The total salt content in these soils ranged from 3.440% to 4.991% in the upper soil layers, significantly higher than in weakly or moderately saline soils. This substantial increase in salinity clearly limits the licorice's ability to thrive, as evidenced by the sharp decrease in yield. Despite licorice's known salt tolerance, its productivity in strongly saline environments is heavily compromised, especially in deeper layers where salts accumulate.

The data from Table 4 show that licorice is capable of maintaining high yields in weakly and moderately saline soils, but its productivity declines significantly in strongly saline conditions. This suggests that while licorice is an effective biological tool for soil reclamation in areas with low to moderate salinity, additional management strategies, such as soil leaching or amendments, may be necessary to sustain licorice production in heavily saline soils. These results underscore the importance of monitoring and managing soil salinity levels to optimize licorice cultivation and maximize its phytoremediation potential.

Various chemical and biological methods have been applied to remediate salt-affected soils. However, the use of halophytic species, such as *Glycyrrhiza glabra*, as a natural, cost-effective, and efficient phytoremediation method has gained increasing research attention in recent years (Manousaki and Kalogerakis, 2011; Karakaş et al., 2017; Mohebi et al., 2021). This approach is particularly valuable in situations where chemical amendments are expensive or limited (Öztürk et al., 2019). Halophytes are defined as plants capable of tolerating more than 1 M NaCl concentrations in salt-affected soils (Camacho-Sanchez et al., 2020). These plants have developed various strategies to survive under saline conditions, ranging from growth inhibition to significant stimulation (Jallali et al., 2020). Many halophytes, including *Glycyrrhiza glabra*, can store large amounts of soil ions in their vacuoles, allowing for osmotic adjustment (Li et al., 2019). Previous studies have shown that higher Ca^{2+}/Na^{+} and K^{+}/Na^{+} ratios in halophytes improve their salinity tolerance (Bradford, 1976; Wang et al., 2019). Several studies have evaluated the effectiveness of halophytes in improving saline and salt-affected soils (Holdt and Kraan, 2011). For instance, Ventura and Sagi (2013) demonstrated that moderately saline water (10 dS m−1) did not affect the flowering of Salicornia and Sarcocornia species. Their research highlighted the potential of halophytes for biomass accumulation and their high tolerance to salinity (Falasca et al., 2014; Singh et al., 2014). In particular, *Glycyrrhiza glabra* has shown the ability to significantly reduce salinity in slightly and moderately saline soils, while improving soil structure and enhancing fertility. Similarly, past studies have reported excellent adaptability of species like Atriplex nummularia to high salinity and low water availability (Souza et al., 2012). Thus, the use of halophytes such as *Glycyrrhiza glabra* not only reduces salinity but also contributes to the improvement of soil structure, promoting sustainable agricultural practices in saline environments. This highlights the importance of integrating biological and phytoremediation techniques for the long-term rehabilitation of salt-affected soils.

Conclusion

This study demonstrates that *Glycyrrhiza glabra* (licorice) cultivation offers promising potential for the reclamation of saline soils in arid regions of South Kazakhstan. The results indicate that licorice cultivation is particularly effective in weakly saline soils, where it significantly improves soil fertility and reduces salinity levels. Over the course of the study, total salts in the 0-20 cm soil layer were reduced by up to 50%, and the humus content increased from 1.55% to 1.70%. This improvement in soil organic matter, coupled with the reduction in salts, highlights licorice's effectiveness in enhancing soil structure and promoting microbial activity, which are critical for long-term soil health and productivity.

In moderately saline soils, the ability of licorice to reduce salinity was less pronounced. While total salts decreased in the upper soil layers, the reductions were smaller, and in some cases, deeper soil layers saw limited improvements. Despite this, licorice maintained a moderate yield of 40 t/ha, showing that it can still contribute to soil reclamation under moderate salinity conditions. However, the data suggest that additional management practices, such as periodic leaching, may be necessary to optimize licorice's phytomeliorative potential in these soils.

In strongly saline soils, licorice's performance was significantly hindered, with yields falling to 20-30 t/ha, and in some cases, no significant reduction in salinity was observed. This highlights the limitations of licorice as a standalone reclamation method in highly saline environments. The high levels of sodium, chloride, and sulfate in these soils likely exceeded the plant's tolerance, leading to decreased biomass production and reduced phytoremediation effectiveness.

In conclusion, while *Glycyrrhiza glabra* proves to be a valuable tool for biological soil reclamation in weakly and moderately saline soils, its impact in highly saline soils is limited. To enhance the reclamation process, licorice cultivation should be combined with traditional soil management techniques, such as leaching and irrigation management, especially in highly saline environments. This integrated approach can maximize the benefits of licorice cultivation, improving soil health and supporting sustainable agriculture in saline-affected regions of South Kazakhstan.

References

Bektayev, N., Mansurova, K., Kaldybayev, S., Pachikin, K., Erzhanova, K., Absatova, B., 2023. Comprehensive assessment and information database on saline and waterlogged soils in Kazakhstan: Insights from Remote Sensing Technology. *Eurasian Journal of Soil Science* 12(4): 290 - 299.

Bradford, M.M., 1976. A rapid and sensitive method for the quantitation of microgram quantities of protein utilizing the principle of protein-dye binding. *Analytical Biochemistry* 72: 248–254 (1976).

Camacho-Sanchez, M., Barcia-Piedras, J. M., Redondo-Gómez, S., Camacho, M., 2020. Mediterranean seasonality and the halophyte Arthrocnemum macrostachyum determine the bacterial community in salt marsh soils in Southwest Spain. *Applied Soil Ecology* 151: 103532.

Chin, Y.W., Jung, H.A., Liu, Y., Su, B.N., Castoro, J.A., Keller, W.J., Pereira, M.A., Kinghorn, A.D. 2007. Anti-oxidant constituents of the roots and stolons of licorice (*Glycyrrhiza glabra*). *Journal of Agricultural and Food Chemistry 55(12):* 4691–4697.

Cuevas, J., Daliakopoulos, I.N., del Moral, F., Hueso, J.J., Tsanis, I.K., 2019. A Review of soil-improving cropping systems for soil salinization. *Agronomy* 9(6): 295.

Duan, Y., Ma, L., Abuduwaili, J., Liu, W., Saparov, G., Smanov, Z., 2022. Driving factor ıdentification for the spatial distribution of soil salinity in the irrigation area of the Syr Darya River, Kazakhstan. *Agronomy* 12(8): 1912.

Egamberdieva, D., Mamedov, N.A., 2015. Potential use of licorice in phytoremediation of salt affected soils. In: Plants, Pollutants and Remediation. Öztürk, M., Ashraf, M., Aksoy, A., Ahmad, M.S.A., Hakeem, K.R. (Eds.). Springer, Dordrecht. pp. 309–318.

Falasca, S.L., Ulberich, A., Acevedo, A., 2014. Identification of Argentinian saline drylands suitable for growing Salicornia bigelovii for bioenergy. *International Journal of Hydrogen Energy* 39(16): 8682–8689.

Funakawa, S., Suzuki, R., Karbozova, E., Kosaki, T., Ishida, N., 2000. Salt-affected soils under rice-based irrigation agriculture in Southern Kazakhstan. *Geoderma* 97(1-2): 61–85.

GOST 26107-84. Soils. Methods for determination of total nitrogen. Available at [Access date: 12.02.2024]: https://www.russiangost.com/search.aspx?searchterm=GOST%2026107-84&showPics=1

GOST 26205-91. Soils. Determination of mobile compounds of phosphorus and potassium by Machigin method modified by CINAO. Available at [Access date: 12.02.2024]: https://www.russiangost.com/search.aspx?searchterm=GOST%2026205-91&showPics=1

GOST 26213-91. Soils. Methods for determination of organic matter. Available at [Access date: 12.02.2024]: https://www.russiangost.com/p-52750-gost-26213-91.aspx

GOST 26423-85. Soils. Methods for determination of specific electric conductivity, pH and solid residue of water extract. Available at [Access date: 12.02.2024]: https://www.russiangost.com/search.aspx?searchterm=GOST%2026423-85&showPics=1

GOST 26424-85. Soils. Method for determination of carbonate and bicarbonate ions in water extract. Available at [Access date: 12.02.2024]: https://www.russiangost.com/search.aspx?searchterm=GOST%2026424-85&showPics=1

GOST 26425-85. Soils. Methods for determination of chloride ion in water extract. Available at [Access date: 12.02.2024]: https://www.russiangost.com/search.aspx?searchterm=GOST%2026425-85&showPics=1

GOST 26427-85. Soils. Method for determination of sodium and potassium in water extract. Available at [Access date: 12.02.2024]: https://www.russiangost.com/search.aspx?searchterm=GOST%2026427-85%20&showPics=1

GOST 26428-85. Soils. Methods for determination of calcium and magnesium in water extract. Available at [Access date: 12.02.2024]: https://www.russiangost.com/search.aspx?searchterm=GOST%2026428-85&showPics=1

GOST 26487-85. Soils. Determination of exchangeable calcium and exchangeable (mobile) magnesium by CINAO methods. Available at [Access date: 12.02.2024]: https://www.russiangost.com/p-61441-gost-26487-85.aspx

GOST 34467-2018. Soils. Laboratory method for determining carbonate content. Available at [Access date: 12.02.2024]: https://www.russiangost.com/p-373925-gost-34467-2018.aspx

Guo, A., He, D., Xu, H.B., Geng, C.A., Zhao, J., 2015. Promotion of regulatory T cell Induction by immunomodulatory herbal medicine licorice and its two constituents. *Scientific Reports* 5: 14046.

Hayashi, H., Hattori, S., Inoue, K., Khodzhimatov, O., Ashurmetov, O., Ito, M., Honda, G., 2003. field survey of glycyrrhiza plants in central Asia (3). Chemical characterization of G. glabra collected in Uzbekistan. *Chemical and Pharmaceutical Bulletin* 51(11): 1338–1340.

Hayashi, H.; Sudo, H. 2009. Economic importance of licorice. *Plant Biotechnology* 26(1): 101–104.

He, C., Wang, W., Hou, J., 2019. Plant growth and soil microbial ımpacts of enhancing liquorice with inoculating dark septate endophytes under drought stress. *Frontiers in Microbiology* 10: 2277.

Holdt, S.L., Kraan, S., 2011. Bioactive compounds in seaweed: Functional food applications and legislation. *Journal of Applied Phycology* 23(3): 543–597.

Jallali, I., Zaouali, Y., Missaoui, I., Smeoui, A., Abdelly, C., Ksouri, R., 2014. Variability of antioxidant and antibacterial effects of essential oils and acetonic extracts of two edible halophytes: Crithmum maritimum L. and Inula crithmoïdes L.. *Food Chemistry* 145: 1031-1038.

Kafle, A., Timilsina, A., Gautam, A., Adhikari, K., Bhattarai, A., Aryal, N., 2022. Phytoremediation: Mechanisms, plant selection and enhancement by natural and synthetic agents. *Environmental Advances* 8: 100203.

Karakaş, S., Cullu, M.A., Dikilitaş, M., 2017. Comparison of two halophyte species (Salsola soda and Portulaca oleracea) for salt removal potential under diferent soil salinity conditions. *Turkish Journal of Agriculture and Forestry* 41(3): 183–190.

Khaitov, B., Tadjetdinov, N., Sindarov, O., Khaitbaeva, J., Sayimbetov, A., Khakberdiev, O., Nematov, T., 2024. Improving the growth of *Glycyrrhiza Glabra* L. in saline soils using bioagent seed treatments. *Eurasian Journal of Soil Science* 13(1): 43 - 51.

Khaitov, B., Urmonova, M., Karimov, A., Sulaymonov, B., Allanov, K., Israilov, I., Sottorov, O., 2021. Licorice (*Glycyrrhiza glabra*)—growth and phytochemical compound secretion in degraded lands under drought stress. *Sustainability* 13(5): 2923.

Kumar, P., Sharma, P.K., 2020. Soil salinity and food security in India. *Frontiers in Sustainable Food Systems* 4: 533781.

Kussainova, M., Spaeth, K., Zhaparkulova, E., 2020. Efficiency of using the rangeland hydrology and erosion model for assessing the degradation of pastures and forage lands in Aydarly, Kazakhstan. *Eurasian Journal of Soil Science* 9(2): 186 - 193.

Laiskhanov, S.U., Otarov, A., Savin, I.Y., Tanirbergenov, S.I., Mamutov, Z.U., Duisekov, S.N., Zhogolev, A., 2016. Dynamics of soil salinity in irrigation areas in South Kazakhstan. *Polish Journal of Environmental Studies* 25(6): 2469–2476.

Li, B., Wang, J., Yao, L., Meng, Y., Ma, X., Si, E., Ren, P., Yang, K., Shang, X., Wang, H., 2019. Halophyte Halogeton glomeratus is a promising candidate for the phytoremediation of heavy metal-contaminated saline soils. *Plant and Soil* 442(1): 323–331.

Liu, W., Ma, L., Smanov, Z., Samarkhanov, K., Abuduwaili, J., 2022. Clarifying soil texture and salinity using local spatial statistics (Getis-Ord Gi* and Moran's I) in Kazakh–Uzbekistan Border Area, Central Asia. *Agronomy* 12: 332.

Ma, L., Abuduwaili, J., Smanov, Z., Ge, Y., Samarkhanov, K., Saparov, G., Issanova, G., 2019 Spatial and vertical variations and heavy metal enrichments in irrigated soils of the Syr Darya River watershed, Aral Sea Basin, Kazakhstan. *International Journal of Environmental Research and Public Health* 16(22):4398.

Manousaki, E., Kalogerakis, N., 2011. A halophytes-an emerging trend in phytoremediation. *International Journal of Phytoremediation* 13(10): 959–969.

Mohebi, Z., Khalasi Ahwaz, L., Heshmati, G.A., 2021. Comparison of diferent methods to estimate forage production of two shrub species Halocnemum strobilaceum (Pall.) Bieb and Halostachys caspica CA Mey (Case Study: Winter Rangelands of Golestan Province, Iran). *Journal of Rangeland Science* 11(2): 171–181.

Mukhopadhyay, R., Sarkar, B., Jat, H.S., Sharma, P.C., Bolan, N.S., 2021. Soil salinity under climate change: Challenges for sustainable agriculture and food security. *Journal of Environmental Management* 280: 111736.

Nainwal, R.C., Chaurasiya, P., Kumar, A., Singh, M., Singh, D., Tewari, S.K., 2024. Phytoremediation: A sustainable approach to combat soil salinity. *Advances in Environmental and Engineering Research* 5(2): 1-11.

Otarov, A., 2014. Concentration of heavy metals in irrigated soils in Southern Kazakhstan. In: Novel measurement and assessment tools for monitoring and management of land and water resources in agricultural landscapes of Central Asia. Mueller, L., Saparov, A., Lischeid, G. (Eds.). Environmental Science and Engineering. Springer, Cham. pp 641–652.

Öztürk, M., Altay, V., Güvensen, A., 2019. Sustainable use of halophytic taxa as food and fodder: an important genetic resource in Southwest Asia. In: Ecophysiology, abiotic stress responses and utilization of halophytes. Hasanuzzaman, M., Nahar, K., Öztürk , M. (Eds.). Springer, Singapore. pp.235–257.

Pachikin, K., Erokhina, O., Funakawa, S., 2014. Soils of Kazakhstan, their distribution and mapping. In: Novel measurement and assessment tools for monitoring and management of land and water resources in agricultural landscapes of Central Asia. Mueller, L., Saparov, A., Lischeid, G. (Eds.). Environmental Science and Engineering. Springer, Cham. pp 519–533.

Saparov, A., 2014. Soil resources of the Republic of Kazakhstan: Current status, problems and solutions. In: Novel measurement and assessment tools for monitoring and management of land and water resources in agricultural landscapes of Central Asia. Mueller, L., Saparov, A., Lischeid, G. (Eds.). Environmental Science and Engineering. Springer, Cham. pp 61–73.

Shahid, S.A., Zaman, M., Heng, L., 2018. Soil salinity: Historical perspectives and a world overview of the problem. In: Guideline for salinity assessment, mitigation and adaptation using nuclear and related techniques. Shahid, S.A., Zaman, M., Heng, L. (Eds.). Springer, Cham. pp. 43–53.

Shaygan, M., Baumgartl, T., 2022. Reclamation of salt-affected land: A review. *Soil Systems* 6(3): 61.

Sherene, T., 2010. Mobility and transport of heavy metals in the polluted soil environment. *Biological Forum- An International Journal* 2(2): 112–121 (2010).

Shrivastava, P., Kumar, R., 2015. Soil salinity: A serious environmental issue and plant growth promoting bacteria as one of the tools for its alleviation. *Saudi Journal of Biological Sciences* 22(2): 123-131.

Singh, D., Buhmann, A.K., Flowers, T.J., Seal, C.E., Papenbrock, J., 2014. Salicornia as a crop plant in temperate regions: selection of genetically characterized ecotypes and optimization of their cultivation conditions. *AoB PLANTS* 6: plu071.

Song, J., Feng, G., Zhang, F., 2006. Salinity and temperature effects on germination for three salt-resistant euhalophytes, Halostachys caspica, Kalidium foliatum and Halocnemum strobilaceum. *Plant and Soil* 279(1): 201–207.

Souza, E.R., dos Santos Freire, M.B.G., da Cunha, K.P.V., do Nascimento, C.W.A., Ruiz, H.A., Lins, C.M.T., 2012. Biomass, anatomical changes and osmotic potential in Atriplex nummularia Lindl. cultivated in sodic saline soil under water stress. *Environmental and Experimental Botany* 82: 20–27.

Stavi, I., Thevs, N., Priori, S., 2021. Soil salinity and sodicity in drylands: A review of causes, effects, monitoring, and restoration measures. *Frontiers in Environmental Science* 9:712831.

Suska-Malawska, M., Sulwiński, M., Wilk, M., Otarov, A., Metrak, M., 2019. Potential eolian dust contribution to accumulation of selected heavy metals and rare earth elements in the aboveground biomass of Tamarix spp. from saline soils in Kazakhstan. *Environmental Monitoring and Assessment* 191: 57.

Suska-Malawska, M., Vyrakhamanova, A., Ibraeva, M., Poshanov, M., Sulwiński, M., Toderich, K., Metrak, M., 2022. Spatial and in-depth distribution of soil salinity and heavy metals (Pb, Zn, Cd, Ni, Cu) in arable irrigated soils in Southern Kazakhstan. *Agronomy* 12: 1207.

Tyurin, I. V., 1965. Organic matter of soil and its role in fertility. Nauka, Moscow. 320p.

Ventura, Y., Sagi, M., 2013. Halophyte crop cultivation: The case for Salicornia and Sarcocornia. *Environmental and Experimental Botany* 92: 144–153.

Wang, L. M., Bu, X.L., Chen, J., Huang, D.F., Luo, T., 2018. Efects of NaCl on plant growth, root ultrastructure, water content, and ion accumulation in a halophytic seashore beach plum (Prunus maritima). *Pakistan Journal of Botany* 50(3): 863–869.

Yertayeva, Z. , Kızılkaya, R., Kaldybayev, S., Seitkali, N., Abdraimova, N., Zhamangarayeva, A., 2019. Changes in biological soil quality indicators under saline soil condition after amelioration with alfalfa (Medicago sativa L.) cultivation in meadow Solonchak. *Eurasian Journal of Soil Science* 8 (3): 189-195.

Yin, X., Feng, Q., Li, Y., Deo, R.C., Liu, W., Zhu, M., Zheng, X., Liu, R., 2022. An interplay of soil salinization and groundwater degradation threatening coexistence of oasis-desert ecosystems. *Science of The Total Environment* 806: 150599.

Zhang, W., Ma, L., Abuduwaili, J., Ge, Y., Issanova, G., Saparov, G., 2019. Hydrochemical characteristics and irrigation suitability of surface water in the Syr Darya River, Kazakhstan. *Environmental Monitoring and Assessment* 191: 572.

Eurasian Journal of Soil Science 2025, 14(1), 38 - 45

Eurasian Journal of Soil Science

Journal homepage : http://ejss.fesss.org

Mathematical modeling of cations from non-edible food waste for the reclamation of sodic and saline soils

Md. Rezwanul Islam [a,b,*], Qingyue Wang [a,*], Sumaya Sharmin [a,b], Weiqian Wang [a], Christian Ebere Enyoh [a]

[a] Graduate School of Science and Engineering, Saitama University, 255 Shimo-Okubo, Sakura-ku, Saitama 338-8570, Japan

[b] Department of Agricultural Extension, Khamarbari, Dhaka 1215, Bangladesh

Article Info

Received : 23.05.2024

Accepted : 09.10.2024

Available online: 12.10.2024

Author(s)

M.R.Islam *

Q.Wang *

S.Sharmin

W.Wang

C.E.Enyoh

* Corresponding author

Abstract

Nutritional disparity is a crucial impediment to agricultural productivity that interferes with soil structural stability and plant growth since more than one-fourth of the total land area is affected, especially by sodicity globally. This study assesses the mathematical models of non-edible food waste, including brinjal waste, potato peel, banana peel, orange peel, eggshell, cow bone, chicken bone, and fish bone. After consumption of the food, the resulting non-edible food waste was cleaned, dried, crushed, and stored separately in aluminum zipper bags. Cation concentrations of the considered waste materials were measured using ion chromatography systems. Then the mathematical models such as Exchangeable Sodium Percentage (ESP), Exchangeable Potassium Percentage (EPP), Sodium Adsorption Ratio (SAR), Potassium Adsorption Ratio (PAR), and Cation Ratio of Soil Structural Stability (CROSS) were assessed considering cation concentrations. The results revealed that Na^+ concentrations ranged from 0.17±0.001 mg/kg in orange peel to 5.21±0.005 mg/kg in chicken bone; K^+ ranged from 0.28±0.003 mg/kg in eggshell to 56.50±0.216 mg/kg in banana peel; Ca^{2+} ranged from 0.30±0.004 mg/kg in potato peel to 1.37±0.049 mg/kg in eggshell; and Mg^{2+} ranged from 0.06±0.004 mg/kg in eggshell to 1.12±0.006 mg/kg in banana peel. The overall concentration sequence was $K^+ > Na^+ > Ca^{2+} > Mg^{2+}$. In addition, animal waste biomass had comparatively high ESP and EPP values for the studied waste biomasses. SAR, PAR, and CROSS models for all studied wastes are suitable for application to sodic and saline soils. In conclusion, non-edible food waste biomass might be a reliable source of cations that is important for soil structural stability and ultimately for plant growth and could be utilized in sodic and saline soils based on the analysis of cationic parameters and mathematical models.

Keywords: Cationic parameters, food waste, soil structural stability, plant growth.

Introduction

Cations (K^+, Na^+, Mg^{2+}, Ca^{2+}, etc.) are critical for agroecosystems as they significantly impact the physico-chemical properties of soil (Qadir et al., 2007), nutrient availability, plant growth, and crop yield (Filho et al., 2020). Specifically, these cations contribute to global soil salinity and sodicity problems, which hinder crop production due to ionic imbalance. Approximately 33% of irrigated land and 20% of total land worldwide are affected by salinity (Machado and Serralheiro, 2017). Additionally, nearly 424 million hectares of topsoil (0–30 cm) and 833 million hectares of subsoil (30–100 cm) have been affected by salt, covering 118 countries (FAO, 2021). The affected topsoil consists of 85% saline soil, 10% sodic soil, and 5% saline-sodic soil, whereas the subsoil comprises 62% saline soil, 24% sodic soil, and 14% saline-sodic soil (FAO, 2021). Salinization is rapidly spreading, affecting 1-2 million hectares of land annually, posing a significant threat to food security

: https://doi.org/10.18393/ejss.1565860 Publisher : Federation of Eurasian Soil Science Societies

: https://ejss.fesss.org/10.18393/ejss.1565860 e-ISSN : 2147-4249

(Hopmans et al., 2021). Soil salinization and sodification are major obstacles to crop production, particularly in drylands (Filho et al., 2020; Stavi et al., 2021). It is predicted that about 50% of the world's crop fields will be affected by salt by 2050 (Jamil et al., 2011).

Plants require 17 essential nutrients for their growth and development (Fageria, 2009), including K^+, Na^+, Mg^{2+}, and Ca^{2+}. Sodium (Na) has also been found beneficial for many C4 plants, such as *Atriplex tricolor* and *Panicum miliaceum* (Arnon and Stout, 1939). Without these essential elements, plants cannot complete their life cycle. Conversely, an excess of these elements causes ionic toxicity. Therefore, balanced nutrient levels promote plant growth, while imbalanced nutrition impedes agricultural production.

Improper waste management, particularly of non-edible food waste, poses a serious problem in developing and underdeveloped countries. Non-edible food waste such as brinjal waste (Quamruzzaman et al., 2020), potato peel (Jekayinfa et al., 2015), banana peel (Pyar and Peh, 2018), orange peel (Abdelazem et al., 2021), eggshell (Ajala et al., 2018), cow bone (Nwankwo et al., 2018), chicken bone (Khalil, 2018), and fish bone (Hooi et al., 2021) have been identified as sources of mineral nutrients. Previous studies of the authors have reported the presence of 17 essential minerals, including cationic nutrients (K, Mg, and Ca), in these plant and animal wastes (Islam et al., 2023).

Thus, these wastes can be potential sources of nutrients, including cations, depending on the soil's nutritional conditions. Additionally, they can add organic matter beneficial for amending sodic and saline soils (Aboelsoud et al., 2020). Achieving a clean environment is crucial for all countries to meet the Sustainable Development Goals (SDGs) established by the UN (UN, 2015). However, there has been no comprehensive assessment of non-edible food waste for improving soil conditions and plant growth. That is why, this study aims to evaluate the potential of non-edible food wastes for enhancing soil health and stability in problematic sodic and saline soils through mathematical modeling of cation dynamics. Therefore, Na^+, K^+, Mg^{2+}, and Ca^{2+} ions were determined using ion chromatography of the mentioned wastes. Then, the mathematical models ESP, EPP, SAR, PAR, and CROSS were calculated considering the ionic concentrations of K^+, Na^+, Mg^{2+}, and Ca^{2+} to assess the potential of non-edible food waste for maintaining soil structural stability and promoting plant growth based on mathematical modeling.

Material and Methods

Sample preparation

Eight non-edible food wastes, namely brinjal waste, potato peel, banana peel, orange peel, eggshell, cow bone, chicken bone, and fish bone, were collected from households at International House-2, Saitama University, Japan. The waste samples were thereafter washed. Then the sample was dried under sunlight to remove the moisture. After being dried, the samples were ground using a standard laboratory grinder (IKA® Japan K.K., Osaka, Japan) and crusher (WB-1, 700 W, Osaka Chemical Co. Ltd., Japan). Then, the samples were kept in a sealed aluminum foil bag temporarily for analysis.

Cation determination

50 mg of each waste biomass were taken in a plastic bottle for ion determination. 10 mL of Ultrapure (Type1) water (Direct-Q® 3 UV Water Purification System) was added. Then the sample solution was subjected to ultrasonic extraction for 30 minutes. After that, the solution was centrifuged for 30 minutes. Then the centrifuged solution was filtered (0.25µm). Then the sample was stored temporarily for analysis. By this time, eluent had been prepared using Na_2CO_3, $NaHCO_3$, and methane sulfonic acid for their ability to effectively elute the targeted cations. The extractant was then placed for analysis. A standard solution was prepared and analyzed. The ionic concentration (mg/kg) of four cations, namely Na^+, K^+, Mg^{2+}, and Ca^{2+}, having three replications, was measured using an ion chromatography system (Dionex ICS-1600, Diotec Tokyo Co., Ltd., Japan).

Mathematical models

Exchangeable Sodium Percentage (ESP)

The ESP was computed as the ratio of Na to the summation of all cations expressed in percentage. The equation is followed in (1) (Richards, 1954).

$$\mathrm{ESP} = \frac{\mathrm{Na^+}}{\mathrm{Na^+ + K^+ + Mg^{2+} + Ca^{2+}}} \times 100 \quad (1)$$

Exchangeable Potassium Percentage (EPP)

The EPP was computed as the ratio of K to the summation of all cations expressed in percentage. The equation is as follows in (2) (Richards, 1954)

$$EPP = \frac{K^+}{Na^+ + K^+ + Mg^{2+} + Ca^{2+}} \times 100 \quad (2)$$

Sodium Adsorption Ratio (SAR)

SAR addresses the effects of sodium on the stability of soil aggregates. SAR was calculated using the mathematical equation (3) (Richards, 1954)

$$SAR = \frac{Na^+}{\sqrt{\frac{(Ca^{2+} + Mg^{2+})}{2}}} \quad (3)$$

Potassium Adsorption Ratio (PAR)

PAR addresses the effects of potassium on the stability of soil aggregates. PAR was calculated using the mathematical equation (4) (Chen et al., 1983)

$$PAR = \frac{K^+}{\sqrt{\frac{(Ca^{2+} + Mg^{2+})}{2}}} \quad (4)$$

Cation Ratio of Structural stability (CROSS)

CROSS considers the effects of all cations on the stability of soil aggregates. It includes the potential negative effects of high sodium (Na), potassium (K), and magnesium (Mg) concentrations. CROSS was estimated using the mathematical equation in (5).

$$CROSS = \frac{Na^+ + 0.56K^+}{\sqrt{\frac{(Ca^{2+} + 0.6Mg^{2+})}{2}}} \quad (5)$$

Statistical analysis

IBM SPSS Statistics 20 and Microsoft office Excel 2013 (Microsoft, Inc, USA) were used for calculation and data analysis. Analysis of variance (ANOVA) was conducted to determine significant differences among treatment groups.

Results and Discussion

Concentration of mono and divalent cations in different non-edible food waste

This study found that non-edible food waste contains a significant amount of monovalent and divalent cations like Na^+, K^+, Ca^{2+}, and Mg^{2+} (Table 1). Sodium ions were the highest in animal-derived wastes (2.24±0.002–5.21±0.005), excluding eggshell, while plant-derived wastes exhibited the lowest concentrations (0.30±0.001), with the exception of potato peel (1.74±0.003). Potassium ions (7.11±0.017–56.50±0.216) and magnesium ions (0.38±0.002–1.12±0.006) were highest in plant-derived wastes, particularly in banana peel, with eggshell showing the lowest values for both elements. Calcium ions were notably high in eggshell (1.37±0.049) and banana peel (1.17±0.003), whereas potato peel had the lowest calcium content (0.30±0.004).

Table 1. Ionic concentration of mono and divalent cations in waste materials

Waste materials	Ion concentration (mg/kg)			
	Na^+	K^+	Ca^{2+}	Mg^{2+}
Brinjal waste	$0.30^{e} \pm 0.001$	$29.57^{b} \pm 0.025$	$0.52^{e} \pm 0.005$	$0.84^{b} \pm 0.001$
Potato peel	$1.74^{d} \pm 0.003$	$26.69^{c} \pm 0.045$	$0.30^{g} \pm 0.004$	$0.79^{c} \pm 0.002$
Banana peel	$0.19^{g} \pm 0.001$	$56.50^{a} \pm 0.216$	$1.17^{b} \pm 0.003$	$1.12^{a} \pm 0.006$
Orange peel	$0.17^{h} \pm 0.001$	$7.11^{d} \pm 0.017$	$1.01^{c} \pm 0.047$	$0.38^{d} \pm 0.002$
Eggshell	$0.25^{f} \pm 0.001$	$0.28^{h} \pm 0.003$	$1.37^{a} \pm 0.049$	$0.06^{g} \pm 0.004$
Cow bone	$2.24^{c} \pm 0.002$	$1.09^{g} \pm 0.008$	$0.46^{f} \pm 0.041$	$0.16^{f} \pm 0.005$
Chicken bone	$5.21^{a} \pm 0.005$	$2.91^{e} \pm 0.017$	$1.02^{c} \pm 0.018$	$0.21^{e} \pm 0.008$
Fish bone	$3.06^{b} \pm 0.003$	$1.84^{f} \pm 0.003$	$0.68^{d} \pm 0.007$	$0.16^{f} \pm 0.001$

Mean values in the column with uncommon superscript letters differ significantly ($p < 0.05$)

The overall trend of cationic distribution followed the following sequence: $K^+ > Na^+ > Ca^{2+} > Mg^{2+}$. K^+ is higher in plant and animal wastes because it is an essential nutrient for both. Since plants and animals require large amounts of potassium for various biological processes, it accumulates in their tissues and, consequently, in

their waste. Na^+ concentrations are lower in both plant and animal wastes compared to K^+. But animal bone contained higher Na^+ compared to non-edible plant waste biomasses because animal bone acts as a reservoir of different minerals including Na^+ and Na^+ is integrated into the mineral matrix of the bone, contributing its stability. The findings regarding the high potassium content in banana peel are consistent with those reported by Jekayinfa et al. (2015), suggesting that these wastes have high potential for use as potassium supplements in deficient soils. In addition, eggshell, chicken bone, fruit peel biomasses contained a higher amount of Ca^{2+} than others mentioned in Table 1 might be used in Ca deficient soils. The result is similar to the findings of Al-awwal and Ali (2015) for eggshell. Calcium is higher in eggshell because it is primarily composed of calcium carbonate ($CaCO_3$). Mg^{2+} was recorded as having the highest concentration in banana peels and comparatively higher in plant waste biomasses. The present study concurs with the findings in brinjal waste, potato peel, banana peel, orange peel, and eggshell reported by Quamruzzaman et al. (2015), Jekayinfa et al. (2015), Pyar and Peh (2018), Abdelazem et al. (2021), Ajala et al. (2018), respectively. As salinity and sodicity are affected mainly by the presence of Na^+ (Rath et al., 2019), non-edible plant waste with lower Na^+ might be suitable for maintaining soil health and supplying essential plant nutrients.

Mathematical modeling of cation of non-edible food waste

Exchangeable sodium percentage (ESP), Exchangeable potassium percentage (EPP), sodium adsorption ratio (SAR), potassium adsorption ratio (SAR) and cationic ratio of structural stability (CROSS) are shown in Figure 1, 2, 3, 4 and 5.

Exchangeable Sodium Percentage (ESP)

The results for the exchangeable sodium percentage are presented in Figure 1. The results showed that the ESP of non-edible food waste ranged from 0.32±0.001 to 56.84±0.64. Cow bone had the highest ESP (56.84±0.64) followed by chicken bone, and fish bone that had ESPs greater than 15. Waste from vegetables and fruits has a lower value (0.32±0.0013-5.89±0.002) from the ESP model than animal waste (13.01±0.0013-56.84±0.64). The ESP value was statistically significant ($p<0.05$).

The ESP model is highly related to soil structure and sodicity. A higher ESP value indicates the presence of more Na^+ over monovalent and divalent cations, resulting in poor soil structure. ESP having ≤15 unlikely effects adversely, whereas >15 implies sodic soil-associated problems on soil structure (USDA, 2007). High ESP insists on soil particle dispersion and nutrient imbalances or deficiencies. Plants grow in a wide range of soils. Trapp et al. (2008), Prasad et al. (2007) and Kumar et al. (2006) described those plants exposed to higher ESP had reduced plant height, branches, leaves, flowers, and fruits. In addition, chlorophyll a and b and carotenoids in leaves decreased with increasing ESP. Anwar et al. (1996) found similar findings with the vetiver plant. Pea and lentil growth is affected even at ESP levels below 15, whereas rice and grass growth continue up to 15 and above 65, respectively. In addition, *A. majus* is more tolerant of sodic soil (ESP 57.4). Barley, linseed, mustard, sunflower, and wheat were supposed to be salt-tolerant crops (Chippa and Lal, 1995). Many halophyte plants can adapt to high-salty areas (Chen and Wang, 2024). Na can be used by glycophytic plants (turnips, beets, and spinach) as well, to such an extent that it can be an alternative to K (Marschner, 1971). It is also essential for Chenopodiaceae, Amaranthaceae, and Cyperaceae plants (Arnon and Stout, 1939). These C4 plants exhibited poor growth, visual deficiency indications such as chlorosis and necrosis, or failed to produce flowers in the absence of Na (Johnston at al., 1988). A recent field study revealed that Na fertilization increased beet yield (Barłóg et al., 2018). It has been reported that tomatoes respond to extra Na stress (Roşca et al., 2023) too. Therefore, cow bone, chicken bone, and fish bone can be added to the Na-deficient soil for the growth of C4 plant (tomato, etc.) that are beneficial for their growth. On the contrary, remaining waste materials can be applied to saline and sodic soil to improve its structure as well as plant growth.

Exchangeable Potassium Percentage (EPP)

The results for the EPP of the non-edible food waste are presented in Figure 2. It represents that the studied waste material possessed a higher EPP with a range of EPP (14.07±0.46 to 95.79±0.028). Vegetables, and fruits waste had a higher EPP value (81.96±0.487 to 95.79±0.028) than animal waste (14.065±0.46-32.07±0.014) with statistically differed ($p<0.05$). Animal waste had a low EPP value, but that is also higher than the critical value of 13. The EPP model is directly proportional to K^+ over monovalent and divalent cations. K^+ is very important for plants to maintain the proper functioning of cell membranes (Wei et al., 2003). It is also a macronutrient, essential for plant growth. A significant increase in crop yield was recorded with increasing EPP (Ravina and Markus, 1975). Clay dispersion has been linked to soils with high exchangeable K levels

(Farahani et al., 2018). According to Dexter and Czy (2000), clay dispersion frequently leads to unfavorable conditions for plant root development, decreases water permeability, which raises the risk of run-off, flooding, and erosion, and may result in anaerobic conditions in soils and crusting of the soil surface. As the EPP value was higher than the critical value, these wastes cannot be applied to saline and sodic soils. According to EPP models, the investigated wastes can be incorporated into K-deficient soils.

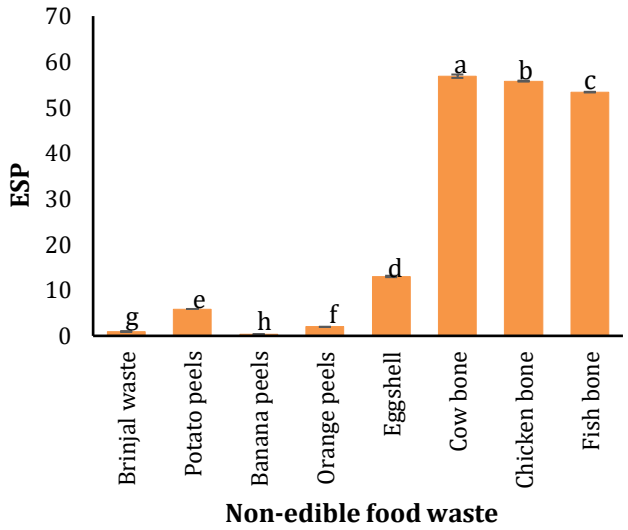

Figure 1. Exchangeable Sodium Percentage (ESP) of non-edible food waste (Mean values on the bars with uncommon superscript letters differ significantly, $p < 0.05$)

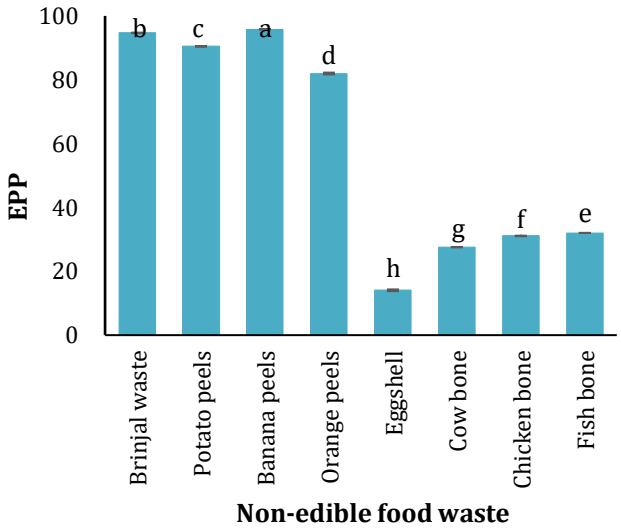

Figure 2. Exchangeable Potassium Percentage (EPP) of non-edible food waste (Mean values on the bars with uncommon superscript letters differ significantly, $p<0.05$)

Sodium Adsorption Ratio (SAR)

The Sodium Adsorption Ratio (SAR) of non-edible food waste is mentioned in Figure 3. All the studied waste biomasses had very low SAR values, with a range of 0.05±0.0001-2.35±0.02. A lower SAR value indicates the presence of less monovalent Na^+ over divalent ions, namely Ca^{2+} and Mg^{2+}. Results also revealed that animal waste like cow bone, chicken bone, and fish bone had a higher value except eggshell that had a lower SAR value. On the other hand, plant waste had the lowest value, apart from potato peels. The recommended value of SAR of <13 is expected to have structural stability (Enyoh and Isiuku, 2020). The considered waste material with a lower SAR value is very conducive to having a good structure with respect to sodium and would allow the growth of plants. Marchuk and Rengasamy (2010) noted a positive association between SAR and clay dispersion. The results indicated that the higher the SAR value, the higher the potassium ion over divalent cations like Ca^{2+} and Mg^{2+}, and vice versa. SAR values indicate a low risk of sodium-induced structural instability, suggesting these wastes can be safely used in sodic soils.

Potassium Adsorption Ratio (PAR)

The PAR value of the studied non-edible food waste biomasses ranged 0.12±0.003-18.65±0.104. Results indicated that all biomasses except banana peels had a lower PAR value than the critical value mentioned in Figure 4. Vegetable and fruit waste biomasses contained a higher PAR value with a range 3.012±0.06-18.65±0.104. Banana peel had the highest PAR value, followed by potato peel, and brinjal waste, respectively. The PAR value does not cover sodium ion concentration. The biomasses with high PAR values contribute to the dispersion. As all the studied materials have a lower PAR value except banana peels, these can be applied to the soil, even saline soil.

Cation Ratio on Structural Stability (CROSS)

The results revealed that the investigated waste materials contained a CROSS-value with a wide range (0.17±0.004 to 11.71±0.06). Animal waste biomass had a lower CROSS value than vegetable and fruit waste. The CROSS value was lower than the critical value of 13 for all waste. The eggshell waste showed the lowest CROSS value (0.17±0.004) whereas banana peel showed the highest value (11.71±0.063). The CROSS model is the most accepted model that covers all causal factors. The lower CROSS value of non-edible food waste implies the comparatively lower presence of monovalent ions (Na^+ and K^+) over divalent cations (Ca^{2+} and Mg^{2+}) and vice versa. Rengasamy and Marchuk (2011) mentioned that low CROSS-links inhibit the dispersion

of soil clay. Al-Hadidi and Al-Ubaydi (2021) also stated similar findings: low CROSS-values prevent dispersion of soil clay but reduce hydraulic conductivity. As the studied waste biomass had a lower CROSS-value than the critical value, these biomasses can be incorporated into any kind of soil, especially highly dispersed soils.

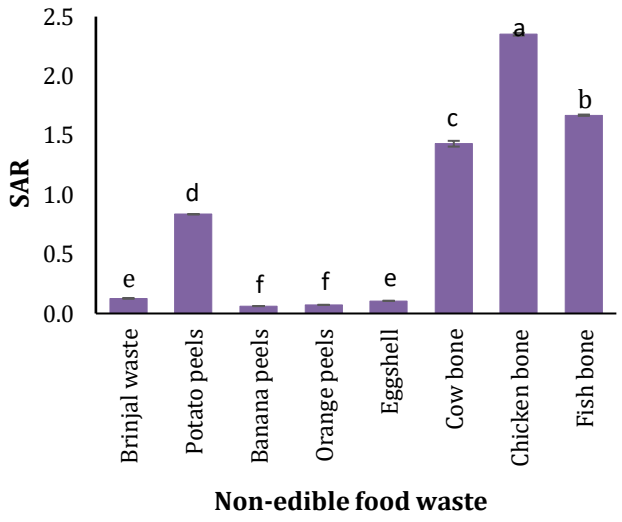

Figure 3. Sodium Adsorption Ratio (SAR) of non-edible food waste (Mean values on the bars with uncommon superscript letters differ significantly, $p < 0.05$)

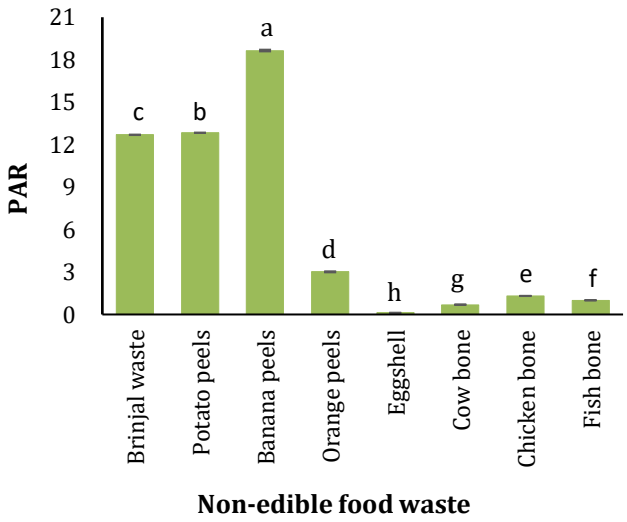

Figure 4. Potassium Adsorption Ratio (PAR) of non-edible food waste (Mean values on the bars with uncommon superscript letters differ significantly, $p<0.05$)

Principal Component Analysis

Figure 6 depicts the principal component analysis (PCA) of mathematical models of cations like ESP, EPP, SAR, PAR, and CROSS, respectively. It was constructed by maximizing the sum of the coefficients of variance of cationic parameters using Kaiser normalization and varimax rotation. Based on the eigenvalue, the principal component analysis was constructed. When it was considered greater than 1, only one component formed. If the eigenvalue was greater than 0.5, two principal components, PCA1 (79.50%) and PCA2 (16.41%), with EPP, PAR, and CROSS (ESP and SAR, respectively), were developed. Results revealed that components EPP, PAR, and CROSS are strongly correlated. The studied non-edible food waste biomasses contained a higher concentration of K^+ as compared to the other mono- and divalent cations, which leads to a strong positive relationship. The ESP and SAR, on the other hand, were strongly correlated because these values are influenced by Na^+. Some of the findings agree with Farahani et al. (2018), where they found relationships between K and Na concentrations, the K:Na ratio, and cationic indicators (CROSS, SAR, PAR, ESP, and EPP) in soils.

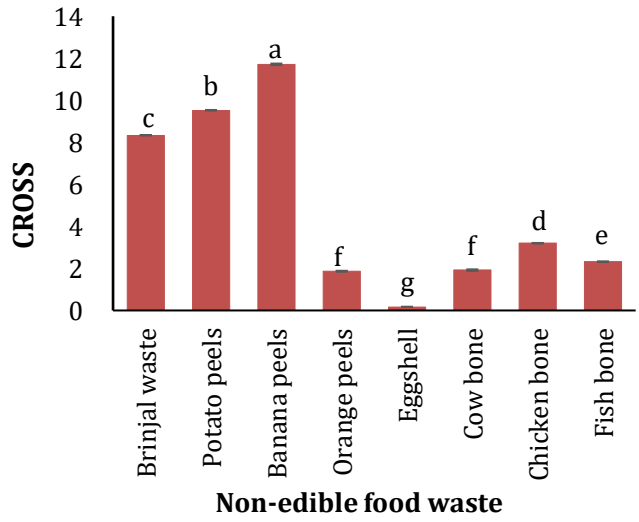

Figure 5. Cation Ratio on Structural Stability (CROSS) of non-edible food waste (Mean values on the bars with uncommon superscript letters differ significantly, $p < 0.05$)

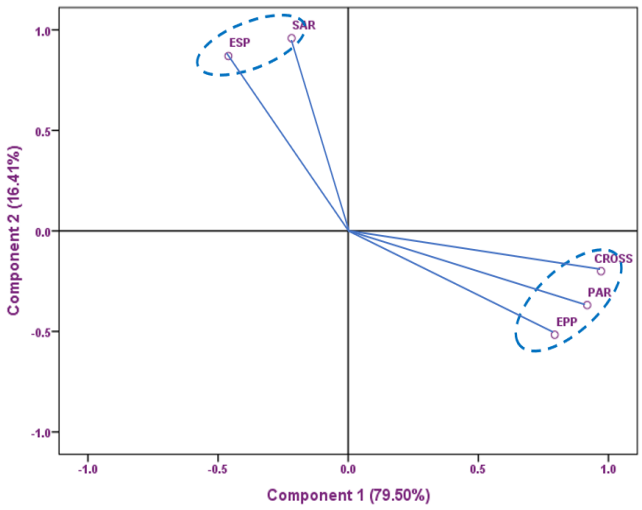

Figure 6. Principal Component analysis (PCA) of mathematical models (ESP, EPP, SAR, PAR, and CROSS)

Conclusion

The non-edible food waste contains a significant amount of monovalent and divalent cationic plant nutrients, viz., K^+, Na^+, Mg^{2+}, and Ca^{2+}, which are essential for soil improvement. The concentration of these cations varies depending on the type of waste material. According to the ESP model, all investigated waste except cow bone, chicken bone, and fish bone waste might be used to make sodic soil. However, the EPP model suggests that considered waste cannot be congenial to address the salinity and sodicity issues but can be added to the K-deficient soil. Nevertheless, based on the SAR, PAR, and CROSS models, the investigated waste can be incorporated into any kind of soil to build a stable soil structure and increase nutrient availability, including saline and sodic soils. This evaluation underscores the potential of non-edible food wastes, particularly banana peels and other plant-derived materials, to serve as sustainable potassium sources and improve soil fertility. Further research should focus on field-scale applications to assess the long-term effects of these wastes on soil structure and fertility.

Acknowledgments

This study was partially supported by the Special Funds for Innovative Area Research (No.20120015, FY 2008-FY2012) and Basic Research (B) (No. 24310005, FY2012-FY2014; No.18H03384, FY2017-FY2020; No.22H03747, FY2022-FY2024) of Grant-in-Aid for Scientific Research of Japanese Ministry of Education, Culture, Sports, Science and Technology (MEXT).

References

Abdelazem, R.E., Hefnawy, H.T., Gehan, A.E., 2021. Chemical composition and phytochemical screening of *Citrus sinensis* (orange) peels. *Zagazig Journal of Agricultural Research* 48 (3): 793-804.

Aboelsoud, H.M., Engel, B., Gad, K.I., 2020. Effect of planting methods and gypsum application on yield and water productivity of wheat under salinity conditions in north Nile Delta. *Agronomy* 10(6): 853.

Ajala, E.O., Eletta, O., Ajala, M.A., Oyeniyi, S.K., 2018. Characterization and evaluation of chicken eggshell for use as a bio-resource. *Arid Zone Journal of Engineering, Technology and Environment* 14 (1): 26-40.

Al-Hadidi, K.E., Al-Ubaydi, M.A., 2021. Impact of cation ratio structure stability (CROSS) on the hydraulic conductivity saturation and clay dispersion for some calcareous soils in north Iraq. *Kirkuk University Journal for Agricultural Sciences* 12 (1): 37–47.

Al-awwal, N.Y., Ali, U.L., 2015. Proximate analyses of different samples of eggshells obtained from Sokoto market in Nigeria. *International Journal of Science and Research* 4(3): 564-566.

Anwar, M., Patra, D.D., Singh, D.V., 1996. Influence of soil sodicity on growth, oil yield and nutrient accumulation in Vetiver (*Vetiveria zizanioides*). *Annals of Arid Zone* 35(1): 49-52.

Arnon, D.I., Stout, P.R., 1939. The essentiality of certain elements in minute quantity for plants with special reference to copper. *Plant Physiology* 14: 371-375.

Barłóg, P., Szczepaniak, W., Grzebisz, W., Pogłodziński, R., 2018. Sugar beet response to different K, Na and Mg ratios in applied fertilizers. *Plant, Soil and Environment* 64 (4): 173–179.

Chen, Y., Banin, A., Borochovitch, A., 1983. Effect of potassium on soil structure in relation to hydraulic conductivity. *Geoderma* 30 (1–4): 135-147.

Chen, J., Wang, Y., 2024. Understanding the salinity resilience and productivity of halophytes in saline environments. *Plant Science* 346: 112171.

Chhipa, B.R., Lal, P., 1995. Na/K Ratios as the basis of salt tolerance in wheat. *Australian Journal of Agricultural Research* 46(3): 533–539.

Dexter, A.R., Czy, A.R., 2000. Effects of soil management on the dispersibility of clay in a sandy soil. *International Agrophysics* 14 (3): 269–272.

Enyoh, C.E., Isiuku, B.O., 2020. Characterisation of some soils from flood basin in Amakohia, Owerri, Nigeria. *International Journal of Environmental Analytical Chemistry* 102 (16): 3766-3785.

Fageria, N.K., 2009. The use of nutrients in crop plants. CRC Press, Boca Raton, FL. 448p.

FAO, 2021. Global Map of Salt-affected Soils (GSASmap). FAO Soils Portal. Food and Agriculture Organization of the United Nations. Available at [Access date: 23.05.2024]: https://www.fao.org/soils-portal/data-hub/soil-maps-and-databases/global-map-of-salt-affected-soils/en/

Farahani, E., Emami, H., Thomas, K., 2018. Impact of monovalent cations on soil structure. Part II. Results of Two Swiss Soils. *International Agrophysics* 32 (1): 69–80.

Filho, J.N.O., Junior, M.J.D., Medeiros, J.F., Vieira, R.C., 2020. Yield and leaf concentrations of nutrients of melon crop and fertility of soil fertigated with N and K. *Revista Brasileira de Engenharia Agrícola e Ambiental* 24 (11): 749–55.

Hooi, M.T., Eunice, S.W.P., Yow, H.Y., David, E., Kim N.X., Choo, H.L., 2021. FTIR spectroscopy characterization and critical comparison of poly(vinyl)alcohol and natural hydroxyapatite derived from fish bone composite for bone-scaffold. *Journal of Physics: Conference Series* 2120: 012004.

Hopmans, J.W., Qureshi, A.S., Kisekka, I., Munns, R., Grattan, S.R., Rengasamy, P., Ben-Gal, A., Assouline, S., Javaux, M., Minhas, P.S., Raats, P.A.C., Skaggs, T.H., Wang, G., Lier, Q.J., Jiao, H., Lavado, R.S., Lazarovitch, N., Li, B., Taleisnik, E., 2021. Critical knowledge gaps and research priorities in global soil salinity. *Advances in Agronomy* 169: 1–191.

Islam, M.R., Wang, Q., Guo, Y., Wang, W., Sharmin S., Enyoh, C.E., 2023. Physico-chemical characterization of food wastes for potential soil application. *Processes* 11 (1): 250.

Jamil, A., Riaz, S., Ashraf, M., Foolad, M.R., 2011. Gene expression profiling of plants under salt stress. *Critical Reviews in Plant Sciences* 30 (5): 435–458.

Jekayinfa, S.O., Bernd, L., Ralf, P., 2015. Biogas production from selected crop residues in Nigeria and estimation of its electricity value. *International Journal of Renewable Energy Technology* 6 (2): 101-118.

Johnston, M., Grof, C.P., Brownell, P.F., 1988. The effect of sodium nutrition on the pool sizes of intermediates of the C4 photosynthetic pathway. *Australian Journal of Plant Physiology* 15: 749-760.

Khalil, S., 2018. Analysis of bone of chicken Gallus gallus domesticus. *International Journal of Innovative Research in Science, Engineering and Technology* 7 (5): 6243–46.

Kumar, D., Singh, K., Chauhan, H.S., Prasad, A., Beg, S.U., Singh, D.V., 2006. Ameliorative potential of *Palma rosa* for reclamation of sodic soils. *Communications in Soil Science and Plant Analysis* 35 (9–10): 1197–1206.

Machado, R.M.A., Serralheiro, R.P., 2017. Soil salinity: effect on vegetable crop growth. management practices to prevent and mitigate soil salinization. *Horticulturae* 3 (2): 30.

Marchuk, A., Rengasamy. P., 2010. Cation ratio of soil structural stability (CROSS). Proceedings of 19th World Congress of Soil Science, Soil Solutions for a Changing World. 1 -6 August 2010, Brisbane, Australia. pp.9-11.

Marschner, H., 1971. Why can sodium replace potassium in plants? Proceedings of 8th Colloquium of the International Potash Institute. Potassium in Biochemistry and Physiology. 15-17 June 1971. Skokloster-Uppsala, Sweden. pp. 50–63.

Nwankwo, I.H., Nwaiwu, N., Nwabanne. J.T., 2018. Production and characterization of activated carbon from animal bone. *American Journal of Engineering Research* 7 (7): 335–341.

Prasad, A., Chattopadhyay, A., Chand, S., Naqvi, A.A., Yadav, A., 2007. Effect of soil sodicity on growth, yield, essential oil composition, and cation accumulation in rose-scented geranium. *Communications in Soil Science and Plant Analysis* 37(13–14): 1805–1817.

Pyar, H., Peh, K.K., 2018. Chemical compositions of banana peels (*Musa sapientum*) fruits cultivated in Malaysia using proximate analysis. *Research Journal of Chemistry and Environment* 22: 108–113.

Qadir, M., Oster, J.D., Schubert, S., Noble, A.D., Sahrawat, K.L., 2007. Phytoremediation of sodic and saline- sodic Soils. *Advances in Agronomy* 96: 197–247.

Quamruzzaman, A.K.M., Khatun, A., Islam, F., 2020. Nutritional content and health benefits of Bangladeshi eggplant cultivars. *European Journal of Agriculture and Food Sciences* 2 (4).

Rath, K.M., Fierer, N., Murphy, D.V., Rousk, J., 2019. Linking bacterial community composition to soil salinity along environmental gradients. *The ISME Journal* 13: 836–846.

Ravina, I., Markus, Z., 1975. The effect of high exchangeable potassium percentage on soil properties and plant growth. *Plant and Soil* 42 (3): 661–672.

Rengasamy, P., Marchuk, A., 2011. Cation Ratio of Soil Structural Stability (CROSS). *Soil Research* 49 (3): 280–285.

Richards, L.A., 1954. Diagnosis and improvement of saline and alkaline soils. Agriculture Handbook, Vol. 60, United States Department of Agriculture (USDA), Washington DC, 160 p.

Roşca, M., Mihalache, G., Stoleru, V., 2023. Tomato responses to salinity stress: From morphological traits to genetic changes. *Frontiers in Plant Science* 14: 1118383.

Stavi, I., Thevs, N., Priori, S., 2021. Soil salinity and sodicity in drylands: A review of causes, effects, monitoring, and restoration measures. *Frontiers of Environmental Science* 9: 712831.

Trapp, S., Feificova, D., Rasmussen, N.F., Gottwein. P.B., 2008. Plant uptake of NaCl in relation to enzyme kinetics and toxic effects. *Environmental and Experimental Botany* 64 (1): 1–7.

UN, 2015. What are the Sustainable Development Goals? United Nations Development Programme. Available at [Access date: 23.05.2024]: https://www.undp.org/sustainable-development-goals

USDA, 2007. Soil survey manual Chapter 3: Examination and description of soils. United States Department of Agriculture (USDA), Natural Resources Conservation Service. Available at [Access date: 23.05.2024]: https://www.nrcs.usda.gov/sites/default/files/2022-09/SSM-ch3.pdf

Eurasian Journal of Soil Science 2025, 14(1), 46 - 57

Eurasian Journal of Soil Science

Journal homepage : http://ejss.fesss.org

Diversity and distribution of arbuscular mycorrhizal fungi associated with vegetable crops in Haryana, India

Anju Tanwar [a,*], Ashok Aggarwal [b], Ishan Saini [c], Tarsem Kumar [d], Mukesh Kumar [e], Sergio T. Pichardo [f]

[a] Department of Botany, Government P.G. College, Ambala Cantt–133001, Haryana, India
[b] Department of Botany, Kurukshetra University, Kurukshetra–136119, Haryana, India
[c] Department of Botany, Indira Gandhi University, Meerpur, Rewari, Haryana, India
[d] Department of Zoology, Government P.G. College, Ambala Cantt–133001, Haryana, India
[e] Department of Botany, Government College Bahadurgarh, Jhajjar-124507, Haryana, India
[f] Abraham Baldwin Agricultural College (ABAC), School of Agriculture and Natural Resources (SANR) Tifton, GA, USA

Article Info
Received : 29.04.2024
Accepted : 24.10.2024
Available online: 27.10.2024

Author(s)
A.Tanwar *
A.Aggarwal
I.Saini
T.Kumar
M.Kumar
S.T.Pichardo

* Corresponding author

Abstract

The optimal growth and development of many vegetable crops hinge significantly upon their reliance on Arbuscular Mycorrhizal Fungi (AMF). Understanding the AMF status of vegetable crops can assist researchers in selecting suitable strains for future experiments. Therefore, a field work was carried out to determine the species diversity and composition of AMF with fifty vegetable crops from seventeen different districts of Haryana. AMF spores were isolated and identified to evaluate AMF density, diversity, and host preference in terms of AMF species richness, abundance and frequency of occurrence. Soil conditions, land use type and its physico–chemical properties played a crucial role in regulating the uneven distribution and composition of AMF. Mycotrophic structures such as linear infection (Arum–type) to coils (Paris–type) arbuscules and vesicles were seen. Interestingly, no correlation was found between spore number and root colonization. Maximum AMF spore density, spore richness and abundance were witnessed in *Zea mays* and *Trigonella foenum–graecum*. Five plants exhibited 100% AMF colonized roots, 15 plants showed above 75% and 12 plants above 50% colonization. Soil pH 6.10 to 7.40 supported the maximal abundance and frequency of occurrence of *Glomus* and *Acaulospora* with 53 species and 18 species followed by *Acaulospora* (18), *Sclerocystis* (10), *Gigaspora* (5), *Entrophospora* (4) and *Sclerocystis* (4). *G. mosseae* was the most preferred species among vegetable crops. Members of non–mycorrhizal families lack root colonization except for *Brassica campestris*, *B. oleracea* var. *botrytis* and *B. Rapa* where 2–11% root colonization was detected. Noticing the abundant AMF diversity of vegetable crops , this investigation expands the scope of detection, selection and inoculation of vegetable crops with suitable AMF species for improving their quality and quantity.

Keywords: Abundance, Frequency of occurrence, Mycorrhizal distribution, Soil properties, Species richness.

Introduction

Exploring the dynamic nexus of plant-root interactions and soil microbiota in the rhizosphere unveils a realm of hidden complexities shaping plant health, nutrient cycling, and ecosystem resilience. Amidst various microbes influencing plants growth and production, the most pervasive and elemental type of relationship is that formed by the fungal endophyte Arbuscular Mycorrhizal Fungi (AMF). Ecological functions of AMF hyphae, have great impacts on global sustainability (Wang et al., 2022). It plays crucial roles in ecosystem

: https://doi.org/10.18393/ejss.1574580
: https://ejss.fesss.org/10.18393/ejss.1574580
Publisher : Federation of Eurasian Soil Science Societies
e-ISSN : 2147-4249

functioning, inclusive of absorption and transport of mineral nutrients (especially P), maintaining soil fertility, amendment of the physical soil ecosystem, modification of plant association with other biota, maintenance of biodiversity and ecosystem stability together with ecological system protection, restoration, and reconstruction (Powell and Rillig, 2018). AMF have significant prominence for agricultural sustainability owing to their multifaceted contribution in assisting plant growth and productivity. This association improves soil properties, nutrient cycling, plants hormonal regulation and defense mechanisms, AMF are widespread in distribution in both natural and agricultural soil as well with almost 230 AMF species of the phylum Glomeromycota are reported till now (Higo et al., 2013). Perhaps that is why they show great diversity within species, genetic and functional as well. Although, the AMF diversity fluctuates from one type of soil to another type of soil and extremely influenced by the type of host plant, physico–chemical and biota of the experimental soil and other growing mediums also (Tanwar et al., 2021). Researchers are of diverse opinion regarding AMF host specificity which ranges from high host specificity (Yang et al., 2012), certain level of host specificity (Bi et al., 2020) to non–host specificity (Santos–González et al., 2006). Moreover, their population is remarkably influenced by both biotic and abiotic communities as well (Wahab et al., 2023). Factors like available nutrient (Johnson et al., 2015), climatic (Li et al., 2010), forage cover (Pellegrino et al., 2020), elevation (Haug et al., 2019), land–use (Melo et al., 2020) can determine the AMF–plant interactions. According to Ma et al. (2023) latitude and soil available phosphorus are the most important predictors of AMF diversity. Given the growing need for sustainable agricultural practices, understanding the role of AMF in nutrient uptake and soil health is crucial for improving vegetable crop productivity. It is also important to know about the species diversity of the AMF in the plant root to get better insight of the mycorrhizal functioning besides adopting their management and preservation (Alguacil et al., 2009). The evaluation of AMF biodiversity of ecological site is relying on evaluating AMF root colonization and AMF spore number. Beside this, few other factors that contribute to the functioning of agricultural performance is AMF biomass which include spores, extraradical and intraradical hyphae and colonized pieces of roots (Higo et al., 2013). AMF status also relies on the time of sampling, soil depth and growth stage of the test plant which increases from initial vegetative state of the plant to completely grown stage.

In nature, most of the vegetable crops are known to be associated with AMF which directly or indirectly influence their growth and production (Tanwar and Aggarwal, 2014). During the last few decades, different aspects of AMF on vegetable crops have been studied extensively in different geographical and agricultural conditions. Work has also been done on studies related to biodiversity of AMF associated with vegetable crops (Castillo et al., 2016). There are several studies on the AMF status in variety of plants from Indian soil also. However, most of the studies are concentrated either on medicinal plants or fruit crops (Khastini et al., 2020) and our present uderstanding on AMF status and morphology in olericultural crop is limited. Therefore, before applying any commercially available inocula via knowing the AMF status and sustenance of crop plant on particular AMF strain is compulsory. In India some previous studies have mainly focused on AMF diversity in cereal crops, whereas this study specifically targets vegetable crops in the region of Haryana, which has unique soil conditions. Furthermore, the research regarding biodiversity of AMF in vegetable crops mainly comes from southern part of India (Kumar and Garampalli, 2013) and literature perusal did not show any authentic study related to AMF status of vegetable crops of Haryana region. Keeping in view the positive impact of AMF on vegetable crops, it became significantly important to emphasize work on monitoring the mycorrhizal status in vegetable crops. Therefore, this study aims to assess the diversity and colonization rate of AMF associated with different vegetable crops grown under specific agro-ecological conditions in Haryana, India.

Material and Methods

Study Site, Sample Collection and Soil Analysis

Seventeen districts of Haryana (Panchkula, Ambala, Kurukshetra, Yamunanagar, Karnal, Kaithal, Panipat, Sonipat, Jind, Rohtak, Hisar, Bhiwani, Rewari, Faridabad, Gurgaon, Sirsa and Fatehabad) were surveyed for the collection of soil samples and plant roots. Thin roots and soil were randomly collected from the rhizosphere of 50 vegetable crops from various districts of Haryana. For the isolation of AMF spores, the soil samples from five randomly selected plants were collected from the depth of 0–30 cm. All the samples were mixed together to make one composite sample. Collected soil was air dried, grounded and sieved through 2mm sieve and kept at 4–10°C for further analysis. Soil Physico–chemical propertieslike pH, electrical conductivity (EC), organic carbon (OC), available phosphorus (P), potassium (K) and Sulphur (S) were analyzed from Directorate of Agriculture, Krishi Bhawan, Sector–21, Panchkula, Haryana, India (Table 1).

Table 1. Physical and chemical characteristics of soil collected from different districts

S. no.	Districts	pH	EC (dS m^{-1})	OC (%)	P (kg m^{-2})	K (kg m^{-2})	S (ppm)
1.	Panchkula	6.1	0.32	0.24	3.70	85.0	18.7
2.	Ambala	6.5	0.12	0.25	5.20	88.0	21.2
3.	Karnal	7.0	0.66	0.43	7.50	112.0	21.7
4.	Kurukshetra	6.8	0.25	0.40	7.30	88.0	14.8
5.	Yamunanagar	6.7	0.41	0.16	4.20	78.0	15.7
6.	Kaithal	7.0	0.44	0.35	7.20	77.5	20.2
7.	Panipat	7.0	0.42	0.24	10.30	98.0	28.2
8.	Sonipat	7.1	0.43	0.25	4.40	90.0	27.6
9.	Jind	7.4	0.40	0.12	13.00	78.0	14.9
10.	Rohtak	6.8	0.44	0.48	8.10	125.0	15.7
11.	Hisar	7.0	0.40	0.42	6.80	115.0	15.7
12.	Bhiwani	7.4	0.41	0.16	13.20	78.0	15.7
13.	Rewari	7.4	0.35	0.44	11.80	85.0	34.4
14.	Faridabad	7.1	0.47	0.31	7.30	75.0	24.2
15.	Gurgaon	6.8	0.36	0.18	3.20	72.0	15.7
16.	Sirsa	7.2	0.47	0.45	12.30	75.0	22.4
17.	Fatehabad	7.2	0.30	0.48	13.80	135.0	17.1

*Electrical conductivity (EC), organic carbon (OC), available phosphorus (P), potassium (K) and Sulphur (S)

Root Colonization

The fine host roots repeatedly washed with water and then cut to make 1cm long segments. These roots were then processed as per rapid clearing and staining technique by Phillips and Hayman's (1970). Plant root colonization assessment was done by Giovannetti and Mosse's (1980) root slide technique. Individual root fragment was conscientiously examined through its entire length to record mycotrophic structures like intra–radical, extra–radical mycelium, hyphal coils, arbuscules and vesicles, first at 100× then at 400×. The colonized roots were photographed with Nikon Coolpix S4000 camera . The percent root colonization was calculated using the following formula:

$$\text{Percentage AM root colonization} = \frac{\text{number of root segments colonized}}{\text{number of root segments studied}} \times 100$$

Isolation and Quantification of AMF Spores

Rhizosphere soil samples were enumerated to detect the presence of AMF spores. Gerdemann and Nicolson's (1963) wet sieving and decanting technique was followed for the isolation of AMF spores. Adoleya and Gaur's (1994) grid line intersect method was followed to quantify AMF spores. Total number of intact spores was counted to calculate spore density and later mounted in polyvinyl lactic acid for identification.

AMF Spore Identification

The spores were identified using the High power research microscope (Suswox Optic, Sudheer Scientific Works–133001, India). The taxonomic identification of AMF spores to species level was done referring the manuals of Schenck and Pérez (1990), Mukerji (1996), Morton and Redecker (2001). Identification was also authenticated from the description in reference cultures in International Culture Collection of Vesicular Arbuscular Mycorrhizal Fungi (http://invam.cag.wvu.edu) and AMF phylogeny (www.amf–phylogeny.com).

AMF Species Richness, Abundance, and Frequency of Occurrence

Number and type of AMF species was used to calculate AMF species richness, species abundance (A) and frequency of occurrence (FO). Species richness (SR) equals total AMF species number in 50 g soil while species abundance (A) equals number of soil samples having particular species.

$$\text{FO}(\%) = \frac{\text{number of soil samples possessing spores of particular species}}{\text{total number of samples analyzed}} \times 100$$

Results

Chemical Analysis of Soil

As per Table 2, the soil pH ranged from 6.10 to 7.40 with minimum with lowest in Panchkula and maximum in Bhiwani, Rewari and Jind. Maximum EC was found in the soil of Karnal (0.66) and minimum in Ambala (0.12) while maximum OC in Rohtak and Fatehabad (0.48) and least in Jind (0.12). Maximum P level was detected in Fatehabad (13.8) and Bhiwani (13.2), while Gurgaon (3.2) had deficient in P. Soil K and S content was also analyzed and none of the soil showed either excess or low level of these nutrients (Table 2).

Table 2. Diversity and distribution of arbuscular mycorrhizal fungi in some vegetable crops of Haryana

S. no	Vegetable crops	Collection site	Pattern of mycorrhization			AMF spore density/50 g soil	AMF root colonization (%)
			M	V	A		
1.	*Abelmoschus esculentus* (Linn.) Moench.	Karnal	+	+	+	239.6 ± 17.90	75.53 ± 5.01
2.	*Allium cepa* Linn.	Panchkula	+	+	+	423.2 ± 20.40	100.00 ± 0.00
3.	*A. sativum* Linn.	Kurukshetra	+	+	-	352.6 ± 12.00	100.00 ± 0.00
4.	*Amaranthustricolor* Linn.	Gurgaon	-	-	-	42.6 ± 7.13	0
5.	*Amorphophallus paeoniifolius* (Dennst.) Nicol.	Kurukshetra	+	-	-	214.2 ± 9.62	33.99 ± 3.65
6.	*Apium graveolens* Linn.	Kurukshetra	+	+	+	219.2 ± 10.00	95.86 ± 3.82
7.	*Beta vulgaris* Linn.	Panipat	-	-	-	114.8 ± 8.22	0
8.	*Brassica campestris* Linn.	Sonipat	+	-	-	21.8 ± 2.38	5.83 ± 0.38
9.	*B. oleracea* var. *botrytis* Linn.	Hisar	+	-	-	35.6 ± 4.39	11.22 ± 1.25
10	*B. oleracea* var. *capitata* Linn.	Yamunanagar	-	-	-	55.5 ± 3.33	0
11	*B. oleracea* var. *gongylodes* Linn.	Yamunanagar	-	-	-	23.0 ± 4.18	0
12	*B. oleracea* var. *italica* Linn.	Karnal	-	-	-	37.0 ± 4.06	0
13	*B. rapa* Linn.	Faridabad	+	-	-	67.8 ± 6.46	2.22 ± 3.04
14	*Capsicum annuum* Linn. (green)	Kurukshetra	+	+	+	342.8 ± 12.20	87.78 ± 5.40
15	*C. annuum* Linn. (red)	Panchkula	+	+	+	376.3 ± 11.30	93.45 ± 3.08
16	*C. annuum* Linn. (yellow)	Ambala	+	+	-	245.4 ± 15.20	75.33 ± 3.40
17	*Chenopodium album* Linn.	Panchkula	-	-	-	18.4 ± 2.30	0
18	*Cicer arietinum* Linn.	Ambala	+	+	+	307.4 ± 10.10	100.00 ± 0.00
19	*Coccinia indica* (Linn.) Voigt	Fatehabad	+	-	-	130.8 ± 4.45	50.60 ± 3.06
20	*Colocasia esculenta* (Linn.) Schott.	Rewari	+	+	-	210.2 ± 7.85	75.00 ± 3.53
21	*Coriandrum sativum* Linn.	Ambala	+	+	+	285.2 ± 6.01	66.43 ± 5.25
22	*Cucumis sativus* Linn.	Yamunanagar	+	+	+	162.0 ± 5.05	57.06 ± 7.25
23	*Cucurbita maxima* Dutch.	Jind	+	-	+	105.4 ± 5.68	69.94 ± 3.64
24	*C. pepo* Linn.	Fatehabad	+	+	+	259.6 ± 12.00	73.50 ± 6.61
25	*Curcuma longa* Linn.	Panchkula	+	+	+	416.0 ± 5.09	95.45 ± 2.34
26	*Daucus carota* Linn.	Sirsa	+	+	+	172.6 ± 5.10	93.87 ± 3.71
27	*Glycine max* (Linn.) Merr.	Jind	+	-	-	125.0 ± 2.91	75.52 ± 5.01
28	*Ipomoea batatas* (Linn.) Lam.	Kurukshetra	+	+	+	138.0 ± 8.69	87.88 ± 7.21
29	*Lagenaria siceraria* (Mol.) Standl. (elongate)	Yamunanagar	+	+	-	217.0 ± 5.15	55.63 ± 4.22
30	*L. siceraria* (Mol.) Standl. (round)	Karnal	+	-	+	244.7 ± 3.76	60.40 ± 3.00
31	*Luffa cylindrica* (Linn.) M.J. Roem.	Sirsa	+	-	-	225.6 ± 6.10	27.66 ± 3.82
32	*Lycopersicon esculentum* Mill.	Gurgaon	+	+	+	284.8 ± 6.14	95.32 ± 4.47
33	*Momordica charantia* Linn.	Rohtak	+	+	+	382.4 ± 8.80	70.45 ± 3.09
34	*M. cochinchinesis* (Lour.) Spreng.	Rewari	+	-	-	117.2 ± 6.45	44.16 ± 5.44
35	*Phaseolus lunatus* (Linn.) Walp.	Kaithal	+	-	-	120.4 ± 3.64	34.72 ± 3.34
36	*P. vulgaris* Linn.	Hisar	+	+	+	224.2 ± 8.38	78.86 ± 4.41
37	*Pisum sativum* Linn.	Gurgaon	+	+	+	339.6 ± 4.03	94.17 ± 3.62
38	*Praecitrullus fistulosus* (Stocks) Pangalo	Ambala	+	-	+	298.0 ± 6.63	33.17 ± 4.00
39	*Raphanus sativus* Linn.	Rohtak	-	-	-	73.4 ± 5.59	0
40	*Solanum melongena* Linn. (white, elongate)	Kaithal	+	+	+	263.8 ± 5.11	64.10 ± 4.90
41	*S. melongena* Linn. (purple, elongate)	Faridabad	+	-	+	364.0 ± 8.69	76.09 ± 3.00
42	*S. melongena* Linn. (purple, round)	Sonipat	+	+	+	244.7 ± 4.55	60.00 ± 0.00
43	*S. tuberosum* Linn.	Faridabad	+	+	-	326.6 ± 8.79	95.58 ± 4.06
44	*Spinacia oleracea* Linn.	Ambala	-	-	-	86.4 ± 9.65	0
45	*Trichosanthes dioica* Roxb.	Panipat	+	+	+	208.6 ± 5.81	54.68 ± 3.72
46	*Trigonella foenum- graecum* Linn.	Panchkula	+	+	+	421.2 ± 13.60	100.00 ± 0.00
47	*Vicia faba* Linn.	Bhiwani	+	+	-	190.2 ± 5.67	25.67 ± 3.47
48	*Vigna radiata* (Linn.) Wilczek	Bhiwani	+	-	-	153.0 ± 4.69	43.50 ± 4.09
49	*V. unguiculata* (Linn.) Walp.	Hisar	+	-	+	317.0 ± 11.30	55.93 ± 2.64
50	*Zea mays* Linn.	Panchkula	+	+	+	514.2 ± 17.90	100.00 ± 0.00

Each value is a mean of five replicates, ±: standard deviation, A: Arbuscule, M: Mycelium, V: Vesicle, +: present, - : absent

AMF spore density

AMF spore propagule density varied greatly among plants (Table 3). Highest mean spore density (514.2±17.9) was found with *Z. mays* followed by *A. cepa*, *T. foenum–graecum* and *Capsicum annuum* (green and red). While less than 100 spores were seen in the members of Amaranthaceae, Brassicaceae and Chenopodiaceae. Sporocarp of several *Glomus* and *Sclerocystis* species and resting spore i.e., chlamydospores were also seen. AMF spore propagules were strikingly low in the soil of Jind, Bhiwani and Rewari. No direct relationship was

observed between soil nutrient status and mycorrhization except with soil pH and P level. Slightly acidic soil of Panchkula and Gurgaon exhibited higher spore density as compared to samples from alkaline soils of Bhiwani and Jind (Table 3).

Table 3. AMF species distribution among studied vegetable crops of Haryana

S. no.	Vegetable crops	Species richness	Diversity of AM fungal species
1.	*Abelmoschus esculentus* (Linn.) Moench.	9	2, 9, 23, 28, 35, 39, 50, 59, 74
2.	*Allium cepa* Linn.	19	2, 5, 9, 10, 22, 23, 30, 34, 39, 43, 50, 55, 58, 59, 70, 75, 77, 78, 90
3.	*A. sativum* Linn.	11	2, 9, 13, 23, 32, 44, 50, 59, 76, 78, 90
4.	*Amaranthustricolor* Linn.	6	2, 31, 47, 59, 68, 75
5.	*Amorphophallus paeoniifolius* (Dennst.) Nicol	10	8, 28, 54, 56, 57, 59, 65, 71, 75, 87
6.	*Apium graveolens* Linn.	7	2, 9, 11, 59, 65, 69, 75
7.	*Beta vulgaris* Linn.	3	5, 34, 59
8.	*Brassica campestris* Linn.	4	9, 23, 29, 59
9.	*B. oleracea* var. *botrytis* Linn.	4	2, 43, 57, 59
10.	*B. oleracea* var. *capitata* Linn.	4	7, 10, 59, 81
11.	*B. oleracea* var. *gongylodes* Linn.	5	23, 43, 48, 50, 75
12.	*B. oleracea* var. *italica* Linn.	7	2, 9, 13, 38, 48, 56, 59
13.	*B. rapa* Linn.	3	2, 7, 59
14.	*Capsicum annuum* Linn. (green)	6	5, 9, 26, 32, 59, 61
15.	*C. annuum* Linn. (red)	8	9, 13, 44, 50, 55, 59, 69, 89
16.	*C. annuum* Linn. (yellow)	6	9, 29, 45, 50, 59, 75
17.	*Chenopodium album* Linn.	5	2, 23, 30, 35, 59
18.	*Cicer arietinum* Linn.	16	2, 9, 12, 24, 25, 44, 52, 59, 62, 66, 67, 71, 75, 79, 81, 90
19.	*Coccinia indica* (Linn.) Voigt	8	12, 19, 28, 39, 59, 64, 86, 87
20.	*Colocasia esculenta* (Linn.) Schott.	6	2, 9, 44, 51, 59, 62
21.	*Coriandrum sativum* Linn.	7	2, 9, 39, 44, 66, 70
22.	*Cucumis sativus* Linn.	7	3, 6, 9, 33, 50, 59, 90
23.	*Cucurbita maxima* Dutch.	6	4, 9, 23, 44, 59, 75
24.	*C. pepo* Linn.	6	9, 12, 29, 36, 44, 77
25.	*Curcuma longa* Linn.	15	6, 8, 9, 15, 18, 21, 43, 50, 53, 59, 69, 81, 83, 86, 88
26.	*Daucus carota* Linn.	7	2, 9, 20, 41, 56, 59, 93
27.	*Glycine max* (Linn.) Merr.	7	4, 25, 42, 44, 50, 59, 78
28.	*Ipomoea batatas* (Linn.) Lam.	7	1, 3, 39, 50, 59, 62, 79
29.	*Lagenaria siceraria* (Mol.) Standl. (elongate)	6	2, 9, 43, 44, 59, 73
30.	*L. siceraria* (Mol.) Standl. (round)	8	1, 8, 15, 48, 49, 52, 57, 59
31.	*Luffa cylindrica* (Linn.) M.J. Roem.	8	2, 8, 9, 35, 45, 54, 59, 84
32.	*Lycopersicon esculentum* Mill.	17	2, 4, 9, 13, 19, 23, 33, 34, 59, 66, 67, 68, 72, 73, 75, 78, 79
33.	*Momordica charantia* Linn.	6	2, 7, 9, 49, 59, 62
34.	*M. cochinchinesis* (Lour.) Spreng.	6	6, 19, 36, 44, 46, 59
35.	*Phaseolus lunatus* (Linn.) Walp.	8	1, 7, 23, 43, 50, 53, 59, 60
36.	*P. vulgaris* Linn.	10	2, 12, 14, 41, 48, 51, 59, 65, 75, 78
37.	*Pisum sativum* Linn.	15	2, 9, 12, 30, 32, 37, 38, 39, 44, 50, 59, 70, 75, 78, 94
38.	*Praecitrullus fistulosus* (Stocks) Pangalo	8	2, 24, 37, 43, 58, 59, 63, 80
39.	*Raphanus sativus* Linn.	4	9, 59, 63, 71
40.	*Solanum melongena* Linn. (white, elongate)	11	6, 9, 10, 32, 44, 47, 50, 59, 64, 69, 92
41.	*S. melongena* Linn. (purple, elongate)	6	1, 2, 28, 43, 50, 59
42.	*S. melongena* Linn. (purple, round)	7	10, 14, 30, 40, 50, 59, 78
43.	*S. tuberosum* Linn.	11	2, 4, 9, 24, 27, 30, 39, 43, 44, 50, 59
44.	*Spinacia oleracea* Linn.	5	2, 23, 58, 59, 65
45.	*Trichosanthes dioica* Roxb.	7	3, 39, 40, 50, 59, 75, 80
46.	*Trigonella foenum- graecum* Linn.	21	2, 5, 9, 29, 30, 31, 38,39,44,50,59,60,63,64,69,75,76,78,81,82, 90
47.	*Vicia faba* Linn.	7	2, 9, 44, 46, 50, 60, 75
48.	*Vigna radiata* (Linn.) Wilczek	8	8, 9, 15, 50, 59, 60, 78, 91
49.	*V. unguiculata* (Linn.) Walp.	7	9, 23, 28, 47, 56, 59, 65
50.	*Zea mays* Linn.	21	2,9,16,17,19,23,26,30,33,36,44,50,58,59,65,69,75, 78, 81, 85, 86

Table 3. (Continue)

Name of AMF species	
1. *Acaulospora appendiculata* Sieverding & Schenck	48. *G. intraradices* Schenck & Smith
2. *A.bireticulata* Rothwell & Trappe	49. *G. invermaium* Hall
3. *A. denticulata* Sieverding & Toro	50. *G. lamellosum* Dalpé, Koske & Tews
4. *A. elegans* Trappe & Gerdemann	51. *G. luteum* Kennedy, Stitz & Morton
5. *A. foveata* Trappe & Janos	52. *G. macrocarpum* Tulasne & Tulasne
6. *A. gedanensis* Blaskowski	53. *G. maculosum* Miller & Walker
7. *A. gerdemannii* Schenck & Nicolson	54. *G. magnicaule* Hall
8. *A. lacunosa* Morton	55. *G. manihotis* Howeler, Sieverding & Schenck
9. *A. laevis* Gerdemann & Trappe	56. *G. melanosporum* Gerdemann & Trappe
10. *A. mellea* Spain & Schenck	57. *G. microcarpum* Tulasne & Tulasne
11. *A. nicolsonii* Walker, Reed & Sanders	58. *G. monosporum* Gerdemann & Trappe
12. *A. rehmii* Sieverding & Toro	59. *G. mosseae* (Nicolson & Gerdemann) Gerdemann & Trappe
13. *A. scrobiculata* Trappe	60. *G. multicaule* Gerdemann & Bakshi
14. *A. sporocarpia* Berch	61. *G. pachycaule* Wu & Chen
15. *A. trappei* Ames & Linderman	62. *G. pallidum* Hall
16. *A. tuberculata* Janos & Trappe	63. *G. pansihalos* Berch & Koske
17. *Acaulospora* sp. 1 (unidentified)	64. *G. pubescens* (Saccardo & Ellis) Trappe & Gerdemann
18. *Acaulospora* sp. 2 (unidentified)	65. *G. reticulatum* Bhattacharjee & Mukerji
19. *Entrophospora infrequens* (Hall) Ames & Scheinder	66. *G. rubiforme* (Gerdemann & Trappe) Almeida & Schenck
20. *Entrophospora* sp. 1 (unidentified)	67. *G. scintillans* Rose & Trappe
21. *Entrophospora* sp. 2 (unidentified)	68. *G. segmentatum* Trappe, Spooner & Ivory
22. *Entrophospora* sp. 3 (unidentified)	69. *G. sinuosum* (Gerdemann & Bakshi) Almeida & Schenck
23. *Glomus aggregatum* Schenck & Smith emend. Koske	70. *G. spinosum* Hu
24. *G. albidum* Walker & Rhodes	71. *G. tenerum* Tandy
25. *G. aurantium* Blaskowski, Blanke, Renker & Buscot	72. *G. tubiformis* Tandy
26. *G. badium* Oehl, Redecker & Sieverding	73. *G. verruculosum* Blaszkowski
27. *G. boreale* (Thaxter) Trappe & Gerdemann	74. *G. vesiculiferum* (Thaxter) Gerdemann & Trappe
28. *G. caledonium* (Nicolson & Gerdemann) Trappe & Gerdeman	75. *G. velum* Porter & Hall
29. *G. claroideum* Schenck & Smith	76. *Gigaspora albida* Schenck & Smith
30. *G. clarum* Nicolson & Schenck	77. *G. calospora* (Nicolson & Gerdemann) Gerdemann
31. *G. clavisporum* (Trappe) Almeida & Schenck	78. *G. gigantea* (Nicolson & Gerdemann) Gerdemann & Trappe
32. *G. constrictum* Trappe	79. *G. margarita* Becker & Hall
33. *G. convolutum* Gerdemann & Trappe	80. *G. pellucida* Nicolson & Schenck
34. *G. coronatum* Giovannetti	81. *G. rosea* Nicolson & Schenck
35. *G. deserticola* Trappe, Bloss & Menge	82. *G. gregaria* Schenck & Nicolson
36. *G. diaphanum* Morton & Walker	83. *Gigaspora* sp. 1 (unidentified)
37. *G. duscii* (Patouillard) Van Hohn	84. *Gigaspora* sp. 2 (unidentified)
38. *G. etunicatum* Becker & Gerdemann	85. *Gigaspora* sp. 3 (unidentified)
39. *G. fasciculatum* (Thaxter) Gerdemann & Trappe emend. Walker & Koske	86. *Sclerocystis coremoides* Berkely & Broome
	87. *S. cunninghamia* Hu
40. *G. formosanum* Wu & Chen	88. *Sclerocystis* sp. 1 (unidentified)
41. *G. fragile* (Berkeley & Broome) Trappe & Gerdemann	89. *Sclerocystis* sp. 2 (unidentified)
42. *G. fragilistratum* Skou & Jacobsen	90. *Scutellospora aurigloba* (Hall) Walker & Sanders
43. *G. fuegianum* (Spegazzini) Trappe & Gerdemann	91. *Scutellospora* sp.2 (unidentified)
44. *G. geosporum* (Nicolson & Gerdemann) Walker	92. *Scutellospora* sp.1= *Dentiscutata sp.* (unidentified)
45. *G. glomerulatum* Sieverding	93. *Scutellospora* sp.3 (unidentified)
46. *G. heterosporum* Smith & Schenck	94. *Scutellospora* sp.4 (unidentified)
47. *G. indicum* Blaskowski, Wubet, Harikumar, Ryszka & Buscot	

Occurrence of AMF Morphological Types

The microscopic analysis of the plant root pieces showed the presence of AMF intercellular hyphae, arbuscules, vesicles and hyphal coils (Figure 1). The presence of linear or parallel mycelium characteristic of Arum–type was seen in majority of the vegetable crops. In contrast, some plants showed the presence of Paris–type, which was characterized by the presence of hyphal coils. Prominent hyphal coils were detected in *T. foenum–graecum* and *S. tuberosum* (Figure 1 G, H). Moreover, several other shape of mycelium (H, Y, T, X, lobed, twisted & beaded) was also encountered (Figure 1 K-P). Root penetration through formation of

appresorium was clearly detected in the root of *P. sativum* and *C. longa* (Figure 1B) while little bit of extraradical mycelium in the form of parallel running hyphae was detected on the root tips of Brassicaceae (Figure 1C). The details of AMF colonization pattern are furnished in Table 2. Vesicles were detected in majority of the plants while arbuscules were rarely found (Figure 1 E,F). Vesicle shape also showed tremendous variation ranging from round (*A. cepa*), oval (*A. sativum*), beaked (*C. longa*), pear (*Zea mays*), rectangular (*L. esculentum*), elliptical (*C. indica*), triangular (*V. unguiculata*) to irregular (*V. faba*, *T. dioica*) either singly, in pairs and in groups (*C. arietinum* and *T. foenum–graecum*). Likewise, globose vesicles with funnel shaped hyphal attachment were mainly formed in *C. arietinum*.

Extend of AMF Colonization

Maximum colonization was recorded in plants collected from Panchkula, Ambala and Kurukshetra district (Table 2). Based on percentage colonization, plants were classified into those having highest (100%), high (75–99.9%), moderate (50–75%), low (25–50%) and least (1–25%) colonization. Highest colonization was observed in *A. cepa*, *A. sativum*, *C. arietinum*, *T. foenum–graecum* and *Z. mays* while least was detected in *B. rapa* (2.22±3.04). Seven members of non-mycorrhizal family Brassicaceae showed low colonization (Table 3).

AMF Species Richness, Spore Abundance and Frequency of Occurrence

Data recorded from Table 4 showed maximum AMF species in *T. foenum–graecum* and *Z. mays* (21 each) followed by *A. cepa* (19), while only 3 species were detected in *B. vulgaris* and *B. rapa*. Altogether 94 species representing different genera of AMF i.e., *Acaulospora*, *Entrophospora*, *Glomus*, *Gigaspora*, *Sclerocystis* and *Scutellopsora* were detected. Two genera viz. *Glomus* and *Acaulospora* were dominantly present. Fifty-three species of *Glomus*, 18 of *Acaulospora*, 10 of *Gigaspora*, 5 of *Scutellospora*, 4 each of *Entrophospora* and *Sclerocystis* were detected. The most frequent species among vegetable crops was putatively assigned to *Glomus mosseae* (now called as *Funneliformis mosseae*) occurring in 46 studied samples with 92% frequency of occurrence (Table 4).

Table 4. Species abundance and frequency of occurrence of isolated AM fungal species

S. no.	Isolated AM fungal species	Species abundance	Frequency of occurrence (%)
1.	*Acaulospora appendiculata* Sieverding & Schenck	2	4
2.	*A.bireticulata* Rothwell & Trappe	26	52
3.	*A. denticulata* Sieverding & Toro	3	6
4.	*A. elegans* Trappe & Gerdemann	4	8
5.	*A. foveata* Trappe & Janos	4	8
6.	*A. gedanensis* Blaskowski	4	8
7.	*A. gerdemannii* Schenck & Nicolson	4	8
8.	*A. lacunosa* Morton	5	10
9.	*A. laevis* Gerdemann & Trappe	30	60
10.	*A. mellea* Spain & Schenck	4	8
11.	*A. nicolsonii* Walker, Reed & Sanders	1	2
12.	*A. rehmii* Sieverding & Toro	5	10
13.	*A. scrobiculata* Trappe	4	8
14.	*A. sporocarpia* Berch	2	4
15.	*A. trappei* Ames & Linderman	3	6
16.	*A. tuberculata* Janos & Trappe	1	2
17.	*Acaulospora* sp. 1 (unidentified)	1	2
18.	*Acaulospora* sp. 2 (unidentified)	1	2
19.	*Entrophospora infrequens* (Hall) Ames & Scheinder	4	8
20.	*Entrophospora* sp. 1 (unidentified)	1	2
21.	*Entrophospora* sp. 2 (unidentified)	1	2
22.	*Entrophospora* sp. 3 (unidentified)	1	2
23.	*Glomus aggregatum* Schenck & Smith emend. Koske	12	24
24.	*G. albidum* Walker & Rhodes	3	6
25.	*G. aurantium* Blaskowski, Blanke, Renker & Buscot	2	4
26.	*G. badium* Oehl, Redecker & Sieverding	2	4
27.	*G. boreale* (Thaxter) Trappe & Gerdemann	1	2
28.	*G. caledonium* (Nicolson & Gerdemann) Trappe & Gerdemann	5	10
29.	*G. claroideum* Schenck & Smith	4	8
30.	*G. clarum* Nicolson & Schenck	7	14
31.	*G. clavisporum* (Trappe) Almeida & Schenck	2	4
32.	*G. constrictum* Trappe	4	8
33.	*G. convolutum* Gerdemann & Trappe	3	6

34.	*G. coronatum* Giovannetti	3	6
35.	*G. deserticola* Trappe, Bloss & Menge	3	6
36.	*G. diaphanum* Morton & Walker	3	6
37.	*G. duscii* (Patouillard) Van Hohn	2	4
38.	*G. etunicatum* Becker & Gerdemann	3	6
39.	*G. fasciculatum* (Thaxter) Gerdemann & Trappe emend. Walker & Koske	9	18
40.	*G. formosanum* Wu & Chen	2	4
41.	*G. fragile* (Berkeley & Broome) Trappe & Gerdemann	2	4
42.	*G. fragilistratum* Skou & Jacobsen	1	2
43.	*G. fuegianum* (Spegazzini) Trappe & Gerdemann	9	18
44.	*G. geosporum* (Nicolson & Gerdemann) Walker	16	32
45.	*G. glomerulatum* Sieverding	2	4
46.	*G. heterosporum* Smith & Schenck	2	4
47.	*G. indicum* Blaskowski, Wubet, Harikumar, Ryszka & Buscot	3	6
48.	*G. intraradices* Schenck & Smith	4	8
49.	*G. invermaium* Hall	2	4
50.	*G. lamellosum* Dalpé, Koske & Tews	21	42
51.	*G. luteum* Kennedy, Stitz & Morton	2	4
52.	*G. macrocarpum* Tulasne & Tulasne	2	4
53.	*G. maculosum* Miller & Walker	2	4
54.	*G. magnicaule* Hall	2	4
55.	*G. manihotis* Howeler, Sieverding & Schenck	2	4
56.	*G. melanosporum* Gerdemann & Trappe	4	8
57.	*G. microcarpum* Tulasne & Tulasne	3	6
58.	*G. monosporum* Gerdemann & Trappe	4	8
59.	*G. mosseae* (Nicolson & Gerdemann) Gerdemann & Trappe	46	92
60.	*G. multicaule* Gerdemann & Bakshi	4	8
61.	*G. pachycaule* Wu & Chen	1	2
62.	*G. pallidum* Hall	4	8
63.	*G. pansihalos* Berch & Koske	3	6
64.	*G. pubescens* (Saccardo & Ellis) Trappe & Gerdemann	3	6
65.	*G. reticulatum* Bhattacharjee & Mukerji	4	8
66.	*G. rubiforme* (Gerdemann & Trappe) Almeida & Schenck	3	6
67.	*G. scintillans* Rose & Trappe	2	4
68.	*G. segmentatum* Trappe, Spooner & Ivory	2	4
69.	*G. sinuosum* (Gerdemann & Bakshi) Almeida & Schenck	6	12
70.	*G. spinosum* Hu	3	6
71.	*G. tenerum* Tandy	3	6
72.	*G. tubiformis* Tandy	1	2
73.	*G. verruculosum* Blaszkowski	2	4
74.	*G. vesiculiferum* (Thaxter) Gerdemann & Trappe	1	2
75.	*G. velum* Porter & Hall	15	30
76.	*Gigaspora albida* Schenck & Smith	2	4
77.	*G. calospora* (Nicolson & Gerdemann) Gerdemann	2	4
78.	*G. gigantea* (Nicolson & Gerdemann) Gerdemann & Trappe	10	20
79.	*G. margarita* Becker & Hall	3	6
80.	*G. pellucida* Nicolson & Schenck	2	4
81.	*G. rosea* Nicolson & Schenck	5	10
82.	*G. gregaria* Schenck & Nicolson	1	2
83.	*Gigaspora* sp. 1 (unidentified)	1	2
84.	*Gigaspora* sp. 2 (unidentified)	1	2
85.	*Gigaspora* sp. 3 (unidentified)	1	2
86.	*Sclerocystis coremoides* Berkely & Broome	3	6
87.	*S. cunninghamia* Hu	2	4
88.	*Sclerocystis* sp. 1 (unidentified)	1	2
89.	*Sclerocystis* sp. 2 (unidentified)	1	2
90.	*Scutellospora aurigloba* (Hall) Walker & Sanders	5	10
91.	*Scutellospora* sp. 2 (unidentified)	1	2
92.	*Scutellospora* sp. 1= *Dentiscutata* sp. (unidentified)	1	2
93.	*Scutellospora* sp. 3 (unidentified)	1	2
94.	*Scutellospora* sp. 4 (unidentified)	1	2

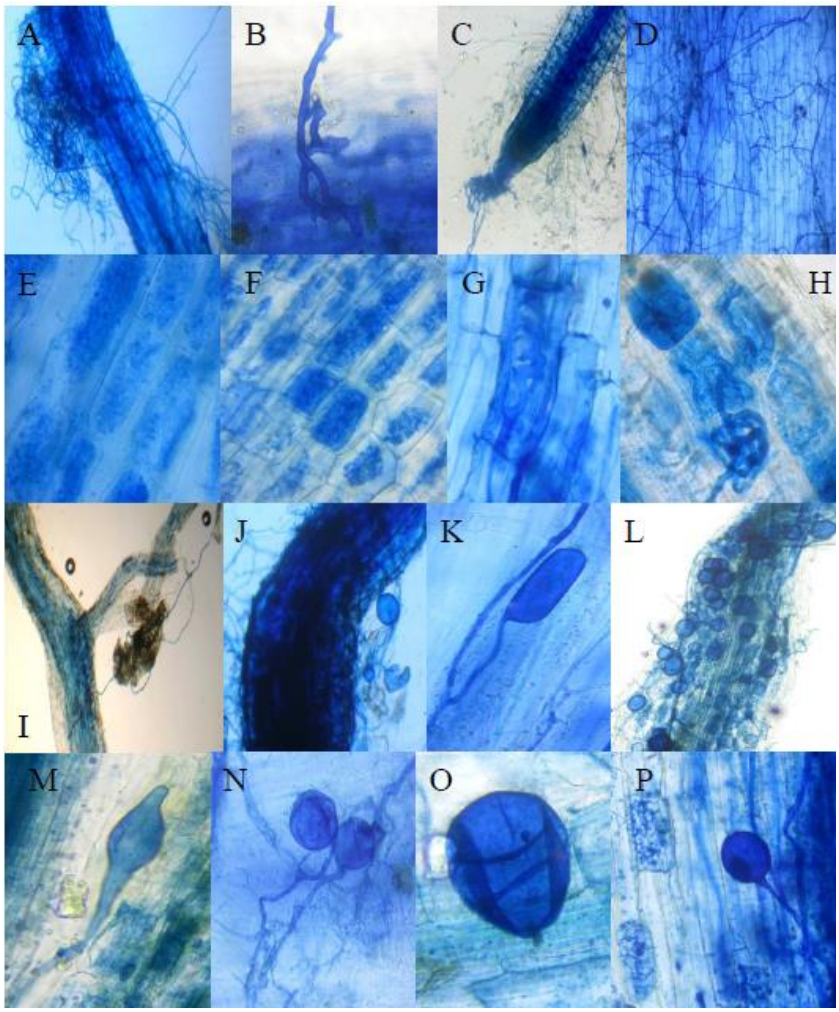

Figure 1. A: Shows the presence of extensive extramatrical mycelium, B: Appresorium formation and intrusion of AMF hyphae into host roots, C: Colonization of root tip, D: Extensive intramatrical mycelium, E-F: Arbuscules, G-H: Paris-type, I: Germinating AMF spore, J: Extra-radical vesicles, K-P: Different types of intra-radical vesicles, K: Rectangular, L: Small, round & scattered, M: Beaked, N: Big, round & paired, O: Pear, P: Globose with funnel shaped hyphal attachment.

Discussion

Considering the high production cost of olericultural crops, the adoption of AMF inoculation practice can substitute the high input production (Tanwar and Aggarwal, 2014). But before that, knowing the AMF status of crop is important for the selection of efficient strain. All the plant species studied in this investigation showed the presence of AMF association indicating that the AMF are widely distributed in studied site. Yet lot of variation was detected among members of same family, same genera and same locality. This confirms host preference as the prime factor determining AMF symbiosis in soil. Perhaps, abundance of AMF species behaves as indicator species for particular habitats and land sites which might provide certain ecosystem services at their habitats (Oehl et al., 2017). Highest mean spore density was found with *Z. mays* and *A. cepa*. Same results have been observed by Sinegani and Sharifi (2007) and Tran et al. (2019) with maximum AMF spore abundance in *A. cepa* and *A. ampeloprasum* var. *porrum* respectively. Likewise, abundant spore population in the rhizosphere soil of *Capsicum annuun* and *Vigna unguiculata* has been documented by Ríos–Ruiz et al. (2019). Distribution of AMF is a contemporary ecological process. Even some of the plant of same species that differ in age harboured distinctive AMF populations (Husband et al., 2002). Not only the AMF spore density but the AMF spore richness and abundance was also found highest in *Zea mays* and *T. foenum–graecum* followed by *A. cepa* and *L. esculentum* while some plants inhabits quite low AMF spores like members of Cucurbitaceae. Several factors contribute to low AMF population in the soil, including presence of different host plant, application of excess fertilizer and time of sampling (Cassazza et al., 2017).

AMF are considered as essential constituent of soil forming symbiosis with plants roots and positively influence ecosystems functioning (Diagne et al., 2020). Among all the studied plants, 5 plants exhibited 100% root colonization, above 75% and above 50% colonized roots were detected in 15 and 12 plants respectively. The presence of high mycorrhization in vegetable crops is mainly due to the high dependency of these crops on AMF as the mycorrhizal status of crops depends upon the physiological status of the host as well as host genotype (Dickie et al., 2013). Koul et al. (2012) observed 70%, 62% and 75% colonization and 17, 12 and 47 AMF propagules in *A. cepa*, *A. sativum* and *T. foenum–graecum* respectively. The discrepancy in the root

colonization could be accredited to the exudation of some specific metabolites from the plant roots that attract the AMF resulting in disparate colonization pattern amidst different plants (Wen et al., 2019).

It was inferred that the low level of spore population was not related to reduce colonization of roots and likewise plants which do not form AMF colonization inhabits acceptable spore number while few plants harbored prominent spore number which is equivalent to the high colonization of roots. These results corroborate with the findings of Sastry and Johri (1999) reporting no relationship between AMF spore number and colonization of root. AMF colonization was not detected in non mycorrhizal families however efficient AMF spores were isolated from their rhizosphere soils. All the members of non–mycorrhizal families lack hyphal infection except for *B. campestris*, *B. oleracea* var. *botrytis*, and *B. rapa* which showed 2–11% colonization. However, colonization in non–mycorrhizal plants has also been witnessed by Poveda et al. (2019) and Adekanmbi and Adewole (2019). This may be due to the intermingling of host plants roots with other mycorrhizal plant grown in the vicinity or it is plausible that crop rotation with mycorrhizal plant may have influenced sporulation in the rhizosphere of non–mycorrhizal plants. But whether an efficient symbiosis capable of benefiting the host plant is formed or not is not known because of the absence of vesicles and arbuscules in these plants. As per the studies of Wang et al. (2024) the topsoil intensify interactions amid root AMF by enhancing competitive relationships.

The data revealed uneven distribution of AMF species diversity that was affected by sampled location, land use type and its physico–chemical properties as well. All the six genera of AMF were detected which were widely distributed in the soil of different districts of Haryana. *Glomus* exhibited maximal abundance and frequency of occurrence followed by *Acaulospora*. Similarly, dominance of *Glomus* followed by *Acaulospora* has also been stated by other workers (Shukla et al., 2013; Gupta et al., 2018; Alrajhi et al., 2024). Members of Glomaraceae family reveal high ecological plasticity to occupy the more diverse habitats (Melo et al., 2020). According to Haug et al. (2019), AMF community compositions are influenced by stochastic processes and habitat filtering. This might also be due to the reason that *Glomus* and *Acaulospora* compete strongly for resources through a variety of strategies as compared to the other AMF genera to establish in the soil. The soil pH ranged from 6.10 to 7.40 i.e., slight acidic to neutral to slight alkaline and the presence of excessive AMF spores in this soil is in accordance with the inference of Jiao et al. (2011) and Parihar et al. (2019) that this pH range favour *Glomus* and *Acaulospora* sporulation and therefore *Acaulospora* was frequently witnessed in the soil of Ambala and Panchkula. Among *Glomus* species, *G. mosseae* and among *Acaulospora* species, *A. laevis* were the most preferred species by vegetable crops.

The AMF spores were isolated from the cultivated agricultural land which is prone to lot of disturbance in the form of various cultivation practices including tillage, implementation of fertilizer, pesticides etc which disturbs the growth and proliferation of AMF hypha and thus reduces the spore formation. In the present study in spite of mechanical disturbances in the cultivated land, AMF status was sufficient enough to provide benefits to the plants. Contrary to this Schalamuk et al. (2006) documented that tillage and fertilization did not affect AMF biodiversity. Interestingly a large number of AMF spores were encountered from the studied site, with highest number in slightly acidic soil of Panchkula, Ambala, Kurukshetra and Gurgaon which were comparatively beneficial for AMF survival confirmed by the frequent occurrence of AMF compared to that of Rewari, Jind and Sirsa that harbour least AMF spore density. This is in accordance with the view of Dessai and Rodrigues (2012) that the soil pH range from acidic to neutral inhabits a more AMF species number as compared to the neutral to slight alkaline soil of other regions and suggest that the soil AMF community can adapt to different environmental conditions and host type. Thorough microscopic investigation of the plant root segments showed the presence of arbuscules, vesicles, hyphal infection which was much toward Arum–type, but in some crops AMF hyphal coils were also seen which belongs to Paris–type. The variations in root colonization are thought to be linked to soil properties and AMF communities (Han et al., 2019).

Conclusion

Vegetable crops are recognized for their pronounced reliance on the existence of symbiotic fungal endophytes to grow, establish and produce yield. The study demonstrates that tomato crops exhibit the highest AMF colonization, which suggests their significant potential for enhancing nutrient uptake efficiency in sustainable vegetable production systems. AMF association with vegetable crops of Haryana was never analyzed before and such recommendations would provide direction for further studies The finding of the present investigation can be pathway for researcher to make AMF formulation to be used in vegetable production system. The outcomes of this inquiry pave the way for researchers to formulate AMF preparations tailored for use in vegetable production systems. The findings of the present investigation highlight the importance of AMF inoculation in vegetable cropping systems to improve nutrient use efficiency, potentially reducing the

dependence on chemical fertilizers and contributing to sustainable agriculture. Furthermore, the practical agricultural implications of this study are to aids researcher in comprehending the diversity and composition of AMF in conjunction with vegetable crops, a fundamental aspect in grasping these crops' dependency on AMF. The regional specific survey of confined number of vegetable species may limit the generalizability of the findings to other agro-ecological zones. Future research should focus on field level validation of AMF inoculation and its long-term effects on soil health and crop productivity under different environmental conditions.

Acknowledgments

The financial assistance in the form of university research scholarship provided by Kurukshetra University Kurukshetra to Anju Tanwar is highly acknowledged. The authors also wish to thank Dr. Vipin Parkash, Scientist, Forest Pathology Division, Forest research Institute Dehradun for identifying AMF spores.

References

Adekanmbi, A.E., Adewole, M.B., 2019. Effects of arbuscular mycorrhiza fungi, organic fertilizer and different moisture regimes on soil properties and yield of *Amaranthus cruentus*. *Journal of Agricultural Science* 64(2): 147–163.

Adholeya, A., Gaur, A., 1994. Estimation of VAM fungal spores in soil. *Mycorrhiza News* 6(1): 10–11.

Alguacil, M.E., Diaz–Pereira del M., Caravaca, F., Frenandez, D.A., Roldán, A., 2009. Increased diversity of arbuscular mycorrhizal fungi in a long term field experiment via application of organic amendments to a semiarid degraded soil. *Applied and Environmental Microbiology* 75(13): 4254–4263.

Alrajhi, K., Bibi, S., Abu-Dieyeh, M., 2024. Diversity, Distribution, and applications of arbuscular mycorrhizal fungi in the Arabian Peninsula. *Saudi Journal of Biological Sciences*. 31(2): 103911.

Bi, Y., Ma, W., Xing, F., Gao, Y., Li, Z., Chen, C., Mu, X., Li, X., Zhu, X., 2020. Diversity and specificity of arbuscular mycorrhizal fungi in the rhizosphere of six plants in the Songnen grassland, China. *Écoscience* 27(1): 11–21.

Cassazza, G., Lumini, E., Ercole, E., Dovana, F., Guerrina, M., Arnulfo, A., Minuto, L., Fusconi, A., Mucciarelli, M., 2017. The abundance and diversity of arbuscular mycorrhizal fungi are linked to the soil chemistry of screes and to slope in the Alpic paleo–endemic *Berardia subacaulis*. *PLoS ONE* 12(2): e0171866.

Castillo, C.G., Borie, F., Oehl, F., Sieverding, E., 2016. Arbuscular mycorrhizal fungi biodiversity: prospecting in Southern–Central zone of Chile. A review. *Journal of Soil Science and Plant Nutrition* 16(2): 400–422.

Dessai, S.A., Rodrigues, B.F., 2012. Diversity studies on arbuscular mycorrhizal fungi in vegetable crop plants of Goa, India. *Plant Pathology and Quarantine* 2(1): 87–101.

Diagne, N., Ngom, M., Djighaly, P.I., Fall, D., Hocher, V., Svistoonoff, S. 2020. Roles of arbuscular mycorrhizal fungi on plant growth and performance: importance in biotic and abiotic stressed regulation. *Diversity* 12**:** 370.

Dickie, I.A., Martínez–García, L.B., Koele, N., Grelet, G.A., Tylianakis, J.M. Peltzer, D.A., Richardson, S.A., 2013. Mycorrhizas and mycorrhizal fungal communities throughout ecosystem development. *Plant and Soil* 367: 11–39.

Gerdemann, J.W., Nicolson, Y.H., 1963. Spores of mycorrhiza *Endogone* species extracted from soil by wet sieving and decanting. *Transactions of the British Mycological Society* 46: 235–244.

Giovannetti, M., Mosse, B., 1980. An evaluation of techniques for measuring vesicular arbuscular infection in roots. New Phytology 84: 489–500.

Gupta, M.M., Gupta, A., Kumar, P., 2018. Urbanization and biodiversity of arbuscular mycorrhizal fungi: The case study of Delhi, India. Revista de Biología Tropical 66(4): 1547–1558.

Han, X., Xu, C., Wang, Y., Huang, D., Fan, Q., Xin, G., Müller, C., 2019. Dynamics of arbuscular mycorrhizal fungi in relation to root colonization, spore density, and soil properties among different spreading stages of the exotic plant three flower beggarweed (*Desmodium triflorum*) in a *Zoysia tenuifolia* lawn. *Weed Science* 67(6): 689–701.

Haug, I., Setaro, S., Suárez, J.P. 2019. Species composition of arbuscular mycorrhizal communities changes with elevation in the Andes of South Ecuador. *PLoS ONE* 14(8): e0221091.

Higo, M., Isobe, K., Yamaguchi, M., Drijber, R.A., Jeske, E.S., Ishii, R., 2013. Diversity and vertical distribution of indigenous arbuscular mycorrhizal fungi under two soybean rotational systems. *Biology and Fertility of Soils* 48(8): 911–922.

Husband, R., Herre, E.A., Turner, S.L., Gallery, R., Young, J.P.W., 2002. Molecular diversity of arbuscular mycorrhizal fungi and patterns of host association over time and space in a tropical forest. *Molecular Ecology* 11: 2669–2678.

Jiao, H., Chen, Y.L., Lin, X.G., Liu, R.J., 2011. Diversity of arbuscular mycorrhiza fungi in greenhouse soils continuously planted to watermelon in North China. *Mycorrhiza* 21: 681–688.

Johnson, J.M., Houngnandan, P., Kane, A. Sanon, K.B., Neyra, M., van Tuinen, D., 2015. Colonization and molecular diversity of arbuscular mycorrhizal fungi associated with the rhizosphere of cowpea (*Vigna unguiculata* (L.) Walp.) in Benin (West Africa): an exploratory study. *Annals of Microbiology* 66: 207–221.

Khastini, R.O., Sari, I.J., Wahyuni, I., Sumantri, A., 2020. The diversity of arbuscular mycorrhizal fungi associated with rambutan tangkue cultivar in Lebak, Banten Province. *AIP Conference Proceedings* 2231: 040047.

Koul, K.K., Agarwal, S., Lone, R., 2012. Diversity of arbuscular mycorrhizal fungi associated with the medicinal plants from Gwalior–Chambal region of Madhya Pradesh, India. *American-Eurasian Journal of Agricultural and Environmental Science* 12(8): 1004–1011.

Kumar, S.C.P., Garampalli, R.H., 2013. Diversity of arbuscular mycorrhizal fungi in irrigated and non–irrigated fields of southern Karnataka, India. *Journal of Environmental Biology* 34: 159–164.

Li, L.F., Li, T., Zhang, Y., Zhao, Z.W., 2010 Molecular diversity of arbuscular mycorrhizal fungi and their distribution patterns related to host–plants and habitats in a hot and arid ecosystem, southwest China. *FEMS Microbiology Ecology* 71(3): 418–427.

Ma, X., Xu, X., Geng, Q., Luo, Y., Ju, C., Li, Q., Zhou, Y., 2023. Global arbuscular mycorrhizal fungal diversity and abundance decreases with soil available phosphorus. *Global Ecology and Biogeography* 32(8): 1423-1434.

Melo, C.D., Walker, C., Freitas, H., Machado, A.C., Borges, P.A.V., 2020. Distribution of arbuscular mycorrhizal fungi (AMF) in Terceira and São Miguel Islands (Azores). *Biodiversity Data Journal* 8: e49759.

Morton, J.B., Redecker, D., 2001. Two new families of Glomales, Archaeosporaceae and Paraglomaceae, with two new genera Archaeospora and Paraglomus, based on concordant molecular and morphological characters. *Mycologia* 93: 181–195.

Mukerji, K.G., 1996. Taxonomy of endomycorrhizal fungi. In: Advances in Botany. Mukerji, K.G., Mathur, B., Chamola, B.P., Chitralekha P. (Eds.). A.P.H. Publishing Corporation, New Delhi, India. pp.211–221.

Oehl, F., Laczko, E., Oberholzer, H.R., Jansa, J., Egli, S., 2017. Diversity and biogeography of arbuscular mycorrhizal fungi in agricultural soils. *Biology and Fertility of Soils* 53: 777–797.

Parihar, M., Rakshit, A., Singh, H.B., Rana, K., 2019. Diversity of arbuscular mycorrhizal fungi in alkaline soils of hot sub humid eco–region of Middle Gangetic Plains of India. *Acta Agricultural Scandinavica Section B—Soil Plant Science* 69(5): 386-397.

Pellegrino, E., Gamper, H.A., Ciccolini, V., Ercoli, L., 2020. Forage rotations conserve diversity of arbuscular mycorrhizal fungi and soil fertility. *Frontiers in Microbiology* 10: 2969.

Phillips, J.M., Hayman, D.S., 1970. Improved produces for clearing roots and staining parasitic and VAM fungi for rapid assessment of infection. *Transactions of the British Mycological Society* 55: 158–161.

Poveda, J., Hermosa, R., Monte, E., Nicolás, C., 2019. *Trichoderma harzianum* favours the access of arbuscular mycorrhizal fungi to non–host Brassicaceae roots and increases plant productivity. *Scientific Reports* 9: 11650.

Powell, J.R., Rillig, M.C., 2018. Biodiversity of arbuscular mycorrhizal fungi and ecosystem function. *New Phytology* 220: 1059–1075.

Ríos–Ruiz, W.F., Barrios–López, L., Rojas–García, J.C., Valdez–Nuñez, R.A., 2019. Mycotrophic capacity and diversity of native arbuscular mycorrhizal fungi isolated from degraded soils. *Scientia Agropecuaria* 10(1): 99–108.

Santos–González, J.C., Finlay, R.D., Tehler, A., 2006. Seasonal dynamics of arbuscular mycorrhizal root colonization in a seminatural grassland. *Applied Environmental Microbiology* 73: 5613–5623.

Sastry, M.S.R., Johri, B.N., 1999. Arbuscular mycorrhizal fungal diversity of stressed soils of Bailadila iron ore sites in Bastar region of Madhya Pradesh. *Current Science* 77(8): 1095–1100.

Schalamuk, S., Velazquez, S., Chidichimo, H., Cabello, M., 2006. Fungal spore diversity of arbuscular mycorrhizal fungi associated with spring wheat: effects of tillage. *Mycologia* 98(1): 16–22.

Schenck, N.C., Pérez, Y., 1990. Manual for the Identification of VA Mycorrhizal Fungi. Synergistic Publications, 286p.

Shukla, A., Vyas, D., Jha, A., 2013. Soil depth: an overriding factor for distribution of arbuscular mycorrhizal fungi. *Journal of Soil Science and Plant Nutrition* 13(1): 23–33.

Sinegani, A.A.S., Sharifi, Z., 2007. The abundance of arbuscular mycorrhizal fungi spores in rhizospheres of different crops. *Turkish Journal of Biology* 31: 181–185.

Tanwar, A., Aggarwal, A., 2014. Multifaceted potential of bioinoculants on red bell pepper (F1 hybrid, Indam Mamatha) production. *Journal of Plant Interactions* 9(1): 82–91.

Tanwar, A., Singh, A., Aggarwal, A., Jangra, E., Pichardo, S.T. 2021. Evaluation of municipal sewage sludge for Arbuscular mycorrhizal fungi inoculum production. *Eurasian Journal of Soil Science* 10(4): 343–353.

Tran, B.T.T., Watts–Williams, S.J., Cavagnaro, T.R., 2019. Impact of an arbuscular mycorrhizal fungus on the growth and nutrition of fifteen crop and pasture plant species. *Functional Plant Biology* 46: 732–742.

Wahab, A., Muhammad, M., Munir, A., Abdi, G., Zaman, W., Ayaz, A., Khizar, C., Reddy, S.P.P., 2023. Role of arbuscular mycorrhizal fungi in regulating growth, enhancing productivity, and potentially influencing ecosystems under abiotic and biotic stresses. *Plants* 12(17): 3102.

Wang, F., Zhang, L., Zhou, J., Rengel, Z., George, T.S., Feng, G., 2022. Exploring the secrets of hyphosphere of arbuscular mycorrhizal fungi: processes and ecological functions. *Plant and Soil* 481: 1–22.

Wang, Z., Zhao, J., Xiao, D., Chen, M., He, X., 2024. Higher colonization but lower diversity of root-associated arbuscular mycorrhizal fungi in the topsoil than in deep soil. *Applied Soil Ecology* 194: 105195.

Wen, Z., Li, H., Shen, Q., Tang, X., Xiong, C., Li, H., Pang, J., Ryan, M.H., Lambers, H., and Shen, J., 2019. Tradeoffs among root morphology, exudation and mycorrhizal symbioses for phosphorus–acquisition strategies of 16 crop species. *New Phytology* 223: 882–895.

Yang, H., Zang, Y., Yuan, Y., Tang, J., Chen, X., 2012. Selectivity by host plants affects the distribution of arbuscular mycorrhizal fungi: evidence from ITS rDNA sequence metadata. *BMC Evolutionary Biology* 12: 50.

Eurasian Journal of Soil Science 2025, 14(1), 58 - 66

Eurasian Journal of Soil Science

Journal homepage : http://ejss.fesss.org

Effect of nitrogen and sulfur combinations on spring wheat (*Triticum aestivum*) growth, yield, and soil nutrient availability in a greenhouse experiment

Gulbaram Nurgaliyeva [a], Aizhan Akmullayeva [b], Gulnar A. Myrzabayeva [c,*], Gulnara Tastanbekova [d], Zhanar Izbassarova [c], Zhanylkhan Bukabayeva [e], Gulnissam Rvaidarova [f], Dastan Mussapirov [c]

[a] West Kazakhstan Agrarian and Technical University named after Zhangir Khan, Uralsk, Kazakhstan
[b] Zhetysu University named after Ilyas Zhansugurov, Taldykorgan, Kazakhstan
[c] Kazakh National Agrarian Research University, Almaty, Kazakhstan
[d] Mukhtar Auezov South Kazakhstan University, Symkent, Kazakhstan
[e] Alikhan Bokeikhan University, Semey, Kazakhstan
[f] Kazakh Scientific Research Institute for Plant Protection and Quarantine, Almaty, Kazakhstan

Article Info
Received : 15.02.2024
Accepted : 25.10.2024
Available online: 01.11.2024

Author(s)
G.Nurgaliyeva
A.Akmullayeva
G.A.Myrzabayeva *
G.Tastanbekova
Z.Izbassarova
D.Mussapirov
Z.Bukabayeva
G.Rvaidarova

* Corresponding author

Abstract

Effective management of nitrogen (N) and sulfur (S) is crucial for maximizing spring wheat productivity, as both nutrients play key roles in improving growth, yield attributes, grain protein content, and soil fertility. Despite their importance, determining the optimal application rates of N and S for enhanced wheat performance remains a challenge. This study was conducted as a pot experiment under controlled greenhouse conditions, with 12 treatments replicated three times and carried out over 85 days. The treatments included a control (0N + 0S), nitrogen-only treatments (40N + 0S, 80N + 0S, 120N + 0S), sulfur-only treatments (30S, 60S), and combined N and S treatments (40N + 30S, 80N + 30S, 120N + 30S, 40N + 60S, 80N + 60S, 120N + 60S). The results revealed that the application of 120N + 60S significantly improved key growth parameters such as plant height, grains per spike, spike density (spike/m^2), and 1000-grain weight. This treatment also resulted in higher grain nitrogen content, N uptake, and protein levels, confirming its superiority over other treatments. Additionally, post-harvest soil analysis indicated increased mineral N and available S levels, while showing a slight decrease in pH and an increase in electrical conductivity (EC). In conclusion, the 120N + 60S combination was identified as the most effective treatment for maximizing wheat yield, improving grain quality, and enhancing soil nutrient availability. However, it is recommended that future studies validate these findings under field conditions, across different soil types and climates, to ensure broader applicability of 120N + 60S as a best practice for wheat cultivation.

Keywords: Wheat productivity, Nitrogen and sulfur fertilization, Grain protein content, Nutrient use efficiency (NUE), Greenhouse pot experiment.

Introduction

Wheat (*Triticum aestivum*) is one of the most important staple crops globally, contributing significantly to food security and human nutrition (Shewry, 2009). Its production is critical, accounting for approximately 20% of the daily caloric intake worldwide, and providing substantial amounts of carbohydrates (55%) and proteins (8-12%). The quality and yield of wheat are influenced by a variety of factors, including environmental conditions, fertilizer management, and the genotype of the cultivated variety (Souza et al., 2004). Most wheat varieties are selected for traits such as milling performance, protein content, and baking

: https://doi.org/10.18393/ejss.1577652
: https://ejss.fesss.org/10.18393/ejss.1577652
Publisher : Federation of Eurasian Soil Science Societies
e-ISSN : 2147-4249

properties (Branlard et al., 2001; Gupta et al., 2021). Therefore, improving wheat growth, yield, and quality is essential for both agricultural productivity and the health benefits wheat provides to the global population (Shiferaw et al., 2013).

A critical factor in maximizing wheat yield and quality is Nutrient Use Efficiency (NUE), which refers to the plant's ability to absorb, store, utilize, and redistribute nutrients efficiently (Ghafoor et al., 2021). NUE is largely influenced by root architecture and growth, particularly in soils containing a mixture of organic and inorganic matter (Panhwar et al., 2019). Additionally, NUE is affected by external factors such as irrigation and fertilizer management. Among essential nutrients, nitrogen (N) plays a pivotal role in enhancing crop growth, as it is a fundamental component of chlorophyll, directly impacting photosynthesis and energy production (Khalofah et al., 2021). Research has shown that effective nitrogen management can significantly improve grain weight and yield, especially in cereal crops like wheat. Furthermore, nitrogen application has been positively correlated with increased protein content in wheat grains, which is a key quality attribute associated with nutritional benefits (Zhang et al., 2021; Alimbekova et al., 2022).

In addition to nitrogen, sulfur (S) is another essential nutrient crucial for plant growth and development. Sulfur is involved in the synthesis of amino acids, such as methionine and cysteine, which are vital for protein formation (Hell, 1997). Studies have shown that balanced sulfur application plays a key role in reducing oxidative stress and improving the plant's internal nutrient reduction mechanisms, ultimately leading to better productivity (Ragab and Saad-Allah, 2021). Sulfur has also been found to enhance the efficiency of nitrogen uptake and utilization, especially in the biosynthesis of protein, as nitrogen cannot optimally perform this function without sufficient sülfür (Wang et al., 2021). This makes sulfur an indispensable component for maximizing wheat grain quality and yield.

Despite the established importance of nitrogen and sulfur for wheat production, there is limited research on the optimal application rates of these nutrients when applied together. Most studies have focused on nitrogen or sulfur individually, but their combined effects on wheat productivity and grain quality remain underexplored. Given that nitrogen and sulfur exhibit a synergistic relationship, particularly in protein synthesis, understanding the best application rates for both nutrients is critical to enhancing wheat's agronomic performance.

Thus, the primary aim of this study is to investigate the combined effects of nitrogen and sulfur on wheat growth, yield, and protein content, with the goal of identifying the optimal application rates for both nutrients. By addressing the gap in the literature, this research seeks to provide valuable insights for improving wheat productivity through better nutrient management strategies. To achieve this, a pot experiment was conducted under controlled greenhouse conditions, using the Omskaya 18 variety of spring wheat, allowing for precise monitoring of plant growth, nutrient uptake, and environmental factors. This experiment serves as an initial step in understanding how nitrogen and sulfur interact to influence wheat performance, and the results will inform future field trials to assess the applicability of these findings under real-world agricultural conditions.

Material and Methods

Soil characteristics

This study was conducted under controlled greenhouse conditions using a randomized complete block design (RCBD) with three replications. The soil properties were determined according to the methods described by Rowell (1996) and Jones (2001). The experimental soil had a silty clay texture, consisting of 45% clay, 15% sand, and 40% silt. The other soil characteristics were as follows: organic matter content of 2.3%, pH (1:1) of 7.65, electrical conductivity (EC) of 0.86 dS/m, $CaCO_3$ content of 13%, total nitrogen (N) of 0.105%, available phosphorus (P) of 4.5 mg/kg, available sulfur (S) of 2176 mg/kg, and available potassium (K) of 195 mg/kg.

Experimental design and applications

Wheat (Triticum aestivum) variety Omskaya 18 was used as the test plant material. Each pot was filled with 5 kg of air-dried soil passed through a 4 mm sieve, and 15 wheat seeds were sown in each pot. The moisture content of the soil was maintained at field capacity throughout the experiment by weighing the pots daily and replacing the water lost through evapotranspiration. The effects of different nitrogen (N) and sulfur (S) levels on wheat growth were investigated. Nitrogen was applied in the form of urea (46% N), and sulfur was applied in the form of potassium sulfate (18% S). The experiment included 12 treatment combinations, with a total of 36 pots. The treatments were as follows:

1. Control (0N + 0S)
2. 40 kg/ha N (40N + 0S)
3. 80 kg/ha N (80N + 0S)
4. 120 kg/ha N (120N + 0S)
5. 30 kg/ha S (30S)
6. 40 kg/ha N + 30 kg/ha S (40N + 30S)
7. 80 kg/ha N + 30 kg/ha S (80N + 30S)
8. 120 kg/ha N + 30 kg/ha S (120N + 30S)
9. 60 kg/ha S (60S)
10. 40 kg/ha N + 60 kg/ha S (40N + 60S)
11. 80 kg/ha N + 60 kg/ha S (80N + 60S)
12. 120 kg/ha N + 60 kg/ha S (120N + 60S)

Plants were harvested after 85 days, when they reached physiological maturity. Soil and plant samples were collected for subsequent analysis.

Measurements and Analysis

Plant analyses: Plant height, number of grains per spike, spikes per square meter, 1000-grain weight, biological yield, and grain yield were determined using gravimetric and counting methods. The results were expressed in kg/ha based on the soil weight in the pots. Nitrogen (N) and sulfur (S) contents in wheat grains were analyzed using the method described by Jones (2001). N and S uptake by plants was calculated using the biological yield and the nutrient content of the plant tissues.

Soil analyses: After the harvest, soil samples were analyzed for pH, electrical conductivity (EC), mineral nitrogen (N), and available sulfur (S) contents using the method outlined by Rowell (1996) and Jones (2001).

Statistical analysis: The data were subjected to analysis of variance (ANOVA), and the means were compared using the least significant difference (LSD) test. Statistical analyses were performed using the SPSS software package.

Results

The application of nitrogen (N) and sulfur (S) significantly affected various growth parameters of wheat, including plant height, grains per spike, spike density (spike/m^2), and 1000-grain weight, as summarized in Table 1. Statistical analysis indicated that nitrogen and sulfur had a significant impact on these parameters, with differences between treatments determined to be statistically significant ($p \leq 0.05$). Below is a detailed breakdown of each parameter:

Table 1. Effect of Nitrogen and Sulfur on Plant Height, Grains per Spike, Spike/m^2, and 1000-Grain Weight

Treatment	Plant Height (cm)	Grains/Spike	Spike/m^2	1000-Grain Weight (g)
0N + 0S	75.3 ± 2.1c	25.4 ± 1.5b	270 ± 15b	40.5 ± 1.2b
40N + 0S	80.1 ± 2.2bc	26.5 ± 1.6b	285 ± 16b	41.2 ± 1.1b
80N + 0S	85.7 ± 2.4b	27.8 ± 1.3ab	310 ± 20ab	42.8 ± 1.3b
120N + 0S	90.5 ± 2.6a	29.1 ± 1.2a	350 ± 18a	44.3 ± 1.4a
40N + 30S	83.9 ± 2.0bc	27.2 ± 1.4b	300 ± 17b	42.3 ± 1.1b
80N + 30S	88.6 ± 2.5ab	28.5 ± 1.3a	335 ± 19a	43.5 ± 1.2a
120N + 30S	92.1 ± 2.7a	29.6 ± 1.1a	360 ± 20a	45.0 ± 1.3a
40N + 60S	84.7 ± 2.3b	27.5 ± 1.4ab	305 ± 18b	42.7 ± 1.2b
80N + 60S	89.4 ± 2.4ab	28.9 ± 1.3a	340 ± 19a	44.0 ± 1.3a
120N + 60S	93.2 ± 2.9a	30.2 ± 1.1a	370 ± 21a	46.1 ± 1.4a

Note: Values followed by different letters (a, b, c) indicate significant differences between treatments at $p \leq 0.05$, based on Fisher's LSD test.

Plant height

Nitrogen and sulfur applications led to a notable increase in plant height, with the highest values observed in treatments where both nitrogen and sulfur were applied at higher rates. The 120N + 60S treatment produced the tallest plants, reaching 93.2 ± 2.9 cm, which was significantly greater compared to the control (75.3 ± 2.1 cm). Plant height increased consistently with higher nitrogen levels, and the addition of sulfur further enhanced this growth. For example, treatments such as 120N + 30S (92.1 ± 2.7 cm) and 80N + 60S (89.4 ± 2.4 cm) also showed significantly higher plant heights compared to both the control and lower nitrogen levels. These results indicate that the combination of nitrogen and sulfur is essential for maximizing plant height.

Grains per spike

The number of grains per spike was also significantly influenced by nitrogen and sulfur application. The highest grain count per spike was recorded in the 120N + 60S treatment (30.2 ± 1.1 grains), which was significantly higher than the control (25.4 ± 1.5 grains). Other treatments, such as 80N + 30S (28.5 ± 1.3 grains) and 120N + 30S (29.6 ± 1.1 grains), also exhibited significantly higher grain counts compared to the control. These results suggest that increasing nitrogen levels, particularly when combined with sulfur, promotes greater spike fertility, leading to a higher number of grains per spike.

Spike/m²

Spike density, measured as the number of spikes per square meter, was significantly affected by nitrogen and sulfur applications. The highest spike density was observed in the 120N + 60S treatment (370 ± 21 spikes/m²), which was significantly greater than the control (270 ± 15 spikes/m²). Similarly, other treatments with higher nitrogen and sulfur levels, such as 120N + 30S and 80N + 60S, also resulted in significantly higher spike densities compared to both the control and lower nitrogen treatments. The results demonstrate that the combined application of nitrogen and sulfur improves spike production, which directly contributes to increased grain yield.

1000-grain weight

The 1000-grain weight, an indicator of grain size and quality, was significantly increased by nitrogen and sulfur applications. The 120N + 60S treatment produced the highest 1000-grain weight (46.1 ± 1.4 g), significantly higher than the control (40.5 ± 1.2 g). Treatments with nitrogen alone, such as 120N + 0S (44.3 ± 1.4 g) and 80N + 0S (42.8 ± 1.3 g), also showed significant improvements in grain weight, though the addition of sulfur further enhanced grain size. Other treatments, such as 120N + 30S (45.0 ± 1.3 g) and 80N + 60S (44.0 ± 1.3 g), also resulted in substantial increases in 1000-grain weight, confirming the importance of sulfur in enhancing grain quality when applied alongside nitrogen.

In summary, the application of nitrogen and sulfur significantly improved all measured growth parameters. Higher rates of nitrogen, particularly when combined with sulfur, consistently led to improved plant height, grain count per spike, spike density, and 1000-grain weight. These results indicate that both nitrogen and sulfur play crucial roles in maximizing wheat growth and yield.

The effects of nitrogen (N) and sulfur (S) on biological yield and grain yield of wheat were significant, as shown in Table 2. The results indicate that both nitrogen and sulfur had a considerable influence on these yield parameters, with statistically significant differences observed between treatments ($p \leq 0.05$).

Table 2. Effect of Nitrogen and Sulfur on Biological Yield and Grain Yield

Treatment	Biological Yield (kg/ha)	Grain Yield (kg/ha)
0N + 0S	5600 ± 150c	2400 ± 100c
40N + 0S	6100 ± 160bc	2650 ± 110b
80N + 0S	6800 ± 170b	2900 ± 120b
120N + 0S	7500 ± 180a	3150 ± 130a
40N + 30S	6400 ± 165bc	2750 ± 115b
80N + 30S	7100 ± 175ab	3000 ± 125ab
120N + 30S	7800 ± 185a	3250 ± 135a
40N + 60S	6600 ± 170b	2850 ± 120b
80N + 60S	7300 ± 180a	3050 ± 130ab
120N + 60S	8000 ± 190a	3350 ± 140a

Note: Letters indicate significant differences ($p \leq 0.05$).

Biological yield

Biological yield, representing the total above-ground biomass, increased significantly with higher nitrogen and sulfur applications. The 120N + 60S treatment produced the highest biological yield, reaching 8000 ± 190 kg/ha, which was significantly greater than the control (5600 ± 150 kg/ha). Treatments with higher nitrogen levels, such as 120N + 30S (7800 ± 185 kg/ha) and 80N + 60S (7300 ± 180 kg/ha), also showed significant improvements in biological yield compared to lower nitrogen or sulfur applications. These findings suggest that the combined application of nitrogen and sulfur maximizes biomass production, with nitrogen playing a primary role, further enhanced by sulfur supplementation.

Grain yield

Grain yield, a key indicator of crop productivity, was similarly influenced by nitrogen and sulfur application. The highest grain yield was recorded in the 120N + 60S treatment (3350 ± 140 kg/ha), significantly higher than the control treatment (2400 ± 100 kg/ha). Higher nitrogen levels alone, such as 120N + 0S (3150 ± 130 kg/ha), resulted in increased grain yield, but the addition of sulfur at both moderate (30S) and high (60S) levels further enhanced the yield. For example, the 120N + 30S treatment resulted in 3250 ± 135 kg/ha, while 80N + 60S produced 3050 ± 130 kg/ha, both significantly higher than lower nitrogen and sulfur treatments.

Overall, the results demonstrate that higher nitrogen levels, especially when supplemented with sulfur, significantly improve both biological and grain yield. These findings highlight the essential role of nitrogen in

enhancing wheat productivity, with sulfur acting as a synergistic element that further boosts the yield potential of the crop.

The effects of nitrogen (N) and sulfur (S) on nitrogen and sulfur uptake in wheat plants were significant, as shown in Table 3. The statistical analysis confirmed that both nitrogen and sulfur levels had a substantial impact on grain nitrogen content, sulfur content, and the total nitrogen and sulfur uptake by the plants ($p \leq 0.05$).

Nitrogen content and uptake

Nitrogen content in the wheat grains increased significantly with higher nitrogen applications, particularly when combined with sulfur. The highest nitrogen content in the grains was recorded in the 120N + 60S treatment, with a value of 2.1 ± 0.1%, which was significantly higher than the control (1.3 ± 0.1%). Similarly, nitrogen uptake by the plants was highest in the 120N + 60S treatment, reaching 55.4 ± 2.7 kg/ha, compared to the control (29.5 ± 2.0 kg/ha). Treatments with moderate nitrogen levels, such as 80N + 60S (48.3 ± 2.5 kg/ha) and 120N + 30S (52.7 ± 2.6 kg/ha), also showed significantly increased nitrogen uptake. These results indicate that higher nitrogen rates lead to increased nitrogen accumulation in the plants, with sulfur further enhancing nitrogen uptake efficiency.

Table 3. Nitrogen and Sulfur Uptake in Wheat Plants

Treatment	Grain N Content (%)	N Uptake (kg/ha)	Grain S Content (%)	S Uptake (kg/ha)
0N + 0S	1.3 ± 0.1c	29.5 ± 2.0c	0.12 ± 0.02c	1.8 ± 0.1c
40N + 0S	1.5 ± 0.1bc	35.7 ± 2.1bc	0.15 ± 0.02bc	2.2 ± 0.1bc
80N + 0S	1.7 ± 0.1b	43.2 ± 2.3b	0.17 ± 0.02b	2.6 ± 0.1b
120N + 0S	1.9 ± 0.1a	50.6 ± 2.5a	0.19 ± 0.02a	3.0 ± 0.1a
40N + 30S	1.6 ± 0.1b	38.5 ± 2.2b	0.18 ± 0.02b	2.8 ± 0.1b
80N + 30S	1.8 ± 0.1ab	45.8 ± 2.3ab	0.20 ± 0.02ab	3.1 ± 0.1ab
120N + 30S	2.0 ± 0.1a	52.7 ± 2.6a	0.22 ± 0.02a	3.4 ± 0.1a
40N + 60S	1.7 ± 0.1b	41.2 ± 2.2b	0.19 ± 0.02b	2.9 ± 0.1b
80N + 60S	1.9 ± 0.1a	48.3 ± 2.5a	0.21 ± 0.02a	3.2 ± 0.1a
120N + 60S	2.1 ± 0.1a	55.4 ± 2.7a	0.23 ± 0.02a	3.6 ± 0.1a

Note: Values followed by different letters (a, b, c) indicate significant differences ($p \leq 0.05$) based on Fisher's LSD test.

Sulfur content and uptake

Sulfur content in the wheat grains followed a similar trend, with significant increases observed in treatments with higher sulfur applications. The highest sulfur content was recorded in the 120N + 60S treatment (0.23 ± 0.02%), which was significantly higher than the control (0.12 ± 0.02%). Sulfur uptake also peaked in the 120N + 60S treatment, reaching 3.6 ± 0.1 kg/ha, compared to the control (1.8 ± 0.1 kg/ha). Other treatments with combined nitrogen and sulfur, such as 80N + 60S (3.2 ± 0.1 kg/ha) and 120N + 30S (3.4 ± 0.1 kg/ha), also demonstrated significantly higher sulfur uptake than the control or nitrogen-only treatments. These results highlight the synergistic effect of nitrogen and sulfur on sulfur uptake, with higher sulfur availability leading to increased absorption by the wheat plants.

In summary, the combined application of nitrogen and sulfur significantly increased both nitrogen and sulfur content in the grains, as well as the total uptake of these nutrients by the wheat plants. Higher nitrogen levels, particularly when paired with sulfur, resulted in greater nutrient accumulation, suggesting that sulfur enhances nitrogen use efficiency and contributes to optimal plant growth.

The effects of nitrogen (N) and sulfur (S) on soil properties after harvest, including mineral nitrogen (N), available sulfur (S), pH, and electrical conductivity (EC), are presented in Table 4. The results demonstrate significant changes in soil nutrient levels and properties due to varying nitrogen and sulfur applications ($p \leq 0.05$).

Mineral nitrogen (N)

Post-harvest mineral nitrogen levels in the soil increased significantly with higher nitrogen applications. The highest mineral N content was recorded in the 120N + 60S treatment, reaching 27.4 ± 0.9 mg/kg, compared to the control (12.1 ± 0.5 mg/kg). Treatments such as 120N + 0S (23.5 ± 0.8 mg/kg) and 80N + 60S (23.1 ± 0.8 mg/kg) also exhibited significantly higher mineral nitrogen levels compared to the control and lower nitrogen treatments. These results suggest that increasing nitrogen application leads to a buildup of residual mineral nitrogen in the soil, which can be beneficial for subsequent crops.

Table 4. Soil Properties Post-Harvest (Mineral N, Available S, pH, EC)

Treatment	Mineral N (mg/kg)	Available S (mg/kg)	pH	EC (dS/m)
0N + 0S	12.1 ± 0.5c	210 ± 15c	7.8 ± 0.1a	0.85 ± 0.05b
40N + 0S	16.4 ± 0.6bc	220 ± 16bc	7.7 ± 0.1a	0.88 ± 0.05b
80N + 0S	19.8 ± 0.7b	230 ± 16b	7.6 ± 0.1ab	0.91 ± 0.05b
120N + 0S	23.5 ± 0.8a	240 ± 17b	7.5 ± 0.1b	0.93 ± 0.05ab
40N + 30S	17.2 ± 0.6bc	250 ± 17ab	7.6 ± 0.1ab	0.92 ± 0.05ab
80N + 30S	21.5 ± 0.7ab	260 ± 18ab	7.5 ± 0.1b	0.95 ± 0.06ab
120N + 30S	25.6 ± 0.8a	270 ± 19a	7.4 ± 0.1b	0.98 ± 0.06a
40N + 60S	18.6 ± 0.7b	260 ± 18ab	7.5 ± 0.1b	0.94 ± 0.05ab
80N + 60S	23.1 ± 0.8a	280 ± 19a	7.4 ± 0.1b	0.99 ± 0.06a
120N + 60S	27.4 ± 0.9a	290 ± 20a	7.3 ± 0.1b	1.02 ± 0.07a

Note: Letters indicate significant differences ($p \leq 0.05$).

Available sulfur (S)

Available sulfur in the soil increased significantly with sulfur applications. The highest available sulfur content was observed in the 120N + 60S treatment (290 ± 20 mg/kg), which was significantly higher than the control (210 ± 15 mg/kg). Other sulfur-supplemented treatments, such as 80N + 60S (280 ± 19 mg/kg) and 120N + 30S (270 ± 19 mg/kg), also showed substantial increases in available sulfur levels compared to nitrogen-only treatments and the control. These results confirm that sulfur applications not only improve plant sulfur uptake but also enhance sulfur availability in the soil after harvest.

Soil pH

Soil pH values showed slight but significant changes following nitrogen and sulfur applications. The control treatment had the highest pH value (7.8 ± 0.1), whereas the pH levels slightly decreased with increasing nitrogen and sulfur applications. The lowest pH value was recorded in the 120N + 60S treatment (7.3 ± 0.1), indicating that higher nitrogen and sulfur applications tend to slightly acidify the soil. However, these changes in pH remain within the neutral to slightly alkaline range, suggesting that nitrogen and sulfur applications did not drastically affect soil acidity.

Electrical conductivity (EC)

Electrical conductivity (EC), an indicator of soil salinity, increased with higher nitrogen and sulfur applications. The highest EC was observed in the 120N + 60S treatment (1.02 ± 0.07 dS/m), which was significantly higher than the control (0.85 ± 0.05 dS/m). Treatments such as 80N + 60S (0.99 ± 0.06 dS/m) and 120N + 30S (0.98 ± 0.06 dS/m) also showed increased EC values compared to lower nitrogen or sulfur applications. The increase in EC is likely due to the addition of nitrogen and sulfur, as these nutrients contribute to the ionic content of the soil.

Discussion

The results of this study clearly demonstrate that the combined application of nitrogen (N) and sulfur (S) significantly enhances wheat growth, yield attributes, and nutrient uptake. The increase in growth and yield characteristics is largely attributable to improved nitrogen and sulfur uptake by the plants. These findings are consistent with previous research, which highlights the critical role of N and S in promoting plant growth, optimizing nitrogen use efficiency, and enhancing protein synthesis in grains.

Nitrogen and sulfur effects on growth and yield

The significant improvement in wheat growth and yield observed in this study can be attributed to better uptake of nitrogen and sulfur, particularly in treatments with higher N and S application rates. The combined application of 120N + 60S led to the highest plant height, spike density, grain yield, and biological yield. This enhancement in growth is likely due to the role of nitrogen in improving leaf surface area and chlorophyll synthesis, which optimizes the photosynthetic process and provides the energy needed for plant growth. Zecevic et al. (2010) noted that nitrogen facilitates cell division, which plays a crucial role in shoot elongation and overall plant height, similar to the findings of this study.

Sulfur, when applied in conjunction with nitrogen, plays a synergistic role in enhancing wheat productivity by improving nitrogen use efficiency (Haneklaus et al., 1999). In the present study, treatments with combined N and S resulted in a significant improvement in grain number per spike and 1000-grain weight, likely due to the favorable environment created for tillering and grain filling. Assefa et al. (2021) also reported similar results, noting that sulfur application improved both grain and straw yields by optimizing nutrient availability. Moreover, Šiaudinis and Lazauskas (2005) found that higher nitrogen doses increased

biological yield and altered vegetative growth characteristics, which aligns with the increase in biological yield observed in this study.

Protein content and nutrient uptake

In addition to improving growth and yield, the application of nitrogen and sulfur significantly increased the protein content in wheat grains. This is in agreement with previous studies, such as those by Wilson et al. (2020) and Liimatainen et al. (2022), who reported that sulfur application enhances the synthesis of amino acids and proteins, leading to higher protein content in grains and leaves. The increase in protein content observed in the 120N + 60S and 120N + 30S treatments in this study can be attributed to sulfur's involvement in the formation of amino acids and its role in activating enzymes that stimulate the production of proteins and vitamins essential for plant metabolism (Haneklaus et al., 1999).

The synergistic interaction between nitrogen and sulfur is well documented in the literature, and this study further confirms the positive effect of S on N uptake. Khandkar and Shinde (1991) demonstrated that the combined effect of S and N fertilizers significantly improved nitrogen uptake in maize plants, a result that is consistent with the findings of this study, where sulfur supplementation significantly enhanced nitrogen assimilation in wheat. The improvement in nitrogen uptake is critical for promoting protein synthesis, as nitrogen is a key component of amino acids, the building blocks of proteins. As Garrido-Lestache et al. (2005) pointed out, the increase in nitrogen supply is strongly correlated with higher protein content, although the effect on protein quality also depends on the wheat variety used, due to differences in nitrogen utilization.

Soil properties post-harvest

The post-harvest soil analysis in this study revealed important changes in soil nutrient levels due to nitrogen and sulfur applications. The increase in residual mineral nitrogen in the soil after high nitrogen treatments, particularly when combined with sulfur, indicates that these nutrients can have a lasting impact on soil fertility. Fuentes et al. (2003), İslamzade et al. (2023; 2024) and Kaliyeva et al. (2024) reported similar findings, noting that residual nitrogen in the soil could benefit subsequent cropping cycles by maintaining higher nutrient availability.

Additionally, the slight decrease in soil pH with increasing nitrogen and sulfur rates aligns with the findings of Barak et al. (1997), who observed soil acidification due to nitrogen fertilization. The increase in electrical conductivity (EC) observed in this study is likely a result of the accumulation of salts from the fertilizers, as noted by Choudhary et al. (2011), and suggests that while the nutrient additions improved plant growth and nutrient uptake, there may be long-term implications for soil salinity that require monitoring in future seasons.

Practical implications for fertilizer management

The findings of this study underscore the importance of balanced nitrogen and sulfur fertilization to maximize wheat productivity. The combined application of 120 kg/ha nitrogen with 60 kg/ha sulfur was particularly effective in enhancing growth, yield, and protein content, indicating that sulfur plays a critical role in complementing nitrogen fertilization by improving nitrogen use efficiency and promoting protein synthesis. This is consistent with the broader body of literature that highlights sulfur's importance in nitrogen metabolism and amino acid formation, leading to improved grain yield and quality (Carciochi et al., 2020; Wilson et al., 2020).

In terms of practical application, these results suggest that sulfur should be included in fertilizer programs, especially in soils where sulfur is deficient or where high rates of nitrogen are applied. The improvement in yield and protein content observed with combined N and S application suggests that wheat farmers can achieve higher productivity and better grain quality by incorporating both nutrients into their fertilization strategies. However, as the slight increase in soil salinity (EC) suggests, continued monitoring of soil conditions is essential to ensure long-term soil health and sustainability.

Conclusion

This pot experiment demonstrated the significant impact of nitrogen (N) and sulfur (S) on wheat growth, yield attributes, and grain protein content. The combined application of 120 kg/ha nitrogen and 60 kg/ha sulfur (120N + 60S) proved to be the most effective treatment, leading to substantial improvements in plant height, spike density, grain number per spike, biological yield, and nutrient uptake. The results indicate that the 120N + 60S combination is a balanced and optimal fertilization strategy for maximizing wheat productivity and enhancing grain quality. However, it is important to note that these findings were obtained under controlled pot experiment conditions. To fully validate the efficacy of the 120N + 60S treatment under real-world agricultural scenarios, further field trials are necessary. Conducting field experiments across

different wheat cultivars, soil types, and environmental conditions will provide more comprehensive insights into how nitrogen and sulfur interactions influence wheat growth in larger-scale farming systems. Wheat growers are encouraged to consider the 120N + 60S combination for improving yield and protein content, but it is also recommended that additional research be undertaken to bridge the gap between pot experiment results and field conditions. Such trials will help determine the most effective nutrient management strategies for achieving maximum crop productivity under variable and dynamic field conditions.

References

Alimbekova, N., Issabekov, B., Orazbayev, S., Yertayeva, Z., Yessengeldiyeva, L., 2022. Morphophysiological response of young Frantoio olive tree under different fertilizer types in sierozem with surface drip irrigation. *Eurasian Journal of Soil Science* 11(1): 86-92.

Barak, P., Jobe, B.O., Krueger, A.R., Peterson, L.A., Laird, D.A., 1997. Effects of long-term soil acidification due to nitrogen fertilizer inputs in Wisconsin. *Plant and Soil* 197(1): 61-69.

Branlard, G., Dardevet, M., Saccomano, R., Lagoutte, F., Gourdon, J., 2001. Genetic diversity of wheat storage proteins and bread wheat quality. *Euphytica* 119: 59-67.

Carciochi, W.D., Salvagiotti, F., Pagani, A., Calvo, N.I.R., Eyherabide, M., Rozas, H.R.S., Ciampitti, I.A., 2020. Nitrogen and sulfur interaction on nutrient use efficiencies and diagnostic tools in maize. *European Journal of Agronomy* 116: 126045.

Choudhary, O.P., Ghuman, B.S., Bijay-Singh, Thuy, N., Buresh, R.J., 2011. Effects of long-term use of sodic water irrigation, amendments and crop residues on soil properties and crop yields in rice–wheat cropping system in a calcareous soil. *Field Crops Research* 121(3): 363-372.

Fuentes, J.P., Flury, M., Huggins, D.R., Bezdicek, D.F., 2003. Soil water and nitrogen dynamics in dryland cropping systems of Washington State, USA. *Soil and Tillage Research* 71(1): 33-47.

Garrido-Lestache, E., López-Bellido, R.J., López-Bellido, L., 2005. Durum wheat quality under Mediterranean conditions as affected by nitrogen rate, timing, and splitting, and by sulfur fertilization. *European Journal of Agronomy* 23(3): 265-278.

Ghafoor, I., Habib-ur-Rahman, M., Ali, M., Afzal, M., Ahmed, W., Gaiser, T., Ghaffar, A., 2021. Slow-release nitrogen fertilizers enhance growth, yield, NUE in wheat crop and reduce nitrogen losses under an arid environment. *Environmental Science and Pollution Research* 28: 43528-43543.

Gupta, R., Meghwal, M., Prabhakar, P.K., 2021. Bioactive compounds of pigmented wheat (Triticum aestivum): Potential benefits in human health. *Trends in Food Science & Technology* 110: 240-252.

Haneklaus, S., Paulsen, H.M., Gupta, A.K., Bloem, E., Schnug, E., 1999. Influence of sulfur fertilization on yield and quality of oilseed rape and mustard. Proceedings of the 10th International Rapeseed Congress, 1999; pp 26–29. Proc. 10th Int. Rapeseed Congress. 26-29 September 1999, Canberra, Australia.

Hell, R., 1997. Molecular physiology of plant sulfur metabolism. *Planta* 202(2): 138-148.

İslamzade, R., Hasanova, G., Asadova, S., 2023. Impact of varied NPK fertilizer application rates and seed quantities on barley yield and soil nutrient availability in chestnut soil of Azerbaijan. *Eurasian Journal of Soil Science* 12(4): 371 - 381.

İslamzade, R., Islamzade, T., Hasanova, G., Huseynova, S.,2024. Babayeva, T.Effect of NPK fertilization and seed rate on barley (Hordeum vulgare) yield, yield component and nitrogen dynamics in semi-arid conditions. *Journal of Agriculture Faculty of Ege University* 61(3): 307–319.

Jones, J.B., 2001. Laboratory guide for conducting soil tests and plant analyses. CRC Press, New York, USA. 363p.

Kaliyeva, S., Suleimenov , B., Rvaidarova, G., Konysbekov, K., Muminova, S., Raimbekova , B., 2024. Effect of fertilizer treatments on sugar beet cultivars: A comprehensive study on crop yield and nutrient contents of soil and plant in chestnut soil of Kazakhstan. *Eurasian Journal of Soil Science* 13(3): 247-253.

Khalofah, A., Khan, M.I., Arif, M., Hussain, A., Ullah, R., Irfan, M., Mahpara, S., Shah, R.U., Ansari, M.J., Kintl, A., Brtnicky, M., Danish, S., Datta, R., 2021. Deep placement of nitrogen fertilizer improves yield, nitrogen use efficiency and economic returns of transplanted fine rice. *PLoS One* 16: e0247529.

Khandkar, U.R., Shinde, D.A., 1991. Phosphorus nutrition of black gram as influenced by P and S Application. *Journal of the Indian Society of Soil Science* 39: 583–585.

Liimatainen, A., Sairanen, A., Jaakkola, S., Kokkonen, T., Kuoppala, K., Jokiniemi, T., Mäkelä, P.S.A., 2022. Yield, quality and nitrogen use of forage maize under different nitrogen application rates in two boreal locations. *Agronomy* 12: *887*.

Panhwar, Q.A., Ali, A., Naher, U.A., Memon, M.Y., 2019. Fertilizer management strategies for enhancing nutrient use efficiency and sustainable wheat production. In: *Organic Farming: Global Perspectives and Methods*. Chandran, S., Unni, M.R., Thomas, S. (Eds.). Elsevier pp. 17-39.

Ragab, G., Saad-Allah, K., 2021. Seed priming with greenly synthesized sulfur nanoparticles enhances antioxidative defense machinery and restricts oxidative injury under manganese stress in *Helianthus annuus* (L.) seedlings. *Journal of Plant Growth Regulation* 40: 1894-1902.

Rowell, D.L., 1996. Soil Science: methods and applications. Longman, UK. 350p.

Shewry, P.R., 2009. Wheat. *Journal of Experimental Botany* 60(6): 1537-1553.

Shiferaw, B., Smale, M., Braun, H.J., Duveiller, E., Reynolds, M., Muricho, G., 2013. Crops that feed the world 10. Past successes and future challenges to the role played by wheat in global food security. *Food Security* 5: 291-317.

Šiaudinis, G., Lazauskas, S., 2005. The effect of nitrogen and sulphur fertilization on tiller formation and grain yield of spring wheat. Research for Rural Development: International Scientific Conference Proceedings, Jelgava, Latvia, 19–22 May 2005. pp 15–18.

Souza, E.J., Martin, J.M., Guttieri, M.J., O'Brien, K.M., Habernicht, D.K., Lanning, S.P., McLean, R., Carlson, G.R., Talbert, L.E., 2004. Influence of genotype, environment, and nitrogen management on spring wheat quality. *Crop Science* 44(2): 425-432.

Wang, Q., Zhang, Y., Wu, H., Xu, N., Li, A., 2021. Effects of sulfur limitation on nitrogen and sulfur uptake and lipid accumulation in *Scenedesmus acuminatus*. *Journal of Applied Phycology* 33: 301-311.

Wilson, t.L., Guttieri, M.J., Nelson, N.O., Fritz, A., Tilley, M., 2020. Nitrogen and sulfur effects on hard winter wheat quality and asparagine concentration. *Journal of Cereal Science* 93: 102969.

Zecevic, V., Knezevic, D., Boskovic, J., Micanovic, D., Dozet, G., 2010. Effect of nitrogen fertilization on winter wheat quality. *Cereal Research Communications* 38: 243–249.

Zhang, Z., Yu, Z., Zhang, Y., Shi, Y., 2021. Optimized nitrogen fertilizer application strategies under supplementary irrigation improved winter wheat (Triticum aestivum L.) yield and grain protein yield. *PeerJ* 9: e11467.

Eurasian Journal of Soil Science 2025, 14(1), 67 - 78

Eurasian Journal of Soil Science

Journal homepage : http://ejss.fesss.org

Adsorption of Pb, Ni and Zn by coastal soils: Isothermal models and kinetics analysis

Tatiana Minkina [a], Tatiana Bauer [a], Oleg Khroniuk [a], Ekaterina Kravchenko [a,*], David Pinsky [b], Anatoly Barakhov [a], Inna Zamulina [a], Elizabeth Latsynnik [a], Svetlana Sushkova [a], Yao Jun [c], Coşkun Gülser [d], Rıdvan Kızılkaya [d]

[a] Southern Federal University, Rostov-on-Don, 344090, Russia

[b] Institute of Physicochemical and Biological Problems of Soil Science, Russian Academy of Sciences, 142290 Pushchino, Russia

[c] China University of Geosciences, School of Water Resources and Environment, Beijing, China

[d] Ondokuz Mayıs University, Faculty of Agriculture, Department of Soil Science and Plant Nutrition, Samsun, Türkiye

Article Info

Received : 21.04.2024

Accepted : 24.10.2024

Available online: 04.11.2024

Author(s)

T.Minkina

T.Bauer

O.Khroniuk

E.Kravchenko *

D.Pinsky

A.Barakhov

I.Zamulina

E.Latsynnik

S.Sushkova

Y.Jun

C.Gülser

R.Kızılkaya

* Corresponding author

Abstract

Coastal areas are facing increasing heavy metal pollution as a result of various anthropogenic activities, posing a serious threat to ecosystems. Modeling and understanding the sorption behavior of heavy metals in soils are essential for assessing their mobility and risk in the coastal landscapes. The aim of this study was to examine the adsorption behavior of Pb^{2+}, Ni^{2+}, and Zn^{2+} by common soil types of the Lower Don and the Taganrog Bay coast in Russia to better understand their potential environmental implications. The soil capacities for heavy metal adsorption and retention were determined using isothermal models. The maximum adsorption capacity and the binding strength parameter for the heavy metals were calculated, revealing significant differences among the soils. Haplic Chernozem emerged with superior values, while Gleyic Solonchak Sulfidic and Umbric Fluvisol trailed the lowest. All soils exhibited a greater adsorption capacity and binding strength for Pb compared to the other metals. The influence of soil characteristics on sorption and retention was also examined. The Pseudo-second-order model provided a more accurate description of the adsorption kinetics of heavy metals by the studied soils. The co-presence of metals in the system affected their sorption by the soils due to competition: soils adsorbed fewer metals but retained them more strongly. These findings are important for developing effective strategies to reduce heavy metal pollution in coastal ecosystems.

Keywords: Heavy metals, Soils, Individual and Competitive adsorption, Adsorption capacity, Binding strength, Kinetics

Introduction

The growth in the Earth's population and the industrialization of human lifestyles inevitably lead to environmental pollution from anthropogenic emissions (Zamora-Ledezma et al., 2021). Soils, nature's universal filters, possess the remarkable ability to absorb, retain, and transform myriad pollutants into benign forms, yet they remain acutely vulnerable to anthropogenic contamination (Vega et al., 2006; Pinskii et al., 2023). Among the most dangerous pollutants for soils are heavy metals (HMs), whose formidable toxicity, tenacity against degradation, propensity for biological accumulation, and pervasive presence render them particularly hazardous (Tepanosyan et al., 2018; Bai et al., 2019). These elements can infiltrate the food chain, jeopardizing the delicate balance of ecosystems and endangering human health alike (Li et al.,

: https://doi.org/10.18393/ejss.1579168

: https://ejss.fesss.org/10.18393/ejss.1579168

Publisher : Federation of Eurasian Soil Science Societies

e-ISSN : 2147-4249

2023). Through this interconnected web of life, the insidious threat of heavy metals looms, casting a shadow over both our environment and the well-being of future generations.

To assess the potential mobility and fate of HMs within naturally contaminated soils, it is crucial to predict both the timing and magnitude of leaching events. This endeavor calls for a thorough exploration of patterns and mechanisms underpinning HM sorption and stabilization within the soil matrix (Liu et al., 2023; Cao et al., 2024). Sorption emerges as a pivotal factor dictating the fate and transport of HMs within ecosystems (Degryse et al., 2009; Bauer et al., 2018; Zwolak et al., 2019). The phenomenon of adsorption governs HM leaching from soil, with the extent of leaching intricately linked to the adsorption equilibrium, which describes the distribution of metals between the solid and liquid phases (Komuro and Kikumoto, 2024). A suite of sorption equilibrium models, including the linear, Freundlich, Langmuir, and Dubinin-Radushkevich equations, have been articulated, with the partitioning coefficient influenced by factors such as pH, temperature, Fe/Mn oxide content, and clay and silt content (Das et al., 2014; Diagboya et al., 2015). Furthermore, numerical models, such as the Pseudo-first order model (PFO, Lagergren model) and the Pseudo-second order model (PSO), have been proposed (Ho and McKay, 1999). These models capture sorption kinetics characterized by rapid sorption at the initial stage, followed by a slower rate later on.

The mechanisms governing HM sorption by soils are remarkably intricate, shaped by a multitude of factors. These include pH levels, ionic strength of the solution, the presence of competing ions, the composition and availability of soil sorption sites, as well as the potential for precipitation on soil particle surfaces and within the liquid phase in the presence of components such as carbonates, phosphates, organic matter, silicates, oxides, and hydroxides (Jalali and Moharrami, 2007; Sipos et al., 2008; Usman, 2008; Fisher-Power et al., 2016; Bauer et al., 2022).

Soil contamination frequently entails the concurrent presence of multiple HMs. In such scenarios, the dynamics and behavior of these HMs are dictated by the competition for sorption sites (Vega et al., 2006; Li et al., 2023). Research on the quantitative patterns of HM sorption by soils has revealed that metals like Ni, Pb, and Zn can compete for adsorption sites on soil particles (Lu and Xu, 2009; Akrawi et al., 2021; Umeh et al., 2021; Kravchenko et al., 2024). Ultimately, the composition and properties of the soil stand as the foremost determinants of HM adsorption (Jalali and Moharrami, 2007; Imoto and Yasutaka, 2020; Daramola et al., 2024).

The exploration of soil sorption capacity within coastal realms assumes profound significance, for these vibrant regions serve as conduits of both natural and anthropogenic transport and deposition (Ward et al., 2020). During these processes, coastal soils embody a protective buffer, sequestering HMs and threatening human health (Yu et al., 2021). The functioning of seaports and shipping are prominent sources of HM pollution in coastal ecosystems, leading to their degradation (Konstantinova et al., 2024). Moreover, these coastal zones provide invaluable ecosystem services and cradle nearly 40% of the global population dwelling within 100 km of the shoreline (Kulp and Strauss, 2019).

Among the most densely populated and heavily utilized areas in southern Russia, the Lower Don region and the coast of the Taganrog Bay of the Azov Sea are engage in a perilous interplay of anthropogenic pressure on the soil degradation, resulting in a concerning the accumulation of priority HMs such as Pb, Ni, and Zn (Konstantinova et al., 2023). These HMs rank among the foremost pollutants to infiltrate the environment, with adverse effects on ecosystems (Najamuddin et al., 2024). The aim of this study is to assess the patterns and mechanisms of mono- and poly-elemental sorption, as well as the sorption kinetics of Pb, Ni, and Zn by coastal soils with varying compositions and properties: Umbric Fluvisol, Gleyic Solonchac Sulfidic, and Haplic Chernozem.

Material and Methods

Soil sampling and analysis

The objects of investigation were the soils of various genesis (zonal, azonal and intrazonal) of the Lower Don and alone the coast of the Taganrog Bay (Rostov region, Russia). The soils were classified as Umbric Fluvisol, Gleyic Solonchac Sulfidic and Haplic Chernozem (IUSS, 2015). Soil samples were meticulously collected to a depth ranging from 0 to 20 cm, then air- dried at ambient temperature before being combiened and sieved through a 1 mm sieve. The main primary physical and chemical characteristics of the studied soils were assessed employing a suite of analytical methods: pH of soil suspension in water was measured according to ISO 10390:2005; the content of soil organic matter (SOM) content was measured according to the sulfochromic oxidation, ISO 14235: 1998; the carbonates content was determined using a Scheibler

apparatus, ISO 10693: 1995; cation exchange capacity (CEC) and exchangeable cations Ca^{2+} and Mg^{2+} were evaluated with by hexamminecobalt trichloride solution in accordance with ISO 23470: 2018. The particle size distribution was determined using the pipette method with the pyrophosphate procedure preparation (Shein, 2009). The total elemental composition (Si, Fe, Al) in the soils was determined by X-ray fluorescent (XRF) scanning spectrometer SPECTROSCAN MAKS-GV.

An X-ray diffractometry using DRON-7 diffractometer in Cu-Ka-filtered radiation was used to determine the mineralogical composition of the clay fraction of soils with a size less than 1 μm. For this purpose, the silt fraction was meticulously isolated from the studied soils (0-20 cm layer) by the sedimentation method according to (Chizhikova et al., 2018). After removing carbonates, the samples were kneaded twice (for 20 min) with a rubber pestle in a paste-like state. The soil samples were transferred to glass containers (3 L) with marks, in which the suspension was elutriated. The soil particles were separated into fractions by immersing the siphon to different depths, draining the liquid at certain intervals into receiving vessels. Upon completion of the elutriation, the suspensions of the soil fractions, except for the silt fraction, were dried and weighed. Concentrated $CaCl_2$ was added to the vessels with the liquid containing the silt fraction (<1 μm) for coagulation, and the highly dispersed particles were precipitated using a centrifuge.

Batch adsorption experiments

The metal adsorption on the soils was studied using a batch experiment. The adsorption experiments were performed in 150 mL Erlenmeyer flasks at 25°C. The Pb^{2+} Ni^{2+} and Zn^{2+} solutions were prepared by dissolving its nitrate salt in deionized water. The initial concentrations of HMs in the solution were 0.05; 0.08; 0.1; 0.3; 0.5; 0.8 and 1.0 mM·L^{-1}. The studied metal solutions contained either one metal or all three metals simultaneously. Five grams of the soil and 50 mL of HMs solution were added to the flasks. The initial pH of the solutions was adjusted using a dilution of 0.01 M KOH and 0.1 M HNO_3 solution. The flasks were sealed with silicon caps and shaken at 200 rpm in a rotary shaker for 1 h and then left in a calm state for 24 h to reach apparent equilibrium. Preliminary studies (Burachevskaya et al., 2023) showed that an apparent adsorption equilibrium was reached within 24 h. After the experiment, the metal ion concentrations remaining in the filtrate were determined using an atomic absorption spectrophotometer (AAS, The MGA-915 AA, Lyumeks, Russia). The amount of metal adsorbed per gram of soil (C_{ad}, mM·kg^{-1}) and the efficiency of adsorption (% adsorbed) were determined using equations (1) and (2), respectively (Daramola et al., 2024):

$$C_{ad} = \frac{(C_i - C_{eq}) \times V}{m}, \quad (1)$$

$$\%\ \text{adsorbed} = \frac{C_i - C_{eq}}{C_i} \cdot 100, \quad (2)$$

where C_i и C_{eq} are initial and equilibrium metal solution concentrations, mM·L^{-1}; V is the volume of the solution, mL; m is the mass of the adsorbent, kg. The information gathered was used to create the adsorption isotherms plot (C_{eq} – C_{ad}).

Adsorption isotherm and kinetic models

Thermodynamic models

The simple Langmuir (3), Freundlich (4) and Dubinin-Radushkevich (Vodyanitskii et al., 2000) (5) models were applied to describe the adsorption characteristics:

$$C_{ad} = C_\infty K_L C_{eq} / (1 + K_L C_{eq}), \quad (3)$$

$$C_{ad} = K_F C_{eq}^{1/n}, \quad (4)$$

$$C_{ad} = C_\infty \exp(-B\varepsilon^2), \quad (5)$$

where C_{ad} is the amount of absorbed metal per unit weight of adsorbent, C_∞ is the maximum adsorption capacity for the metal, mM·kg^{-1}; K_L is the constant of the Langmuir model related to the affinity of the binding sites (Cui et al., 2016), L·mM^{-1}; C_{eq} is the concentration of metal at equilibrium, мМ·L^{-1}; K_F is the Freundlich adsorption constant, L·kg^{-1}; 1/n is the Freundlich exponent related to adsorption intensity (Cui et al., 2016); B is a constant related to the mean free energy of sorption per mole of the adsorbate mol^2·kJ^{-2}; ε is Polanyi potential, which is equal to $RTln[KC_p / (1 + KC_{eq})]$, where K is an empirical parameter which is necessary for straightening experimental curves and obtaining quantitative values.

The Gibbs free energy (ΔG) was calculated using the equation (6):

$$\Delta G = - RTlnK_L, \quad (6)$$

where R is the gas constant, equals to 8.31 J·mol^{-1}·K^{-1}; T is the absolute temperature, K; K_L is the Langmuir constant.

To calculate the binding energy in equation (5), Hobson's formula (1969) is used for the average energy value (7):

$$E = B^{-1/2} / \sqrt{2} \quad (7)$$

Kinetic models

In order to investigate the mechanisms involved during the adsorption processes, a study was conducted to examine the dynamics of HM adsorption by the studied soil types. The concentration of HM in the initial solution with a volume of 50 mL was 0.5 мМ·L^{-1}. Soil weighing 5 g was added to the system. The interaction times of the suspensions were 1, 2, 5, 15, 30, 60, 180, 360 and 1440 minutes, with constant stirring on a shaker. The models of pseudo-first order and pseudo-second order (Ho and McKay, 1999) were used to describe the kinetics of adsorption and identify the limiting stage of the process.

$$Q_t = Q_e \left(1 - e^{-k_1 t}\right), \quad (8)$$

$$Q_t = \frac{k_2 Q_e^2 t}{1 + k_2 Q_e t}, \quad (9)$$

where Q_e and Q_t are the amount of sorbed metal per unit mass of the sorbent in equilibrium (the value is determined empirically) and at time t (min), mM·kg^{-1}; K_1 is the sorption rate constant of the pseudo–first order model, min^{-1}, K_2 is the sorption rate constant of the pseudo-second order model, kg·mM^{-1}·min^{-1}.

Statistical analysis

The experiments on adsorption isotherms and kinetics were performed in triplicate, and the standard deviation error bars in the graphs are from 3 replicates. All the calculation data were processed using Origin 2019® software. The R^2 values were used to compare the performance of the Langmuir, Dubinin-Radushkevich, and Freundlich models.

Results and Discussion

Characteristics of studied soils

The main physicochemical properties of the studied soils are given in Table 1. The soils were slightly alkaline. The $CaCO_3$ content varied from 1.1 to 7.6%. The SOM content ranged from 1.4 to 3.1%. The sum of exchangeable cations of Ca^{2+} and Mg^{2+} varied from 2.0 to 32.7 cmol(+)/kg. The content of the physical clay fraction (particle size <10 μm) in the studied soils ranged from 21.4 to 47.3%, and that of clay particles (<1 μm) was 10.5-24.0%. The mineralogy of the soils and their silt fractions indicates that smectite and hydrosludes are dominant. Kaolinite and chlorite are found in smaller amounts in all samples (Table 2).

Table 1. Physicochemical properties of studied soils, layer 0-20 cm

pH	$CaCO_3$ (%)	SOM (%)	Ca^{2+}, cmol(+)/kg	Mg^{2+}, cmol(+)/kg	$\Sigma Ca^{2+}+Mg^{2+}$, cmol(+)/kg	SiO_2 (%)	Fe_2O_3 (%)	Al_2O_3 (%)	Physical clay (particle size <10 μm)	Clay (particle size <1 μm)
Umbric Fluvisol										
8.1	7.6	1.4	1.1	16.7	2.0	18.7	71.7	3.0	21.4	10.5
Gleyic Solonchac Sulfidic										
7.9	1.1	1.7	21.0	2.2	23.2	45.3	4.9	10.1	36.1	20.2
Haplic Chernozem										
7.5	1.9	3.1	26.9	5.8	32.7	68.5	4.5	11.0	47.3	24.0

Table 2. Total content of dominant clay minerals in studied soils and their silt fractions

Studied soil	Hydrosludes (%)		Smectite phase (%)		Kaolinite + Chlorite (%)		Quartz (%)
	In soil as a whole	In fraction < 1 μm	In soil as a whole	In fraction < 1 μm	In soil as a whole	In fraction < 1 μm	
Umbric Fluvisol	4.6	34.0	5.8	49.0	2.1	17.0	49.5
Gleyic Solonchac Sulfidic	14.7	66.0	2.9	13.0	4.7	21.0	40.6
Haplic Chernozem	7.8	32.0	13.2	54.0	3.4	14.0	30.1

Individual adsorption of HMs by soils

Adsorption isotherms

Figure 1 illustrates the efficiency of individual HM adsorption by the studied soils. At initial concentrations of HM ions in solution reaching up to 1.0 mM L^{-1}, the soils exhibited notable sorption percentages: Pb^{2+} – 91.42–99.64%, Ni^{2+} – 42.00–91.33%, and Zn^{2+} – 31.4–90.0%. As the concentration of the initial solutions escalated, the percentage of Pb^{2+} sorbed by Gleyic Solonchak Sulfidic and Haplic Chernozem soils remained nearly constant at around 99.6%, while in Umbric Fluvisol, this value decreased to 91.42%. The sorption capacity of the soils for Ni^{2+} and Zn^{2+}, in all cases, followed the hierarchy: Haplic Chernozem > Gleyic Solonchak Sulfidic ≥ Umbric Fluvisol. This highlights the different buffer capacities of the soils and, consequently, the varying strengths of metal cation retention in different soil types. It further reveals the intricate interactions between adsorbed cations and the soils, as well as changes in the mechanisms of Ni and Zn adsorption by the soil absorption complex (SAC) as the metal ions concentration in the solution increases. Table 3 and Figure 2 present the data on the adsorption of Pb^{2+}, Ni^{2+} and Zn^{2+} cations by Umbric Fluvisol, Gleyic Solonchac Sulfidic and Haplic Chernozem.

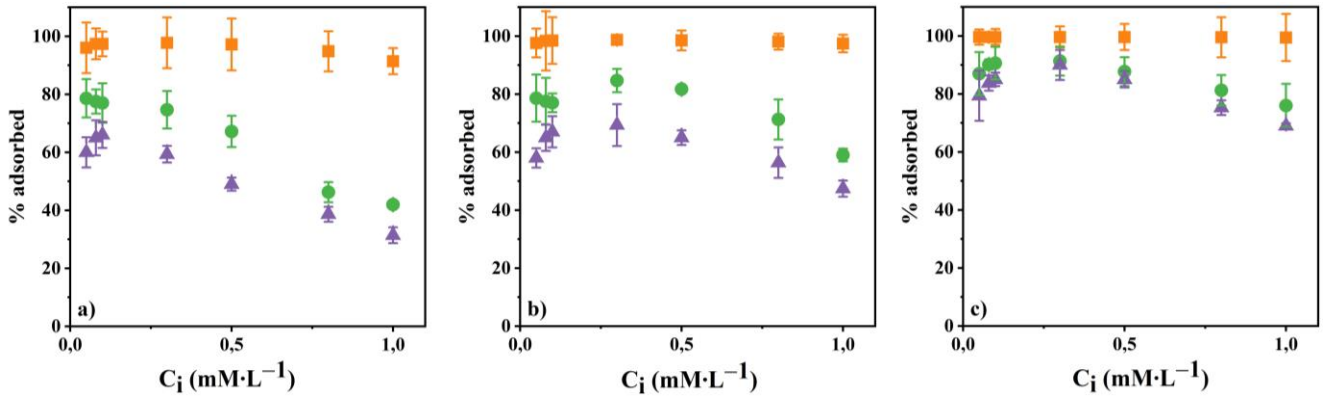

Figure 1. The efficiency of individual adsorption (% adsorbed) of HMs by the Umbric Fluvisol (a), Gleyic Solonchac Sulfidic (b) and Haplic Chernozem (c)

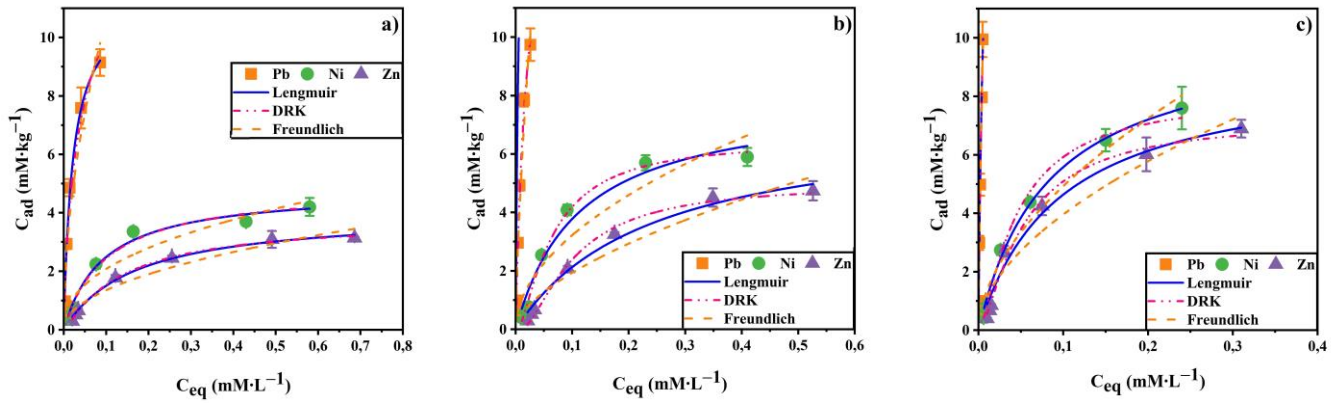

Figure 2. Individual adsorption isotherms for HMs by the Umbric Fluvisol (a), Gleyic Solonchac Sulfidic (b) and Haplic Chernozem (c)

Table 3. Individual adsorption isotherm parameters of HMs by Umbric Fluvisol, Gleyic Solonchac Sulfidic and Haplic Chernozem

Soil	Metal	Langmuir model				Dubinin-Radushkevich model			
		K_L, L·mM^{-1}	C_∞, mM·kg^{-1}	−ΔG, kJ·M^{-1}	R^2	C_∞, mM·kg^{-1}	E, kJ·M^{-1}	K	R^2
Umbric Fluvisol	Pb	46.79	11.51	9.53	0.992	11.13	4.29	8	0.981
	Ni	10.72	4.81	5.88	0.985	4.88	4.98	1	0.984
	Zn	6.01	4.02	4.44	0.995	3.71	4.44	1	0.998
Gleyic Solonchac Sulfidic	Pb	50.15	17.55	9.70	0.991	16.91	4.50	8	0.987
	Ni	9.01	7.97	5.45	0.964	8.90	4.45	1	0.969
	Zn	4.16	7.25	3.53	0.985	6.49	3.94	1	0.996
Haplic Chernozem	Pb	133.03	23.69	12.12	0.996	23.78	5.53	10	0.997
	Ni	12.20	10.16	6.20	0.996	11.35	5.06	1	0.997
	Zn	10.52	9.06	5.83	0979	10.85	4.60	1	0.981

The isotherms depicting HM adsorption by soils exhibit a convex profile, a hallmark of Langmuir isotherms (Figure 2). The variations among these isotherms illuminate the unique adsorption capacities different soils possess for the HMs in question. At the initial phases of adsorption, the binding sites with the greatest interaction energy between sorbate and sorbent are swiftly occupied. As these prime sites become saturated, the binding strength decreases, and the amount of adsorbed substance diminishes. During this process, the nature of the sorption compounds formed changes – from inner-sphere complexes to outer-sphere ones (Sosorova et al., 2018). The specific transitions in HM-soil interaction mechanisms are intricately tied to the properties of the adsorbed cations. Across the concentration spectrum of the analyzed solutions (0.05–1.0 mM L^{-1}), all soil types exhibit a pronounced preference for Pb^{2+} over Ni^{2+} and Zn^{2+}, a phenomenon evident in the contours of the isotherms and their alignment with the ordinate axis. In examining the isotherm approximation data via Equations (3) – (5), it became apparent that both the Langmuir and Dubinin-Radushkevich equations were adept at encapsulating the HM adsorption dynamics of the studied soils, whereas the Freundlich equation proved less fitting (Figure 2).

The investigation has unveiled that the C∞ value for the examined soils diminishes in the following hierarchy: $Pb^{2+} > Ni^{2+} \geq Zn^{2+}$ (Table 3). In contrast, the KL value—reflective of the energetic interplay between the adsorbed cations and soil adsorption capacity (SAC)—exhibits a descending order of $Pb^{2+} > Ni^{2+} > Zn^{2+}$. The adsorption potential of an ion appears to correlate tentatively with specific characteristics including hydrolyzability, electronegativity, and the softness parameter, as posited by Misono (1967). Notably, discrepancies in the computed parameters hinge predominantly on electronegativity values: Pb^{2+} at 2.33, followed by Ni^{2+} at 1.99, and Zn^{2+} trailing at 1.65 (McBride, 1994). Lead further boasts a superior softness metric (Pb^{2+} at 3.58, Ni^{2+} at 2.82, Zn^{2+} at 2.34), which influences the metal's affinity for soil entities, facilitating the establishment of covalent π-bonds (Basta and Sloan, 1999; Sposito, 2008; Shaheen et al., 2012). Additionally, the hydrolysis of metal ions is crucial to their soil adsorption dynamics. Abd-Elfattah and Wada (1981) identified the hydrolysis constant (pK_1) as a pivotal index of metal selectivity in soil contexts, with pK_1 values of 7.8 for Pb^{2+} and 9.9 for Ni^{2+} (Brown and Ekberg, 2016). Lower pK_1 values denote heightened interactions through the formation of inner-sphere complexes or sorption reactions (Park et al., 2016).

It has been noted that the Gibbs free energy (ΔG) derived from the Langmuir equation and the interaction energy of adsorbed heavy metals (HMs) with soil adsorption capacity (SAC) as calculated by the Dubinin-Radushkevich equation diverge markedly. In all instances, the adsorption energy derived from the Dubinin-Radushkevich equation was considerably lower (Table 3). Nonetheless, both models converge on a singular insight: the ranking of the analyzed metals, based on ΔG and E values, remains steadfast. The computed C∞ values for the individual cations exhibit remarkable consistency across models, revealing no significant disparities (Table 3). Among the evaluated soils, the calculated values of C∞ and KL adhere to the hierarchy: Haplic Chernozem > Gleyic Solonchak Sulfidic > Umbric Fluvisol. These variances largely stem from differences in soil texture, soil organic matter (SOM), exchangeable cations, and carbonate concentrations. In Umbric Fluvisol, these parameters are at their nadir, culminating in a diminished buffering capacity against heavy metals (Table 1, 3). The negative Gibbs free energy values (ΔG) (Table 3), ascertained through the Langmuir equation, affirm that the adsorption of HMs by soils unfolds as a spontaneous process, with ΔG directly proportional to KL: the higher the KL, the more pronounced the change in Gibbs energy.

Correlation analysis

Table 4 elegantly illustrates the correlation coefficients that intertwine various soil properties with sorption parameters (KL and C∞) for the metals Pb, Ni, and Zn. These coefficients unveil the intricate relationships governing soil characteristics and metallic behavior.

Table 4. The correlation coefficients between K_L and C_∞ for each metal and selected soil characteristics

Metals	pH	$CaCO_3$	SOM	Ca^{2+}	Mg^{2+}	$\Sigma Ca^{2+}+Mg^{2+}$	SiO_2	Fe_2O_3	Al_2O_3	Physical clay (particle size <10 μm)	Clay (particle size <1 μm)
K_L											
Pb	-0.956	-0.430	0.991	0.702	-0.312	0.761	0.864	-0.534	0.614	0.843	0.741
Ni	-0.623	0.154	0.744	0.177	0.279	0.262	0.428	0.036	0.061	0.393	0.233
Zn	-0.814	-0.124	0.899	0.441	0.004	0.518	0.660	-0.240	0.333	0.631	0.491
C_∞											
Pb	-0.983	-0.801	0.938	0.953	-0.719	0.976	0.999	-0.866	0.911	0.909	0.968
Ni	-0.957	-0.862	0.895	0.980	-0.790	0.994	0.998	-0.915	0.950	0.891	0.990
Zn	-0.939	-0.889	0.868	0.990	-0.824	0.930	0.993	-0.937	0.967	0.995	0.911

For Pb^{2+}, KL exhibits a profound negative correlation with pH (r = -0.956) and a striking positive correlation with soil organic matter (SOM) (r = 0.991). Additional positive correlations are noted with $\Sigma Ca^{2+}+Mg^{2+}$ (r = 0.761), SiO_2 (r = 0.864), and particles smaller than 1 μm (r = 0.741). The C∞ value for Pb^{2+} mirrors this trend, revealing strong negative correlations with pH (r = -0.983) and $CaCO_3$ (r = -0.801), while displaying robust positive correlations with SOM (r = 0.938), Ca^{2+} (r = 0.953), and SiO_2 (r = 0.999).

For Ni^{2+}, KL reveals a moderate negative correlation with pH (r = -0.623) and a positive correlation with SOM (r = 0.744), though other correlations remain generally weak. The C∞ values for Ni^{2+}, however, showcase compelling negative correlations with pH (r = -0.957) and $CaCO_3$ (r = -0.862), alongside substantial positive correlations with SOM (r = 0.895), Ca^{2+} (r = 0.980), and $\Sigma Ca^{2+}+Mg^{2+}$ (r = 0.994).

For Zn^{2+}, KL displays a strong negative correlation with pH (r = -0.814) and a positive correlation with SOM (r = 0.899), though correlations with other soil properties are moderate. The C∞ values for Zn^{2+} reflect strong negative correlations with pH (r = -0.939) and $CaCO_3$ (r = -0.889), as well as significant positive correlations with SOM (r = 0.868), Ca^{2+} (r = 0.990), and $\Sigma Ca^{2+}+Mg^{2+}$ (r = 0.930). Notably, a striking positive correlation emerges with the content of particles smaller than 10 μm (r = 0.995).

The sorption parameters of soils regarding heavy metals are predominantly shaped by pH, soil organic matter (SOM), and clay content. At diminished pH levels, numerous metallic ions manifest as cations, displaying an increased affinity for adsorption onto negatively charged soil particles. Conversely, elevated pH levels may hinder this process; here, the formation of hydroxide complexes occurs, yielding compounds less susceptible to adsorption. The role of SOM is intricately tied to its organic functional groups, notably carboxyl and phenolic entities, which adeptly bind metal cations, thereby enhancing the likelihood of complex formations. Furthermore, clay minerals, with their expansive specific surface area and considerable cation exchange capacity, significantly boost the adsorption of metals within the soil matrix (Bradl, 2004). In essence, these intertwined factors create a dynamic interplay, dictating the availability and mobility of heavy metals in the soil environment, ultimately impacting their ecological fate.

Adsorption kinetics

The kinetic data were meticulously analyzed to ascertain both the rate of adsorption and its nature—whether it be chemisorption or physisorption. The influence of contact time on heavy metals (HMs) adsorption by soils is illustrated in Figure 3.

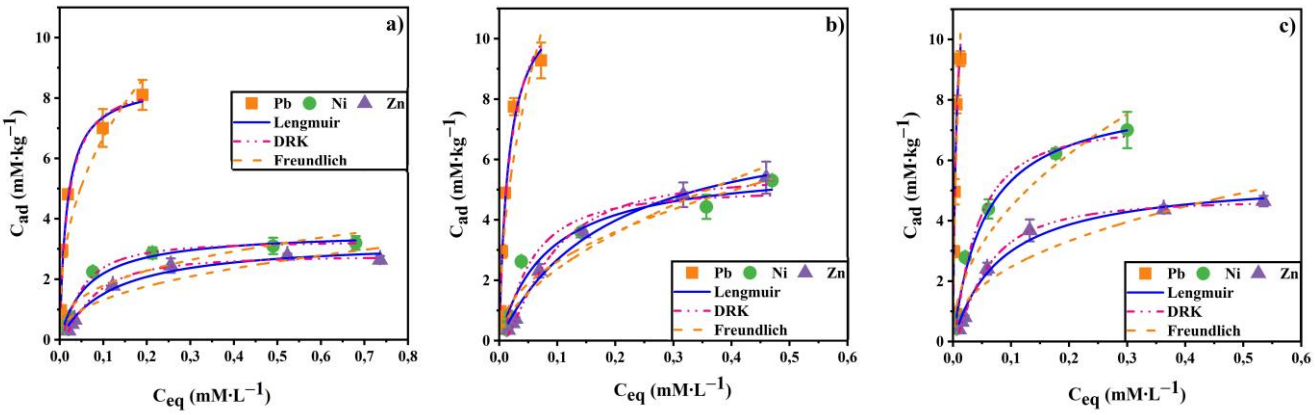

Figure 3. Kinetics of individual adsorption for HMs by Umbric Fluvisol (a), Gleyic Solonchac Sulfidic (b) and Haplic Chernozem (c)

To elucidate the findings, nonlinear statistical analysis was employed to adeptly fit Eqs. (8) and (9) to the experimental kinetic data, as detailed in Table 5. Notably, the quantity of adsorbed HMs escalated in tandem with contact time (see Figure 3). This adsorption process exhibited a notably rapid rate, achieving equilibrium within the observed timeframe of a day. After three hours, the curves began to level off, signifying a negligible change in the quantity of metals absorbed by the soil over time. This behavior may be ascribed to the profusion of active sites on the soil surface that initially facilitate swift sorption. However, as these sites gradually become occupied, the rate of sorption slows, reflecting the intricate interplay between time and the dynamic availability of adsorption sites.

The findings illuminate the intricate dynamics of heavy metal ion adsorption by soils, unfolding in two distinct stages. The initial phase is a swift dance of rapid surface adsorption, predominantly driven by the magnetic pull of electrostatic attraction and ion exchange (Mouni et al., 2009). This is succeeded by a more

languid stage, potentially characterized by the diffusion of ions into the soil's granular embrace (Karavanova and Schmidt, 2001). Data summarized in Table 3 affirm that the pseudo-second order equation most aptly captures the essence of the sorption process, with R^2 values soaring high between 0.914 and 0.965, a stark contrast to the subdued values of the pseudo-first order model, which languish between 0.597 and 0.760 (Table 5). This analysis underscores chemisorption as the rate-limiting step, relegating diffusion to a role of little consequence.

At equilibrium, the K_2 values delineate a hierarchy of sorption rates: Pb^{2+} reigns supreme over Zn^{2+} and Ni^{2+} in both Umbric Fluvisol and Haplic Chernozem, while in Gleyic Solonchac Sulfidic, Zn^{2+} commands attention with Pb^{2+} closely trailing. Notably, the sorption capacity (Q_e) for Pb^{2+} consistently eclipses that of Zn^{2+} and Ni^{2+} across all examined soils (Table 5).

Table 5. Kinetic model parameters of the HMs adsorption by studied soils

Soil	Metal	Q_e, mM·kg^{-1}	PFO model		PSO model	
			R^2	K_1, min^{-1}	R^2	K_2, kg·mM^{-1}·min^{-1}
Umbric Fluvisol	Pb	4.754	0.597	0.0034	0.952	0.0481
	Ni	3.572	0.646	0.0032	0.942	0.0352
	Zn	3.090	0.760	0.0032	0.903	0.0427
Gleyic Solonchac Sulfidic	Pb	4.925	0.655	0.0033	0.943	0.0379
	Ni	4.157	0.647	0.0034	0.938	0.0377
	Zn	3.262	0.539	0.0039	0.923	0.0641
Haplic Chernozem	Pb	4.992	0.608	0.0035	0.936	0.0431
	Ni	4.404	0.741	0.0032	0.936	0.0257
	Zn	4.021	0.720	0.0032	0.915	0.0346

Competitive adsorption of HMs by soils

Adsorption isotherms

The principal force that governs the sorption of heavy metal cations by the examined soils, when subjected to solutions containing all three cations simultaneously, is their inherent competition for limited sorption sites. In the realm of competitive adsorption, the soils consistently exhibit a diminished sorption capacity with escalating initial heavy metal concentrations (Figure 4), a phenomenon amplified in contrast to mono-element adsorption. The efficiency of adsorption for each metal unfolds as follows: Pb^{2+} – 81.02-99.00%; Ni^{2+} – 32.00-93.00%; Zn^{2+} – 26.40-81.25%. The overarching absorption capacity is hierarchically ordered as: Haplic Chernozem > Gleyic Solonchac Sulfidic > Umbric Fluvisol.

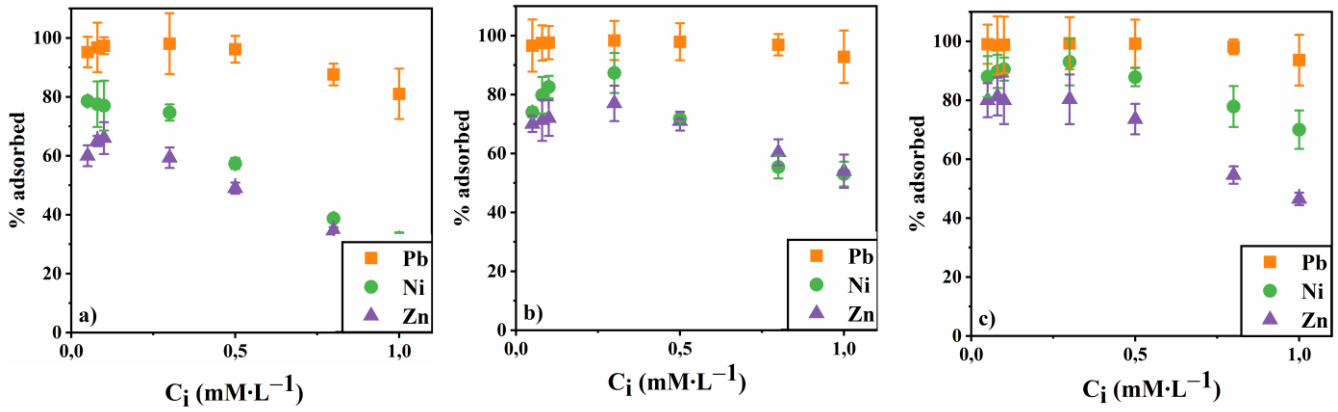

Figure 4. The efficiency of HMs adsorption (% adsorbed) by the Umbric Fluvisol (a), Gleyic Solonchac Sulfidic (b) and Haplic Chernozem (c) during polyelement pollution

Figure 5 elucidates the sorption isotherms of Pb^{2+}, Ni^{2+}, and Zn^{2+} within multi-metal solutions. Given the constrained sorption capacities during polycationic adsorption, the energy associated with each cation, articulated through the constant K_l , rises, while the peak adsorption ($C\infty$) wanes compared to mono-element scenarios (Tables 3, 6). This trend elucidates the competitive dynamics hindering the adsorption of individual ions. Furthermore, the interplay between adsorption sites and ion competition substantially diminishes overall adsorption capacity. Thus, the governing mechanisms of interaction for Pb^{2+}, Ni^{2+}, and Zn^{2+} with the studied soils persist consistently across both mono-element and poly-element sorption processes.

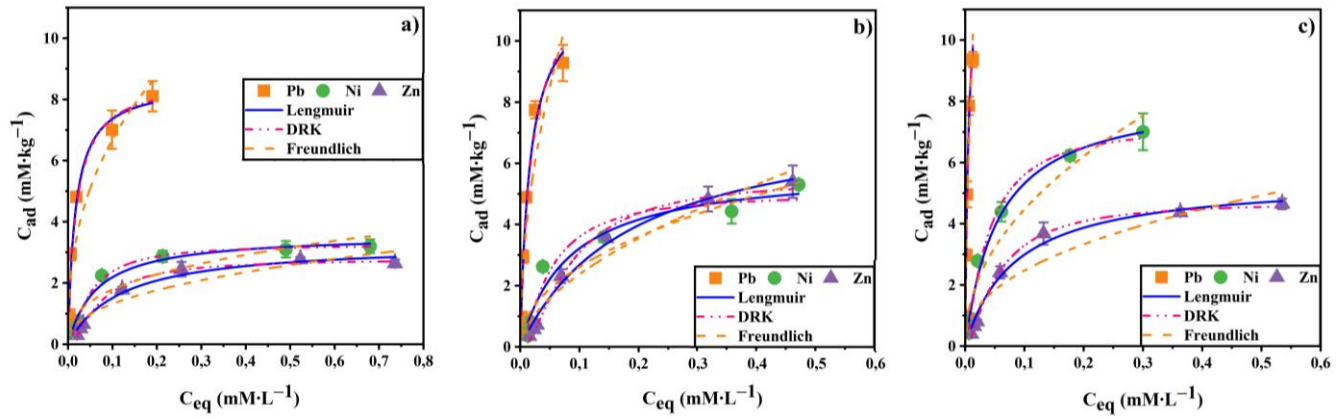

Figure 5. Competitive adsorption isotherms for HMs by the Umbric Fluvisol (a), Gleyic Solonchac Sulfidic (b) and Haplic Chernozem (c)

Table 6. Competitive adsorption isotherm parameters of HMs by studied soils

Soil	Metal	Langmuir equation model				Dubinin-Radushkevich model			
		K_L, L·mM^{-1}	C_∞, mM·kg^{-1}	−ΔG, kJ·M^{-1}	R^2	C_∞, mM·kg^{-1}	E, kJ·M^{-1}	K	R^2
Umbric Fluvisol	Pb	61.64	8.56	10.21	0.978	8.34	3.73	15	0.962
	Ni	15.59	3.59	6.80	0.980	3.84	5.30	1	0.971
	Zn	8.47	3.30	5.29	0.979	3.35	4.57	1	0.983
Gleyic Solonchac Sulfidic	Pb	62.41	11.78	10.24	0.978	11.43	3.74	15	0.951
	Ni	12.14	5.87	6.19	0.952	5.32	3.13	5	0.952
	Zn	5.34	7.70	4.15	0.989	7.15	4.23	1	0.995
Haplic Chernozem	Pb	173.48	14.06	12.77	0.978	13.78	4.23	30	0.960
	Ni	17.90	8.30	7.15	0.987	8.84	4.61	2	0.984
	Zn	12.05	5.48	6.17	0.986	5.87	4.96	1	0.984

In the intricate dance of competition among three metal ions, the inherent properties of these metals profoundly influence their sorption capabilities within the embrace of soil. Across all soil types, the affinity for Pb^{2+} stands out markedly, eclipsing that of its counterparts. When these metals vie for a common adsorption site, the resilient Pb^{2+} can displace Ni^{2+}, which in turn may usurp Zn^{2+} position. This dynamic interplay reveals a deeper truth: the presence of competing ions compels an increase in the bond strength between metals and soil particles, thereby diminishing the overall absorption capacity compared to scenarios involving single-component systems.

Adsorption kinetics

The dynamics of competitive heavy metal (HM) adsorption are revealed in Figure 6. The sorption capacity of these metals (Q_e) diminishes with their simultaneous introduction into the examined soils, in stark contrast to the singular adsorption of each metal, as illustrated in Figure 6. Such trends align seamlessly with the adsorption isotherms, rooted in the competition for active sorption sites within the soil matrix. This phenomenon may stem from the repulsive electrostatic forces that arise among the three ions present in multi-element systems. Notably, Pb^{2+} exhibits the most favorable sorption rates, signifying its greater affinity over Ni^{2+} and Zn^{2+}, which present similar data profiles.

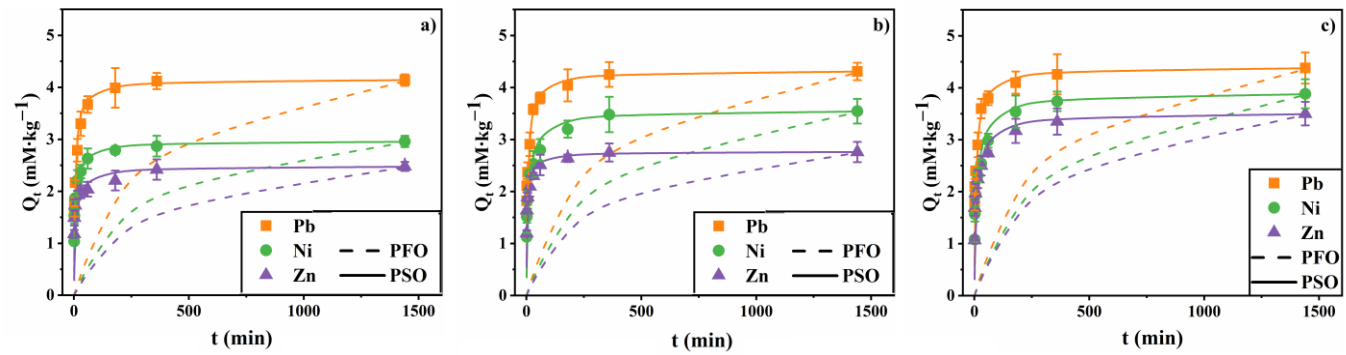

Figure 6. Kinetics of competitive HMs adsorption by Umbric Fluvisol (a), Gleyic Solonchac Sulfidic (b) and Haplic Chernozem (c)

The correlation coefficients (R^2) reinforce this finding, showcasing elevated values for the pseudo-second order (0.922-0.974) compared to the pseudo-first order (0.580-0.753). Additionally, the K_2 value constants (Table 7) reveal marginally lower figures (0.0201-0.0626), suggesting a slight extension of time necessary to reach equilibrium. This observation can be attributed to the intensified competition for active sites, which leads to a deceleration in the adsorption process.

Table 7. Kinetic model parameters of the competitive HMs adsorption by studied soils

Soil	Metal	Q_e, mM·kg^1	PFO model		PSO model	
			R^2	K_1, min^{-1}	R^2	K_2, kg·mM^{-1}·min^{-1}
Umbric Fluvisol	Pb	4.157	0.641	0.0033	0.968	0.0374
	Ni	2.965	0.580	0.0036	0.973	0.0479
	Zn	2.488	0.679	0.0032	0.922	0.0537
Gleyic Solonchac Sulfidic	Pb	4.324	0.641	0.0033	0.957	0.0391
	Ni	3.565	0.716	0.0031	0.957	0.0260
	Zn	2.764	0.585	0.0037	0.964	0.0626
Haplic Chernozem	Pb	4.386	0.623	0.0039	0.974	0.0267
	Ni	3.909	0.753	0.0031	0.949	0.0201
	Zn	3.513	0.709	0.0034	0.943	0.0243

Conclusion

The physicochemical, mineralogical, and sorption characteristics of coastal soils from the Lower Don region and the Taganrog Bay coast in southern Russia were meticulously examined. This study delved into the individual and competitive sorption processes of heavy metals Pb^{2+}, Ni^{2+}, and Zn^{2+}, employing sorption isotherms to unveil the underlying interactions within these soils. In every instance, the sorption phenomena were aptly encapsulated by the Langmuir model. The resulting sorption isotherms delineated a hierarchy of metal affinity: Pb > Ni > Zn, and illuminated distinct soil types: Haplic Chernozem > Gleyic Solonchak Sulfidic > Umbric Fluvisol. Experiments on the competitive sorption of heavy metals unveiled variable selective sorption sites among the soils for each metal; lead emerged as the predominant adsorbate, while nickel and zinc exhibited diminished adsorption under competitive conditions. Correlation analysis underscored the pivotal roles of pH, soil organic matter, and clay content in facilitating heavy metal adsorption. Notably, the pseudo-second-order kinetic model emerged as a superior descriptor of the adsorption dynamics, emphasizing chemisorption as the rate-limiting step, with diffusion playing a subordinate role. These insights underscore the urgent need for effective strategies to combat heavy metal pollution and safeguard coastal ecosystems.

Acknowledgments

The study was carried out with the financial support of the Russian Science Foundation, Russian Federation, project no. 20-14-00317.

References

Abd-Elfattah, A., Wada, K., 1981. Adsorption of lead, copper, zinc, cobalt, and cadmium by soils that differ in cation-exchange materials. *European Journal of Soil Science* 32(2): 271-283.

Akrawi, H., Al-Obaidi, M., Abdulrahman, C.H., 2021. Evaluation of Langmuir and Frendlich isotherm equation for Zinc Adsorption in some calcareous soil of Erbil province north of Iraq. *IOP Conference Series: Earth and Environmental Science* 76(1): 012017.

Bai, J., Zhao, Q., Wang, W., Wang, X., Jia, J., Cui, B., Liu, X., 2019. Arsenic and heavy metals pollution along a salinity gradient in drained coastal wetland soils: depth distributions, sources and toxic risks. *Ecological indicators* 96: 91-98.

Basta, N., Sloan, J., 1999. Bioavailablility of heavy metals in strongly acidic soils treated with exceptional quality biosolids. *Journal of Environmental Quality* 28(2): 633-638.

Bauer, T., Pinskii, D., Minkina, T., Nevidomskaya, D., Mandzhieva, S., Burachevskaya, M., Chaplygin, V., Popileshko, Y., 2018. Time effect on the stabilization of technogenic copper compounds in solid phases of Haplic Chernozem. *Science of the Total Environment* 626: 1100-1107.

Bauer, T.V., Pinskii, D.L., Minkina, T.M., Shuvaeva, V.A., Soldatov, A.V., Mandzhieva, S.S., Tsitsuashvili, V.S., Nevidomskaya, D.G., Semenkov, I.N., 2022. Application of XAFS and XRD methods for describing the copper and zinc adsorption characteristics in hydromorphic soils. *Environmental Geochemistry and Health* 44(2): 335-347.

Bradl, H.B., 2004. Adsorption of heavy metal ions on soils and soils constituents. *Journal of Colloid and Interface Science* 277(1): 1-18.

Brown, P.L., Ekberg, C., 2016. Hydrolysis of metal ions. John Wiley and Sons, Weinheim, Germany. 917p.
Burachevskaya, M., Minkina, T., Bauer, T., Lobzenko, I., Fedorenko, A., Mazarji, M., Sushkova, S., Mandzhieva, S., Nazarenko, A., Butova, V., 2023. Fabrication of biochar derived from different types of feedstocks as an efficient adsorbent for soil heavy metal removal. *Scientific Reports* 13: 2020.
Cao, W., Qin, C., Zhang, Y., Wei, J., Shad, A., Qu, R., Xian, Q., Wang, Z., 2024. Adsorption and migration behaviors of heavy metals (As, Cd, and Cr) in single and binary systems in typical Chinese soils. *Science of the Total Environment* 950: 175253.
Chizhikova, N., Khitrov, N., Varlamov, E., Churilin, N., 2018. The profile distribution of minerals within the solonetz in Yergeni. *Dokuchaev Soil Bulletin* 91: 63-84.
Cui, X., Hao, H., Zhang, C., He, Z., Yang, X., 2016. Capacity and mechanisms of ammonium and cadmium sorption on different wetland-plant derived biochars. *Science of the Total Environment* 539: 566-575.
Daramola, S., Demlie, M., Hingston, E., 2024. Mineralogical and sorption characterization of lateritic soils from Southwestern Nigeria for use as landfill liners. *Journal of Environmental Management* 355: 120511.
Das, B., Mondal, N., Bhaumik, R., Roy, P., 2014. Insight into adsorption equilibrium, kinetics and thermodynamics of lead onto alluvial soil. *International Journal of Environmental Science and Technology* 11: 1101-1114.
Degryse, F., Smolders, E., Parker, D., 2009. Partitioning of metals (Cd, Co, Cu, Ni, Pb, Zn) in soils: concepts, methodologies, prediction and applications–a review. *European journal of Soil Science* 60(4): 590-612.
Diagboya, P.N., Olu-Owolabi, B.I., Adebowale, K.O., 2015. Effects of time, soil organic matter, and iron oxides on the relative retention and redistribution of lead, cadmium, and copper on soils. *Environmental Science and Pollution Research* 22: 10331-10339.
Fisher-Power, L.M., Cheng, T., Rastghalam, Z.S., 2016. Cu and Zn adsorption to a heterogeneous natural sediment: Influence of leached cations and natural organic matter. *Chemosphere* 144: 1973-1979.
Ho, Y.-S., McKay, G., 1999. Pseudo-second order model for sorption processes. *Process biochemistry* 34(5): 451-465.
Hobson, J.P., 1969. Physical adsorption isotherms extending from ultrahigh vacuum to vapor pressure. *The Journal of Physical Chemistry* 73(8): 2720-2727.
Imoto, Y., Yasutaka, T., 2020. Comparison of the impacts of the experimental parameters and soil properties on the prediction of the soil sorption of Cd and Pb. *Geoderma* 376: 114538.
ISO 10390:2005. Soil quality — Determination of pH. Available at [Access date: 21.04.2024]: https://www.iso.org/obp/ui/#iso:std:iso:10390:ed-2:v1:en
ISO 10693:1995. Soil quality — Determination of carbonate content — Volumetric method. Available at [Access date: 21.04.2024]: https://www.iso.org/obp/ui/#iso:std:iso:10693:ed-1:v1:en
ISO 14235:1998. Soil quality — Determination of organic carbon by sulfochromic oxidation. Available at [Access date: 21.04.2024]: https://www.iso.org/obp/ui/#iso:std:iso:14235:ed-1:v1:en
ISO 23470:2018. Soil quality — Determination of effective cation exchange capacity (CEC) and exchangeable cations using a hexamminecobalt(III)chloride solution. Available at [Access date: 21.04.2024]: https://www.iso.org/obp/ui/#iso:std:iso:23470:ed-2:v1:en
IUSS, 2015. World reference base for soil resources 2014 International soil classification system for naming soils and creating legends for soil maps. Update 2015. World Soil Resources Reports 106. Food and Agriculture Organization of the United Nations (FAO), Rome, Italy. 192p. Available at [Access date: 21.04.2024]: http://www.fao.org/3/i3794en/I3794en.pdf
Jalali, M., Moharrami, S., 2007. Competitive adsorption of trace elements in calcareous soils of western Iran. *Geoderma* 140(1-2): 156-163.
Karavanova, E.I., Schmidt S.Yu., 2001. Sorption of water-soluble copper and zinc compounds by forest litter. *Eurasian Soil Science* 34(9): 967-974.
Komuro, R., Kikumoto, M., 2024. IntraPD model: Leaching of heavy metals from naturally contaminated soils. *Environmental Pollution* 340: 122861.
Konstantinova, E., Minkina, T., Nevidomskaya, D., Lychagin, M., Bezberdaya, L., Burachevskaya, M., Rajput, V. D., Zamulina, I., Bauer, T., Mandzhieva, S., 2024. Potentially toxic elements in urban soils of the coastal city of the Sea of Azov: Levels, sources, pollution and risk assessment. *Environmental Research* 252: 119080.
Konstantinova, E., Minkina, T., Nevidomskaya, D., Mandzhieva, S., Bauer, T., Zamulina, I., Voloshina, M., Lobzenko, I., Maksimov, A., Sushkova, S., 2023. Potentially toxic elements in surface soils of the Lower Don floodplain and the Taganrog Bay coast: sources, spatial distribution and pollution assessment. *Environmental Geochemistry and Health* 45(1): 101-119.
Kravchenko, E., Sushkova, S., Raza, M. H., Minkina, T., Dudnikova, T., Barbashev, A., Maksimov, A., Wong, M.H., 2024. Ecological and human health impact assessments based on long-term monitoring of soil PAHs near a coal-fired power plant. *Environmental Geochemistry and Health* 46: 288.
Kulp, S.A., Strauss, B.H., 2019. New elevation data triple estimates of global vulnerability to sea-level rise and coastal flooding. *Nature Communications* 10: 4844.
Li, Y., Liu, J., Wang, Y., Tang, X., Xu, J., Liu, X., 2023. Contribution of components in natural soil to Cd and Pb competitive adsorption: semi-quantitative to quantitative analysis. *Journal of Hazardous Materials* 441: 129883.

Liu, H., Xie, J., Cheng, Z., Wu, X., 2023. Characteristics, chemical speciation and health risk assessment of heavy metals in paddy soil and rice around an abandoned high-arsenic coal mine area, Southwest China. *Minerals* 13(5): 629.

Lu, S., Xu, Q., 2009. Competitive adsorption of Cd, Cu, Pb and Zn by different soils of Eastern China. *Environmental Geology* 57: 685-693.

McBride, M.B., 1994. Environmental chemistry of Soils. Oxford University Press. 406p.

Misono, M., Ochiai, E., Saito, Y., Yoneda, Y., 1967. A new dual parameter scale for the strength of Lewis acids and bases with the evaluation of their softness. *Journal of Inorganic and Nuclear Chemistry* 29(11): 2685-2691.

Mouni, L., Merabet, D., Robert, D., Bouzaza, A., 2009. Batch studies for the investigation of the sorption of the heavy metals Pb^{2+} and Zn^{2+} onto Amizour soil (Algeria). *Geoderma* 154(1-2): 30-35.

Najamuddin, Inayah, Labenua, R., Samawi, M.F., Yaqin, K., Paembonan, R.E., Ismail, F., Harahap, Z.A., 2024. Distribution of heavy metals Hg, Pb, and Cr in the coastal waters of small islands of Ternate, Indonesia. *Ecological Frontiers* 44(3): 529-537.

Park, J.-H., Ok, Y.S., Kim, S.-H., Cho, J.-S., Heo, J.-S., Delaune, R.D., Seo, D.-C., 2016. Competitive adsorption of heavy metals onto sesame straw biochar in aqueous solutions. *Chemosphere* 142: 77-83.

Pinskii, D., Shary, P., Mandzhieva, S., Minkina, T., Perelomov, L., Maltseva, A., Dudnikova, T., 2023. Effect of composition and properties of soils and soil-sand substrates contaminated with copper on morphometric parameters of barley plants. *Eurasian Soil Science* 56(3): 352-362.

Shaheen, S.M., Derbalah, A.S., Moghanm, F., 2012. Removal of heavy metals from aqueous solution by zeolite in competitive sorption system. *International Journal of Environmental Science and Development* 3(4): 362-367.

Shein, E., 2009. The particle-size distribution in soils: problems of the methods of study, interpretation of the results, and classification. *Eurasian Soil Science* 42: 284-291.

Sipos, P., Németh, T., Kis, V.K., Mohai, I., 2008. Sorption of copper, zinc and lead on soil mineral phases. *Chemosphere* 73(4): 461-469.

Sosorova, S.B., Merkusheva, M.G., Boloneva, L.N., Ubuguno, L.L., 2018. Parameters of sorption of cobalt and nickel ions by salt marshes of Western Transbaikal. *Agrochemistry* 9: 69–79. [In Russian]

Sposito, G., 2008. The chemistry of soils. Second edition. Oxford university press, USA. 329p.

Tepanosyan, G., Sahakyan, L., Belyaeva, O., Asmaryan, S., Saghatelyan, A., 2018. Continuous impact of mining activities on soil heavy metals levels and human health. *Science of the Total Environment* 639: 900-909.

Umeh, T.C., Nduka, J.K., Akpomie, K.G., 2021. Kinetics and isotherm modeling of Pb (II) and Cd (II) sequestration from polluted water onto tropical ultisol obtained from Enugu Nigeria. *Applied Water Science* 11: 65.

Usman, A.R.A., 2008. The relative adsorption selectivities of Pb, Cu, Zn, Cd and Ni by soils developed on shale in New Valley, Egypt. *Geoderma* 144(1-2): 334-343.

Vega, F.A., Covelo, E.F., Andrade, M., 2006. Competitive sorption and desorption of heavy metals in mine soils: influence of mine soil characteristics. *Journal of Colloid and Interface Science* 298(2): 582-592.

Vodyanitskii, Y.N., Rogova, O., Pinskii, D.L., 2000. Application of the Langmuir and Dubinin-Radushkevich equations to the description of Cu and Zn adsorption in rendzinas. *Eurasian Soil Science* 33(11): 1226-1233.

Ward, N.D., Megonigal, J.P., Bond-Lamberty, B., Bailey, V.L., Butman, D., Canuel, E.A., Diefenderfer, H., Ganju, N.K., Goñi, M.A., Graham, E.B., Hopkinson, C.S., Khangaonkar, T., Langley, J.A., McDowell, N.G., Myers-Pigg, A.N., Neumann, R.B., Osburn, C.L., Price, R.M., Rowland, J., Sengupta, A., Simard, M., Thornton, P.E., Tzortziou, M., Vargas, R., Weisenhorn, P.B., Windham-Myers, L., 2020. Representing the function and sensitivity of coastal interfaces in Earth system models. *Nature Communications* 11(1): 2458.

Yu, D., Wang, Y., Ding, F., Chen, X., Wang, J., 2021. Comparison of analysis methods of soil heavy metal pollution sources in China in last ten years. *Chinese Journal of Soil Science* 52(4): 1000.

Zamora-Ledezma, C., Negrete-Bolagay, D., Figueroa, F., Zamora-Ledezma, E., Ni, M., Alexis, F., Guerrero, V.H., 2021. Heavy metal water pollution: A fresh look about hazards, novel and conventional remediation methods. *Environmental Technology and Innovation* 22: 101504.

Zwolak, A., Sarzyńska, M., Szpyrka, E., Stawarczyk, K., 2019. Sources of soil pollution by heavy metals and their accumulation in vegetables: A review. *Water, Air, and Soil Pollution* 230: 164.

Eurasian Journal of Soil Science 2025, 14(1), 79 - 86

Eurasian Journal of Soil Science

Journal homepage : http://ejss.fesss.org

Identification and degradation potential of microplastics by indigenous bacteria isolated from Putri Cempo Landfill, Surakarta, Indonesia

Retno Rosariastuti *, Muhammad Hafizh Husna Prakosa, Sutami Sutami, Sumani Sumani, Purwanto Purwanto

Department of Soil Science, Faculty of Agriculture, Universitas Sebelas Maret, Surakarta, 57126, Indonesia

Article Info

Received : 20.05.2024
Accepted : 05.11.2024
Available online: 11.11.2024

Author(s)

R.Rosariastuti *
M.H.H.Prakosa
S.Sutami
S.Sumani
P.Purwanto

* Corresponding author

Abstract

Plastic waste on agricultural land can break down into microplastics (< 5 mm), which plants can absorb through their roots, potentially inhibiting plant growth. Utilizing microplastic-degrading bacteria isolated from landfills offers a potential solution to microplastic contamination in agriculture. This study aimed to isolate and identify bacteria from the Putri Cempo Landfill and evaluate their ability to degrade different types of plastic contaminants found in agricultural environments. Microorganisms were isolated from soil samples using Soil Extract Media (SEM), and pure cultures were established. Bacterial isolates were tested for their microplastic-degrading potential using polyethylene terephthalate (PET) plastic fragments. Molecular analysis was conducted to determine the taxonomy of the bacteria. Further degradation tests were performed on different types of microplastic contaminants (mulch, polybags, and sacks) to identify the most degradable material. Six bacterial isolates were obtained, with isolates CP1 and CP2 demonstrating microplastic degradation rates of 2.43% and 1.15%, respectively, over a 20-day incubation period. Molecular analysis identified CP1 as *Bacillus anthracis str.* and CP2 as *Bacillus cereus ATCC 14579*. Subsequent degradation tests on various agricultural microplastic contaminants revealed that sack materials treated with Bacillus cereus showed the highest degradation rate, with an 8.8% weight reduction, while polybag materials showed the lowest degradation rate, with a weight loss of only 0.59%.

Keywords: *Bacillus* sp., Bacterial Isolation, Microplastic Degradation, Molecular Analysis, Putri Cempo Landfill.

Introduction

The widespread use of plastics has resulted in significant pollution, affecting various environments, including agricultural land. Plastics are resistant to decomposition, leading to their accumulation in the soil. Through biological, chemical, and physical processes, plastics break down into smaller fragments, often less than 5 mm in size, known as microplastics (Hartmann et al., 2019; Wang et al., 2021). Agricultural practices rely extensively on plastic products like mulch, polybags, and sacks, making them a primary source of plastic contamination on farms. These plastics, once in the soil, can degrade further and contribute to microplastic pollution in agricultural fields (Zhang et al., 2020).

Microplastics dispersed in soil can negatively impact water flow, reduce soil aeration, and inhibit microbial activity (Khalid et al., 2023). They can also penetrate plants through cracks or breaks in young roots, spreading through the xylem or phloem systems (Li et al., 2020). The xylem system transports microplastics to the leaves, where they accumulate, impairing physiological processes, stressing plants, and reducing fertility (Lian et al., 2020). The presence of microplastics in plants poses further risks to human health, as they can enter the food chain and potentially cause cancer over time due to dioxin emissions. Dioxins, which are known carcinogens, are produced when plastics are exposed to heat or radiation (Alabi et al., 2019).

: https://doi.org/10.18393/ejss.1582987
: https://ejss.fesss.org/10.18393/ejss.1582987
Publisher : Federation of Eurasian Soil Science Societies
e-ISSN : 2147-4249

Remediation of microplastic-contaminated soil can be achieved through bioremediation, which utilizes living organisms to break down and eliminate microplastics. This process accelerates natural degradation by leveraging the metabolic capabilities of microorganisms to convert harmful substances into harmless ones (Dash et al., 2013). The use of isolated microorganisms, such as bacteria and fungi, as biodegradation agents for polymer-based materials has been widely explored. Previous studies have identified several bacterial species, including *Pseudomonas aeruginosa* (Jeon, 2015), *Bacillus* spp. (Auta et al., 2018; Harshvardhan, 2013), and *Rhodococcus* spp. (Auta et al., 2018), as effective bioremediation agents that can utilize polymers as their sole carbon source, thus reducing the polymer's mass. For instance, *Pseudomonas* sp. strains isolated from landfill environments have been shown to degrade polyethylene (PE) plastic mulch (Hou et al., 2022).

This study aims to identify bioremediation agents capable of degrading microplastic contaminants originating from agricultural plastic waste. Microorganisms were isolated from the Putri Cempo Landfill in Surakarta City, Indonesia, which serves as the largest site for plastic waste accumulation in the area (Prasenja et al., 2022). Despite the abundant availability of plastic waste at this site, no prior research has focused on isolating microplastic-degrading bacteria from this landfill or evaluating their potential for reducing microplastic contamination in agricultural soils.

Material and Methods

Sample collection

Sampling was conducted in May 2023 at the Putri Cempo Landfill, Surakarta City, Central Java, Indonesia (coordinates: 7º32'11.6309 "S - 110º51'18.52550 "E). Soil samples were randomly collected from a depth of 10 cm in three different locations where plastic waste was prevalent. The first sample was taken by the roadside, where large waste transportation machinery frequently passes. The second sample was collected from a mixed pile of garbage and soil, while the third sample was obtained from an area with significant vegetation surrounding the landfill. The soil samples were placed in sterile containers, stored in a cool box, and transported to the laboratory for analysis. Following the protocol of Rosariastuti et al. (2023), soil samples were handled with gloves and stored in a cool, sterile environment.

Material and equipment

The materials used included soil samples from the Putri Cempo Landfill and various growth media: Nutrient Agar (NA) composed of 10 g/L beef extract, 10 g/L peptone, 5 g/L NaCl, 1,000 mL distilled water, and 15 g/L agar; Nutrient Broth (NB) with 3 g/L beef extract and 10 g/L peptone; and Soil Extract Media (SEM) prepared with 100 g of landfill soil, 900 mL distilled water, and 40 g NA. Essential equipment used in the experiments included a spectrophotometer, vortex mixer, incubator, autoclave, pH meter, Erlenmeyer flasks, refrigerator, hot plate, shaker, micropipette, analytical balance, Petri dishes, and stirrer.

Analysis of collected soil samples

Soil quality parameters, including Cation Exchange Capacity (CEC), pH, and organic carbon content, were measured to evaluate the soil's suitability for supporting bacterial growth and activity, factors that influence the abundance of indigenous bacteria at the Putri Cempo Landfill.

Isolation and purification of bacteria

Five grams of soil sample were added to 45 mL of physiological saline solution and diluted up to 10^{-7}. Aliquots of 0.1 mL from the 10^{-3}, 10^{-5}, and 10^{-7} dilutions were inoculated onto Soil Extract Agar Media (SEAM) using the spread plate method, followed by incubation at 27°C for 48 hours. Bacterial colonies were isolated using sterilized inoculation loops and transferred to Petri dishes via the streak plate method. This purification process was repeated 10 times to obtain pure bacterial isolates, which were then cultured on Nutrient Agar plates and stored at 4°C for further use. The purification aimed to enhance the bacteria's activity, stability, and shelf life (Javed et al., 2018).

Initial screening

Pure bacterial isolates were subjected to initial screening by inoculating them on agar media amended with 1x1 cm pieces of microplastic (Yang et al., 2014). The microplastic pieces were surface sterilized by soaking in 70% alcohol overnight. The bacterial inoculation was conducted using the point inoculation method, and plates were incubated for five days. Based on the microbial growth area, six isolates with the highest potential for microplastic degradation were selected for further testing.

Analysis of bacterial growth curve

To evaluate bacterial growth dynamics, isolates were inoculated in NB media and observed periodically for turbidity at 600 nm wavelength using a spectrophotometer, every six hours. The bacterial growth curve,

reflecting cell growth dynamics, was categorized into five phases: lag, log (exponential), stationary, death, and long-term stationary (Park et al., 2023).

Microplastic degradation test

The degradation test aimed to evaluate the capacity of bacterial isolates from the Putri Cempo Landfill to break down microplastics. Polyethylene terephthalate (PET) microplastic fragments, 5 mm in diameter, were pre-weighed and surface sterilized by soaking in 70% alcohol overnight. The degradation medium was sterile NB in 50 mL glass bottles. Bacteria were inoculated into the medium and allowed to reach the stationary phase. At this point, the sterilized microplastic was added to the medium and incubated for 20 days on a shaker at 60 rpm (Vianti and Purwiyanto, 2020). After incubation, the microplastic was filtered and weighed to assess weight loss due to bacterial degradation.

Molecular identification

Genomic DNA of bacterial isolates was extracted using the Quick-DNA Magbead Plus kit (D4082; Zymo Research, Irvine, CA, USA). PCR amplification was performed using the MyTag HS Red Mix (Bioline, BIO-25048), with primers 27F (5'-AGAGTTTGATCNTGGCTCAG-3') and 1492R (5'-TACGGYTACCTTGTTACG-3'), targeting the 16S rRNA gene. PCR involved 9.5 µL ddH_2O, 12.5 µL MyTaq Red Mix, 1 µL of 20 pmol 27F primer, 1 µL of 20 pmol 1492R primer, and 1 µL DNA extract. Sequencing was performed using the bi-directional Sanger method, and DNA sequences were analyzed for similarities using the BLAST program in the NCBI database, followed by phylogenetic tree construction.

Contamination degradation test

The microplastic degradation test involved two selected bacterial isolates, with a control setup lacking bacteria. The experiment followed a factorial design based on a Completely Randomized Design (CRD) with two factors: type of contamination (A1: mulch, A2: polybag, A3: sack) and bacterial treatment (B0: no bacteria, B1: isolate CP1, B2: isolate CP2). Microplastic contaminants (5 mm in size) were pre-weighed and surface sterilized. Bacteria (1 loop) were inoculated into NB media and incubated for 24 hours before the medium was amended with microplastic. Incubation continued for 20 days at 60 rpm under room temperature, after which the microplastics were filtered and weighed to measure weight loss due to degradation.

Results and Discussion

Soil chemical analysis

The chemical analysis of soil from Putri Cempo Landfill (Table 1) revealed favorable conditions for bacterial growth, with results showing a neutral pH, high Cation Exchange Capacity (CEC), and high C-organic content. Bacteria thrive in neutral pH environments, as they facilitate optimal metabolic activities. The high CEC indicates the soil's capacity to retain and exchange essential nutrients, such as calcium, magnesium, and potassium, which are critical for bacterial growth. These findings align with Ding et al. (2017), who observed that a high CEC enhances nutrient availability for soil bacteria. Similarly, the high C-organic content provides the necessary energy and carbon source for bacteria, supporting overall microbial activity, as noted by Lee et al. (2020).

Table 1. Results of Soil Chemical Analysis at Putri Cempo Landfill

Location	Analysis	Result	Class
TP	pH	7.12	Neutral
	CEC (me/100g)	26.62	High
	C-Organic (%)	3.60	High

Soil bacteria isolation, purification, and initial screening

The suitable soil conditions facilitated robust bacterial growth during isolation on SEM media, resulting in 27 bacterial isolates. The purification process, as described by Figueroa-Bossi et al. (2022), aimed to isolate single colonies for pure culture growth. It involved four stages of dilution, using varying ratios of soil extract and distilled water, followed by the use of pure NA media. This approach enhanced the growth of single bacterial colonies, making subsequent molecular analyses more efficient.

Initial screening of the 27 isolates revealed that six of them were capable of forming colonies in the presence of plastic. Consistent with Park and Kim (2019), the selection criteria focused on the isolates' ability to utilize PE microplastics as the sole carbon source. The screening process eliminated bacteria that could not tolerate plastic-contaminated environments, supporting findings by Dussud et al. (2018), who demonstrated that bacteria could colonize both biodegradable and non-biodegradable plastics.

Microplastic degradation test

The microplastic degradation test was conducted during the log phase, where bacterial activity is at its peak, ensuring optimal conditions for degradation (Wijanarka et al., 2016). As shown in Figure 1, bacterial isolates reached their highest growth rate by the 12th hour, marking the best time for the microplastic degradation test. Among the six isolates tested, only three showed measurable weight reduction of PET microplastics during the incubation period (Table 3). PET was chosen for this test due to its classification as a biodegradable plastic by microorganisms and enzymes (Ru et al., 2020).

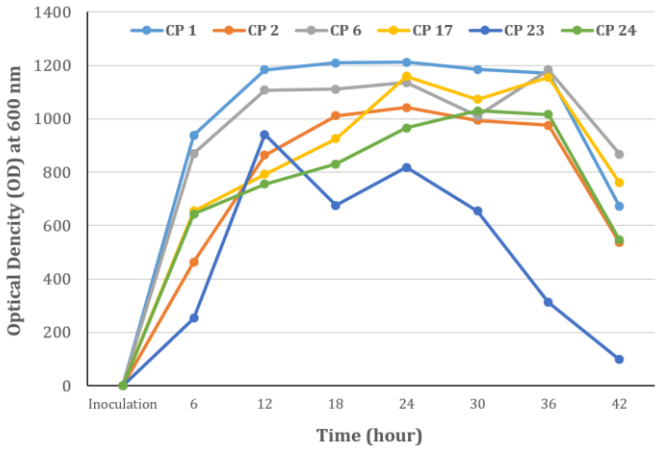

Figure 1. Growth curve of bacterial isolates

Results indicate that only a few isolates demonstrated significant degradation ability, suggesting that factors such as microplastic type, size, pH, salinity, and temperature play crucial roles (Chen et al., 2017). The reduction in microplastic weight was attributed to bacterial metabolic processes that break down the polymer structure into simpler compounds. Mukherjee et al. (2016) observed that bacteria like *Bacillus licheniformis* and *Lysinibacillus fusiformis* initiate microplastic degradation by forming surface cracks, leading to loose chemical bonds such as carbonyl groups, ketones, and aldehydes. Auta et al. (2018) described the degradation process as a two-step mechanism: bacteria first attach to the polymer's surface, form colonies, and then secrete extracellular enzymes that cleave the polymer chains into metabolizable monomers.

Table 2. Optical Density (OD) at 600 nm

Code	Inoculation	6	12	18	24	30	36	42
CP 1	0	939	1184	1210	1212	1185	1170	672
CP 2	0	464	864	1012	1043	994	976	537
CP 6	0	870	1108	1111	1136	1011	1184	867
CP 17	0	655	793	926	1159	1073	1155	760
CP 23	0	253	942	676	818	655	312	98
CP 24	0	644	756	831	966	1030	1017	546
P 2 5	0	925	1125	1147	1202	1238	1195	600

Table 3. Result of Microplastic Degradation Test

Code	Initial weight (mg)	Final weight (mg)	Difference (mg)	% Reduction
CP1	8.34	8.24	0.10	1.15
CP2	8.20	8.00	0.20	2.43
CP6	8.40	8.36	0.04	0.41
CP17	8.27	8.27	0.00	0
CP23	8.76	8.76	0.00	0
CP24	8.60	8.60	0.00	0

Molecular identification of bacteria

The molecular identification of bacterial isolates CP1 and CP2 revealed DNA sequence lengths of 1421 bp and 1424 bp, respectively. BLAST (Basic Local Alignment Search Tool) analysis was used to compare these sequences with entries in the NCBI GenBank database. Results for isolate CP1 (Table 4) indicated a high percentage identity with several *Bacillus* species, including *Bacillus cereus* strain CM 2010 (16S ribosomal RNA, partial sequence), *Bacillus paramycoides* strain MLCCC 1A04089 (16S ribosomal RNA, partial sequence), and *Bacillus anthracis* strain Vollum (complete genome). Phylogenetic analysis (Figure 2) demonstrated that CP1 is closely related to *Bacillus anthracis* str. Collum, confirming its classification within the genus *Bacillus*. As described by Horiike (2016), phylogenetic analysis helps explain evolutionary

relationships among organisms, with the phylogenetic tree serving as a visual representation of these relationships. *Bacillus anthracis* is one of seven species closely related to *Bacillus cereus*.

Similarly, BLAST analysis for isolate CP2 (Table 5) revealed matches with *Bacillus cereus* ATCC 14579 (complete genome) and several other *Bacillus cereus* strains, confirming that CP2 belongs to the genus *Bacillus*. The phylogenetic tree (Figure 3) further identified isolate CP2 as closely related to *Bacillus cereus* ATCC 14579, supporting its classification within the *Bacillus* genus.

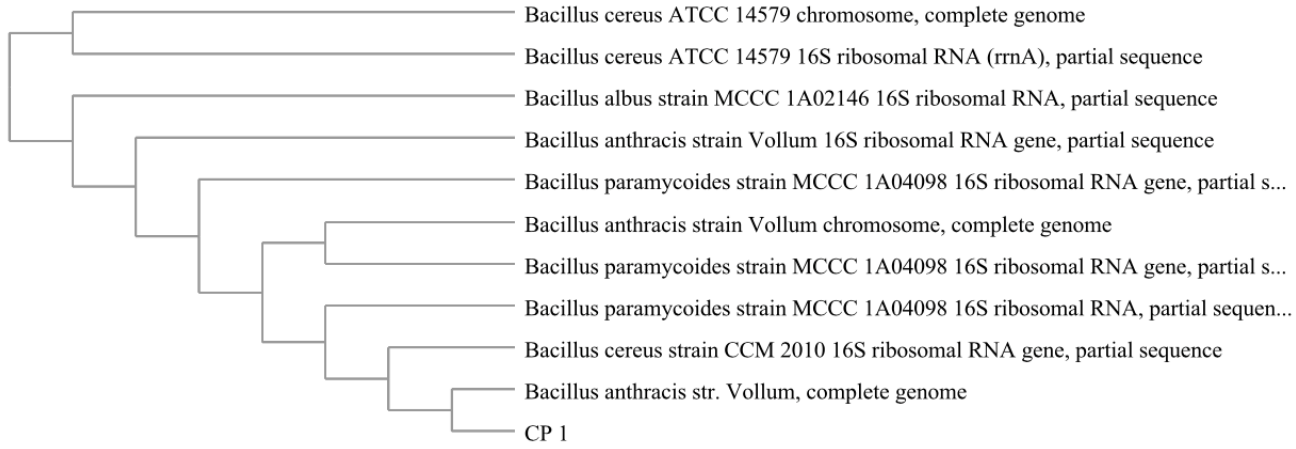

Figure 2. Phylogenetic tree of CP1, based on 16S rRNA gene sequence

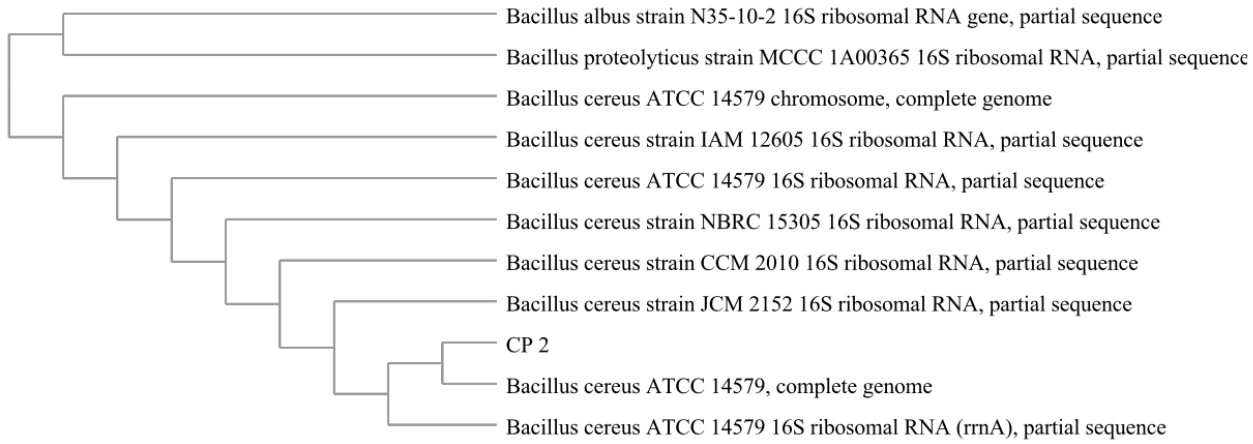

Figure 3. Phylogenetic tree of CP2, based on 16S rRNA gene sequence

Table 4. BLAST result from CP 1 bacterial isolates

Description	Max score	Total score	Query cover	E value	Per. ident	Accession
Bacillus cereus strain CM 2010 16S ribosomal RNA gene, partial sequence	2615	2615	100%	0.0	99.86%	KY628813.1
Bacillus paramycoides strain MCCC 1A04098 16S ribosomal RNA, partial sequence	2615	2615	100%	0.0	99.86%	NR_157734 1
Bacillus anthracis strain Vollum chromosome, complete genome	2615	28703	100%	0.0	99.86%	CP076225.1
Bacillus anthracis str. Vollum, complete genome	2615	28663	100%	0.0	99.86%	CP007666.1
Bacillus paramycoides strain MCCC 1A04098 16S ribosomal RNA gene _ partial sequence	2614	2614	100%	0.0	99.86%	MW065486.1
Bacillus anthracis strain Vollum 16S ribosomal RNA gene, partial sequence	2612	2612	100%	0.0	99.79%	AF290553.1
Bacillus albus strain MCCC 1A02146 16S ribosomal RNA, partial sequence	2610	2610	100%	0.0	99.79%	NR_157729.1
Bacillus paramycoides strain MCCC 1A04098 16S ribosomal RNA gene, partial sequence	2606	2606	99%	0.0	99.79%	MK183820.1
Bacillus cereus ATCC 14579 chromosome, complete genome	2604	33858	100%	0.0	99.72%	CP034551.1
Bacillus cereus ATCC 14579 16S ribosomal RNA (ImA), partial sequence	2604	2604	100%	0.0	99.72%	NR_074540.1

Table 5. BLAST results from CP2 bacterial isolates

Description	Max score	Total score	Query cover	E value	Per. ident	Accession
Bacillus cereus ATCC 14579 chromosome, complete genome	2614	33983	100%	0.0	99.79%	CP034551.1
Bacillus cereus ATCC 14579 16S ribosomal RNA (rRNA), partial sequence	2614	2614	100%	0.0	99.79%	NR_074540.1
Bacillus cereus strain JCM 2152 16S ribosomal RNA, partial sequence	2614	2614	100%	0.0	99.79%	NR_113266.1
Bacillus cereus strain CM 2010 16S ribosomal RNA.partial sequence	2614	2614	100%	0.0	99.79%	NR_115714.1
Bacillus cereus strain NBC 15305 16S ribosomal RNA. partial sequence	2614	2614	100%	0.0	99.79%	NR_112630.1
Bacillus cereus ATCC 14579 16S ribosomal RNA partial sequence	2614	2614	100%	0.0	99.79%	NR_114582.1
Bacillus cereus ATCC 14579 complete genome	2614	33950	100%	0.0	99.79%	AE016877.1
Bacillus cereus strain AM 12605 16S ribosomal RNA, partial sequence	2614	2614	100%	0.0	99.79%	NR_115526.1
Bacillus albus strain N35-10-2 16S ribosomal RNA gene, partial sequence	2612	2612	99%	0.0	99.79%	OQ876685.1
Bacillus proteolyticus strain MCCC 1A00365 16S ribosomal RNA. partial sequence	2608	2608	100%	0.0	99.72%	NR_157735.1

Contamination degradation test

The results of microplastic degradation testing for various contaminants on agricultural land, as shown in Figure 4, indicated that all treatments resulted in increased degradation compared to the control group. ANOVA analysis, performed with a 95% confidence level, revealed that both the type of plastic contamination and the bacterial isolate significantly influenced the percentage of microplastic degradation, with a notable interaction between the two factors. Figure 4 illustrates the results of the Duncan's Multiple Range Test (DMRT), which assessed the degradation rates of different combinations of bacterial isolates and plastic types. The highest degradation rate was observed in the A3B2 treatment (sack + *Bacillus cereus*), which showed a 100% increase over the control treatment (A3B0: sack + no bacteria) and a 23.7% higher degradation than the second-best treatment (A3B1: sack + *Bacillus anthracis*). The lowest degradation was recorded in the A2B2 treatment (polybag + *Bacillus cereus*), indicating that polybags are more resistant to bacterial degradation. However, even this treatment demonstrated a significant improvement, achieving a 100% degradation rate compared to the control (A2B0: polybag + no bacteria).

Bacillus cereus has been identified as an effective microplastic degrader, commonly found in soil, plants, and food. Research by Auta et al. (2018) demonstrated that *Bacillus cereus* isolated from mangrove sediments in Peninsular Malaysia could degrade polypropylene (PP) microplastics by 6.6% over 40 days. The higher degradation rates for sack materials can be attributed to their thin sheets and the elemental composition of biodegradable PP, making them more accessible for microbial action. In contrast, thicker polybags and HDPE (High-Density Polyethylene) plastics are more challenging to degrade due to their dense, non-porous structures. Mohanan et al. (2020) found that PP degrades more readily by microorganisms compared to HDPE and polyethylene (PE). The lean plastic mulch and silver-black mulch, made from PE fabric, are more difficult to degrade, as their outer layer often contains a thin metallic film (e.g., aluminum) that adds to the complexity of the degradation process.

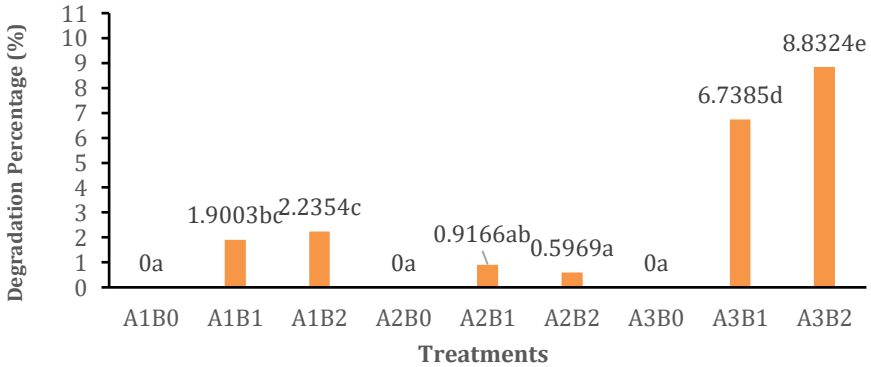

Figure 4. The influence of the type of bacteria and type of plastic on the percentage of plastic weight reduction

Conclusion

The study identified *Bacillus anthracis* and *Bacillus cereus* as microplastic-degrading bacteria in soil samples collected from the Putri Cempo Landfill. Degradation tests on various plastic contaminants commonly found in agricultural settings revealed that no degradation occurred in the control treatment, which lacked bacterial isolates. The highest degradation rate was observed with *Bacillus cereus* on sack material, achieving an 8.83% reduction, followed by *Bacillus anthracis* on the same material with a 6.73% reduction. The CP2 bacterial isolate also showed degradation potential on mulch, with a 2.23% reduction. These results indicate that sack materials are the most susceptible to microbial degradation, while polybag materials present the greatest resistance. The findings confirm that *Bacillus* species can effectively degrade microplastics, demonstrating their potential for bioremediation in agricultural soils.

References

Alabi, O.A., Ologbonjaye, K.I., Awosolu, O., Alalade, O.E., 2019. Public and environmental health effects of plastic wastes disposal: A review. *Journal of Toxicology and Risk Assessment* 5(2): 1-13.

Auta, H.S., Emerinke. C.U., Jayanthi, B., Fauziah, S.H., 2018. Growth kinetics and biodeterioration of polypropylene microplastics by Bacillus sp. and Rhodococcus sp. isolated from mangrove sediment. *Marine Pollution Bulletin* 127: 15–21.

Chen, Q., Li. J., Liu, M., Sun, H., Bao, M., 2017. Study on the biodegradation of crude oil by free and immobilized bacterial consortium in marine environment. *PLoS ONE* 12(3): e0174445.

Dash, H.R., Mangwani, N., Chakraborty, J., Kumari, S., Das, S., 2013. Marine bacteria: Potential candidates for enhanced bioremediation. *Applied Microbiology and Biotechnology* 97(2): 561–571.

Ding, L.J., Su, J.Q., Li, H., Zhu, Y.G., Cao, Z.H., 2017. Bacterial succession along a long-term chronosequence of paddy soil in the Yangtze River Delta, China. *Soil Biology and Biochemistry* 104: 59–67.

Dussud, C., Hudec, C., George, M., Fabre, P., Higgs, P., Bruzaud, S., Delort, A.M., Eyheraguibel, B., Meistertzheim, A.L., Jacquin, J., Cheng, J., Callac, N., Odobel, C., 2018. Colonization of non-biodegradable and biodegradable plastics by marine microorganisms. *Frontiers in Microbiology* 9: 1571.

Figueroa-Bossi, N., Balbontín, R., Bossi, L. 2022. Basic Bacteriological Routines. *Cold Spring Harbor Protocols* 2022(10): 462–468.

Harshvardhan. K., Jha. B. 2013. Biodegradation of low-density polyethylene by marine bacteria from pelagic waters, Arabian Sea, India. *Marine Pollution Bulletin* 77(1–2): 100–106.

Hartmann, N.B., Hüffer, T., Thompson, R.C., Hassellöv, M., Verschoor, A., Daugaard, A.E., Rist, S., Karlsson, T., Brennholt, N., Cole, M., Herrling, M.P., Hess, M.C., Ivleva, N.P., Lusher, A.L., Wagner, M.,2019. Are we speaking the same language? Recommendations for a definition and categorization framework for plastic debris. *Environmental Science and Technology* 53(3): 1039–1047.

Horiike, T. 2016. an Introduction To Molecular Phylogenetic Analysis. *Reviews in Agricultural Science* 4: 36–45.

Hou, L., Xi, J., Liu, J., Wang, P., Xu, T., Liu, T., Qu, W., Lin, Y.B., 2022. Biodegradability of polyethylene mulching film by two Pseudomonas bacteria and their potential degradation mechanism. *Chemosphere* 286: 131758.

Javed, S., Azeem, F., Hussain, S., Rasul, I., Siddique, M.H., Riaz, M., Afzal, M., Kouser, A., Nadeem, H., 2018. Bacterial lipases: A review on purification and characterization. *Progress in Biophysics and Molecular Biology* 132: 23–34.

Jeon, H.J., Kim, M.N., 2015. Functional analysis of alkane hydroxylase system derived from Pseudomonas aeruginosa E7 for low molecular weight polyethylene biodegradation. *International Biodeterioration and Biodegradation* 103: 141–146.

Khalid, N., Aqeel, M., Noman, A., Rizvi, Z.F., 2023. Impact of plastic mulching as a major source of microplastics in agroecosystems. *Journal of Hazardous Materials* 445: 130455.

Lee, S.A., Kim, J.M., Kim, Y., Joa, J.H., Kang, S.S., Ahn, J.H., Kim, M., Song, J., Weon, H.Y., 2020. Different types of agricultural land use drive distinct soil bacterial communities. *Scientific Reports* 10: 17418.

Li, L., Luo, Y., Li, R., Zhou, Q., Peijnenburg, W.J.G.M., Yin, N., Yang, J., Tu, C., Zhang, Y., 2020. Effective uptake of submicrometre plastics by crop plants via a crack-entry mode. *Nature Sustainability* 3: 929–937.

Lian, J., Wu, J., Xiong, H., Zeb, A., Yang, T., Su, X., Su, L., Liu, W., 2020. Impact of polystyrene nanoplastics (PSNPs) on seed germination and seedling growth of wheat (Triticum aestivum L.). *Journal of Hazardous Materials* 385: 121620.

Mohanan, N., Montazer, Z., Sharma, P.K., Levin, D.B., 2020. Microbial and enzymatic degradation of synthetic plastics. *Frontiers in Microbiology* 11: 580709.

Mukherjee, S., Chowdhuri, U.R., Kundu, P.P., 2016. Bio-degradation of polyethylene waste by simultaneous use of two bacteria: Bacillus licheniformis for production of bio-surfactant and Lysinibacillus fusiformis for bio-degradation. *RSC Advances* 6: 2982–2992.

Park, S., Kang, S.E., Kim, S.J., Kim, J., 2023. Graphene-encapsulated yeast cells in harsh conditions. *Fungal Biology* 127: 1389–1396.

Park, S.Y., Kim, C.G., 2019. Biodegradation of micro-polyethylene particles by bacterial colonization of a mixed microbial consortium isolated from a landfill site. *Chemosphere* 222: 527–533.

Prasenja, Y., Putra, J.H., Hidayati, K. 2022. Prediksi daya dukung dan daya tampung Tempat Pembuangan Akhir Putri Cempo Surakarta. *Majalah Geografi Indonesia* 36(1): 62-67.

Rosariastuti, R., Sutami, Nugraha, S., Amanto, B.S., 2023. Bacterial diversity in the western slopes of Mount Lawu, Karanganyar, Indonesia. *Biodiversitas* 24(4): 2125–2133.

Ru, J., Huo, Y., Yang, Y., 2020. Microbial degradation and valorization of plastic wastes. *Frontiers in Microbiology* 11: 1–20.

Vianti, R.O., Purwiyanto, A.I., 2020. Purifikasi Dan Uji Degradasi Bakteri Mikroplastik Dari Perairan Muara Sungai Musi, Sumatera Selatan. *Maspari Journal : Marine Science Research* 12(2): 29–36

Wang, L., Liu, Y., Kaur, M., 2021. Phytotoxic effects of polyethylene microplastics on the growth of food crops soybean (Glycine max) and mung bean (vigna radiata). *International Journal of Environmental Research and Public Health* 18(20): 10629.

Wijanarka, W., Kusdiyantini, E., Parman, S., 2016. Screening cellulolytic bacteria from the digestive tract snail (Achatina fulica) and test the ability of cellulase activity. *Biosaintifika: Journal of Biology & Biology Education* 8(3): 385-391.

Yang, J., Yang, Y., Wu, W.M., Zhao, J., Jiang, L., 2014. Evidence of polyethylene biodegradation by bacterial strains from the guts of plastic-eating waxworms. *Environmental Science and Technology* 48(23): 13776–13784.

Zhang, B., Yang, X., Chen, L., Chao, J., Teng, J., Wang, Q., 2020. Microplastics in soils: a review of possible sources, analytical methods and ecological impacts. *Journal of Chemical Technology and Biotechnology* 95(8): 2052–2068.

Eurasian Journal of Soil Science 2025, 14(1), 87 - 97

Eurasian Journal of Soil Science

Journal homepage : http://ejss.fesss.org

Zeolite-based nano phosphatic fertilizer for enhancing phosphorus availability in acidic soils of Assam, India

Sukanya Pachani [a], Gayatri Goswami Kandali [a,*], Binoy Kumar Medhi [a], Lakshi Saikia [b], Anjali Basumatary [a], Mahima Begum [c], Samikhya Bhuyan [d]

[a] Department of Soil Science, College of Agriculture, Assam Agricultural University, Jorhat – 785013, Assam, India
[b] Materials Sciences & Technology Division, CSIR – North East Institute of Science and Technology, Jorhat – 785006, Assam, India
[c] Department of Agronomy, College of Agriculture, Assam Agricultural University, Jorhat – 785013, Assam, India
[d] Department of Soil Science and Agricultural Chemistry, Rajiv Gandhi University, Rono Hills, Doimukh, Arunachal Pradesh – 791112, India

Article Info
Received : 08.05.2024
Accepted : 11.11.2024
Available online: 14.11.2024

Author(s)
S.Pachani
G.G.Kandali *
B.K.Medhi
L.Saikia
A.Basumatary
M.Begum
S.Bhuyan

Abstract

Considering the fixation and low availability of conventional phosphatic fertilizer in acidic soil, zeolite based nano phosphatic fertilizer was synthesized to investigate its release characteristics in acidic soil system via *invitro* studies. Result revealed that surface modification through a cationic surfactant improved the adsorption capacity of zeolite for phosphorus by 60%. Under the incubation study, the zeolite based nano phosphatic fertilizer sustained the release of phosphorous up to 90 days of incubation against 32 days under conventional SSP. The 100% replacement of RDP through nano fertilizer registered the maximum release of P in soil up to 9.36 mg/kg which was 23.80% higher than conventional SSP (7.56 mg/kg). The study release kinetics also revealed parabolic diffusion equation (3.012 µg/g/day) as the most suitable module for describing the P release as compared to other kinetic modules. Thus, zeolite can be used as carrier material for preparation of nano fertilizer for sustainable release of P for longer period of time under acidic soil.

Keywords: Zeolite, nano fertilizer, slow release, acid soil, parabolic diffusion, soil chemistry.

* Corresponding author

Introduction

Phosphorus, an essential macronutrient required for agricultural production (Wahid et al., 2020) is a principal component of cell membrane system, chloroplast, and mitochondria (Cordell et al., 2014). The requirement of phosphorous for various metabolic activities including growth of various plant parts of plant is already well established (Bindraban et al., 2020). Plants generally take up inorganic phosphorus ($H_2PO_4^-$ and HPO_4^{2-}) from soil solutions (Ibrahim et al., 2022), which accounts for about 35% to 70% of the total phosphorus present in soil system (Wilson et al., 2019). However, the movement of phosphorus in soil is subjected to different forms of losses, making it hurdle for a healthy growth of the crop. In acidic and highly weathered soils, 75-80% (Mahmood et al., 2021) of applied P is fixed onto the surfaces of Fe and Al oxides and hydroxides (Prüter et al., 2020) besides clay mineral lattices to form various complexes (Arai and Sparks, 2007), thereby reducing the available P concentration necessary for plant uptake. Leaching is another form of loss of P from the soil solution (Wakelin et al., 2017). Commercially available P sources, heretofore, are utilized to upgrade the agronomic production to meet the basic requirement (Sharpley et al., 2018). These sources contain water soluble phosphate salts which hardly provide 10-25% (Tarafdar et al., 2015) of P to the crops and the rest often wind up percolating to surface water bodies and coastal ecosystems through run-off or seepage, exacerbating the environmental degradation caused by

: https://doi.org/10.18393/ejss.1585148
: https://ejss.fesss.org/10.18393/ejss.1585148
Publisher : Federation of Eurasian Soil Science Societies
e-ISSN : 2147-4249

eutrophication (Conjin et al., 2018). Nano fertilizer shows promising outcomes to improve nutrient availability by exploring unique properties of nanoparticles (Poddar et al., 2018, Noruzi et al., 2023). They are nutrient carriers of dimensions ranging from 1-100 nm in size (Liu and Lal, 2014), having high surface area to volume ratio (Kumar et al., 2017). One of the major attributes is that they have small particle size (Chinnamuthu and Boopathi, 2009) which provides better penetration into the cell, activating plant and microbial functions for more plant nutrients uptake (Montalvo et al., 2015). Apart from increasing the yield and quality of agricultural produce, nano fertilizer improves the soil health creating favourable habitat for soil flora and fauna (Tarafdar et al., 2015).

The surface modified zeolite can be explored as one of the carrier options for preparation of zeolite based nano phosphatic fertilizer (Bhardwaj et al., 2014) which absorbs both positive (K^+, NH_4^+) and negative (NO_3^-, PO_4^{3-}) ions for its slow release to soil system (Solanki et al., 2015). Zeolites are alumino-silicate minerals, which have a molecular sieve action due to their open channel network; they are composed of SiO_4 tetrahedra linked with oxygen sharing the negative charge created by the presence of AlO_2^- which is balanced by cations that neutralize the charge deficiency (Jakkula and Wani, 2018). The preferential ion exchange property of zeolite (Wei et al., 2011) help the plants to utilize most of the nutrients by minimizing waste either through leaching (Subramanian and Thirunavukkarasu, 2017), volatilization or fixation in the soil (Dhansil et al., 2018). Therefore, the present investigation was carried out to study and analyse the feasibility of zeolite enabled phosphatic nano fertilizer for P availability in strongly acidic (pH < 5.5) environment. The nutrient uptake capacity of the synthesized nanofertilizer was studied, followed by comparative assessment of nutrient leaching patterns of P from nanofertilizer and conventional fertilizer. An evaluation of different reduced doses of nano fertilizer was also carried out to gauge the optimum dose economically and ecologically important for maintaining balanced crop nutrition.

Material and Methods

Fertilizer preparation

The synthesis of surfactant modified zeolite (SMZ) and zeolite based nano fertilizer for P was done following the standard procedure (Bansiwal et al., 2006). As shown in Figure 1, the synthesis of the nano fertilizer, Zeolite A (Sigma Aldrich), hexadecyltrimethylammonium bromide (HDTMABr) (Sigma Aldrich, ≥ 98%) were used 1:100 ratio. The mixture was stirred with 1M concentration of KH_2PO_4 solution for 8 hours. A 1:10 (solid to liquid) ratio followed by distillation and air drying. The dried sample was grounded to a finer particle size. Similarly, nutrient incorporation was carried out on unmodified zeolite to study the effect of surface modification on nutrient uptake capacity in comparison to surfactant modified zeolite.

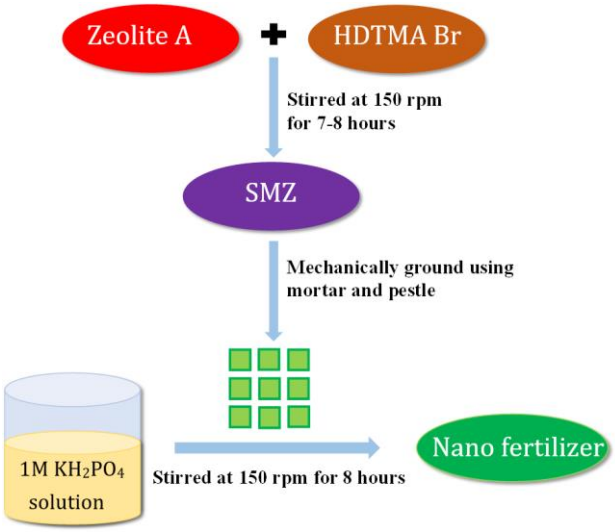

Figure 1. Schematic representation of preparation of Zeolite based nano P fertilizer

Characterization of the nano fertilizer

The unmodified zeolite and surfactant modified zeolite based nano phosphatic fertilizer were characterized by Powder X-ray diffractometer, Scanning Electron Microscope, Transmission Electron Microscope and Brunauer-Emmett-Teller adsorption isotherm. Crystal phase identification was conducted by powder X-ray diffraction. The powder X-ray diffractometer measurement was carried out on a Rigaku Ultima IV X-ray diffractometer of 2θ range using a Cu-Kα source of wavelength, λ = 1.54 Å. For examining the surface morphology, scanning electron microscopy images were acquired using a Carl Zeiss SIGMA scanning

electron microscope. The compositional analysis of the synthesized nanoparticles was carried out by Energy Dispersive X-ray spectroscopy on an Oxford EDS attached to the same instrument. The particle size of the nano-fertilizer was assessed from the Transmission Electron Microscope images, which were recorded on a JEOL, JEM-2100 Plus Electron Microscope. Specific surface area, pore volume and pore diameter were analysed by Brunauer-Emmett-Teller surface area analyser on an Autosorb- iQ (Quantach – rome USA) adsorption analyser. The samples were degassed at 150ºC for 16 hours.

Collection and processing of soil for experimentation

The soil samples were collected from three different locations based on texture representing major soil orders of Assam, India. The vegetation cultivation area of Dhekorgorah block (Latitude: 26°82'18" N; Longitude: 94°31'53" E) of Jorhat district was taken for the soil order Inceptisols (silty clay loam). The rice cultivation area of Regional Agriculture Research Station (RARS), Titabar (Latitude: 26°34'51" N; Longitude: 94°10'50" E) was selected for soil order Alfisols (clay loam). The alluvium rich soil of Majuli (Latitude: 27°03'55" N; Longitude: 94°16'57" E) was taken for soil order Entisols (sandy clay loam). To conduct the incubation study, bulk surface soil samples (0-15 cm) from each site were collected and prepared following standard procedures. The analysis of initial soil parameters prior to application of fertilizers are given in Table 1.

Table 1. Initial physico-chemical properties of the soils

Parameters	Jorhat	Titabar	Majuli
Soil order	Inceptisol	Alfisol	Entisol
pH (soil:water :: 1:2.5)	5.34	5.07	5.53
Electrical conductivity (dSm^{-1})	0.02	0.03	0.03
Particle size distribution			
Sand (%)	19.00	42.00	60.00
Silt (%)	47.00	20.00	15.00
Clay (%)	34.00	38.00	25.00
Textural class	Silty clay loam	Clay loam	Sandy clay loam
Bulk density (g/cm^3)	1.35	1.32	1.39
Particle density(g/cm^3)	2.49	2.39	2.46
Moisture content at Field Capacity (%)	28.37	30.70	27.45
Organic carbon (%)	0.87	0.78	0.93
Available N (kg/ha)	347.61	298.70	361.70
Available P_2O_5 (kg/ha)	25.57	19.47	38.89
Available K_2O (kg/ha)	174.18	118.51	229.28
Exchangeable Ca^{2+}(cmol(p+)/kg)	1.87	2.73	3.21
Exchangeable Mg^{2+} (cmol(p+)/kg)	0.79	1.94	2.13
Cation Exchange Capacity (CEC)(cmol(p+)/kg)	8.19	8.22	7.23
Available S (mg/kg)	13.38	12.81	20.65

Incubation study

About 200 g of finely ground processed soil was placed in plastic containers of capacity 500 g and fertilizer was applied based on the recommended dose of fertilizer for maize (60:40:40 @ N: P_2O_5:K_2O kg/ha) before the incubation study. Recommended dose N and K remained constant throughout the treatments and P was supplied as per treatment mentioned below. Soils were incubated at room temperature (± 27°C) in the laboratory. A total of 10 sets were prepared for each periodical assessment for better results. The containers were partially closed for better gaseous exchange and limiting moisture loss. Soil moisture was maintained at field capacity during the entire period of experimentation. The loss in water content in soil was monitored at 3 days interval by addition of water as determined by the loss in weight of the containers.

Treatments included:

T_1 = Absolute control

T_2 = RDP through single superphosphate (SSP)

T_3 = RDP through nano fertilizer

T_4 = 2.5 times reduction of RDP from T_3

T_5 = 5 times reduction of RDP from T_3

T_6 = 10 times reduction of RDP from T_3

Samples were collected from the respective set at 0, 4, 7, 15, 22, 32, 44, 58, 74 and 90 days of incubation for analysis of the release pattern of P from the chemical and synthesized nano-fertilizer.

Kinetic equations

The rate kinetics of P was assessed based on first order, second order and parabolic diffusion as per the equations [3]:

$$\text{First order} : \text{Log}C_t = \text{Log}C_o - kt$$
$$\text{Second order} : 1/C_t = 1/C_o + kt$$
$$\text{Parabolic diffusion} : C_t/C_o = b + kt^{1/2}$$

Where,

C_t = cumulative concentration of available P (µg/g)
C_o = concentration of P which can be released at equilibrium (µg/g)
k = rate constant
b = C_t/C_o when k = 0 or t = 0 (dimensionless)
t = time (days of incubation)

Statistical analysis

The data obtained under different treatments of each soil was statically analysed to see the significance of variance using Analysis of Variance (ANOVA) at 0.05 significance using IBM Statistical Package for Social Sciences (SPSS) Version 20. To compare the means post hoc analysis was done using Duncan's Multiple Range Test (DMRT).

Results and Discussion

Fertilizer characterization

The crystal phase of the synthesized nano P fertilizer was examined by the X–ray powder diffraction as displayed in Figure 2. The crystallinity of zeolite remained the same as diffraction peaks at 8.93° and 24.06° with indexes of (0 2 0) and (4 0 0) respectively, was seen in the spectrum, which is similar to parent zeolite (Mikhak et al., 2017). This suggests that there were no major structural changes in zeolite framework due to addition of HDTMABr surfactant except for minor changes in the intensity of the band's peak suggesting the retention of P ion within the porous structure of zeolite (Abdul Majid et al.,2018; Mir et al., 2020). The surface morphology of unmodified and modified zeolite was envisaged by scanning electron microscope as depicted in Figure 3. It was observed that the zeolite was of cubical geometry and the crystal lattice was mostly bound aggregates of small cubic particles. However, this was not clearly observed in case of modified zeolite. The particles of the modified zeolite appeared to have broken edges and corners possibly due to HDTMABr coverage on the external surface area of the crystal lattice, which also depicted the adsorption of P and other ion. Similar observations were also reported (Bansiwal et al., 2006; Yan et al., 2014).

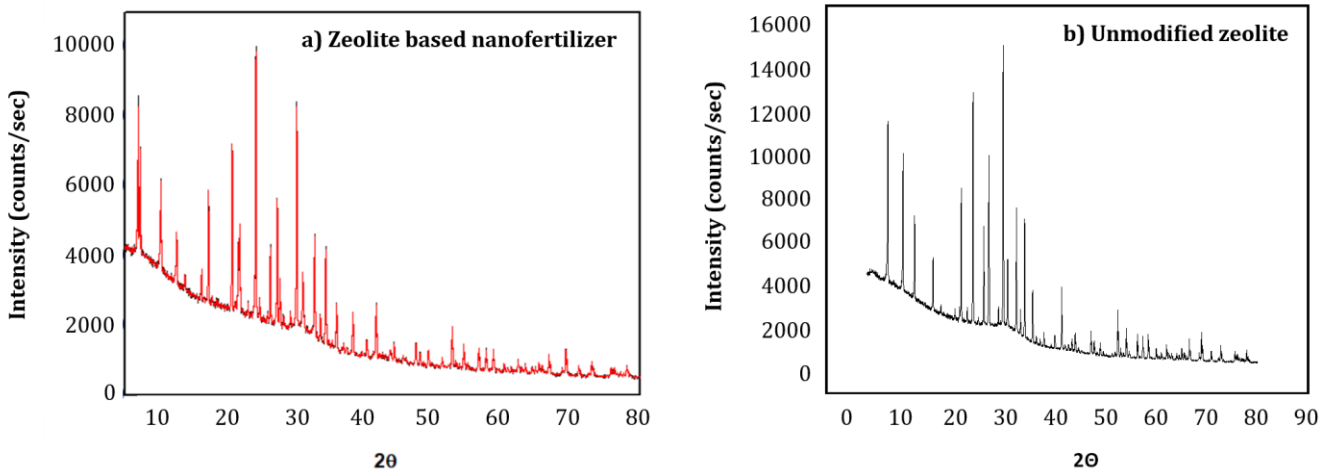

Figure 2. XRD (Powder X-ray diffractometer) patterns of (a) synthesized nano phosphorus fertilizer and (b) parent zeolite (for reference)

The elemental composition of the nano-fertilizer was acquired from the EDX pattern which established the existence of C, N, O, Al, Si, Br, Na, P and K in the compound. During the EDX measurement, different areas were focused, and the corresponding peaks are shown in the figure 4. The addition of surfactant greatly increased adsorption of added P upto 7.4% in nano fertilizer which was 60% greater than the unmodified zeolite. This implies that the surface modification altered the surface charge on zeolite which led to better adsorption of the anion (Akrami et al.,2019). Adsorption of K was also noted from the spectrum of the

sample, probably due to presence of available exchange sites inside the crystal lattice of zeolite. Therefore, stacking of positively charged ions such as K in the pores can be attained together with the negatively charged ions such as P on their surface (Singh et al., 2018; Hagab et al .2018).

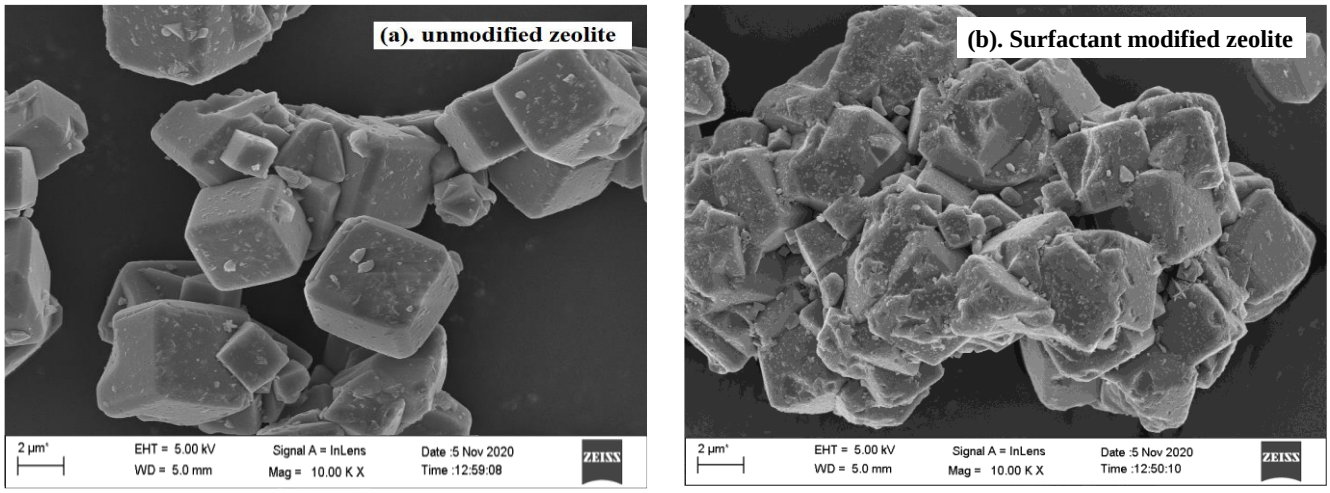

Figure 3. SEM images of (a) unmodified zeolite and (b) modified zeolite fertilizer

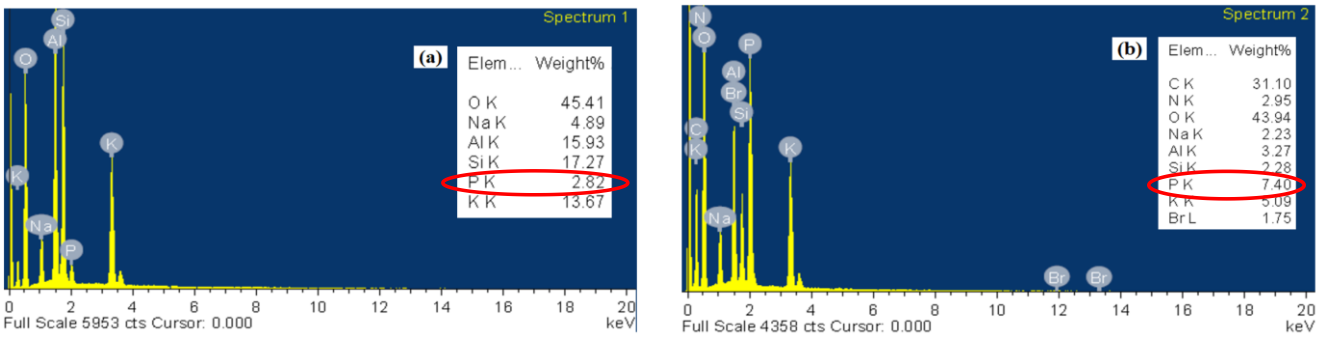

Figure 4. EDX pattern of the nano-fertilizer; (a) spectrum of unmodified zeolite loaded with phosphorus and (b) spectrum of surfactant modified zeolite loaded with phosphorus

From the figure 5, it can be seen that average particle size of zeolite based nano P fertilizer < 100 nm which clearly falls within the nanoparticle range of 1-100 nm (Liu and Lal, 2014; Montalvo et al., 2015). The small black dots observed in the images (Fig. 5a & 5b) were most probably the nutrient particles. As seen in the Figure 5(a), the channel like structures depicted the pores of the nano zeolite particles. In the closer resolution of the sample clear lattice fringes were seen which assured high crystallinity of the nanostructure (Figure 5c). Almost all the particles had been converted to nano zeolite particles as evident from the small black dots found in the images.

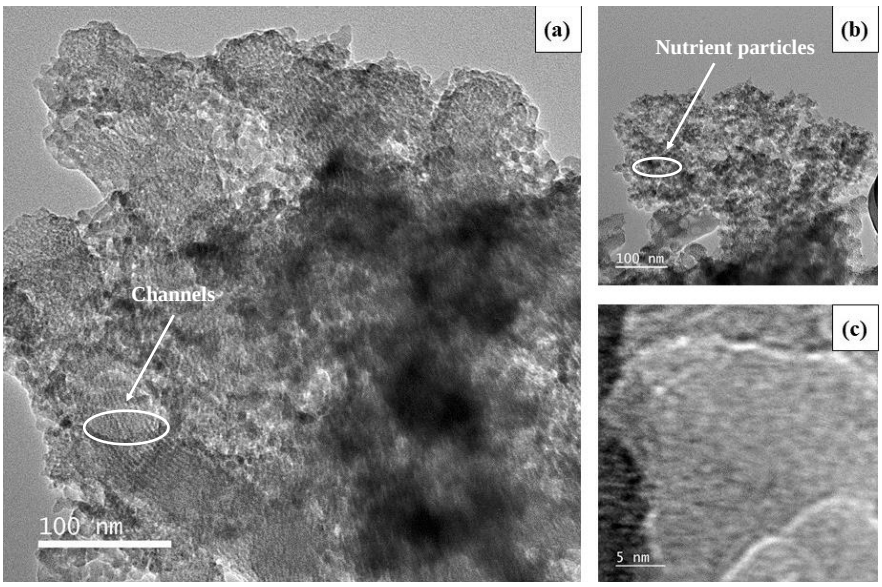

Figure 5. TEM image of the synthesized nano fertilizer

The data presented on Table 2 clearly illustrated that the specific surface area of the modified nano zeolite fertilizer comparatively less (90.07 m^2/g) than the unmodified zeolite (262.72 m^2/g). The specific surface area of zeolite was reduced due to surface modification and subsequent phosphorus loading (Salako et al., 2020). This means that in the pore space of zeolite, P had been loaded which had decreased the pore diameter. Hence, there was overall reduction of surface area of the fertilizer. The pore size was found to be microporous (< 20 nm) in diameter.

Table 2. Surface area, Pore volume and Pore diameter of unmodified and modified zeolite

Sl. No.	Parameters	Unmodified zeolite	Nano P fertilizer
1.	Surface area (m^2/g)	262.72	90.07
2.	Pore volume (cm^3/g)	0.129	0.016
3.	Pore diameter (nm)	6.2	1.2

Release pattern of P

The release pattern of P presented in Figure 6 clearly illustrated that incubation days and clay proportion of the soils played a significant role on release of P in the soil environment and showed a strong and positive interaction between level of treatments and days of incubation. The mean P concentration in control was seen to be declining from 0 to 22 days, then rising from 22 to 44 days, and again decreasing from 44 to 74 days with a slight increase from 74 to 90 days. The overall P level indicated that it was in well maintained equilibrium with respect to the initial P concentration of the soil. The P concentration in T_2 was observed to decrease from 0 to 7 days, with increase from 7 to 32 days. The maximum peak of P release was obtained on 32 days of incubation, after which there was a sharp decline in the release trend which continued up to 90 days of incubation. This might be attributed to low nutrient use efficiency (10-25%) of conventional phosphatic fertilizer (Tarafdar et al., 2015) where about 75-80% of the applied P is fixed by soil solids (Mahmood et al., 2021). Similarly, Dhansil et al. (2018) also reported that in case of chemical fertilizer, the availability of phosphorus greatly increased up to 30 days of incubation and declined afterwards.

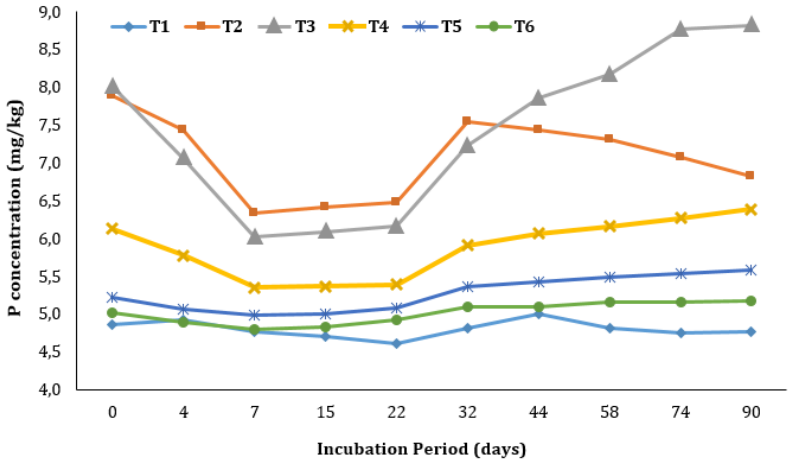

Figure 6. Release of P (mg/kg) as influenced by different levels of treatment over days of incubation (T1= Absolute control, T2 = RDP through single superphosphate, T3= RDF through nano fertilizer, T4 = 2.5 times reduction of RDP from T3, T5 = 5 times reduction of RDF from T3, T6 = 10 times reduction of RDP from T3) Error bars: standard deviation, N = 46

On the contrary, the release of phosphorus from nano fertilizer, showed a gradual increase after 22 days of incubation which was sustained throughout the investigation period. Similar observations have been reported through investigation of nano P formulations in acidic culture media (Mahmood et al., 2021). The release pattern was also similar for the reduced dosages of nano fertilizer applied in the different soil types. The maximum value was recorded on 90 days of incubation with further increasing trend as seen from the Figure 6. T_3 showed the highest increase in mean P levels compared to the other treatments. The slow release of nano-fertilizer might be attributed to the porous structural framework of the zeolite carrier (Singh et al., 2018). The phosphorus adsorbed onto the crystal lattice of zeolite most probably had undergone interaction between the surfaces inside the pores as well as surfaces outside the pores. The loosely bound elements and/or compounds from the top of the surface would release first, then the second layer would contribute and thereafter layer by layer the adsorbed phosphorus would be released by the nano-fertilizer. The influence of several biotic and abiotic factors of soil environment such as soil pH, temperature, humidity, etc., on the fertilizer allowed the zeolite to slowly detach nutrients from its structure (Bharadwaj et al., 2014)

Table 3: Effect of different fertilizer levels on P release in different soil types

Soil type	Treatment	P release
Sandy Clay Loam	T_1	7.51 ± 0.11a
	T_6	7.82 ± 0.25b
	T_5	8.03 ± 0.21b
	T_4	8.64 ± 0.37c
	T_2	9.91 ± 0.49d
	T_3	10.28 ± 1.04e
Silty Clay Loam	T_1	4.81 ± 0.11a
	T_6	5.07 ± 0.21b
	T_5	5.28 ± 0.22b
	T_4	5.88 ± 0.38c
	T_2	7.08 ± 0.52d
	T_3	7.42 ± 1.04e
Clay Loam	T_1	3.70 ± 0.94a
	T_6	3.99 ± 0.14b
	T_5	4.22 ± 0.22b
	T_4	4.79 ± 0.37c
	T_2	5.93 ± 0.58d
	T_3	6.17 ± 1.02d

Means under the same letter in a column are not significantly different at $p \leq 0.001$
*Average ± standard error, treatment has been arranged as descending order.

The P release pattern from the sandy clay loam textured soil presented in Figure 7a revealed highest P concentration in RD of P was applied through nano-fertilizer (10.28 ± 1.04) at 90 days of incubation, which was statistically higher than P released from SSP fertilizer (9.91 ± 0.49). Similarly, in silty clay loam textured soil (Figure 7b) and clay loam textured soil (Figure 7c) the mean P level of T_3 (7.42 ± 1.04; 6.17 ± 1.02, respectively) was found to be highest amongst all the treatment levels.

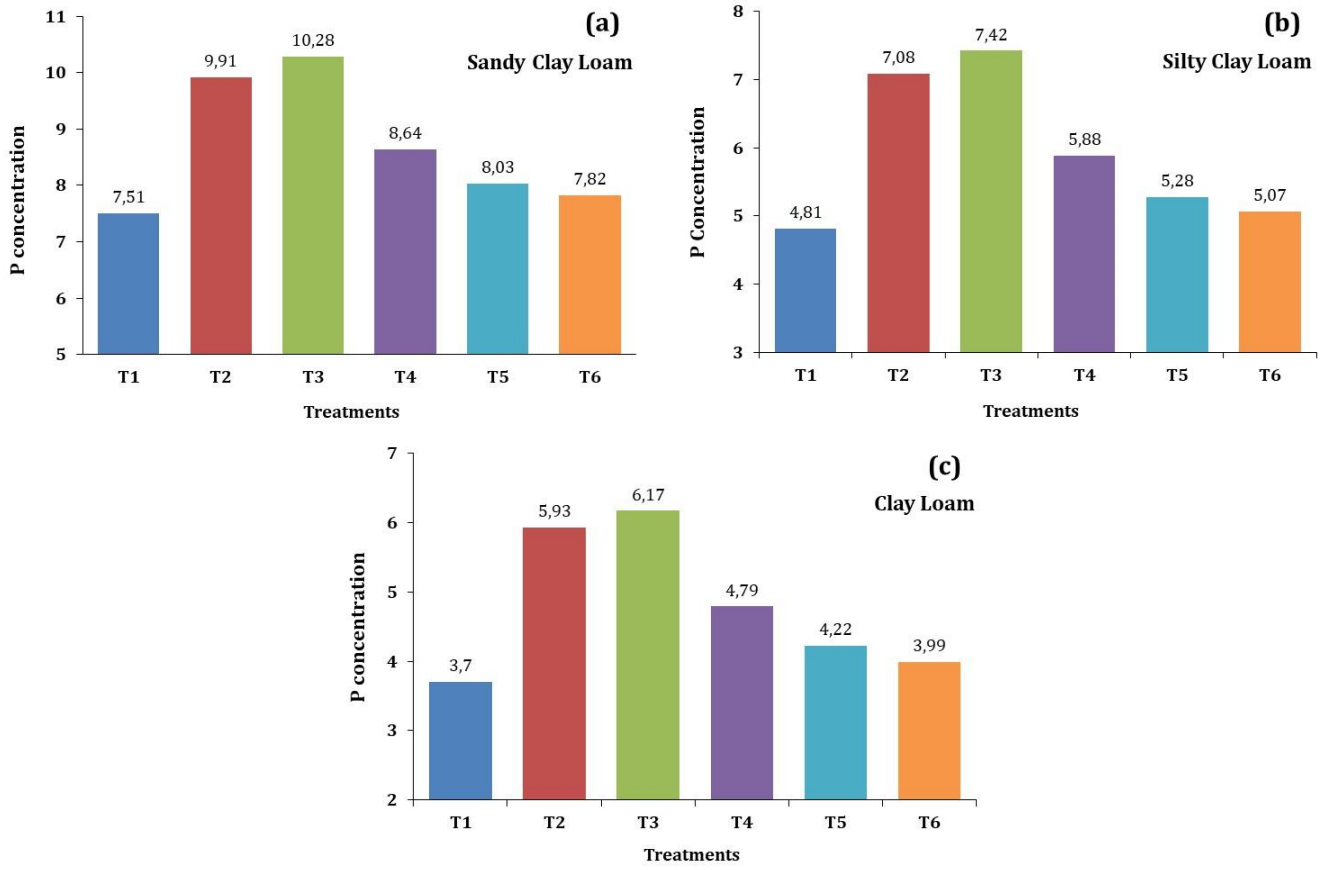

Figure 7. Phosphorus release pattern from different soil due to different treatment levels

The variation in clay content affects the P release pattern in different types of soil as shown in Figure 8. The phosphorus release followed the sequence: sandy clay loam > silty clay loam > clay loam. This might be due to presence of higher content of clay, organic carbon and free oxides of Fe and Al in clay loam textured soil as compared to the other soils, which resulted in more adsorption of P by soil matrix. In contrast, the sandy clay

loam textured soil contained lesser amount of clay, organic carbon and free oxides of Fe and Al, thereby more available phosphorus concentration was being released into the soil solution. Similar observations were reported during other investigations (Prakash et al., 2017; Gupta et al., 2020).

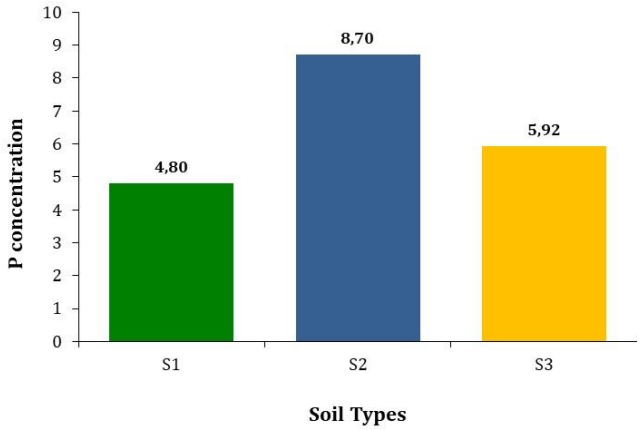

Figure 8. Differences in clay content influence the release of P in soil: sandy clay loam (S2) > silty clay loam (S3) > clay loam (S1)

Kinetics of Phosphate release in soil

The first order kinetic constant was found to increase from T_2 to T_6 in all the three types of soil as noted from Tables 4, 5 and 6. This might be due to less fixation of phosphorus by the sesquioxides content of the soil. The first order kinetic model was unable to describe the P release in soil, due to the uncertainty of the model to explain the concentration of P in soil – water system, whether the contribution of P was from the soil solution or the exchange sites on the clay surfaces (Sparks, 2003). In case of second order kinetics, there was a decrease in rate constant (KcII) value which probably meant that there was increase in the release of P which is dependent upon both soil solution and soil matrix (Sanyal, 2018). The presence of negative sign indicates that as it is inverse of cumulative concentration of available phosphorus ($1/C_t$), while plotting the graph, the slope is from left to right in descending order as depicted in Figure 9. Lower values of correlation coefficients in second order kinetic constants than first order in all the treatments might be due to involvement of solid matrix in regulating equilibrium P concentrations in solution (Medhi et al., 2012).

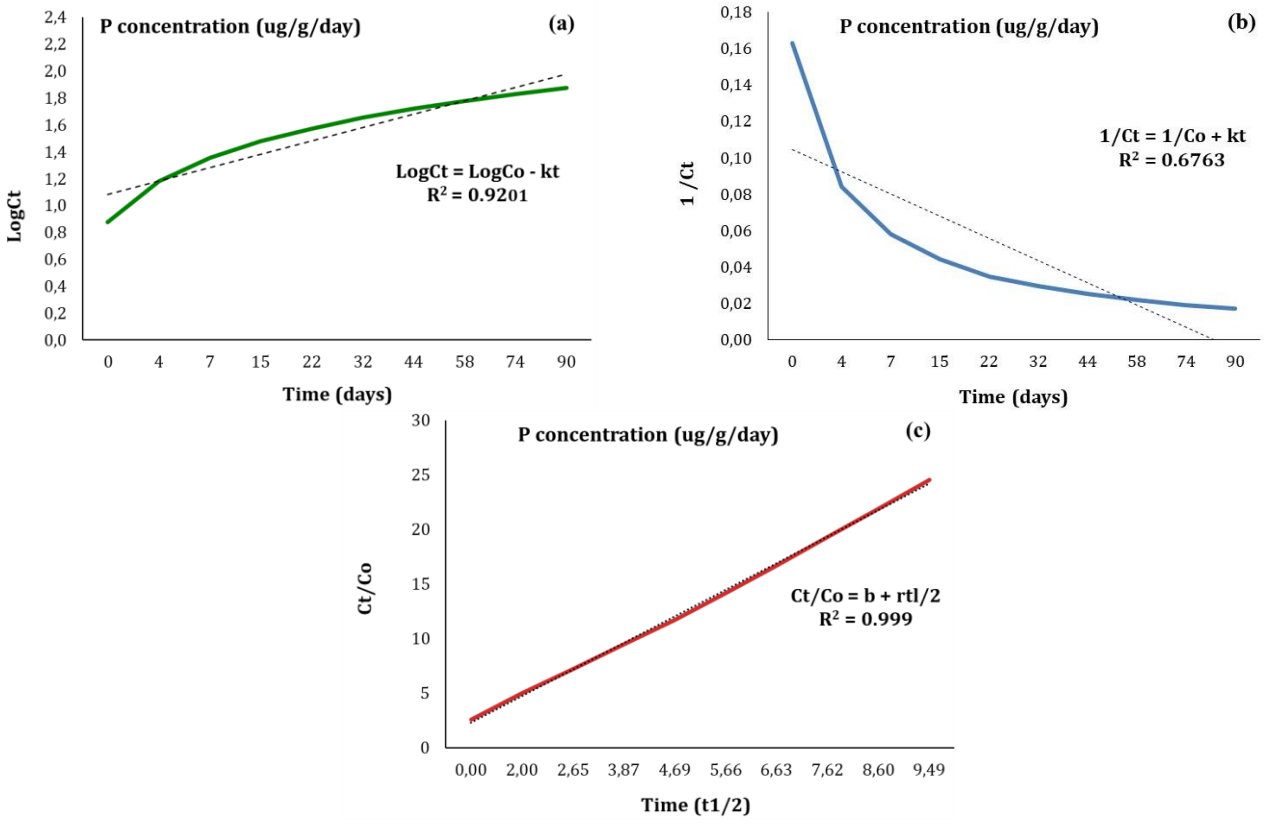

Figure 9. Kinetics of P release in soil system: (a) first order kinetic model, (b) second order kinetic model and (c) parabolic diffusion kinetic model

Table 4. Kinetic parameters from linear regression analysis of first order, second order and parabolic diffusion kinetic models of P release in sandy clay loam soil

Treatments	P release kinetics								
	First order			Second order			Parabolic diffusion		
	Equation	KcI ($\mu g\ g^{-1}day^{-1}$)	R^2	Equation	KcII ($g\ \mu g^{-1}day^{-1}$)	R^2	Equation	Kcp ($\mu g\ g^{-1}day^{-1}$)	R^2
T_1=Absolute control	$logC_t$=0.099t+0.793	0.099	0.906	$1/C_t$=-0.015t+0.143	-0.015	0.654	$C_t/C_o=2.010t^{1/2}$+0.040	2.010	1
T_2=RDF through SSP	$logC_t$=0.096t+0.985	0.096	0.920	$1/C_t$=-0.009t+0.091	-0.009	0.681	$C_t/C_o=2.909t^{1/2}$+0.245	2.909	0.999
T_3=RDF through nano fertilizer	$logC_t$=0.097t+0.971	0.097	0.939	$1/C_t$=-0.009t+0.091	-0.009	0.705	$C_t/C_o=3.012t^{1/2}$+0.357	3.012	0.994
T_4=2.5 times reduction of RDF from T_3	$logC_t$=0.098t+0.876	0.098	0.920	$1/C_t$=-0.012t+0.116	-0.012	0.676	$C_t/C_o=2.432t^{1/2}$+0.114	2.432	0.999
T_5=5 times reduction of RDF from T_3	$logC_t$=0.101t+0.812	0.101	0.916	$1/C_t$=-0.014t+0.135	-0.014	0.666	$C_t/C_o=2.210t^{1/2}$+0.220	2.210	0.999
T_6=10 times reduction of RDF from T_3	$logC_t$=0.100t+0.797	0.100	0.913	$1/C_t$=-0.014t+0.140	-0.014	0.664	$C_t/C_o=2.102t^{1/2}$+0.127	2.102	0.999

Table 5. Kinetic parameters from linear regression analysis of first order, second order and parabolic diffusion kinetic models of P release in silty clay loam soil

Treatments	P release kinetics								
	First order			Second order			Parabolic diffusion		
	Equation	KcI ($\mu g\ g^{-1}day^{-1}$)	R^2	Equation	KcII ($g\ \mu g^{-1}day^{-1}$)	R^2	Equation	Kcp ($\mu g\ g^{-1}day^{-1}$)	R^2
T_1=Absolute control	$logC_t$=0.099t+0.793	0.099	0.906	$1/C_t$=-0.015t+0.143	-0.015	0.654	$C_t/C_o=2.010t^{1/2}$+0.040	2.010	1
T_2=RDF through SSP	$logC_t$=0.096t+0.985	0.096	0.920	$1/C_t$=-0.009t+0.091	-0.009	0.681	$C_t/C_o=2.909t^{1/2}$+0.245	2.909	0.999
T_3=RDF through nano fertilizer	$logC_t$=0.097t+0.971	0.097	0.939	$1/C_t$=-0.009t+0.091	-0.009	0.705	$C_t/C_o=3.012t^{1/2}$+0.357	3.012	0.994
T_4=2.5 times reduction of RDF from T_3	$logC_t$=0.098t+0.876	0.098	0.920	$1/C_t$=-0.012t+0.116	-0.012	0.676	$C_t/C_o=2.432t^{1/2}$+0.114	2.432	0.999
T_5=5 times reduction of RDF from T_3	$logC_t$=0.101t+0.812	0.101	0.916	$1/C_t$=-0.014t+0.135	-0.014	0.666	$C_t/C_o=2.210t^{1/2}$+0.220	2.210	0.999
T_6=10 times reduction of RDF from T_3	$logC_t$=0.100t+0.797	0.100	0.913	$1/C_t$=-0.014t+0.140	-0.014	0.664	$C_t/C_o=2.102t^{1/2}$+0.127	2.102	0.999

Table 6. Kinetic parameters from linear regression analysis of first order, second order and parabolic diffusion kinetic models of P release in clay loam soil

Treatments	P release kinetics								
	First order			Second order			Parabolic diffusion		
	Equation	KcI ($\mu g\ g^{-1}day^{-1}$)	R^2	Equation	KcII ($g\ \mu g^{-1}day^{-1}$)	R^2	Equation	Kcp ($\mu g\ g^{-1}day^{-1}$)	R^2
T_1=Absolute control	$logC_t$=0.1t+0.684	0.1	0.907	$1/C_t$=-0.019t+0.184	-0.019	0.653	$C_t/C_o=1.595t^{1/2}$+ 0.013	1.595	0.999
T_2=RDF through SSP	$logC_t$=0.096t+0.804	0.096	0.934	$1/C_t$=0.011t+0.108	-0.011	0.710	$C_t/C_o=2.445t^{1/2}$+0.014	2.445	0.998
T_3=RDF through nano fertilizer	$logC_t$=0.096t+0.798	0.096	0.947	$1/C_t$=-0.011t+0.108	-0.011	0.725	$C_t/C_o=2.500t^{1/2}$ +0.311	2.500	0.992
T_4=2.5 times reduction of RDF from T_3	$logC_t$=0.098t+0.691	0.098	0.923	$1/C_t$=-0.014t+0.142	-0.014	0.679	C_t/C_o =1.983$t^{1/2}$+ 0.076	1.983	0.998
T_5=5 times reduction of RDF from T_3	$logC_t$=0.101t+0.607	0.101	0.918	$1/C_t$=-0.018t+0.171	-0.018	0.668	C_t/C_o =1.780$t^{1/2}$+ 0.248	1.780	0.999
T_6=10 times reduction of RDF from T_3	$logC_t$=0.101t+0.690	0.101	0.915	$1/C_t$=-0.019t+0.179	-0.019	0.665	$C_t/C_o=1.682t^{1/2}$ + 0.167	1.682	0.999

In parabolic diffusion kinetic model, strong and significant positive correlation between cumulative P desorbed and $t^{1/2}$ reflected that rate of release of P is synchronizing with time or rather a good state of equilibrium is achieved (Medhi et al., 2012). The rate constant of parabolic diffusion (Kcp) equation was the highest in treatment receiving nano-fertilizer (T3) in all the three types of soil, which indicated that there was sustained release of P as well as longevity of the fertilizer. The coefficient of determination was highest for the parabolic diffusion kinetic equation as compared to the other two kinetic models. Several authors have reported similar findings that parabolic diffusion was the best fit (R^2> 0.95) to describe the release of phosphorus in soil which is a diffusion-controlled process rather than mass flow or root interception (Islas-Espinoza et al., 2014; Singh and Prakash, 2014; Azadi and Baghernejad, 2019) .

Conclusion

The modified zeolite framework witnessed adsorbing both positive and negative ions for its slow release into the soil system throughout the incubation period which may likely be the solution to the major problem of phosphorus fertilization in acid soil which arises due to fixation by sesquioxides. The highest rate constant of parabolic diffusion model was found for the treatment receiving nano-enabled recommended P, which further emphasizes on the sustained release of phosphorous into the soil solution.

Hence, it can be concluded that nutrient use efficiency of phosphatic fertilizers can be significantly improved by nano phosphorus. Zeolite could potentially and simultaneously adsorb both negative and positively charged ions that might possibly be explored as good source of nano carriers for preparation of nano-enabled fertilizers having both positive and negative charged ions. Thus, conventional chemical fertilizers (SSP) can be effectively supplemented by nano phosphatic fertilizer in acidic soil environment.

References

Abdul Majid, S., Ahmad Mir, M., Mir, J.M., 2018. Nitrate and phosphate sorption efficiency of mordenite versus zeolite-A at the convergence of experimental and density functionalized evaluation. *Journal of the Chinese Advanced Materials Society* 6(4): 691-705.

Akrami, Z., Norouzi, S., Bagherzadeh, M., 2019. Immobilization of modified zeolite on polyethylene surface: characterization and its application towards phosphate removal and microalgae growth. *SN Applied Sciences* 1(10): 1183.

Arai, Y., Sparks, D.L., 2007. Phosphate reaction dynamics in soils and soil minerals: a multiscale approach. *Advances in Agronomy* 94: 135-179.

Azadi, A., Baghernejad, M., 2019. Application of kinetic models in describing soil phosphorus release and relation with soil phosphorus fractions across three soil toposequences of calcareous soils. *Eurasian Soil Science* 52(7): 778-792.

Bansiwal, A.K., Rayalu, S.S., Labhasetwar, N.K., Juwarkar, A.A., Devotta, S., 2006. Surfactant modified zeolite as a slow release fertilizer for phosphorus. *Journal of Agricultural and Food Chemistry* 54(13): 4773-4779.

Bhardwaj, P., Sharma, M., Sharma, M., Tomar, R., 2014. Removal and slow release studies of phosphate on surfactant loaded hydrothermally synthesized silicate nanoparticles. *Journal of the Taiwan Institute of Chemical Engineers* 42(5): 2649-2658.

Bindraban, P.S., Dimkpa, C.O., Pandey, R., 2020. Exploring phosphorus fertilizers and fertilization strategies for improved human and environmental health. *Biology and Fertility of Soils* 56(3): 299-317.

Chinnamuthu, C.R., Boopathi, P.M., 2009. Nanotechnology and agroecosystem. *Madras Agricultural Journal* 96(1/6): 17-31.

Conijn, J.G., Bindraban, P.S., Schröder, J.J., Jongschaap, R.E.E., 2018. Can our global food system meet food demand within planetary boundaries? *Agriculture, Ecosystems & Environment* 251: 244-256.

Cordell, D., Neset, T.S.S., 2014. Phosphorus vulnerability: a qualitative framework for assessing the vulnerability of national and regional food systems to the multi-dimensional stressors of phosphorus scarcity. *Global Environmental Change* 24: 108-122.

Dhansil, A., Zalawadia, N.M., Prajapat, B.S., Yadav, K., 2018. Effect of nano phosphatic fertilizer on nutrient content and uptake by pearl millet (Pennisetum glaucum L.) crop. *International Journal of Current Microbiology and Applied Sciences* 7(12): 2327-2337.

Gupta, A.K., Maheshwari, A., Khanam, R., 2020. Assessment of phosphorus fixing capacity in different soil orders of India. *Journal of Plant Nutrition* 42(15): 2395-2401.

Hagab, R.H., Kotp, Y.H., Eissa, D., 2018. Using nanotechnology for enhancing phosphorus fertilizer use efficiency of peanut bean grown in sandy soil. *Journal of Advanced Pharmacy Education and Research* 8(3): 59-67.

Ibrahim, E.A., El-Sherbini, M.A.A., Selim, E.M., 2022. Effects of biochar on soil properties, heavy metal availability and uptake, and growth of summer squash grown in metal-contaminated soil. *Scientia Horticulturae* 301: 111097.

Islas-Espinoza, M., Solís-Mejía, L., Esteller, M.V., 2014. Phosphorus release kinetics in a soil amended with biosolids and vermicompost. *Environmental Earth Sciences* 71: 1441-1451.

Jakkula, V.S., Wani, S.P., 2018. Zeolites: Potential soil amendments for improving nutrient and water use efficiency and agriculture productivity. *Scientific Reviews & Chemical Communications* 8(1): 119.

Kumar, K., Smita, L., Cumbal., Debut, A., 2017. Green synthesis of silver nanoparticles using Andean blackberry fruit extract. *Saudi Journal of Biological Sciences* 24(1): 45-50.

Liu, R., Lal, R., 2014. Synthetic apatite nanoparticles as a phosphorus fertilizer for soybean (Glycine max). *Scientific Reports* 4: 5686.

Mahmood, M., Tian, Y., Ma, Q., Hui, X., Elrys, A.S., Ahmed, W., Mehmood, S., Wang, Z., 2021. Changes in phosphorus fractions in response to long-term nitrogen fertilization in loess plateau of China. *Field Crops Research* 270: 108207.

Medhi, B.K., Ruhal, D.S., Singh, C.P., Grover, D.K., Sarma, A., 2012. Effect of levels of phosphate and organic manures on phosphate supplying capacity and P-kinetics in wheat grown in a TypicHaplustept soil. *Crop Research* 44(1&2): 20-25.

Mikhak, A., Sohrabi,A., Kassaee, M.Z., Feizian, M., 2017. Synthetic nanozeolite/nanohydroxyapatite as a phosphorus fertilizer for German chamomile (Matricariachamomilla L.). *Industrial Crops and Products* 95: 444-452.

Mir, J.M., Ahmad Mir, M., Abdul Majid, S., 2020. Molecular electron density and nitrate-phosphate sorption efficiency of zeolite-A: physico-chemical and DFT analyses. *Indian Journal of Chemistry* 59A: 939-947.

Montalvo, D., Mclaughlin, M.J, Degryse, F., 2015. Efficacy of hydroxyapatite nanoparticles as phosphorus fertilizer in andisols and oxisols. *Soil Science Society of America Journal* 79: 551-558.

Noruzi, M., Hadian, P., Soleimanpour, L., Ma'mani, L., Shahbazi, K., 2023. Hydroxyapatite nanoparticles: an alternative to conventional phosphorus fertilizers in acidic culture media. *Chemical and Biological Technologies in Agriculture* 10(1): 71-76.

Poddar, K., Vijayan, J., Ray, S., Adak, T., 2018. Nanotechnology for sustainable agriculture. In: Biotechnology for Sustainable Agriculture : Emerging Approaches and Strategies. Singh, R.L., Mondal, S. (Eds.). Woodhead Publishing, pp.281-303.

Prakash, D., Benbi, D.K., Saroa, G.S., 2017. Clay, organic carbon, available P and calcium carbonate effects on phosphorus release and sorption-desorption kinetics in alluvial soils. *Communications in Soil Science and Plant Analysis* 48(1): 92-106.

Prüter, J., Leipe, T., Michalik, D., Klysubun, W., Leinweber, P., 2020. Phosphorus speciation in sediments from the Baltic Sea, evaluated by a multi-method approach. *Journal of Soils and Sediments* 20: 1676-1691.

Salako, O., Kovo, A.S., Abdulkareem, A.S., Yusuf, S.T., Afolabi, E.A., Auta, M., 2020. The effect of synthesized NPK loaded surfactant modified zeolite A based fertilizer in tomato (Lycopersycum esclentum) cultivation. *Journal of Nigerian Society of Chemical Engineers* 35(1): 50-63.

Sanyal, S.K., 2018. A textbook of soil chemistry. Astral International Pvt. Limited, India. 306p.

Sharpley, A., Jarvie, H., Flaten, D., Kleinman, P., 2018. Celebrating the 350th anniversary of phosphorus discovery: A conundrum of deficiency and excess. *Journal of Environmental Quality* 47(4): 774-777 .

Singh, D.J.. Sarkar, S.D., Mittal, S., Dhaka, R., Maiti, P., Singh, A., Raghav, T., Solanki, D., Ahmed, N., Singh, S.B., 2018. Zeolite reinforced carboxymethyl cellulose-Na+-g-cl-poly(AAm) hydrogel composites with pH responsive phosphate release behaviour. *Journal of Applied Polymer Science* 136(15): 47332.

Singh, P., Prakash, D., 2014. Phosphorus dynamics in soils as influenced by the application of organic sources: A review. *Indian Journal of Fertilisers*. 10(10): 16-26.

Solanki, P., Bhargava, A., Chhipa, H., Jain, N., Panwar, J. 2015. Nano-fertilizers and their smart delivery system. In: Nanotechnologies in food and agriculture. Rai, M., Ribeiro, C., Mattoso, L., Duran, N. (Eds.). Springer, Cham. pp. 81-101.

Sparks, D.L., 2003. Environmental soil chemistry. Elsevier, 352p.

Subramanian, K.S., Thirunavukkarasu, M., 2017. Nano-fertilizers and nutrient transformations in soil. In: Nanoscience and Plant–Soil Systems. Ghorbanpour, M., Manika, K., Varma, A. (Eds.). Springer Cham. pp. 305-319.

Tarafdar, J.C., Rathore, I., Thomas, E., 2015. Enhancing nutrient use efficiency through nano technological interventions. *Indian Journal of Fertilizers* 11(12): 46-51.

Wahid, F., Fahad, S., Danish, S., Adnan, M., Yue, Z., Saud, S., Siddiqui, M.H., Brtnicky, M., Hammerschmiedt, T., Datta, R., 2020. Sustainable management with mycorrhizae and phosphate solubilizing bacteria for enhanced phosphorus uptake in calcareous soils. *Agriculture* 10(8): 334.

Wakelin, S.A., Condron, L.M., Gerard, E., Dignam, B.E.A., Black, A., O'Callaghan, M., 2017. Long-term P fertilisation of pasture soil did not increase soil organic matter stocks but increased microbial biomass and activity. *Biology and Fertility of Soils* 53: 511-521.

Wei, Y.X., Ye, Z.F., Wang, Y.L., Ma, M.G., Li, Y.F., 2011. Enhanced ammonia nitrogen removal using consistent ammonium exchange of modified zeolite and biological regeneration in a sequencing batch reactor process. *Environmental Technology* 32(12): 1337–1343.

Wilson, J.. Elliott, J., Macrae, M., Glenn, A., 2019. Near-surface soils as a source of phosphorus in snowmelt runoff from cropland. *Journal of Environmental Quality* 48(4): 921-930.

Yan, Z., Lin, Z., Kai, M., Guozhu, M., 2014. The surface modification of zeolite 4A and its effect on the water-absorption capability of starch-g-poly (acrylic acid) composite. *Clay and Clay Minerals* 62(3): 211-223.

Eurasian Journal of Soil Science 2025, 14(1), 98 - 106

Eurasian Journal of Soil Science

Journal homepage : http://ejss.fesss.org

Sustainable nutrient management and agricultural productivity in chernozem soils of the Kostanay Region, Kazakhstan

Zhenis Zharlygassov [a], Niyazbek Kalimov [a,*], Assiya Ansabayeva [a], Zhaxylyk Zharlygassov [a], Elena Moskvicheva [a], Rahila İslamzade [b], Abdurrahman Ay [c], İzzet Akça [d,e], Rıdvan Kızılkaya [c,e]

[a] Akhmet Baitursynuly Kostanay Regional University, Faculty of Agricultural Sciences, Department of Agronomy, Kostanay, Kazakhstan

[b] Sumgayit State University, Sumgayit, Azerbaijan

[c] Ondokuz Mayıs University, Faculty of Agriculture, Department of Soil Science and Plant Nutrition, Samsun, Türkiye

[d] Ondokuz Mayıs University, Faculty of Agriculture, Department of Plant Protection, Samsun, Türkiye

[e] Agrobigen Research & Development Trade Ltd.Co, Samsun Technopark, Samsun, Türkiye

Article Info

Received : 11.05.2024

Accepted : 21.11.2024

Available online: 28.11.2024

Author(s)

Z.Zharlygassov

N.Kalimov *

A.Ansabayeva

Z.Zharlygassov

E.Moskvicheva

R.İslamzade

A.Ay

İ.Akça

R.Kızılkaya

* Corresponding author

Abstract

Chernozem soils, known for their high organic matter and fertility, are crucial for agricultural productivity in northern Kazakhstan's Kostanay region. This study evaluated the physical, chemical, and biological properties of these soils to assess their suitability for crop production and propose sustainable management practices. Soil samples were collected from 0-20 cm depths across various locations to represent the region's main nutrient profile. Physical analyses included texture determination, while chemical analyses measured pH, electrical conductivity (EC), organic matter, and nutrient levels (N, P, K, Ca, Mg, Fe, Cu, Zn, and Mn) using standard methods. Biological assessments focused on microbial biomass carbon (C_{mic}), basal soil respiration (BSR), dehydrogenase and catalase activities, as well as Cmic: Corg and metabolic quotient (qCO_2) ratios. Results indicated high organic matter content (mean 4.49%), sufficient total nitrogen (>0.25%), and high levels of potassium and calcium. However, phosphorus levels were low (<8 mg kg^{-1}), marking it as a key limiting nutrient. Biological analysis revealed robust microbial activity, with high catalase activity supporting aerobic processes, but low C_{mic}: C_{org} and qCO_2 values suggested limited microbial biomass, potentially slowing organic matter decomposition. This trait, while preserving organic matter, may restrict nutrient mineralization, impacting crop nutrient availability. Based on these findings, we recommend prioritizing phosphorus and potassium fertilization integrated with organic matter management to balance nutrient levels and enhance crop productivity. The application of liquid or solid organic or organomineral fertilizers is suggested to maintain soil organic matter and promote sustainable practices. Additionally, foliar applications of manganese and iron, along with nitrogen supplementation, are recommended to address micronutrient deficiencies and support plant growth. Overall, sustainable management of Chernozem soils in Kostanay requires balanced nutrient management, organic matter preservation, and targeted micronutrient interventions to ensure long-term fertility and productivity.

Keywords: Chernozem Soils, Soil Fertility, Nutrient Management, Organic Matter, Sustainable Agriculture.

Introduction

Chernozem soils, characterized by their high organic matter and humus content, provide ideal conditions for productive agriculture. These unique soils are found in limited regions around the world, with significant

: https://doi.org/10.18393/ejss.1592633

: https://ejss.fesss.org/10.18393/ejss.1592633

Publisher : Federation of Eurasian Soil Science Societies

e-ISSN : 2147-4249

concentrations in countries such as Russia, Ukraine, Kazakhstan, Canada, and the United States. The largest concentration of Chernozems is within the expansive steppe regions of Russia and Ukraine, known as the "Black Earth Belt," which accounts for approximately 60% of the world's total Chernozem areas (Yapiyev et al., 2018; Djalankuzov et al., 2004). Globally, Chernozem soils are estimated to cover over 230 million hectares, with about 25 million hectares located within Kazakhstan's borders. This distribution makes Kazakhstan a significant repository for these highly productive soils (Funakawa et al., 2004; Rolinski et al., 2021). Chernozem soils are not only vital for agricultural productivity but also play a crucial role in climate change mitigation due to their high organic carbon content and capacity for atmospheric carbon sequestration.

In Kazakhstan, Chernozem soils are primarily concentrated in the northern regions, playing a crucial role in the country's grain production. Kazakhstan has a total land area of 272 million hectares, with approximately 30 million hectares allocated for agricultural activities, of which 23 million hectares are active farmlands (Djalankuzov et al., 2004). The extensive Chernozem regions in northern Kazakhstan account for over 20% of the country's arable land, making them a key resource for grain production and a major contributor to food security (Kusherbayev et al., 2023). Additionally, Chernozem soils, with their rich organic carbon content, are effective in sequestering atmospheric carbon, thus holding significant potential in mitigating climate change impacts (Funakawa et al., 2004).

However, Kazakhstan's Chernozem soils have undergone various changes over time due to agricultural policies and intensive land use. Notably, during the Soviet era, the "Virgin Lands Campaign" opened millions of hectares to agriculture, disrupting the natural balance of these soils and leading to organic matter loss and declining soil quality (Yapiyev et al., 2018; Karbozova–Saljnikov et al., 2004). For example, while traditional Chernozem soils generally contain 5-6% organic carbon, the campaign resulted in losses of up to 11%, reducing organic carbon levels to 4.5-5%. In some areas of northern Kazakhstan, the continuous practice of fallow rotation and monoculture wheat cultivation has led to organic carbon reductions of 28-30% (Karbozova–Saljnikov et al., 2004; Funakawa et al., 2004; Kalimov et al., 2024). These losses have been exacerbated by fallow practices, which, while aimed at increasing the soil's water retention capacity, ultimately accelerate organic matter mineralization and carbon depletion over time.

Kazakhstan's Chernozem soils remain a crucial resource for the country's agricultural sustainability and food security. However, fertilizer applications on these lands are typically not based on soil analysis, leading to suboptimal management practices. In wheat cultivation, farmers often rely on limited nitrogen and phosphorus applications alongside seeding, resulting in a decline in the organic matter content and levels of essential nutrients in Chernozem soils. The objective of this study is to comprehensively analyze the physical, chemical, and biological properties of Chernozem soil samples from the Kostanay region of northern Kazakhstan to evaluate their suitability for sustainable agricultural production. Specifically, the study aims to identify nutrient limitations and other soil characteristics that may affect crop growth and productivity. By examining these properties, the research seeks to propose evidence-based fertilization strategies and soil management practices that balance nutrient levels, maintain soil organic matter, and support long-term agricultural sustainability. Through this evaluation, nutrient deficiencies and other limiting factors affecting agricultural productivity will be identified, guiding the development of effective practices to optimize soil fertility and enhance crop productivity. The main research questions addressed in this study include identifying nutrient deficiencies present in Chernozem soils, assessing whether the biological activities of these soils are sufficient to sustain long-term productivity, and determining the most effective fertilization and soil management strategies to enhance soil fertility and crop yield.

Material and Methods

Study Area and Soil Sampling

This study was conducted in the Kostanay region of northern Kazakhstan, an area characterized by Chernozem soils, known for their high fertility and significance for agricultural activities. The region has a continental climate, marked by cold winters and warm summers. Long-term and 2023 climate data, including precipitation and temperature for the sampling sites, are presented in Figure 1. In 2023, the annual total rainfall in Kostanay was 447.2 mm, significantly exceeding the long-term annual average of 340 mm. Monthly rainfall showed notable deviations from the average, with August experiencing an exceptionally high rainfall of 102.4 mm, compared to the long-term average of 35 mm. On the other hand, spring months (March to May) received lower-than-average rainfall, which may affect early crop development, whereas higher-than-average rainfall in summer and fall could potentially benefit mid-season crop growth but may also increase the risk of waterlogging in certain areas.

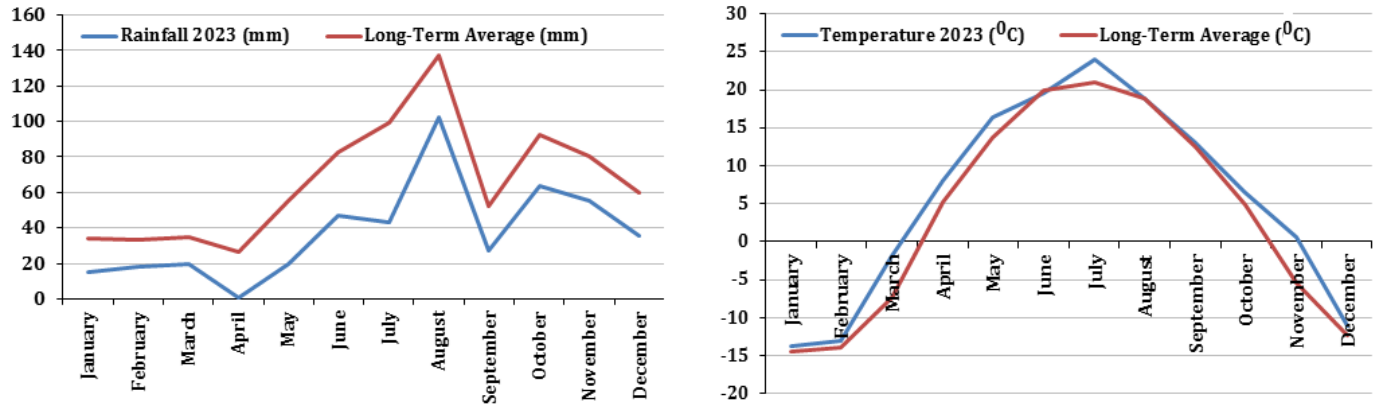

Figure 1. Monthly rainfall and temperature data for 2023 compared to long-term averages in Kostanay, Kazakhstan.

The region's temperature patterns also exhibit significant seasonal fluctuations. In 2023, the average annual temperature was 5.6°C, slightly higher than the long-term average of 3.6°C. Monthly temperatures in 2023 showed some deviations from historical averages, with warmer-than-average conditions in March (−1.9°C compared to −7.4°C long-term average) and November (0.6°C compared to −5.5°C). The summer months, particularly July, experienced above-average temperatures, reaching 24°C compared to the long-term average of 20.9°C. These temperature deviations may impact crop growth cycles and influence the region's agricultural productivity.

Sampling Procedure

The soil samples were collected from Chernozem areas, allowing for a broad examination of the soil's physical, chemical, and biological properties. Soil samples were collected from a depth of 0-20 cm according to Jones (2001), as this layer is critical for nutrient availability and root development in agricultural systems. At each sampling location, multiple sub-samples were collected and combined to form a composite sample, ensuring a representative sample for each site by accounting for spatial heterogeneity. A portion of the collected soil samples was stored at +4°C for biological analyses. The remaining soil samples were air-dried, sieved to 2 mm, and stored for further physical and chemical analysis.

Physical and Chemical Analyses

To determine the physical and chemical properties of the soil, various standard methods were employed. Soil texture was analyzed using the hydrometer method (Bouyoucous, 1951). For chemical analyses, soil pH was measured in a 1:1 soil-to-water suspension using a pH meter (Peech, 1965), and electrical conductivity (EC) was measured in a 1:1 soil-to-water extract (Rowell, 1996). Organic matter content was determined by the Walkley-Black method (Walkley and Black, 1934), while total carbonate content was analyzed using the Scheibler calcimeter (Loeppert and Suarez, 1996). Total nitrogen (N) was measured using the Kjeldahl method (Bremner, 1965a), and mineral nitrogen (NH_4 and NO_3) contents were extracted with 1N KCl and determined by the Kjeldahl distillation method (Bremner, 1965b). The C/N ratios of the soils were calculated based on the total organic C and N determined in the analyses (Rowell, 1996). Available phosphorus (P) was assessed using the Olsen method with a 0.5 M $NaHCO_3$ extraction, which is suitable for calcareous soils like Chernozems (Olsen and Dean, 1965). Exchangeable cations (K, Ca, Mg, and Na) were extracted with 1 N ammonium acetate; K and Na were determined by flame photometry, while Ca and Mg were measured by EDTA titration (Pratt, 1965; Heald, 1965). Available micronutrients, including Fe, Cu, Zn, and Mn, were determined by DTPA extraction followed by Atomic Absorption Spectrophotometry (Lindsay and Norvell, 1978).

Biological Analysis

Microbial biomass carbon (C_{mic}) was determined by the substrate-induced respiration method of Anderson and Domsch (1978), while basal soil respiration (BSR) was measured according Anderson (1982). Dehydrogenase activity (DHA) was analyzed following Pepper (1995), and catalase activity (CA) was measured using the Beck method (Beck, 1971). The $C_{mic}/_{Corg}$ ratios (The microbial biomass C to total organic C ratio) and metabolic quotient (qCO_2) calculated by dividing the CO_2-C released from the sample in 1 h by the biomass C content, were also obtained (ŠantruuČková and SiraŠicraba, 1991).

Data Analysis

The data from the physical, chemical, and biological analyses were compiled to assess the variability of soil properties across different sites. The suitability of Chernozem soils for specific crops, including wheat, barley, potatoes, corn, and soybeans, was evaluated by examining nutrient levels and other soil characteristics in each sample. Sustainable fertilization recommendations were developed by identifying nutrient limitations and proposing strategies to address deficiencies for optimal crop growth.

Results and Discussion

In this study, the fertility status of the Chernozem soils collected from the Kostanay region of Kazakhstan was determined by analyzing their physical, chemical, and biological properties, as shown in Table 2.

Table 2. Physical, Chemical, and Biological Properties of Chernozem Soils Collected from the Kostanay Region of Kazakhstan

Parameters (n=12)	Minimum	Maximum	Average
Clay, %	15,63	59,50	41,02
Silt, %	13,05	31,38	22,45
Sand, %	22,58	71,32	36,53
pH	6,01	7,50	6,79
Electrical Conductivity, µS cm^{-1}	151,40	628,70	304,30
Organic Matter, %	3,07	5,81	4,49
$CaCO_3$, %	0,14	1,45	0,40
C/N ratio	5,93	10,88	7,92
Nutrient Content of the Soils			
Total N, %	0,24	0,44	0,33
Available P, mg kg^{-1}	3,03	14,79	6,58
Available K, mg kg^{-1}	240,17	963,18	619,33
Available Ca, mg kg^{-1}	1668,60	8022,16	3775,42
Available Mg, mg kg^{-1}	678,61	3258,72	2453,98
Available Fe, mg kg^{-1}	0,70	11,47	4,29
Available Cu, mg kg^{-1}	0,20	0,47	0,34
Available Zn, mg kg^{-1}	0,98	16,68	7,13
Available Mn, mg kg^{-1}	0,27	1,18	0,62
Exchangeable Cations			
Exchangeable Ca, me $100g^{-1}$	8,34	40,11	18,88
Exchangeable Mg, me $100g^{-1}$	5,66	27,16	20,45
Exchangeable Na, me $100g^{-1}$	0,95	2,25	1,24
Exchangeable K, me $100g^{-1}$	0,62	2,47	1,59
Exchangeable Na Percentage (ESP), %	1,78	4,96	3,05
Ca/K ratio	6,62	37,26	13,57
Mg/K ratio	3,49	26,78	15,06
Biological Properties			
Basal soil respiration (BSR), mg CO_2 g^{-1} $24h^{-1}$	0,008	0,067	0,026
Microbial biomass carbon (C_{mic}), mg C g^{-1} $24h^{-1}$	11,566	24,207	16,310
C_{mic}:C_{org}	0,450	0,937	0,636
Metabolic coefficient (qCO_2)	0,001	0,005	0,002
Dehydrogenase activity (DHA), µgTPF g^{-1} $24h^{-1}$	26,140	56,692	43,792
Catalase activity (CA), ml O_2 g^{-1} $3min^{-1}$	127,792	267,080	202,391

Soil Physical Properties

- The Chernozem soils from the Kostanay region exhibited a range of textures, as shown in Table 2. Clay content ranged from 15.63% to 59.50% (average 41.02%), silt content from 13.05% to 31.38% (average 22.45%), and sand content from 22.58% to 71.32% (average 36.53%). These results indicate that the predominant soil texture is clay or sandy clay loam, which is beneficial for water retention and nutrient-holding capacity, essential for supporting crop growth (USDA, 2001).

Soil Chemical Properties

- **pH and Electrical Conductivity (EC):** The pH of the soil samples varied from 6.01 to 7.50 (average 6.79), indicating slightly acidic to neutral conditions. Electrical conductivity (EC) ranged from 151.40 to 628.70 µS cm^{-1} (average 304.30 µS cm^{-1}), confirming non-saline conditions (<980 µS cm^{-1}) suitable for crop production (USDA, 2001).

- **Organic Matter and $CaCO_3$ Content:** The organic matter content ranged from 3.07% to 5.81% (mean 4.49%), indicating sufficient levels (>3%) for maintaining soil fertility. The $CaCO_3$ content was low, ranging from 0.14% to 1.45% (mean 0.40%), classifying the soils as non-calcareous (<2%), which supports better nutrient availability (Hazelton and Murphy, 2007).

Nutrient Content Analysis

- **Total Nitrogen (N) and C/N Ratio:** The total nitrogen content ranged from 0.24% to 0.44% (mean 0.33%), which is sufficient (>0.25%) for supporting plant growth. The average C/N ratio was 7.92, reflecting balanced decomposition rates and nutrient availability (Hazelton and Murphy, 2007).
- **Phosphorus (P):** vailable phosphorus was consistently low, ranging from 3.03 to 14.79 mg kg^{-1} (mean 6.58 mg kg^{-1}), indicating a limitation for optimal crop production (<8 mg kg^{-1}). This deficiency could restrict root growth and reduce yield potential (Hazelton and Murphy, 2007).
- **Potassium (K), Calcium (Ca), and Magnesium (Mg):** Available potassium levels varied from 240.17 to 963.18 mg kg^{-1} (mean 619.33 mg kg^{-1}). Calcium ranged from 1668.60 to 8022.16 mg kg^{-1} (mean 3775.42 mg kg^{-1}), and magnesium from 678.61 to 3258.72 mg kg^{-1} (mean 2453.98 mg kg^{-1}). High levels of potassium, calcium, and magnesium (>250 mg kg^{-1}, >2860 mg kg^{-1}, and >115 mg kg^{-1}, respectively) support plant structure and stress resistance. However, imbalances in the Ca/K and Mg/K ratios could affect nutrient uptake efficiency. Although these levels are generally sufficient, the Ca/K and Mg/K ratios, averaging 13.57 and 15.06 respectively, highlight potential imbalances that may influence nutrient absorption. Ideal Ca/K and Mg/K ratios are typically lower (optimum Ca/K ratio is 12, and Mg/K ratio is 2), suggesting that these imbalances could impact plant growth and nutrient uptake (Hazelton and Murphy, 2007).
- **Micronutrients:** Available Fe levels ranged from 0.70 to 11.47 mg kg^{-1} (mean 4.29 mg kg^{-1}), and Mn levels ranged from 0.27 to 1.18 mg kg^{-1} (mean 0.62 mg kg^{-1}), both indicating potential deficiencies (<4.5 mg Fe kg^{-1} and <14 mg Mn kg^{-1}). Zn (mean 7.13 mg kg^{-1}) and Cu (mean 0.34 mg kg^{-1}) levels were sufficient (>0.7 mg Zn kg^{-1} and >0.2 mg Cu kg^{-1}) for plant health (Lindsay and Norvell, 1978).

Soil Biological Properties

- **Basal Soil Respiration (BSR)**: BSR ranged from 0.008 to 0.067 mg CO_2 g^{-1} $24h^{-1}$ (average 0.026 mg CO_2 g^{-1} $24h^{-1}$), reflecting energy utilization by soil microflora and indicating the efficiency of organic carbon breakdown, despite some debate over its interpretation (Wardle and Ghani, 1995).
- **Microbial Biomass Carbon (C_{mic})**: C_{mic} values ranged from 11.57 to 24.21 mg C g^{-1} (average 16.31 mg C g^{-1}). Microbial biomass carbon plays a vital role as a component of soil organic matter and is integral to the biogeochemical cycling of essential nutrients (C, N, P, S) and related energy flows (Smith and Paul, 1990; Meli et al., 2002; Kızılkaya et al., 2004).
- **C_{mic} : C_{org} Ratio and Metabolic Quotient (qCO_2)**: The C_{mic} : C_{org} ratio (average 0.636) and the metabolic quotient (qCO_2) (average 0.002) suggest that while the microbial community is present and functional, it operates with limited efficiency, potentially affecting nutrient mineralization (Hart et al., 1989; Anderson and Domsch, 1989; Insam et al., 1989). The qCO_2, which assesses specific microbial respiration, shows that lower values indicate higher efficiency per unit of microbial biomass. The average value of 0.002 aligns with studies indicating efficient carbon use but slower organic matter decomposition rates (Wardle and Ghani, 1995; Kızılkaya and Hepşen, 2007).
- **Dehydrogenase and Catalase Activity**: Dehydrogenase activity (DHA), which ranged from 26.14 to 56.69 µg TPF g^{-1} $24h^{-1}$ (average 43.79 µg TPF g^{-1} $24h^{-1}$), was high, suggesting active metabolic processes (Gong, 1997; Obbard, 2001; Kızılkaya, 2008). Catalase activity (CA) varied from 127.79 to 267.08 ml O_2 g^{-1} $3min^{-1}$ (average 202.39 ml O_2 g^{-1} $3min^{-1}$), further indicating strong aerobic microbial activity (Pascual et al., 1998; Durmuş and Kızılkaya, 2022; Toor et al., 2024).

In recent years, the results of soil fertility analyses conducted in the Kostanay region show similarities with the findings of this study. However, when compared to data from past decades, a declining trend in organic matter content has been observed. This can be attributed to several factors, including agricultural practices, climate conditions, and soil management strategies. Long-term monoculture cropping can lead to soil fatigue and reduced organic matter (Belete and Yadete, 2023). Continuous tillage and soil disturbance are significant contributors to organic matter loss. Furthermore, extensive and non-analysis-based use of chemical fertilizers can disrupt natural soil biological cycles, leading to a decline in organic matter levels. The sufficient inorganic nitrogen and a C/N ratio of approximately 7.9 in mature plant areas support this observation. This can hinder the regeneration of organic matter in the soil over time, leading to further

declines. Additionally, the inadequate retention or removal of plant residues post-harvest may contribute to the reduction in organic matter levels.

In this study, which aimed to evaluate the biological properties of Chernozem soils in Kazakhstan's Kostanay region, it was determined that the soils had sufficient levels of biological activity. The high catalase activity indicated robust aerobic microbial processes. However, the C_{mic} : C_{org} ratio and the qCO_2 values were found to be relatively low, suggesting limited microbial biomass. This observation implies that, while the microbial population is present, it does not actively decompose organic material at a rapid rate. This can be advantageous, as it indicates that the existing organic matter is not rapidly depleted. However, in agricultural contexts, this limitation may pose a challenge for nutrient mineralization and availability, potentially impacting crop productivity.

Plant Nutrition Strategies

he development of targeted plant nutrition strategies is crucial for maximizing crop productivity and maintaining soil health, especially in regions like the Kostanay area where nutrient imbalances and environmental challenges can significantly impact agricultural outcomes. Considering the nutrient content of the Chernozem soils and their effects on plant growth, appropriate strategies are essential. In Kazakhstan's Kostanay region, the main crops grown in Chernozem soils are wheat, barley, potatoes, corn, and soybeans. Table 3 presents the amounts of nutrients removed by these crops and the levels of plant-available nutrients in the region's Chernozem soils.

Table 3. Nutrient removal by major crops and available nutrient content in Chernozem soils of the Kostanay region

Crops	N, kg ha^{-1}	P_2O_5, kg ha^{-1}	K_2O, kg ha^{-1}	CaO, kg ha^{-1}	MgO, kg ha^{-1}
Wheat	190	80	250	40	40
Barley	120	50	220	40	40
Potatoes	500	200	600	200	100
Corn	770	140	390	180	70
Soybeans	250	130	280	60	60
Chernozem Soils	418 (299 – 556)*	38 (17 – 85)*	1870 (724 – 2902)*	13214 (5840-28078)*	10225 (2827-13578)*

* Values in parentheses represent the minimum and maximum nutrient levels in the Chernozem soils of the region.

An analysis of the available nutrient content in Chernozem soils and the nutrient uptake by crops during a growing season (Table 3) reveals that phosphorus is insufficient for all crops, and nitrogen is inadequate for potatoes and corn. Potassium, calcium, and magnesium levels are adequate for all crops, but their balance is skewed. The ideal Ca/K ratio is 12, but in Chernozem soils, it averages 13.57. Similarly, the ideal Mg/K ratio is 2, but it averages 15.06 in these soils. This indicates that despite adequate potassium levels, crops—especially potatoes and corn—may respond positively to potassium fertilization. Therefore, phosphorus and potassium among the macronutrients, and manganese and iron among the micronutrients, are identified as critical nutrients for crop cultivation in the region.

The study emphasizes that maintaining soil organic matter, which has declined over the years, should be central to fertilization programs for Kostanay's Chernozem soils. Intensive nitrogen fertilization could narrow the C/N ratio, accelerating the mineralization of soil organic matter. Therefore, careful nitrogen management is required, and phosphorus and potassium fertilizers should be applied during seeding. Instead of chemical fertilizers, using liquid or solid organic or organomineral P and K fertilizers is recommended. This practice helps maintain soil organic matter and promotes environmentally sustainable agriculture.

The application of liquid organomineral PK fertilizers, which contain no carrier materials, could offer a more conservation-focused approach. Liquid organomineral fertilizers offer several advantages over granulated types (Paré et al., 2010; Šarauskis et al., 2021; de Melo Benites et al., 2022; Sobreira et al., 2024):

- **Enhanced Nutrient Availability:** Liquid fertilizers are already dissolved, allowing immediate nutrient uptake by plant roots. This promotes faster and more effective absorption, especially during critical early growth stages.
- **Reduced Dependence on Water:** Granulated fertilizers need soil moisture to dissolve, which can be challenging under water-limited conditions. Liquid fertilizers provide nutrients directly, reducing reliance on external water sources. This is particularly important given the increasing frequency of droughts and irregular rainfall patterns due to climate change.

- **Adaptation to Climate Challenges:** Global warming leads to prolonged dry periods and reduced water availability, hindering traditional fertilization methods. Liquid organomineral fertilizers ensure essential nutrients are accessible to crops even under suboptimal moisture conditions.
- **Ease of Application:** Liquid fertilizers can be applied through existing irrigation systems or sprayed directly on the soil surface, saving time and ensuring uniform nutrient distribution.

Given the limitations of granulated fertilizers—particularly their dependency on sufficient moisture for nutrient release—liquid organomineral fertilizers offer a resilient alternative suitable for the changing climate. They provide immediate nutrient availability, enhance nutrient use efficiency, and contribute to long-term soil health by adding organic matter. This reduces nutrient leaching and supports microbial activity, which is essential for sustained soil fertility. Additionally, the insufficient levels of manganese and iron are significant barriers to achieving desired yields in crop production. Therefore, foliar application of these micronutrients is necessary. Supplementing nitrogen through foliar feeding along with micronutrients can significantly boost plant production while helping preserve soil organic matter.

Conclusion

This study reveals the critical nutrient imbalances in the Chernozem soils of Kazakhstan's Kostanay region and highlights the need for targeted fertilization strategies to optimize crop productivity and promote long-term soil health. The findings underscore the widespread deficiency of phosphorus for all major crops, with additional nitrogen deficits observed specifically in potatoes and corn. While potassium, calcium, and magnesium levels are generally sufficient, the skewed Ca/K and Mg/K ratios suggest that crops, particularly high-demand species like potatoes and corn, may still respond positively to supplemental potassium.

Sustaining soil organic matter, which has shown a declining trend in recent years, must be a primary consideration in developing fertilization programs for this region. Excessive nitrogen applications risk narrowing the C/N ratio, accelerating organic matter decomposition. Therefore, careful nitrogen management, combined with phosphorus and potassium fertilization at seeding, is essential to balance crop needs with soil conservation. Implementing liquid or solid organic and organomineral P and K fertilizers offers a more sustainable alternative to traditional chemical fertilizers, helping to maintain soil structure and organic content over time.

The study also identifies the low levels of micronutrients, particularly manganese and iron, as significant barriers to achieving optimal yields. Foliar application of these nutrients, combined with nitrogen, is recommended to enhance plant growth and reduce reliance on soil-stored nutrients, further aiding in the preservation of organic matter.

These recommendations aim to improve short-term crop productivity while fostering sustainable soil management practices. Implementing this comprehensive approach—balancing nutrient inputs, conserving organic matter, and addressing micronutrient deficiencies—ensures the long-term sustainability and productivity of the Chernozem soils in Kostanay and similar regions facing climate and environmental challenges.

Acknowledgement

The authors gratefully acknowledge Agrobigen R&D Ltd. Co., Türkiye, for their financial support of this research (Project No. AGROBIGEN.2022.03.05). Their contribution was essential for the successful completion of this study.

References

Anderson, J.P.E., 1982. Soil respiration. In. Methods of soil analysis, Part 2- Chemical and Microbiological Properties. Page, A.L., Keeney, D. R., Baker, D.E., Miller, R.H., Ellis, R. Jr., Rhoades, J.D. (Eds.). ASA-SSSA, Madison, Wisconsin, USA. pp. 831-871.

Anderson, J.P.E., Domsch, K.H., 1978. A physiological method for the quantative measurement of microbial biomass in soils. *Soil Biology and Biochemistry* 10: 215 – 221.

Beck, T.H., 1971. Die Messung derkKatalasen aktivität Von Böden. *Zeitschrift für Pflanzenernährung und Bodenkunde* 130(1): 68-81.

Belete, T., Yadete, E., 2023. Effect of Mono Cropping on Soil Health and Fertility Management for Sustainable Agriculture Practices: A Review. *Journal of Plant Sciences* 11(6): 192-197.

Bouyoucous, G.J., 1951. A recalibration of the hydrometer method for making mechanical analysis of soils. *Agronomy Journal* 43: 434-438.

Bremner, J.M,, 1965a. Total Nitrogen. In: Methods of Soil Analysis, Part 1 Physical and Mineralogical Methods. Black, C.A., Evans, D.D., White, J.L., Ensminger, L.E., Clark F.E. (Eds.), Soil Science Society of America. Madison, Wisconsin, USA. pp. 1149–1178.

Bremner, J.M,, 1965b. Inorganic Forms of Nitrogen. In: Methods of Soil Analysis, Part 1 Physical and Mineralogical Methods. Black, C.A., Evans, D.D., White, J.L., Ensminger, L.E., Clark F.E. (Eds.), Soil Science Society of America. Madison, Wisconsin, USA. pp. 1179–1237.

de Melo Benites, V., Dal Molin, S.J., Menezes, J.F.S., Guimarães, G.S., de Almeida Machado, P.L.O., 2022. Organomineral fertilizer is an agronomic efficient alternative for poultry litter phosphorus recycling in an acidic ferralsol. *Frontiers in Agronomy* 4: 785753.

Djalankuzov, T.D., Rubinshtejn, M.I., Sulejmenov, B.U., Oshakbaeva, Z.O., Busscher, W.J., 2004. Kazakhstan. *Journal of Soil and Water Conservation* 59 (2): 34A-35A.

Durmuş, M., Kızılkaya, R., 2022. The effect of tomato waste compost on yield of tomato and some biological properties of soil. *Agronomy* 12(6): 1253.

Funakawa, S., Nakamura, I., Akshalov, K., Kosaki, T., 2004. Soil organic matter dynamics under grain farming in Northern Kazakhstan. *Soil Science and Plant Nutrition* 50(8): 1211-1218.

Gong, P., 1997. Dehydrogenase activity in soil: A comparison between the TTC and INT assay under their optimum conditions. *Soil Biology and Biochemistry* 29(2): 211-214.

Hart, P.B.S., August, J.A., West, A.W., 1989. Long-term consequences of topsoil mining on select biological and physical characteristics of two New Zealand loessial soils under grazed pasture. *Land Degradation and Rehabilitation* 1: 77-88.

Hazelton, P., Murphy, B., 2007. Interpreting soil test results. What do the numbers mean? CSIRO Publishing, Melbourne. Australia. 152p.

Heald, W.R., 1965. Calcium and Magnesium. In: Methods of soil analysis. Part 2. Chemical and microbiological properties. Black, C.A., Evans, D.D., White, J.L., Ensminger, L.E., Clark F.E. (Eds.), Soil Science Society of America. Madison, Wisconsin, USA. pp. 999-1010.

Insam, H., Parkinson, D., Domsch, K.H., 1989. Influence of macroclimate on soil microbial biomass. *Soil Biology and Biochemistry* 21: 211-221.

Jones, J.B., 2001. Laboratory guide for conducting soil tests and plant analyses. CRC Press, New York, USA. 363p.

Kalimov, N., Bodryy, K., Shilo, E., Kaldybaev, D., Bodraya, M., 2024. Impact of tillage and crop rotations on soil organic matter content in Northern Kazakhstan's chernozem soils: A 10-year study (2011-2021). *Eurasian Journal of Soil Science* 13(1): 35 - 42.

Karbozova–Saljnikov, E., Funakawa, S., Akhmetov, K., Kosaki, T., 2004. Soil organic matter status of Chernozem soil in North Kazakhstan: effects of summer fallow. *Soil Biology and Biochemistry* 36(9): 1373-1381.

Kızılkaya, R., 2008. Dehydrogenase activity in Lumbricus terrestris casts and surrounding soil affected by addition of different organic wastes and Zn. *Bioresource Technology* 99(5): 946–953.

Kızılkaya, R., Aşkın, T., Bayraklı, B., Sağlam, M., 2004. Microbiological characteristics of soils contaminated with heavy metals. *European Journal of Soil Biology* 40(2): 95-102.

Kızılkaya, R., Hepşen, Ş., 2007. Microbiological properties in earthworm *Lumbricus terrestris* L. cast and surrounding soil amended with various organic wastes. *Communication in Soil Science and Plant Analysis* 38(19-20): 2861-2876.

Kusherbayev, S., Amanzhol, I., Seilkhanova, Zh., Duanbekova, G., Kapparova, T., 2023. The influence of soil-drying inputs on the soil and the productivity of crops. *Scientific Horizons* 26(12): 76-87.

Lindsay, W.L., Norvell, W.A., 1978. Development of a DTPA soil test for zinc, iron, manganese, and copper. *Soil Science Society of America Journal* 42(3): 421-428.

Loeppert, R.H., Suarez, D.L., 1996. Carbonate and gypsum. In: Methods of Soil Analysis. Part 3 Chemical Methods, 5.3. Sparks, D., Page, A., Helmke, P., Loeppert, R., Soltanpour, P.N., Tabatabai, M.A., Johnston C.T., Sumner M.E. (Eds.). American Society of Agronomy, Madison, Wisconsin, USA, pp. 437-475.

Meli, S., Porto, M., Belligno, A., Bufo, S.A., Mazzatura, A., Scapa, A., 2002. Influence of irrigation with lagooned urban wastewater on chemical and microbiological soil parameters in a citrus orchard under Mediterranean condition. *Science of The Total Environment* 285: 69-77.

Obbard, J.P., 2001. Ecotoxicological assessment of heavy metals in sewage sludge amended soils. *Applied Geochemistry* 16: 1405-1411.

Olsen,S.R., Dean, L.A., 1965. Phosphorus. In: Methods of soil analysis. Part 2. Chemical and microbiological properties. Black, C.A., Evans, D.D., White, J.L., Ensminger, L.E., Clark F.E. (Eds.), Soil Science Society of America. Madison, Wisconsin, USA. pp. 1035-1049.

Paré, M.C., Allaire, S.E., Parent, L.E., Khiari, L., 2010. Variation in the physical properties of organo-mineral fertilisers with proportion of solid pig slurry compost. *Biosystems Engineering* 106(3): 243-249.

Pascual, J.A., Hernandez, T., Garcia, C., Ayuso, M., 1988. Enzymatic activities in an arid soil amend with urban organic wastes: laboratory experiment. *Bioresource Technology* 64: 131-138.

Peech, M., 1965. Hydrogen-Ion Activity. In: Methods of soil analysis. Part 2. Chemical and microbiological properties. Black, C.A., Evans, D.D., White, J.L., Ensminger, L.E., Clark F.E. (Eds.), Soil Science Society of America. Madison, Wisconsin, USA. pp. 914-926.

Pepper, I.L., Gerba, C.P., Brendecke, J.W., 1995. Environmental microbiology: a laboratory manual. Academic Press Inc. New York, USA.

Pratt, P.F., 1965. Potassium. In: Methods of soil analysis. Part 2. Chemical and microbiological properties. Black, C.A., Evans, D.D., White, J.L., Ensminger, L.E., Clark F.E. (Eds.), Soil Science Society of America. Madison, Wisconsin, USA. pp. 1022-1030.

Rolinski, S., Prishchepov, A.V., Guggenberger, G., Bischoff, N., Kurganova, I., Schierhorn, F., Müller, D., Müller, C., 2021. Dynamics of soil organic carbon in the steppes of Russia and Kazakhstan under past and future climate and land use. *Regional Environmental Change* 21: 73.

Rowell, D.L., 1996. Soil Science: methods and applications. Longman, UK. 350p.

ŠantruuČková, H., SiraŠicraba, M., 1991. On the relationships between specific respiration activity and microbial biomass in soils. *Soil Biology and Biochemistry* 23(6): 525–532.

Šarauskis, E., Naujokienė, V., Lekavičienė, K., Kriaučiūnienė, Z., Jotautienė, E., Jasinskas, A., Zinkevičienė, R., 2021. Application of granular and non-granular organic fertilizers in terms of energy, environmental and economic efficiency. *Sustainability* 13: 9740.

Smith, J.L., Paul, E.A., 1990. Significance of soil microbial biomass estimation: Soil Biochemistry. Bollag, J.W., Stotzky, G. (Eds.). Volume 6, Marcel Dekker Inc. New York, USA. pp. 357-396.

Sobreira, H.A., Ferreira, M.V., Faria, A.M., de Assunção, R.M.N., 2024. Commercial organomineral fertilizer produced through granulation of a blend of monoammonium phosphate and pulp and paper industry waste post-composting. *Industrial Crops and Products* 222: 119816.

Toor, M.D., Kızılkaya, R., Anwar, A., Koleva, L., Eldesoky, G.E., 2024. Effects of vermicompost on soil microbiological properties in lettuce rhizosphere: An environmentally friendly approach for sustainable green future. *Environmental Research* 243: 117737.

USDA, 2001. Soil Quality Test Kit Guide. United States Department of Agriculture, Agricultural Research Service, Natural Resources Conservation Service, Soil Quality Institute. USA. 82p. Available at [Access date: : 11.05.2024]: https://www.nrcs.usda.gov/sites/default/files/2022-10/Soil%20Quality%20Test%20Kit%20Guide.pdf

Walkley, A., Black, C.A., 1934. An examination of the Degtjareff method for determining soil organic matter and a proposed modification of the chromic acid titration method. *Soil Science* 37(1): 29–38.

Wardle, D.A., Ghani, A., 1995. A critique of the microbial metabolic quotient (qCO2) as a bioindicator of disturbance and ecosystem development. *Soil Biology and Biochemistry* 27: 1601-1610.

Yapiyev, V., Gilman, C., Kabdullayeva, T., Suleimenova, A., Shagadatova, A., Duisembay, A., Naizabekov, S., Mussurova, S., Sydykova, K., Raimkulov, I., Kabimoldayev, I., Abdrakhmanova, A., Omarkulova, S., Nurmukhambetov,D., Kudarova, A., Malgazhdar, D., Schönbach, C., Inglezakis, V., 2018. Top soil physical and chemical properties in Kazakhstan across a north-south gradient. *Scientific Data* 5: 180242.